BLDSC NO:- DX75650/87

LOUGHBOROUGH
UNIVERSITY OF TECHNOLOGY
LIBRARY

AUTHOR/FILING TITLE
ALI, Q R

ACCESSION/COPY NO.
013469/02

VOL. NO.

CLASS MARK
LOAN COPY

- 1 JUL 1994

30 JUN 1995

001 3469 02

AIRCRAFT LOAD ALLEVIATION BY SPECIFYING ITS CLOSED-LOOP EIGENSTRUCTURE

by

Q. R. Ali, B.Sc., B.Tech.(Hons.)

A doctoral thesis

submitted in partial fulfillment of the requirements

for the award of

the degree of Ph.D. of the Loughborough University of Technology

January, 1987

SUPERVISOR: D. McLean, Ph.D., C.Eng., F.Inst.M.C., M.I.E.E.

Formerly of Department of Transport Technology

Loughborough University of Technology

© Qazi Rashid Ali, 1987.

Loughborough University
of Technology Library
Date July 87
Class
Acc. No. 013469/02

DEDICATION

"To the men and women who have the ability to control everything,

but themselves remain uncontrolled....."

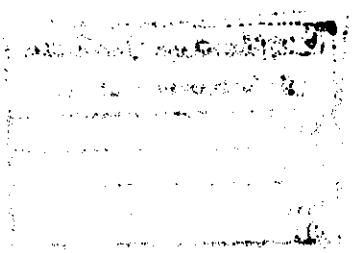

DECLARATION

This thesis is the outcome of the research carried out by the author in the Department of Transport Technology at Loughborough University of Technology and represents the independent work of the author; the work of others has been referenced where appropriate.

The author also certifies that neither the thesis nor the original work contained herein has been submitted to any other institution for a degree.

Qazi Rashid Ali

ACKNOWLEDGEMENTS

The author would like to express his gratitude to his parents Col. (retd.) Qazi Rasheed Ali and Jamila Rasheed for their endless encouragement, continuing love and support throughout his education.

The author is indebted to Prof. D. McLean for his guidance and inspiration at every stage of this research work, and also for providing an opportunity to acquire knowledge under his counsel.

SUMMARY

Reduction of aircraft loads, arising as a result of manoeuvre commands or atmospheric turbulence, by means of active control is an important problem in flight control. A variety of methods of designing appropriate control systems to achieve such reduction are available, but not every method is effective. A feature of this research work is the use of an eigenvalue/eigenvector assignment method using full state variable feedback, to design aircraft load alleviation control systems.

It is known that an eigenvalue associated with a mode determines the overall speed of the response, its corresponding eigenvector distributes the mode in the response. The inadequacies of a eigenvalue assignment method using the generalised control canonical form and of the linear quadratic design method, to achieve the desired eigenvectors was demonstrated by considering the performance of lateral feedback controllers designed using these methods, for the model of L-1011 Tristar aircraft. For the same aircraft model it was demonstrated that the specified eigenvalues and eigenvectors could be achieved through eigenvalue/eigenvector assignment method.

The effectiveness of the technique of an eigenvalue/eigenvector assignment, for load alleviation control in manoeuvres and in atmospheric turbulence, was demonstrated using a mathematical model of a large flexible transport aircraft, the C-5A Galaxy. The model description included the rigid body dynamics, the first six flexural modes, unsteady aerodynamic effects, and the dynamics of the actuators. Atmospheric turbulence was simulated by passing white noise through a Dryden filter. Assessment of the reduction achieved was based on the steady-state and the root mean square (RMS) values of the bending moments and torsional moments at five specific wing stations. These moments were represented by output equations, related to the state equation used to represent the C-5A.

Finally, the robust nature of the proposed feedback laws was demonstrated by considering reduced order feedback laws derived from the reduced order models. It was shown that if at least Law Gamma is available for feedback then manoeuvre load control and gust load alleviation would be possible. It was shown that if some state variables of the aircraft are unavailable for measurement then a full order observer could be designed by using the eigenpair assignment method. Full order observers were used to reconstruct the complete state vector from available measurements. The effect of observer dynamics on the observed states and hence on load alleviation was demonstrated by considering three separate observers. It was also shown that the error between the actual states and the estimated states converged to zero more rapidly as the dynamics of the observer are made fast. The estimated full state variable feedback control system was synthesised digitally by using the simulation language ACSL. The effect of different sampling frequencies on the dynamics of the observer and hence on load alleviation was also demonstrated.

CONTENTS

LIST OF FIGURES

LIST OF TABLES

Chapter 6:

LIST OF SYMBOLS AND ABBREVIATIONS

Lower case English

a	Scalar
a_y	Lateral acceleration at the centre of gravity.
$\bar{c}$	Mean aerodynamic chord
e_{ij}	Elements of matrix E
g	Acceleration due to gravity
k	Rank of matrix S_λ
m	Dimension of control vector
n	Dimension of state vector
n_2	Conversion factor
p	Dimension of the output vector
$\hat{q}$	Pitch rate
q	Normalised pitch rate
r	Yaw rate
$r_{w.o}$	Washed out yaw rate
t	Independent variable, time
u	Forward aircraft speed
w	Vertical velocity
w_g	Vertical gust velocity
x_7	Washout filter state

Vectors

c	Command vector
e	Error vector defined as the difference between the measured and estimated state vectors
r	Forcing vector
u	Control vector

$\mathbf{u}^o$	Optimal control vector
$\mathbf{u}_o$	Vector of unit step inputs
$\mathbf{u}_s$	Eigenvector of matrix $\mathbf{U}_s$
$\mathbf{v}_s$	Eigenvector of matrix $\mathbf{V}_s$
$\mathbf{w}$	Command vector
$\mathbf{x}$	State vector
$\mathbf{x}(0)$, $\mathbf{x}_{ic}$, $\mathbf{x}_o$	Initial state vectors
$\mathbf{x}_e$	Estimated state vector
$\mathbf{x}_{ss}$	Steady-state vector
$\mathbf{y}$	Output vector
$\mathbf{y}_m$	Measured output vector
$\mathbf{z}$	Transformed state vector
$\mathbf{z}_t$	Transformed vector

Upper case English

$E_j(.)$	Dimensional stability derivative of the j^{th} flexural mode due to $(.)^{\dagger}$
$G_T(s)$	Transfer function representing the Küssner dynamics associated with the tail
$\tilde{G}_T(s)$	Approximation to the transfer function representing the Küssner dynamics associated with the tail
$G_W(s)$	Transfer function representing the Küssner dynamics associated with the wing
$\tilde{G}_W(s)$	Approximation to the transfer function representing the Küssner dynamics associated with the wing
$G_{w_g}(s)$	Transfer function representing the gust dynamics
J	Scaler performance index
J(c)	Dimensionless lift on a lifting surface

J_w	Dimensionless lift growth on the wing
J_T	Dimensionless lift growth on the tail
$K1_{(.)}$, $K2_{(.)}$	Feedback gains
L_w	Scale length of the gust
$L'_{(.)}$	Rolling moment stability derivative due to changes in (.)†
$M_{(.)}$	Pitching moment stability derivative due to changes in (.)
$N'_{(.)}$	Yawing moment stability derivative due to changes in (.).
T_d	Time delay
T_T	Time delay representing the delayed appearance of the gust at the tail
T_w	Time delay representing the delayed appearance of the gust at the wing.
U_o	Trimmed forward airspeed of the aircraft.
$X_{(.)}$	Longitudinal force stability derivative due to changes in (.).
$Y_{(.)}$	Sideforce stability derivative due to changes in (.).
$Z_{(.)}$	Vertical force stability derivative due to changes in (.).

Matrices

$\mathbf{A}$	Coefficient matrix
$\mathbf{A_D}$	Desired closed-loop matrix
$\mathbf{A_{11}}$, $\mathbf{A_{12}}$	Sub matrices of matrix $\hat{\mathbf{A}} = \mathbf{T^{-1}A\,T}$
$\mathbf{A_{21}}$, $\mathbf{A_{22}}$	Sub matrices of matrix $\hat{\mathbf{A}} = \mathbf{T^{-1}A\,T}$
$\mathbf{B}$	Control driving matrix
$\mathbf{C}$	Output matrix
$\mathbf{C_m}$	Measured output response matrix
$\mathbf{D}$	Output driving matrix

† (.) denotes any of the defined state variables

E	Forcing matrix
F	Coefficient matrix in the generalised control canonical form
F_e	Estimator coefficient matrix
G	Driving matrix in the generalised control canonical form
G_e	Estimator gain matrix
G_o	Control weighting matrix
G_η	Noise driving matrix
I	Identity matrix
K, K_o	Feedback gain matrices.
M_λ, N_λ	Sub matrices of R_λ
P	Control transformation matrix
Q	State weighting matrix
R_λ	Matrix which forms the basis for the null-space of S_λ
S	Solution of the Riccati equation
S_λ	Matrix defined as $[\lambda I - A \mid B]$
T	State transformation matrix
U_s	Unitary matrix in singular value decomposition
V	Modal matrix
V_c	Closed-loop modal matrix
V_o	Matrix of selected closed-loop eigenvectors
V_s	Unitary matrix in singular value decomposition
W	Matrix of eigenvectors
W_o	Matrix containing eigenvectors $\underline{\omega}_{\kappa_i}$
Z	Controllability matrix

Greek characters

β	Side slip angle
β_{ic}	Initial value of the sideslip angle

χ	Control invariant
δ_a	Aileron deflection
δ_r	Rudder deflection
δ_e	Elevator deflection
δ_{e_i}	Inboard elevator deflection
δ_{e_o}	Outboard elevator deflection
γ	Mach number correction factor
ϕ	Roll angle
v_{ij}	eigenvector components of v_i
λ_i	i^{th} eigenvalue
σ	real part of the eiegnvalue
σ_s	i^{th} singular value
σ_{w_g}	Standard deviation of the vertical gust velocity
θ	pitch angle
ψ	yaw angle
$\psi_K(t)$	Küssner function
ω	Spatial frequency
ω_j	Frequency of the j^{th} flexural mode
ω_n	Natural frequency
ξ_k	Flexural mode displacement of the k^{th} mode
η	White noise
ζ	Damping ratio
ζ_j	Damping ratio of the j^{th} flexural mode
Φ_{w_g}	Power spectral density of gust velocity
Φ_η	Power spectral density of white noise

Vectors

$\underline{\alpha}$	vector defined as $\mathbf{V^{-1}x(o)}$
$\underline{v}_i$	eigenvector corresponding to λ_i

$\underline{\omega}_{\kappa_i}$	eigenvector belonging to matrix M_λ
$\underline{\rho}_{\kappa_i}$	eigenvector belonging to matrix N_λ
$\underline{\Psi}$	Co-state vector

Matrices

Ω	Feedback matrix
Σ	Diagonal matrix whose elements are singular values
Λ	Diagonal matrix whose elements are λ_i's

Operators

s	Laplace variable
>	Greater than
$\leq$	Less or equal to
$\int$	Integral
$\partial/\partial t$	Partial differential
d/dt	Differential
$\|\| . \|\|$	Norm
$\mathcal{H}$	Hamiltonian
$<\cdot , \cdot>$	Inner product
$(.)^T$	Transpose
$(.)^{-1}$	Inverse
$(.)^*$	Conjugate
$(.)^H$	Hermitian
$(.)^\dagger$	Generalised Inverse

Abbreviations

ALDCS	Active lift distribution control system
AR	Aspect ratio
BM	Bending moment
EPAM	Eigenpair assignment method
EFSVF	Estimated full state variable feedback
FM	Flexural mode
FSVF	Full state variable feedback
GCCF	Generalised control canonical form
GLA	Gust load alleviation
LQP	Linear quadratic problem
MLC	Manoeuvre load control
RMS	Root mean square
SLA	Structural load alleviation
TM	Torsional moment
WSn	Wing station 'n' , n = 1, 2, ..., 5

CHAPTER 1

INTRODUCTION

1.1 Introduction

When an aircraft is in flight, it experiences accelerations at various body stations as a result of,

(i) control surface deflections

(ii) variations in engine Thrust

(iii) encountering atmospheric turbulence.

The accelerations thus developed translate directly as the loads on the aircraft structure. In the prediction of design loads on an airplane structure in an accelerated flight condition, it is usually assumed that the airplane is perfectly *rigid.* Structural components designed by loads computed on this basis may fail due to dynamic overstress. External loads that are applied not only cause translation and rotation of the aircraft as a whole, but tend to excite the natural modes of vibration of the structure. The additional inertial forces associated with these vibrations produce the dynamic overstress. Dynamic stresses are usually manifested in the form of increased bending and torsional stresses in the structural components of the wing and fuselage.

During flight, deflections of the structure tend to distribute the aerodynamic loads and may cause their distribution to be significantly different from that computed on the basis of *rigidity* . The altered load distribution may cause degradation of the performance and handling qualities. Structural flexibility may not be objectionable; aeroelastic phenomena arise when structural deformations induce other aerodynamic forces. The elastic and aerodynamic interaction may become smaller as equilibrium is attained or *diverge* resulting in destruction of structural components. The aerodynamic and elastic interactions and their influence on modern airplane design are fully discussed by Bisplinghoff et al [1955].

Modern aircraft are designed to attain maximum aerodynamic efficiency with minimal structural weight. A primary result of search for higher performance is that, with greatly altered geometry of recently designed aircraft, a new class of flight control problems has emerged and has required methods of solution substantially different from those employed to solve conventional problems

of flight control.[¶] The need to minimise the loads on the aircraft, either overall, or at specific locations, the suppression of flutter [§], or the minimisation of the effects upon the motion of aircraft when it encounters atmospheric turbulence are all members of this new class of problems.

To solve these problems of flight control and to enhance the performance of the aircraft, it is now considered more effective to use active control technology (ACT) rather than to employ hardware modifications. ACT encompasses six major control functions, namely

(i)	Relaxed Static Stability	(RSS)
(ii)	Manoeuvre Load Control	(MLC)
(ii)	Fatigue Reduction	(FR)
(iv)	Ride Control	(RC)
(v)	Flutter Mode Control	(FMC)
(vi)	Gust Load Alleviation	(GLA)

The two control functions of interest in this research study were MLC and GLA. The purpose of MLC is to redistribute the lift on the wing during manoeuvring flight. By deflecting control surfaces symmetrically (such as flaps and ailerons) on the wing, it is possible to reduce incremental stresses through the shift inboard of the *centre of lift* of the wing. Thus enabling a reduction of the wing root bending moment. MLC is referred to in some publications as active lift distribution control system (ALDCS), Stone et al[1972]. GLA techniques are concerned with reducing the peak loads and the number of cycles on the airframe when encountering turbulence. It involves controlling (reducing) the contributions of the rigid-body dynamics and/or of the structural deformations to the aircrafts motion.

[¶] Conventional methods of synthesising flight control systems include Root-Locus and frequency response methods which have been used essentially for single input single output (SISO) systems.

[§] An aeroelastic phenomenon.

The amplitudes of the response caused by the structural flexibility can be reduced if,

(i) the amount of energy transferred from the gust input to the structural modes is reduced.

(ii) any energy absorbed by the structural modes is dissipated rapidly.

Both methods should be employed simultaneously because the only method of reducing the energy transfer is to apply a countering force from another source, say, the deflection of a control surface. Such a method requires an accurate knowledge of the stability derivatives which govern the equations of motion of the aircraft. Since these derivatives can change their values extensively and quickly due to variations in the mass of the vehicle, in the dynamic pressure and in the nature of atmospheric turbulence, the dynamics of the aircraft are known too imperfectly to admit perfect cancellation of the forces. Once the energy has been absorbed by the structural modes, the dissipation can be controlled effectively by augmenting their damping. Other control functions of ACT are discussed by Holloway [1973].

Aircraft having flexibility can develop both large amplitude motion and accelerations due to structural modes over and above that due to the rigid-body modes. These accelerations as previously stated may arise due to turbulence or due to manoeuvres. In any event, the magnitude of disturbances can seriously affect the aircrafts structural life, crew fatigue (due to increased work load), and passenger comfort and safety of a transport aircraft. Furthermore repeated high levels of stress and high peak loads influence the structure from both the ultimate strength and fatigue standpoints, Newberry [1969]. These facts, along with the increasing capabilities of ACT in accomplishing the control of rigid-body and structural dynamics to alleviate these areas of concern, was dominant motivation for initiating the Load Alleviation and Mode Stabilisation (LAMS) program. The work on LAMS was conducted on the Boeing B-52 aircraft to demonstrate the capabilities of an advanced flight control system to alleviate gust loads and to control the structural modes using aerodynamic control surfaces as force producers, Burris & Bender [1969].

Applications of ACT to achieve MLC, RC, and GLA are numerous. For example Erkelens & Schuring [1975] proposed a ride control system fro the Fokker F-27 aircraft. Reductions in the vertical accelerations arising due to atmospheric turbulence, of up to 50% were obtained by the use of fast moving flaps, commanded by a vertical acceleration sensor. Other benefits of ACT have been realised on a derivative of the L-1011 Tristar {L-1011-3 (ACS)} by design of a control system which offers improved fuel efficiency. An increase in the wing span of nine feet is responsible for the improved fuel efficiency. In order to minimise the impact of increased wing span on the structural loads and structural weight, an Active Control System (ACS) has been developed concurrently with the increased wing span. The ACS provides MLC and GLA through symmetric deflection of ailerons, commanded by acceleration sensors, Gould [1985].

The C-5A is the largest transport aircraft manufactured by Lockheed Corporation, of America. It first entered service with the United States Air Force in September 1969. Just before delivery there was a technical setback when in July 1969 a wing test specimen failed structurally, at 1.25 times the design load limit. This load figure was significantly below the strength required for demonstration of aircraft's planned structural life. A modification programme to introduce reinforcement at eleven points in the wing was undertaken resulting in a reduction of the payload carrying capacity by 7.5% , (Air International [1984]). Even after these modifications, there remained a problem in the wing durability that threatened reduce the operational life to less than 7500 hours rather than the intended 30,000 hours. Since sixty sets of wings had already been produced, attention was given urgently to achieving alleviation of wing loads by the means of ACT.

Conventional methods of designing feedback control systems, such as the use of Root-Locus, frequency response etc, are ineffective for the structural load alleviation problem being considered, since conventional methods are essentially for single input single output (SISO) systems. It is known (to be shown later) from system dynamics that such alleviation can be obtained by simultaneous use of additional control inputs. Thus modern control methods, which explicitly take into account the multivariable nature of the load alleviation problem, have to be

used.

1.2 Review of Feedback Methods

The equations of motions governing a dynamical system can be represented by a state equation viz:

$$\dot{\mathbf{x}} = \mathbf{A}\,\mathbf{x} + \mathbf{B}\,\mathbf{u}\ , \qquad 1.1$$

$$\mathbf{y} = \mathbf{C}\,\mathbf{x}\ , \qquad 1.2$$

where $\mathbf{x}$ is the state vector $\in \mathcal{R}^n$, $\mathbf{u}$ is the control vector $\in \mathcal{R}^m$, $\mathbf{y}$ is the output vector $\in \mathcal{R}^p$ (where $p < n$), $\mathbf{A}$ is the coefficient matrix of order $[n * n]$, $\mathbf{B}$ is the control driving matrix of order $[n * m]$, $\mathbf{C}$ is the output matrix of order $[p * n]$. The purpose of multivariable control is to alter the system dynamics when the loop is closed. The closure of the loop is accomplished by a feedback law of the type,

$$\mathbf{u} = \mathbf{K}\,\mathbf{x}\ , \qquad 1.3$$

where $\mathbf{K}$ is a feedback matrix of order $[m * n]$. Such a method of feedback control is termed state variable feedback. After the introduction of feedback, equation 1.1 clearly assumes the form,

$$\dot{\mathbf{x}} = (\mathbf{A} + \mathbf{BK})\,\mathbf{x}\ . \qquad 1.4$$

The roots of the characteristic equation, $\det\{s\,\mathbf{I} - (\mathbf{A}+\mathbf{BK})\}=0$, are termed the poles (or the eigenvalues) of the closed-loop system and are associated with the dynamical modes of the closed-loop system. The mechanism of obtaining a control law which results in the closed-loop system having the desired eigenvalues is termed Eigenvalue Assignment.

Wonham [1967] showed that the poles of a closed-loop system may be placed arbitrarily using state variable feedback if and only if the system is controllable (N.B. If rank(A,B)=n then the system is said to be fully controllable). Similar results were presented by Simon & Mitter [1968] and Porter & Carter [1968]. Often, all of the state variables of the system are not available for measurement instead only the output vector is available for feedback. Brasch & Pearson [1970] presented a method of arbitrarily assigning 'p' poles of the closed-loop system by using output feedback ($\mathbf{u} = \mathbf{K}\,\mathbf{y}$), assuming that matrix C is of full rank. The approach used by Brasch & Pearson was not to estimate inaccessible states [N.B. The work of Luenberger [1966] involved design of observers in which the inaccessible states were estimated] and then use these estimates to control , but rather to simply control an unaugmented system using available measurements. Independent, but similar results were presented by Davison [1970]. Since 1970 there have been numerous publications on the subject of eigenvalue assignment, and the methods have been applied to various problems of flight control.

It is known that a free response of a dynamical system is given by a linear combination of the modes of the system, where the mode shapes are determined by the eigenvectors and the time-domain characteristics by the corresponding eigenvalues, Porter & Crossley [1975]. A feedback method which assigns not only the prescribed closed-loop eigenvalues but also the corresponding eigenvectors will obviously be better than the pure eigenvalue assignment. Moore [1976], identified the freedom offered by state variable feedback beyond specification of closed-loop eigenvalues in the case where the closed-loop eigenvalues are distinct. Moore's results included a method of computing the feedback matrix which yields the prescribed eigenvalues and the eigenvectors. The assumption of distinct eigenvalues was dispensed with in a later paper by Klein & Moore [1977].

Porter & D'Azzo [1978][1,2] and Srinathkumar [1978] were among the early researchers in the area of eigenvalue/eigenvector assignment. Since 1978, Broussard et al [1980], Daywansa & Mukundan [1982], Fahmy & O'Reilly [1982], Owens & Mielke [1982], Andry et al [1983],

Shapiro & Chung [1984], Soroka & Shaked [1983], Fahmy & Tantawy [1984] and Mielke & Tung [1985] have presented papers on the subject. Although some of the methods have been applied to design stability augmentation systems for aircraft, none of the methods have been applied to design control systems appropriate to MLC, SLA and GLA.

It is not feasible to discuss in detail here every published method but a number of features of some of the methods are outlined. Moore [1976] derived the necessary and sufficient conditions for the existence of a real feedback matrix such that the resulting closed-loop system would exhibit the specified eigenvalues and eigenvectors. A necessary condition required the computation of the closed-loop eigenvectors such that they spanned the null space of the matrix $[\lambda \mathbf{I}-\mathbf{A} \mid \mathbf{B}]$. The method is restricted by the requirements, that all the specified closed-loop eigenvalues must be distinct. The closed-loop eigenvectors are calculated as a solution of simultaneous linear equations. Porter & D'Azzo [1978] presented a method of calculating a feedback matrix which assigned not only the closed-loop Jordan canonical form, but also the eigenvectors and the generalised eigenvectors. Such vectors are generated from a sequence of equations, the method depends upon selecting from a computed set linearly independent eigenvectors. Moore's method, however, required the specification of distinct closed-loop eigenvalues; while Porter's method is capable of assigning eigenvalues of certain geometric and algebraic multiplicities.

Owens & Mielke's work is essentially the same as Moore's work, in which an achievable closed-loop eigenvector is obtained by projecting the desired closed-loop eigenvector on to the null-space of the matrix $[\lambda \mathbf{I}-\mathbf{A} \mid \mathbf{B}]$. Once a feedback gain matrix is determined by the initial eigenvalue/eigenvector assignment, the feedback gain matrix is checked for elements whose magnitudes are not acceptable. If reduction in the elements is required, then a new set of eigenvectors is obtained by a gradient search procedure. The extent of gain reduction is dependent upon the specified eigenvalues, the desired eigenvectors and the system dynamics. The method presented by Owens & Mielke does enable such gain modifications. However, incorrect specification of the eigenvectors will, in general, result in large gains. Therefore it is

because of the need to reduce the magnitude of the gains, that a modification procedure is required. It will be shown later (chapter 3) that eigenvectors cannot be assigned *totally arbitrarily* but have to be selected according to the dynamical considerations.

The work of Andry et al is a straightforward extension of Moore's work; the closed-loop eigenvectors are required to belong to the sub-space of the matrix $[(\lambda \mathbf{I} - \mathbf{A})^{-1}\mathbf{B}]$. An achievable closed-loop eigenvector is obtained by projecting the desired closed-loop eigenvector on to this sub-space by minimising the 2-norm of the difference between the desired eigenvectors and the achievable eigenvectors. The restriction of the method lies in the fact that the specified closed-loop eigenvalues must be distinct. Clearly if an eigenvalue belonging to the open-loop spectrum is specified for the closed-loop, the inverse of the matrix $(\lambda \mathbf{I} - \mathbf{A})$ is not defined. Moreover the method is dependent upon selecting suitable eigenvectors in the first instance, for if the selected eigenvector is orthogonal to the sub-space of the matrix $[(\lambda \mathbf{I} - \mathbf{A})^{-1}\mathbf{B}]$ then the achievable eigenvector cannot be made to span this sub-space.

The freedom to assign the eigenpairs associated with the flexural modes can be useful in achieving SLA, by assigning the dynamic characteristics of the flexural modes. A new eigenvalue/eigenvector assignment method (EPAM) is presented in this thesis which is subsequently applied to obtain MLC & GLA. The method presented uses complex singular value decomposition method to compute the basis for the null space of $[\lambda\mathbf{I}-\mathbf{A} \mid \mathbf{B}]$. The method presented is a "direct method", in which null space eigenvectors are assigned in the closed-loop thus avoiding the method of eigenvector projection commonly in use.

The question of when to use state or output feedback is a matter of system considerations. For example, in the design of stability augmentation systems (SAS) for aircraft, state variable feedback may be employed. The mathematical models on which the SAS are based, usually comprised of only the rigid-body dynamics. The state vector is usually measurable and therefore state variable feedback posses no great difficulty. However, in some cases the entire state vector is usually unavailable for feedback and therefore output feedback techniques have to be used.

Srinathkumar [1978] and Porter & Bradshaw [1978] have shown that the eigenvalues/eigenvectors of a linear continuous-time system can be assigned by using output feedback. However it suffices to say that if the *missing* states can be estimated from the knowledge of the available measurements then state variable feedback is not so objectionable, provided the robustness properties of the feedback scheme can be demonstrated.

1.3 Problem Description

A number of methods of synthesising control systems by the use of modern control techniques to achieve MLC and GLA have been proposed by Stone et al[1972], Konar et al[1976], McLean[1976], Harvey & Pope[1977] and Prasad[1980], for example. Most of the published work has been concerned with the design of control systems for structural load alleviation (SLA), manoeuvre load control (MLC) and gust load alleviation (GLA), using the solution of the Linear Quadratic Problem (LQP)¶. However, a deficiency of the LQP method for the purposes of SLA lies in the fact that the modal characteristics of the flexural modes, such as frequency and damping, are arbitrarily assigned and that the selection of the weighting matrices used in the scalar performance criterion do not relate to the required system performance; thus a trial and error approach is often adopted for the selection of the weighting matrices.

¶ The method is based on minimising a scalar performance index of the type,

$$J = \frac{1}{2}\int_0^\infty \{ y^T Q\, y + u^T G_o\, u \}\, dt \quad ,$$

where the matrices Q and G_o are termed the weighting matrices. The control law is calculated as,

$$u = - G_o^{-1} B^T S\, x \quad ,$$

where S is the solution of the algebraic Riccati equation.

Since the precise assignment of the eigenvalues and eigenvectors is not possible by the use of feedback controllers designed by the LQP method, the effect of altering the modal characteristics of the flexural modes has not previously been studied in a direct way. The aim of this research study was the development of an eigenvalue/eigenvector assignment [eigenpair assignment method (EPAM)] method to achieve SLA. In particular the effect of altering the characteristics of the flexural modes and effects of such eigenpair assignment on the structural loads on the wing of the C-5A which may arise owing either to manoeuvre commands or to atmospheric turbulence were to be studied. It is known that, if structural loads on the aircraft being studied are to be reduced, then the rates and the displacements associated with the flexural modes must be reduced. The problem therefore is the assignment of appropriate eigenpairs (associated with the flexural modes) by EPAM which will result in the desired reductions.

One of the prime objectives of this research study was to obtain reductions in the bending and torsional moments observed at five specific wing stations. Since these moments are related to the flexural modes any reductions realised in the peak and root mean square (RMS) values of the rates and displacements of the flexural modes will reflect in the bending and torsional moment response. A set of control system design objectives appropriate to SLA defined earlier by Stone et al[1972]. In order to quantitatively access the reductions in the bending and torsion moments and also to validly compare the merits of control systems designed for SLA, by the use of LQP method and those designed by the proposed EPAM, same objectives as those defined by Stone et al [1972] were used in this study. These are listed below:

1) For MLC, a 30% reduction is required in the steady state value of the bending moment (BM) observed at Wing station one (W.S.1).

2) For GLA a 30% reduction is required in the RMS value of the BM at W.S.1, with an increase of not more than 5% in the RMS value of the Torsional moment (TM) observed at the same station.

3) Handling Qualities of the aircraft must not be impaired by feedback.

The percentage figures in objectives (1) and (2) though arbitrary if achieved, represent a substantial improvement in the durability of the aircraft's wing.

1.4 Scope of the thesis

In chapter 2, equations of motion are presented for an aircraft considered as a rigid-body. The assumptions relevant to the inclusion of flexibility effects of the aircraft structure are also presented. Considerations pertinent to the identification of the stability derivatives, for the case when the aircraft is considered as a rigid-body are also presented. For an aircraft whose dynamics is modelled by an appropriate state equation the matrix equations which determine the time response, are developed in terms of eigenvalues and eigenvectors for the cases relating to manoeuvre commands and initial conditions on the state vector. A state space model is presented in this chapter describing the rigid body lateral dynamics of the L-1011 Tristar aircraft. The model, which is of a relatively low order, is presented primarily to assist in the understanding of the role of eigenvalues and eigenvectors in the dynamic performance of the aircraft, merely to illustrate the numerical effectiveness, and to facilitate comparisons of results obtained by feedback controllers designed by the methods presented in chapter 3.

Three feedback methods for obtaining control laws using full state variable feedback (FSVF) are presented in chapter 3. The first method involves assignment of specified closed-loop eigenvalues, termed eigenvalue assignment. The second method is based on the solution of the linear quadratic problem (LQP). And the third method assigns both the closed-loop eigenvalues and eigenvectors; this is referred to as the Eigenpair Assignment Method (EPAM). To the knowledge of the author this particular method has not been presented before. FSVF controllers are designed for the lateral dynamics of the L-1011 using each of the three feedback methods to augment the stability. Comparisons of the performance when using feedback control are presented, both in terms of the dynamic response and the closed-loop eigenpairs which result.

The advantages of designing a feedback controller using the proposed eigenpair assignment are demonstrated here. It is shown that the prescribed eigenvalues and the corresponding eigenvectors are achieved by the EPAM. The specification of eigenpairs is based on physical requirements rather than on arbitrary selection. The dynamic model of the lateral motion of the L-1011 is of a relatively low order, and is used merely to illustrate the numerical effectiveness of the various methods and to facilitate comparisons between them.

Incorporation of the dynamic effects corresponding to the structural flexibility and unsteady aerodynamics into the model based upon rigid-body dynamics tend to increase the complexity of the resulting model. A mathematical model which takes into account these effects for a large transport aircraft, the C5-A Galaxy is presented in detail in chapter 4.

In chapter 5 the design of feedback controllers appropriate to SLA, MLC, GLA using the proposed EPAM is dealt with. The effect on the bending and torsional moments, of altering the damping ratios associated with the flexural modes is investigated. Two schemes for specification of eigenvectors corresponding to the flexural modes are presented; the computed feedback laws corresponding to each of the schemes results in a radically different dynamic response. The extent of reductions obtained in some bending and torsional moments by using the controller designed by EPAM and using those designed by Prasad[1980] using the LQP method are also compared.

In chapter 6 the same FSVF control law designed in chapter 5 is applied to the off-nominal system having altered stability derivatives associated with the flexural modes. The effects of such changes in the aircraft 's dynamic representation are presented here. The robust nature of the proposed feedback laws designed by EPAM is demonstrated by considering reduced order feedback laws derived from the reduced order models. These reduced order controllers are applied to the model of the aircraft presented in chapter 4. It is shown here that if at least Law Gamma (lowest order of FSVF control law which required 6 states to be measured) is available for feedback then SLA would be possible. It is also shown that if some of the aircrafts states are

unavailable for measurement then a full order observer can be designed by using the EPAM. To the knowledge of the author such a method of synthesis of a full order observer using the EPAM does not appear to have been presented by any author before. The effect of observer dynamics on the observed states and hence on load alleviation is demonstrated by considering three separate observers. It is shown in this chapter that the error between the actual states and the estimated states converges to zero more rapidly as the dynamics of the observer are made fast. The estimated full state variable feedback (EFSVF) control system is synthesised digitally by using the advanced continuous simulation language (ACSL). The effect of different sampling frequencies on the observer dynamics is also demonstrated. Finally, considerations for practical implementation of EFSVF controllers using a single chip microcontroller are presented.

The outcome of this research is summarised in chapter 7, where recommendations for further work are also presented.

CHAPTER 2

REPRESENTATION OF AIRCRAFT DYNAMICS

2.1 Aircraft Rigid Body Motion

In the analysis of stability and control of an aircraft, considered as a rigid body, the equations of motion are usually derived in **stability** axis system, see for example figure 2.1. The motion of an aircraft is usually separable into two distinct components:

a) **Longitudinal**:(symmetric), involves aircraft motion in the plane of symmetry, especially pitching and heave motion.

b) **Lateral**: (asymmetric), involves aircraft motion out of plane of symmetry, for example, roll, yaw sideslip, etc.

Shown in figure 2.1 are the notation and definition of the angular rates, the translational velocities, and the forces and moments about each axis. The primary flight control surfaces, namely ailerons, rudder and elevators are also shown on figure 2.1. The equations of motion, based on small perturbation derived in stability axis system, in terms of dimensional stability derivatives, can be shown to be (McRuer et al[1973]):

Longitudinal perturbed equations

$$\dot{u} = X_u u + X_{\dot{w}} \dot{w} + X_w w + X_{\hat{q}} \hat{q} - g\theta + \sum_{i=1}^{m} X_{\delta_i} \delta_i \qquad 2.1$$

$$\dot{w} = Z_u u + Z_{\dot{w}} \dot{w} + Z_w w + (Z_{\hat{q}} + U_o)\hat{q} + \sum_{i=1}^{m} Z_{\delta_i} \delta_i \qquad 2.2$$

$$\dot{\hat{q}} = M_u u + M_{\dot{w}} \dot{w} + M_w w + M_{\hat{q}} \hat{q} + \sum_{i=1}^{m} M_{\delta_i} \delta_i \qquad 2.3$$

$$\dot{\theta} = \hat{q} \qquad 2.4$$

Lateral perturbed equations

$$\dot{v} = Y_v v + Y_p p + (Y_r - U_o) r + g\phi + \sum_{i=1}^{m} Y_{\delta_i} \delta_i \qquad 2.5^{\S}$$

$$\dot{p} = L_v' v + L_p' p + L_r' r + \sum_{i=1}^{m} L_{\delta_i}' \delta_i \qquad 2.6^{\P}$$

$$\dot{r} = N_v' v + N_p' p + N_r' r + \sum_{i=1}^{m} N_{\delta_i}' \delta_i \qquad 2.7^{\P}$$

$$\dot{\phi} = p \qquad 2.8$$

$$\dot{\psi} = r \qquad 2.9$$

The equations above are for equilibrium flight condition, with assumptions that the steady pitch rate Q_o, roll rate P_o, yaw rate R_o, lateral velocity V_o and vertical velocity W_o are equal to zero. The perturbation variables, u, v, w, p, $\hat{q}$, r, θ, φ, ψ are denoted in figure 2.1. Each of the stability derivatives $X_{(.)}$, $Y_{(.)}$ and $Z_{(.)}$ denotes a change of force (about respective axis) due to changes in $(.)^{\dagger}$. Similarly stability derivatives $L'_{(.)}$, $M_{(.)}$ and $N'_{(.)}$ denotes a change of moment (about respective axis) due to changes in $(.)^{\dagger}$. Finally, δ_i represents the deflections of the i^{th} control surface. It is convenient to represent the system of first order linear differential equations (equations 2.1 - 2.9) by a state variable equation, viz;

$$\dot{x} = A x + B u \quad , \qquad 2.10$$

where **x** is the state vector $\in \Re^n$, **u** is a control vector $\in \Re^m$, **A** is a coefficient matrix of order $[n * n]$, **B** is a driving matrix of order $[n * m]$.

---

§ g is the acceleration due to gravity (m/s^2)

¶ $$L'_{(.)} = \frac{L_{(.)} + \frac{I_{xz}}{I_{xx}} N_{(.)}}{(1 - \frac{I_{xz}^2}{I_{xx} I_{zz}})} \quad , \quad N'_{(.)} = \frac{N_{(.)} + \frac{I_{xz}}{I_{zz}} L_{(.)}}{(1 - \frac{I_{xz}^2}{I_{xx} I_{zz}})}$$

† (.) denotes any of the variables u, v, w, p, $\hat{q}$, r, δ

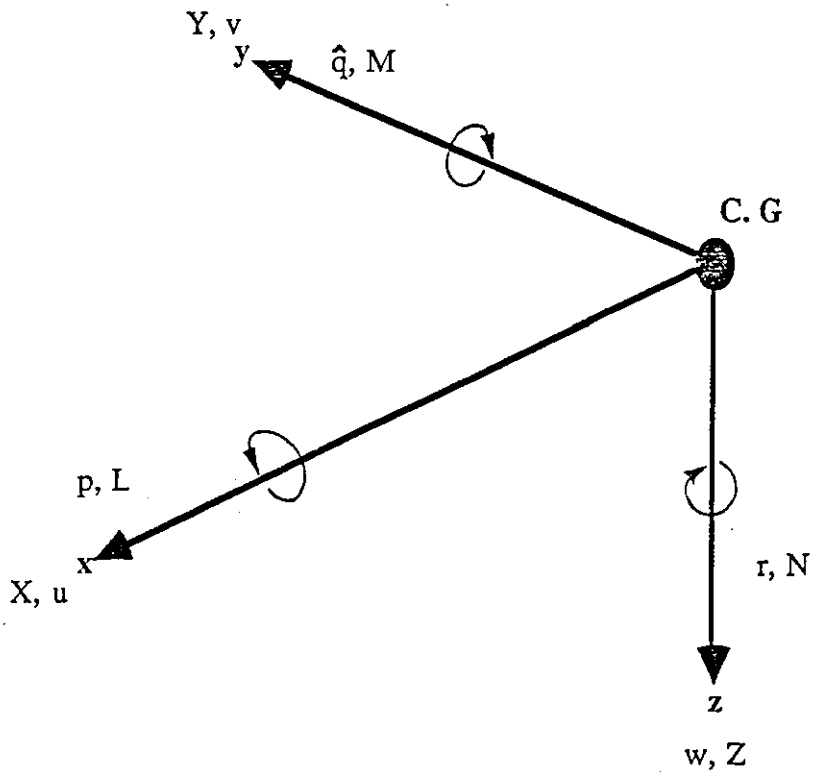

Variable	Definition	Units
p, q̂, r	Roll rate, Pitch rate, Yaw rate	rad/s
L, M, N	Rolling Moment, Pitching moment, Yawing moment	N-m
X, Y, Z	Longitudinal, Lateral , Vertical Forces	N
u, v, w	Longitudinal, lateral, vertical velocities	m / s

Figure 2.1 : Aircraft stability axis system and variable definition

In AFCS work the state vector usually consists of the aircraft's state variables, such as perturbation velocities, angular rates and displacements. The coefficient matrix A contains the stability derivatives $X_{(.)}$, $Y_{(.)}$, $Z_{(.)}$, $L'_{(.)}$, $M_{(.)}$, $N'_{(.)}$ and also quantities such as U_o, and g, where (.) has been defined earlier. The driving matrix **B** usually consists of the derivatives X_δ, Y_δ, Z_δ, L'_δ, M_δ and N'_δ. The state equation can be used to model an aircraft's longitudinal, or its lateral dynamics, or both.

2.1.1 Identification of the Stability Derivatives

Although the stability derivatives X_u, M_w etc in equations 2.1 - 2.9 can be predicted by theoretical analysis or by means of wind tunnel measurements, the requirement for more precise experimentally determined stability and control derivatives is based on the following applications:

(i) Producing the data needed for comprehensive flight simulations. This applies to the fixed, moving-base flight simulators and basic computer simulations.

(ii) Design of stability augmentation systems (SAS). The stability and control derivatives, which are used to define the model of the aircraft, have to be known accurately before any control synthesis procedure can be used.

(iii) Providing data for comparisons which result purely from analytical techniques and wind tunnel testing.

(iv) Proving the flying qualities of the aircraft as laid down in the specifications.

(v) Improvement of testing and data evaluation methods. The necessity of this application is based on economic considerations and the fact that the results from the testing of prototype aircraft contribute more and more towards production decisions.

The identified data can lead to a mathematical model with which investigations may be made of specific flight condition of interest. The extraction of the stability derivatives entails three elements:

- excitation of the modes of motion,
- measurement of the response variables,
- extraction of derivatives from measured data.

The type of flight test manoeuvres used to extract the stability and control derivatives is very important. A manoeuvre which excites all of the aircraft modes and tends to isolate the effects of the individual derivatives is highly desirable. The measured response of the aircraft has to be sensitive to the derivatives that are being identified. This is necessary for obtaining good estimates of the derivatives from the flight data. The dynamic range of the instruments/sensors and their signal-to-noise ratio characteristics impose limitations on the type and magnitude of the manoeuvre. The relationship between input design and instrumentation specification have been emphasised by Sorenson [1972]. Many methods of extracting the stability derivatives from flight data have been proposed ¶,§. Limitations and applicability of some of the methods is outlined below:

Time Vector Method

The time vector methods for derivative extraction are derived from the time-invariance of the amplitude and phase relations between the state variables of an damped second order system and the derivatives and integrals of the state variables. This invariance is then used to determine the values of the amplitude-phase relations, thereby determining the aircraft stability and control derivatives. The main disadvantage of the method is that it can only be applied to stick-fixed transient-oscillations. The method works only if the damping ratios of the responses are less than or equal to 0.3.

¶ *Methods for Aircraft State and Parameter Identification.* **AGARD-CP-172,** 1974

Papers presented at a specialist's meeting of the flight mechanics panel of AGARD held at NASA Langley Research Center, Hampton, Virginia, USA 5-8 November 1974.

§ *Parameter Estimation Techniques and Applications in Aircraft Flight Testing.* **NASA TN D-7647,** 1974

A Symposium held at the NASA flight Research Center, April 24-25, 1973

Analogue-Matching Methods

The analogue matching technique in principle is an output error method, because the method strives to iteratively minimise the errors between the simulated responses and the measured responses. This is accomplished by manually manipulating the derivatives in the analogue representation of the aircraft (NB. The initial values of the derivatives in the analogue model are usually obtained from analytical methods or by wind tunnel measurements). The method works most successfully only when a single control surface is moved and then only when the manoeuvres are simple.

Equation Error Methods

The equation error methods are basically least squares techniques in which the square of the equation error is minimised. The procedure is, by using the equations of motion, to express the stability and control derivatives as functions of the measured responses, this results in n or more linear equations in n unknowns. Since these methods do not take into account the measurement or instrumentation noise, they result in biased estimates of the stability and control derivatives.

Output Error Methods

Output error methods minimise the square of the the error between the measured aircraft responses and the output of a model used to represent the aircraft. Some of the output error methods are based on Newton-Raphson, Gradient Methods and the Kalman Filtering techniques. These methods assume measurement noise but do not cater for measurements made in the presence of atmospheric turbulence. The main disadvantage of the output error methods is that, because they do not include process noise (gusts, modelling errors etc) in their performance criterion, the results are degraded when process noise exists.

Maximum Likelihood (ML)

The ML technique of extracting stability and control derivatives, for linear or non-linear aircraft models, from flight data containing both measurement and process noise is widely used, Stepner & Mehra [1973]. The method involves three steps: (1) Kalman Filtering to estimate the states and generate a residual sequence, (2) a modified Newton-Raphson algorithm to estimate the derivatives, and (3) an algorithm to estimate the mean and variance of the measurement and process noise.

Since neither flight testing facilities nor measured flight data were available to the author, the stability and control derivative data used were taken from published sources. The data pertinent to the rigid-body lateral dynamics of one of the aircraft studied in this work (the L-1011 Tristar aircraft) were taken from Andry et al [1983]. The mathematical model representing the rigid-body lateral dynamics of the L-1011 is presented in section 2.3. The other model was obtained from Harvey & Pope [1977].

All aircraft have observable structural modes which usually cause no problems because their frequencies are much higher than those of the rigid-body modes. Generally, if the frequencies of the structural modes are more than a factor of five to ten times the highest frequency of the rigid-body mode, they can be neglected. The estimate of the stability and control derivatives are unaffected by high frequency structural noise. However, if the frequencies of the rigid-body modes and the structural modes are close then special care is required in the estimation of these derivatives. Two approaches can be taken. The structural modes can be treated as known and their effect subtracted from the data before the derivatives are extracted. The second and more difficult approach is to model the structural modes as well as the rigid-body modes and estimate the unknown coefficients for all the modes as in Schwanz & Wells [1974].

2.2 Flexibility Effects

In the case of an aircraft considered as a rigid-body, the motion of a body-element in Newtonian space is fully defined when its position vector in body-fixed axes system is known,and the motion of that axis system relative to an axis system fixed on earth is also known (the equations of motion presented in the preceding chapter are in stability axes system, which are a simplification of the equations of motion in body-fixed axes system. The assumptions necessary to transform the equations in body-fixed axes to stability axes are given in McRuer et al [1973]). Within the body-fixed frame of reference there is no motion of body-elements relative to one another. In the case of flexing bodies such as deformable aircraft, however, it is apparent that a local deformation motion will be superimposed on an overall spatial motion.

But it is by no means obvious how the respective contributions, from the two sources, to the total motion of a body-element are precisely to be defined. As in the case of rigid aircraft the total motion is ultimately referred to a set of earth-fixed axes, while it is reasonable to suppose that local deformations will be referred to a set of axes moving, in a general way, with the aircraft. As in the rigid aircraft case the complete motion may be referred to the same set of moving axes, which may be regarded as a generalisation of the body-fixed axes used to represent rigid-body dynamics. To quote Milne [1964], 'The specification of such an axes system is not obvious or unique'. Since (in general for a flexing body) the centre of mass does not remain coincident with a particular material point, it is not so obvious a choice for origin as in the case of rigid-body. Furthermore, even if the origin is fixed at a material point, it will not be possible to select rectangular axes which contain the same aggregates of material points at all stages of motion.

Milne [1964], Taylor [1971] favoured the mean-body axes for representation of flexibility effects, with origin of this axis system at the c. of g. of the aircraft. An alternative approach is the use of attached-axes [Milne [1964]]. These are body-fixed axes whose origin and orientation are fixed in an in-finitesimally small material portion of the aircraft. It is assumed that one can

find a small portion of the aircraft which is either essentially rigid or otherwise is such that the axes always remain mutually perpendicular. This axis system is called the body-fixed axis, and can be thought of as a generalisation of the body-fixed axes used for the rigid aircraft. It is noted that, even if the origin of the plane of reference is at the c. of g. when the aircraft is undeformed, it will not necessarily remain so when deformation occurs.

The equations of motion using the body-fixed axes are conveniently derived using Lagrange's equation for a non-inertial frame of reference, in conjunction with the equations based on principle of momentum. For the application of this form of Lagrange's equation it is necessary that the linear and angular velocities of the frame of reference should be independent at all instants of the deformational degrees of freedom (N.B. the motion of the frame of reference defined by the body-fixed axes, relative to an inertial frame, will be a function of the generalised co-ordinates of the body freedoms only). Thus these freedoms should consist only of displacements relative to the frame of reference. In particular any natural modes will have to be modified by the addition of certain amounts of rigid-body motion. This introduces a certain amount of ill-conditioning, [Woodcock [1971]]. However, this can be normally avoided by a suitable choice of the origin of the body-fixed axis. The following points are observed while carrying out an analysis for a deformable aircraft:

1) A convenient geometrical point of the aircraft is chosen as the reference point of the aircraft.It is chosen to avoid ill-conditioned equations of motion, which may result from an inappropriate choice.

2) Body-fixed axes are used whose orientation is fixed in an in-finitesimally small portion of the aircraft which include the reference point. This portion is assumed to be effectively rigid.

3) The motion of the aircraft is considered to be a perturbation of some given motion. The datum motion is not necessarily level flight with constant linear velocity and zero angular velocity. If the datum motion is one in which no deformation of the aircraft occurs then

equations of motion will be ones with constant coefficients. If only a small amount of deformation occurs during the datum motion then the equations of motion for small perturbations of datum motion will again be ones with constant coefficients but for 'large' perturbations time-varying coefficients appear.

4) The equations of motion are obtained from Lagrange's equations for a non-inertial frame and from the principle of momentum. Displacements are used as the unknowns. The generalised co-ordinates of the deformational degrees of freedom have to be such that the position of reference point and the orientation of the body axes are both independent of them.

For details of the derivation of equations of motion, see Milne [1964], Taylor [1971], Woodcock [1971] and Schwanz [1972], for example.

In actuality, a flexible aircraft structure has an infinite number of degrees of freedom making the exact analysis almost impossible. Approximations are often used to reduce the system to a system having finite degrees of freedoms. The following approximations are often used:

Quasi-Static : The motions of the structure are assumed to be in phase with the rigid body motion; with the acceleration of the elastic motion being taken as instantaneous. The method is used primarily for handling qualities, studies particularly for the design of stability augmentation systems for elastic aircraft where there is a wide frequency separation between the rigid body modes and the flexural modes.

Modal Substitution : The motions of the structure are assumed to be related to the orthogonal, in-vacuum eigenvectors (which are real).

Residual Stiffness : The mode shapes representing the elastic motion in the modal substitution formulation are separated into 'retained' and 'deleted' modes. The deleted modes are represented in the dynamic stability analysis as quasi-static aeroelastic corrections, using a

correction factor related to the deleted modes and the stiffness of the 'free-free' structure.

Residual Flexibility : Similar to residual stiffness formulation, except the quasi-static aeroelastic correction factor is related to the retained modes and the flexibility of the 'free-free' structure.

Modal Truncation : The deleted modes of residual flexibility are not represented by any correction factor.

The motion of the structure is represented by modes of vibrations, which are infinite in number. Using one of the approximations described earlier, the motion of the structure is usually described by the retained modes of vibration. A model of C-5A Galaxy was used in this research study to demonstrate that SLA could be achieved by feedback control. A 79^{th} order model representing the longitudinal dynamics of the C-5A Galaxy, was originally formulated by Honeywell Systems Incorporated, Minneapolis. The model contained the description of the longitudnal rigid-body dynamics, first fifteen flexural modes of the wing, Wagner dynamics*, Küssner dynamics† , Padé approximations§, actuator dynamics and the gust dynamics.

In the work of Harvey and Pope [1977], this model was reduced to a 42^{nd} order model using the method of **Modal truncation** (the Wagner dynamics were omitted). The 42^{nd} order model was then reduced to a 24^{th} order model, which included only the first six flexural modes of the wing, other modes in the model being the same as in the 42^{nd} order model. The 24^{th} order model was derived by **Residualisation**. The data pertinent to the model were taken from Harvey & Pope. The flight condition parameters and details of the model are presented in chapter 4.

---

* Wagner dynamics relate to the development of lift on an lifting surface due to step change in the angle of attack of the surface.

† Küssner dynamics relate to the development of lift on an lifting surface when it encounters a step gust.

§ Padé approximation is a ratio of polynomials used to represent a pure time delay.

2.3 Lateral Model of the L-1011 Tristar

The mathematical model of one of the aircraft studied in this research work, the L-1011 Tristar, is the same as that used by Andry et al[1983], for the design of a lateral feedback controller. The stability-axes model includes the rigid body aircraft dynamics, the actuator dynamics, and the dynamics of a washout filter¶ whose input is yaw rate. The lateral equations, which are valid for a particular cruise flight condition, may be represented by an state variable equation such as equation 2.10. The state and control vectors are defined as :

$$\mathbf{x} = \begin{bmatrix} \delta_r \\ \delta_a \\ \varphi \\ r \\ p \\ \beta \\ x_7 \end{bmatrix} \equiv \begin{bmatrix} x_1 \\ x_2 \\ x_3 \\ x_4 \\ x_5 \\ x_6 \\ x_7 \end{bmatrix} , \qquad 2.11$$

$$\mathbf{u} = \begin{bmatrix} \delta_{r_c} \\ \delta_{a_c} \end{bmatrix} \equiv \begin{bmatrix} u_1 \\ u_2 \end{bmatrix} . \qquad 2.12$$

δ_r is the rudder deflection, in rads; δ_a is the aileron deflection, in radians; φ is the roll angle, in radians; r is the yaw rate, in rad/s; p is the roll rate, in rad/s; β is the sideslip angle, in radians ($\beta = v/U_o$, v is the sideslip velocity) and x_7 is the washout filter state, δ_{r_c} and δ_{a_c} are the rudder and aileron commands.

¶

If the washed out yaw rate is defined as,

$r_{w.o} = r - x_7$, where x_7 is a washout filter state, then the transfer function $\frac{r_{w.o}(s)}{r(s)}$ can be expressed as,

$\frac{r_{w.o}(s)}{r(s)} = 1 - \frac{x_7(s)}{r(s)}$. If the transfer function $\frac{x_7(s)}{r(s)} = \frac{a}{s+a}$ then,

$\frac{r_{w.o}(s)}{r(s)} = 1 - \frac{a}{s+a} = \frac{s}{s+a}$, is the transfer function of the washout filter.

Rigid body loads arise when any of the aircraft's states is disturbed from its trim value by some atmospheric disturbance or when the pilot applies a manoeuvre command. Whenever an aircraft is disturbed, accelerations are produced at various body stations. For lateral motion acceleration at the c. of g. is given by,

$$a_{y_{cg}} = U_o\dot{\beta} - g\varphi + U_o r \quad . \tag{2.13}$$

Let,

$$y_5 = a_{y_{cg}} , \tag{2.14}$$

then the output y_5 can be expressed by an equation related to the states and controls such that,

$$\mathbf{y} = \mathbf{C}\,\mathbf{x} + \mathbf{D}\,\mathbf{u} \quad , \tag{2.15}$$

where **y** is the output vector $\in \Re^p$, **x** and **u** were defined in equation 2.10, **C** is a coefficient matrix of order [p * n], **D** is a coefficient matrix of order [p * m]. The matrices **A, B, C, D** for the L-1011 are presented in appendix A. For the L-1011 the output vector was defined as,

$$y = \begin{bmatrix} r_{w.o} \\ p \\ \beta \\ \varphi \\ a_y \end{bmatrix} = \begin{bmatrix} y_1 \\ y_2 \\ y_3 \\ y_4 \\ y_5 \end{bmatrix} \quad , \tag{2.16}$$

where $r_{w.o}$ is the washed out yaw rate, see footnote on previous page.

2.4 Uncontrolled Dynamics of the L-1011 Tristar.

For the model of the L-1011 Tristar, described in section 2.3, the corresponding eigenvalues of the coefficient matrix A are shown in table 2.1. Associated with these eigenvalues are the following modes of motion:

1. A lightly damped oscillatory mode,the 'Dutch roll mode'.
2. A monotonic mode, of relatively long time constant, the 'Spiral mode'.
3. A monotonic mode, of relatively short time constant, the 'Roll subsidence mode'.
4. The real modes associated with, the rudder and the aileron actuators and the washout filter.

MODE	EIGENVALUE
Rudder	-20.0
Aileron	-25.0
Dutch Roll	$-0.12 \pm j\ 1.27$
Spiral	-0.009
Roll Subsidence	-1.087
Washout	-0.5

Table 2.1: Open-loop eigenvalues

The time response of the output variables $r_{w.o}$, p, β, φ and $a_{y_{cg}}$ to an initial condition on the sideslip angle of 0.02 radians is shown as figure 2.2. Although the aircraft's dynamic response is seen to be stable, it is very lightly damped. From figure 2.2 it is seen that the response of $a_{y_{cg}}$ is oscillatory. Since persistent levels of acceleration can cause passenger and crew discomfort, it means that the damping should be augmented, i.e., the eigenvalues corresponding to the dutch roll mode, the spiral and the roll subsidence modes must be modified.The damping ratio of the dutch roll mode can be inferred from table 2.1 to be 0.094 and the undamped natural

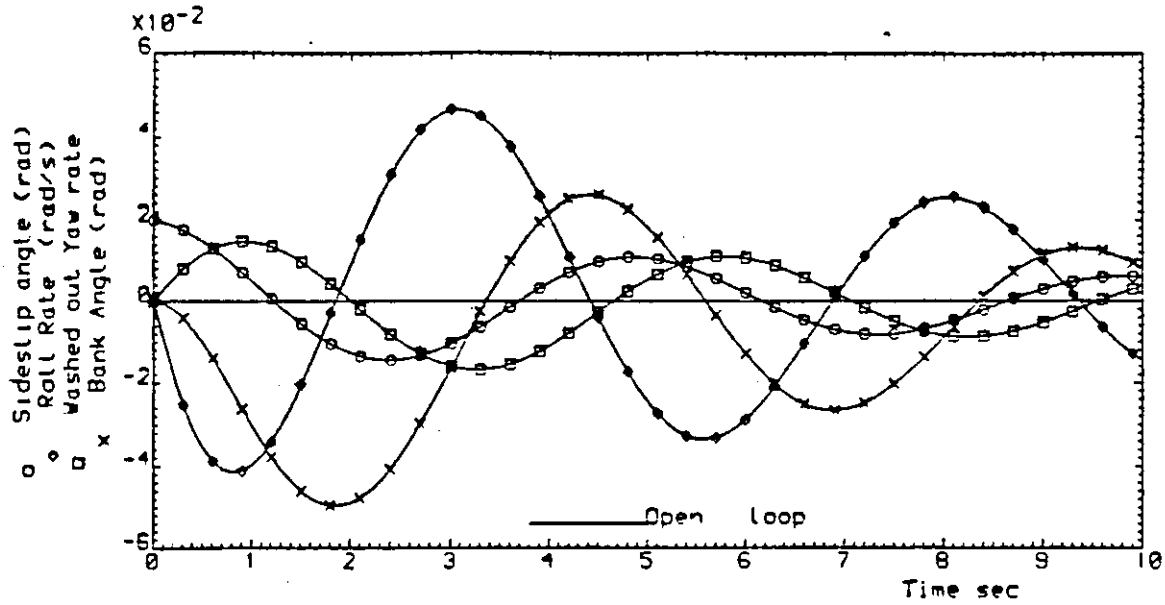

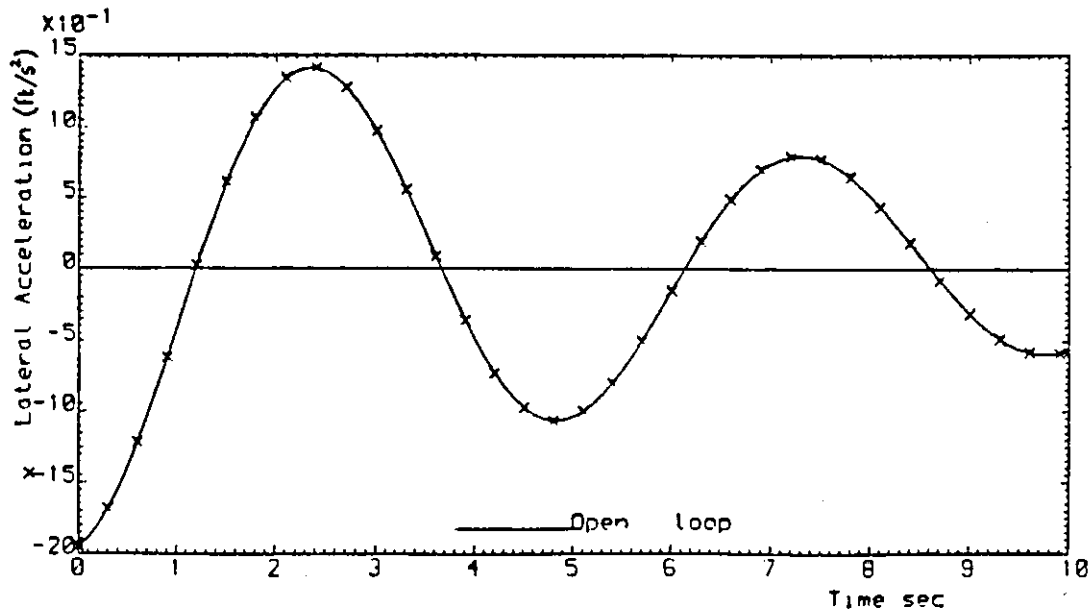

Figure 2.2 : Un-controlled response for β_{ic}= 0.02 radians

frequency* is 1.276 rad/s.

From inspection of equation 2.15, it is seen that damping in the lateral acceleration response will be augmented if any of the variables β, r and φ have added damping. Since the variables β and r constitute the dutch roll mode (which is seen to be very lightly damped), any improvement in the dutch roll damping would reflect in the lateral acceleration response.

---

* If an eigenvalue is represented as,

$$\lambda_1, \lambda_2 = -\sigma \pm j\,\omega \quad ,$$

then,

$$\zeta\omega_n = \sigma \ , \qquad \text{(i)}$$

$$\omega_n\sqrt{1-\zeta^2} = \omega \ . \quad \text{(ii)}$$

Therefore from (i) and (ii),

$$\zeta = \frac{\sigma}{\omega_n} \ , \quad \text{and} \quad \omega_n = \sqrt{\sigma^2+\omega^2} \ .$$

2.5 Influence of Eigenvalues/Eigenvectors on Dynamic Response

Consider the state equation defined earlier as equation 2.10, viz;

$$\dot{\mathbf{x}} = \mathbf{A}\,\mathbf{x} + \mathbf{B}\,\mathbf{u} \quad .$$

The numerical solution of the state equation may be obtained after diagonalisation, usually obtained by the eigenvalues and the eigenvectors of the coefficient matrix A. The eigenvalues λ_i and eigenvectors ν_i of the coefficient matrix satisfy the following equation, viz;

$$\mathbf{A}\,\underline{\nu}_i = \lambda_i\,\underline{\nu}_i \quad , \qquad \text{for } i = 1, \ldots, n \quad . \tag{2.17}$$

The non-singular modal matrix V, whose columns are the eigenvectors of the matrix A is defined by,

$$\mathbf{V} = [\underline{\nu}_1 , \underline{\nu}_2 , \ldots, \underline{\nu}_n \,] \quad . \tag{2.18}$$

By using the modal matrix diagonalisation of the state equation can be obtained by the transformation,

$$\mathbf{x} = \mathbf{V}\,\mathbf{z}_t \quad , \tag{2.19}$$

where $\mathbf{z}_t$ is the transformed state vector $\in \Re^n$. After substitution of equation 2.19, the transformed system is given by,

$$\mathbf{V}\,\dot{\mathbf{z}}_t = \mathbf{A}\,\mathbf{V}\,\mathbf{z}_t + \mathbf{B}\,\mathbf{u} \quad . \tag{2.20}$$

Multiplication of equation 2.20 by $\mathbf{V}^{-1}$ yields,

$$\dot{z}_t = V^{-1}A\ V\ z_t + V^{-1}B\ u\ . \qquad 2.21$$

Equation 2.21 can be simplified by equating the matrix $V^{-1}A\ V$ to the matrix Λ such that,

$$\Lambda = V^{-1}A\ V\ . \qquad 2.22$$

Substitution of equation 2.22 in equation 2.21 yields,

$$\dot{z}_t = \Lambda\ z_t + V^{-1}\ B\ u\ . \qquad 2.23$$

Since matrices Λ and A are similar[§], their eigenvalues are the same. Λ is a diagonal matrix whose principal elements are the eigenvalues of matrix A, i.e., $\Lambda = \text{diagonal}[\lambda_1, \lambda_2, ..., \lambda_n]$.

The solution of equation 2.23 can be shown to be,

$$z_t(t) = e^{\Lambda t}z_t(0) + \int_0^t e^{\Lambda(t-\tau)}\ V^{-1}\ B\ u(\tau)\ d\tau\ . \qquad 2.24$$

---

§ Definition : If there exist a non-singular matrix V such that $V^{-1}\ AV = \Lambda$, then Λ is said to be similar to A.

Theorem : Similar matrices have same characteristic equation and same eigenvalues.

Proof: Since

$$\text{Det}\ V^{-1}\ \text{Det}\ V = \text{Det}\ (V^{-1}V) = \text{Det}\ I = 1$$

we have

$$\text{Det}\ (\Lambda - \lambda I) = \text{Det}\ \{ V^{-1}\ (A - \lambda I)\ V \}$$

$$= \text{Det}\ V^{-1}\ \text{Det}(A - \lambda I)\ \text{Det}\ V$$

$$= \text{Det}\ (A - \lambda I)$$

proved.

Where $z_t(0)$ consists of the initial values of the transformed state variables. Transforming back into the original state space via equation 2.19, results in,

$$x(t) = V\, e^{\Lambda t} V^{-1} x(0) + V \int_0^t e^{\Lambda(t-\tau)} V^{-1} B\, u(\tau)\, d\tau \ . \qquad 2.25$$

The first term on the right hand side of equation 2.25 is the zero input response, and the second term is the zero state response. Expansion of the first term yields,

$$x(t) = \left[\underline{v}_1, \underline{v}_2, \ldots, \underline{v}_n \right] \begin{bmatrix} e^{\lambda_1 t} & \cdot & \cdot & 0 \\ \cdot & \cdot & \cdot & \cdot \\ \cdot & \cdot & \cdot & \cdot \\ 0 & \cdot & \cdot & e^{\lambda_n t} \end{bmatrix} \left[\underline{v}_1, \underline{v}_2, \ldots, \underline{v}_n \right]^{-1} x(0) \ . \qquad 2.26$$

Simplification of equation 2.26 can be obtained by defining,

$$\underline{\alpha} = [\underline{v}_1 , \underline{v}_2 , \ldots, \underline{v}_n \ ]^{-1} x(0) \ . \qquad 2.27$$

Expansion of equation 2.26 after substitution of equation 2.27 yields,

$$\begin{aligned} x_1(t) &= v_{11} e^{\lambda_1 t} \alpha_1 + v_{12} e^{\lambda_2 t} \alpha_2 + \ldots + v_{1n} e^{\lambda_n t} \alpha_n \\ &\cdot \quad \cdot \quad \cdot \quad \cdot \\ &\cdot \quad \cdot \quad \cdot \quad \cdot \\ x_n(t) &= v_{n1} e^{\lambda_1 t} \alpha_1 + v_{n2} e^{\lambda_2 t} \alpha_2 + \ldots + v_{nn} e^{\lambda_n t} \alpha_n \end{aligned} \qquad 2.28$$

Expansion of the zero state response is performed, by assuming that the input vector $\mathbf{u}(t)$ is a vector of unit step functions $\mathbf{u}_o$. The zero state response term of equation 2.25 can be written as,

$$x(t) = V\, e^{\Lambda t} \left\{ \int_0^t e^{-\Lambda \tau}\, d\tau \right\} \; V^{-1}\, B\, u_o \quad . \tag{2.29}$$

After integration of $\left\{ \int_0^t e^{-\Lambda \tau}\, d\tau \right\}$, equation 2.29 becomes,

$$x(t) = V\, e^{\Lambda t} \{ -1/\Lambda\, (e^{-\Lambda t} - 1) \} V^{-1} B\, u_o \quad . \tag{2.30}$$

Simplification of 2.30 can be obtained by defining,

$$\underline{\mu} = -1/\Lambda\, (V^{-1} B\, u_o) \, ,$$

hence equation 2.30 can be written as,

$$x(t) = V\, (1 - e^{\Lambda t}\,)\, \underline{\mu} \quad . \tag{2.31}$$

Equation 2.31 can be expanded into,

$$\begin{aligned} x_1(t) &= \nu_{11}(1 - e^{\lambda_1 t})\mu_1 + \nu_{12}(1 - e^{\lambda_2 t})\mu_2 + \ldots + \nu_{1n}(1 - e^{\lambda_n t})\mu_n \\ &\vdots \qquad\qquad \vdots \qquad\qquad \vdots \qquad\qquad \vdots \\ x_n(t) &= \nu_{n1}(1 - e^{\lambda_1 t})\mu_1 + \nu_{n2}(1 - e^{\lambda_2 t})\mu_2 + \ldots + \nu_{nn}(1 - e^{\lambda_n t})\mu_n \end{aligned} \tag{2.32}$$

The terms, $e^{\lambda t}$ in equations 2.28 and 2.32 are termed the modes of the system. From an examination of equations 2.28 and 2.32 it is seen that the eigenvalues* must be negative if the state variables are to have a stable response (as positive values would imply an increasing exponential function with time). The eigenvalues λ_i determine the rate of decay of the modes, hence influencing the settling time of the state variables. Whereas the eigenvectors govern the participation of the modes in the state variable response. For example, if eigenvector component v_{11} , in equation 2.28 is zero, then the mode $e^{\lambda_1 t}$ will not participate in the response of the state variable x_1. In order to examine the extent of mode participation, in this research work, the eigenvectors $\underline{v}_i$ were normalised such that,

$$\| \underline{v}_i \|_2 = 1.0 \qquad 2.33$$

If the diagonal elements v_{ii} of the modal matrix V are unity and the remaining elements are zero (which implies V is an identity matrix), then the i^{th} mode will participate only in the i^{th} state variable response. In such an event full decoupling of the modes of the motion will result.

---

* So far it has been assumed that the eigenvalues are real. Whenever eigenvalues occur as complex conjugate pairs the corresponding eigenvectors are also complex.

2.6 Open-loop Eigenvectors of the L-1011 Tristar

The uncontrolled dynamics of the L-1011 is explained in terms of its open-loop eigenvectors. It was shown in section 2.5, how the eigenvectors distribute the modes in the state variable response. The open-loop eigenvectors of the L-1011 are presented in table 2.2.

MODE	Dutch Roll	Roll Subs.	Spiral	Rudder	Aileron	Washout
Eigenvalue	-0.117 +j 1.269	-1.087	-0.009	-20.0	-25.0	-0.5
States	E I G E N V E C T O R S*					
δ_r	0.0	0.0	0.0	0.999	0.0	0.0
δ_a	0.0	0.0	0.0	0.0	0.999	0.0
φ	-0.050 -j 0.574	-0.677	0.998	0.001	-0.002	0.0
r	-0.213 +j 0.160	-0.016	0.038	0.037	0.001	0.0
p	-0.734	0.736	-0.009	-0.018	0.047	0.0
β	-0.135 -j 0.172	0.012	0.004	0.001	0.0	0.0
x_7	0.346 +j 0.094	0.014	0.039	-0.001	0.0	1.0

Table 2.2: Open-loop eigenvectors of the L-1011

* Eigenvector components have been rounded to three decimal places. For a complex eigenvalue, eigenvector corresponding to only the positive imaginary part is shown.

The response of roll rate due to an initial condition on any of the states, by using the eigenvector components presented in table 2.2 and by using equation 2.28 can shown to be:

$$p(t) = -0.734\, e^{(-0.117+j1.269)\,t}\alpha_1 - 0.734\, e^{(-0.177-j1.269)\,t}\alpha_2 + 0.736\, e^{-1.087\,t}\alpha_3$$
$$- 0.009\, e^{-0.009\,t}\alpha_4 - 0.018\, e^{-20\,t}\alpha_5 + 0.047\, e^{-25\,t}\alpha_6 + 0.0\, e^{-0.5\,t}\alpha_7 \ ,$$

which can be approximated to,

$$p(t) = -0.734\, e^{(-0.117+j1.269)\,t}\alpha_1 - 0.734\, e^{(-0.177-j1.269)\,t}\alpha_2 + 0.736\, e^{-1.087\,t}\alpha_3 \ ,$$

where the constants α_1, α_2, α_3 are defined by equation 2.27. From the equation presented above it can be seen that the dutch roll mode will participate in the response of roll rate. Thus coupling the rolling and the yawing motions of the aircraft. If the yawing and the rolling motions are to be decoupled then it would be necessary to modify the eigenvectors corresponding to the dutch roll mode. Roll subsidence and the spiral modes are seen to be predominantly contributing to the rolling motion variables. The lack of damping in the dutch roll mode and lack of stability in the other modes translates into the L-1011 having a very lightly damped response, as indicated by figure 2.2. In order to improve the dynamic response full state variable feedback is required.

2.7 Concluding Remarks

Three methods for obtaining full state variable feedback (FSVF) control laws are presented in chapter 3. The first method assigns the specified closed-loop eigenvalues, termed eigenvalue assignment. The second method is based on the solution of the linear quadratic problem (LQP). And the third method which assigns both the closed-loop eigenvalues and eigenvectors termed as Eigenpair assignment method (EPAM) . At this stage however it is sufficient to mention that a feedback control law which assigns both the specified closed-loop eigenvalues and the eigenvectors will, result in the closed-loop system having the desired dynamic performance.

CHAPTER 3

FEEDBACK METHODS

3.0 Introduction

Conventional methods of designing feedback control systems, essentially for single input single output (SISO) systems, are ineffective for the structural load alleviation problem being considered, since it is known from a study of system dynamics that such alleviation can be obtained by the simultaneous use of number of control inputs. In this chapter three modern methods of obtaining multivariable feedback control are presented and discussed.

3.1 EigenvalueAssignment by Generalised Control Canonical Form

The dynamic performance of a linear multivariable control system whose plant is described by equation 2.1 can be assessed by examining the eigenvalues of the coefficient matrix A. The time constants of a real modes are the inverse of the associated real eigenvalues, and the damping and frequency of oscillatory modes can be inferred from the associated complex conjugate eigenvalues. If the performance of the dynamic system is unsatisfactory, then it may be necessary to alter the system eigenvalues by feedback such that the eigenvalues of the closed-loop reflect the desired performance requirements.

Canonical forms for multivariable systems, such as those presented by Luenberger [1967] for example, can be used in eigenvalue assignment techniques, and it is known that, by using state variable feedback, the eigenvalues of such linear multivariable systems can be assigned arbitrarily. Computational algorithms to arrive at the Luneberger canonical form have been presented by Applevich [1974] and, Jordan & Sridhar [1973]. The algorithm proposed by Applevich was used in this research.

The Luenberger canonical form, which exhibits inherent properties of the mathematical structure of a control system which are particularly advantageous in the design of control systems using full state variable feedback. The generalised Control Canonical form (GCCF) may be obtained

directly from the Luenberger canonical form. The GCCF while not the only form (others include the phase-variable or Jordan forms) can be used in eigenvalue assignment schemes. The GCCF form is well suited for higher order systems, because the process of arriving at the required form involves elementary matrix row and column operations. Consider the state variable description of the dynamic system as defined by equation 2.1,

$$\dot{\mathbf{x}} = \mathbf{A}\,\mathbf{x} + \mathbf{B}\,\mathbf{u} \ .$$

The state equation may be transformed into the Generalised Control Canonical form,viz.

$$\dot{\mathbf{z}} = \mathbf{G}\,\mathbf{z} + \mathbf{F}\,\mathbf{c} \ , \qquad 3.1$$

where, $\mathbf{z}$ is the transformed state vector $\in \Re^n$, $\mathbf{c}$ is a command vector $\in \Re^m$, $\mathbf{G}$ is the coefficient matrix of order $[n * n]$, $\mathbf{F}$ is the driving matrix of order $[n * m]$. The matrices $\mathbf{F}$ and $\mathbf{G}$ have the following forms,

$$\mathbf{G} = \text{Block diagonal}\left[\mathbf{G}_{\chi_1}, \mathbf{G}_{\chi_2}, \mathbf{G}_{\chi_3}, \ldots, \mathbf{G}_{\chi_m}\right] \ , \qquad 3.2$$

$$\mathbf{F} = \text{Block diagonal}\left[\mathbf{F}_{\chi_1}, \mathbf{F}_{\chi_2}, \mathbf{F}_{\chi_3}, \ldots, \mathbf{F}_{\chi_m}\right] \ . \qquad 3.3$$

Where the sub-matrices $\mathbf{G}_{\chi_i}$ and $\mathbf{F}_{\chi_i}$, are of the order $[\chi_i * \chi_i]$ and $[\chi_i * 1]$ respectively. The subscripts χ_i are called the control invariants [Wonham & Morse [1972]] and can be computed from the controllability matrix, $\mathbf{Z}$, viz,

$$\mathbf{Z} = [\mathbf{B} \mid \mathbf{AB} \mid \mathbf{A}^2\mathbf{B} \mid \mathbf{A}^3\mathbf{B} \mid \ldots \mid \mathbf{A}^{n-1}\,\mathbf{B}] \ . \qquad 3.4$$

Assuming controllability, let the left-most n linearly independent columns of the matrix $\mathbf{Z}$, be rearranged to form a matrix $\mathbf{Z}_o$, i.e.,

$$Z_o = [b_1, Ab_1, A^2 b_1, \ldots, A^{\chi_1 - 1} b_1, b_2, \ldots, A^{\chi_m - 1} b_m] \ , \qquad 3.5$$

where b_i denotes the column in the matrix **B**. The control invariants, χ_i for i=1,2...,m are an ordered set of integers, equal in number to the dimension of the control vector **u** , (i.e., m) and have properties such that,

$$\chi_1 \geq \chi_2 \geq \chi_3 \geq \ldots \chi_m \geq 0 \ , \qquad 3.6$$

$$\chi_1 + \chi_2 + \chi_3 + \ldots + \chi_m = \text{rank}(\mathbf{AB}) \leq n \ . \qquad 3.7$$

To arrive at the GCCF, equation 3.1 must be transformed in the following manner,

1. Transformation of the state vector

The state vector **x** can be transformed into another vector by the transformation,

$$\mathbf{z} = \mathbf{T}^{-1} \mathbf{x} \ ,$$

or,

$$\mathbf{x} = \mathbf{T}\, \mathbf{z} \ . \qquad 3.8$$

Substitution of equation 3.8 in equation 2.1 yields

$$\mathbf{T}\, \dot{\mathbf{z}} = \mathbf{A}\, \mathbf{T}\, \mathbf{z} + \mathbf{B}\, \mathbf{u} \ , \qquad 3.9$$

multiplication of equation 3.9 by $\mathbf{T}^{-1}$ yields,

$$\dot{\mathbf{z}} = \mathbf{T}^{-1}\mathbf{A}\mathbf{T}\, \mathbf{z} + \mathbf{T}^{-1}\mathbf{B}\, \mathbf{u} \ . \qquad 3.10$$

The transformation matrix **T**, can be calculated using the algorithm presented by Applevich,

based on elementary row and column operations operations.

2. Transformation of the control vector

The control vector **u** can be transformed into another vector by the transformation,

$$\mathbf{d} = \mathbf{P}^{-1}\,\mathbf{u} \ ,$$

or,

$$\mathbf{u} = \mathbf{P}\,\mathbf{d} \ . \qquad 3.11$$

Where **P** is a non-singular matrix of order [m * m], **d** is the transformed control vector $\in \Re^m$. Substitution of equation 3.11 in equation 3.10 yields,

$$\dot{\mathbf{z}} = \mathbf{T}^{-1}\,\mathbf{A}\,\mathbf{T}\,\mathbf{z} + \mathbf{T}^{-1}\mathbf{B}\,\mathbf{P}\,\mathbf{d} \ . \qquad 3.12$$

3. Introduction of transformed state variable feedback

In order to transform equation 3.12 in the GCCF, feedback control law of the type,

$$\mathbf{d} = \mathbf{c} - \mathbf{K}_o\,\mathbf{z} \ , \qquad 3.13$$

is required. The matrix $\mathbf{K}_o$ in equation 3.13 is a feedback matrix of order [m * n] and **c** is some command vector $\in \Re^m$. Substitution of equation 3.13 in 3.12 yields,

$$\dot{\mathbf{z}} = \mathbf{T}^{-1}\mathbf{A}\,\mathbf{T}\,\mathbf{z} + \mathbf{T}^{-1}\mathbf{B}\,\mathbf{P}\,(\mathbf{c} - \mathbf{K}_o\,\mathbf{z}) \ . \qquad 3.14$$

Rearranging equation 3.14,

$$\dot{\mathbf{z}} = (\,\mathbf{T}^{-1}\mathbf{A}\,\mathbf{T} - \mathbf{T}^{-1}\mathbf{B}\,\mathbf{P}\,\mathbf{K}_o)\mathbf{z} + \mathbf{T}^{-1}\mathbf{B}\,\mathbf{P}\,\mathbf{c} \ , \qquad 3.15$$

which can be simplified into,

$$\dot{z} = G\,z + F\,c \qquad 3.16$$

only if the matrices K_o and P can be found. The matrices G and F of order [n * n] and [n * m] respectively can be formed directly from the knowledge of the control invariants, with each sub-matrix defined in equations 3.2 and 3.3 having the following generalised control canonical form,

$$G_{\chi_i} = \begin{bmatrix} 0 & 1 & 0 & 0 & . & . & . & 0 \\ 0 & 0 & 1 & 0 & . & . & . & 0 \\ . & . & . & . & . & . & . & . \\ . & . & . & . & . & . & . & . \\ 0 & 0 & 0 & 0 & . & . & . & 1 \\ 0 & 0 & 0 & 0 & . & . & . & 0 \end{bmatrix}, \qquad 3.17$$

each block G_{χ_i} is of the order of [χ_i * χ_i], and ,

$$F_{\chi_i} = \begin{bmatrix} 0 \\ 0 \\ . \\ . \\ . \\ 1 \end{bmatrix}, \qquad 3.18$$

each block F_{χ_i} is of the order of [χ_i * 1], it is noted from equation 3.18 that,

$$F_{\chi_i}^{T} * F_{\chi_i} = I \ .$$

To determine the matrices K_o and P , equations 3.15 and 3.16 are compared resulting in,

$$G = T^{-1}A\,T - T^{-1}\,B\,P\,K_o \ , \qquad 3.19$$

$$F = T^{-1}\,B\,P \ . \qquad 3.20$$

Substitution of equation 3.20 in 3.19 and after rearangement yields,

$$F K_o = T^{-1} A T - G \ . \qquad 3.21$$

Equation 3.21 is a simultaneous matrix linear equation from which the feedback matrix K_o can be found as follows,

$$K_o = F^{\dagger} (T^{-1} A T - G) \qquad 3.22$$

where $F^{\dagger}$ is the generalised inverse of F and is of the order of [m * n]. Matrix P can be determined from equation 3.20. Equation 3.16 represents the open-loop transformed system. The eigenvalues of matrix G are, located at the origin, and if the eigenvalues are required to be relocated then feedback is required. In order to assign the eigenvalues, to the desired locations, consider a feedback law of the type,

$$c = \Omega \ z + w \ , \qquad 3.23$$

where Ω is a feedback matrix of order [m * n], and w is a command vector $\in \Re^m$ which drives the closed-loop system. Substitution of equation 3.23 in 3.16 yields,

$$\dot{z} = (G + F \Omega) z + F w \ , \qquad 3.24$$

alternatively,

$$\dot{z} = A_D z + F w \ . \qquad 3.25$$

Where A_D is the desired closed-loop matrix, selected to have the form,

$$A_D = \text{Block diagonal} \left[A_{D_1}, A_{D_2}, \ldots, A_{D_m} \right] . \qquad 3.26$$

Each block A_{D_i} is in companion form and has the order [χ_i * χ_i]. Comparing equation 3.24 and 3.25,

$$G + F \Omega = A_D \ . \qquad 3.27$$

Since $F^T F = I_m$ equation 3.27 can be written as,

$$\Omega = F^T [A_D - G] \ . \qquad 3.28$$

Transforming into original state space by means of equations 3.11, 3.13 and 3.23 and assuming that the system is driven by initial conditions on the states, the control **u** (for **w** = 0) is given by,

$$\mathbf{u} = \mathbf{P}\,\mathbf{d} = \mathbf{P} (\Omega - K_o)\,\mathbf{z} \ . \qquad 3.29$$

The non-singular matrix P, is determined as a solution of simultaneous matrix linear equation 3.20 , viz.,

$$(T^{-1}B)\,P = F \ . \qquad 3.30$$

Since, **x** = T **z**, equation 3.29 becomes,

$$\mathbf{u} = P\,(\Omega - K_o)T^{-1}\mathbf{x} \ , \qquad 3.31$$

which can be written in the form,

$$\mathbf{u} = K\,\mathbf{x} \ . \qquad 3.32$$

Where $K=P\,(\Omega - K_o)T^{-1}$ is a feedback matrix of order [m * n]. The closed-loop system described by equations 2.1 and 3.32 will possess the prescribed eigenvalues. Some noteworthy

features of eigenvalue assignment method are summarised below;

a) Although the specified eigenvalues may be complex, the determination of the feedback matrix K requires only real arithmetic (this is illustrated in later sections).

b) An important property,viz, controllability, of the pair (AB) can be assessed from examining the control invariants. For example, if the sum of invariants in equation 3.7 is equal to n, then full state controllability is indicated; whereas if the sum of invariants is r, then $n-r$ state variables are uncontrollable.

c) If some of the states are uncontrollable, then the matrix $T^{-1}AT$ equation 3.10 has the form,

$$T^{-1} A T = \hat{A} = \begin{bmatrix} A_{11} & A_{12} \\ A_{21} & A_{22} \end{bmatrix}, \qquad 3.33$$

where the matrix A_{11} contains the controllable part and matrix A_{22} of order $[n-r * n-r]$, contains the uncontrollable part. Matrix A_{22} is carried through the analyses; therefore the eigenvalues of the matrix A_{22}, which are also the uncontrollable eigenvalues of matrix A, are unchanged by feedback. (N.B. Matrix $T^{-1}AT = \hat{A}$ is similar to matrix A, since similar matrices have the same eigenvalues, therefore eigenvalues of $\hat{A}$ will be exactly those of A, Noble & Daniel [1977]).

3.2 Linear Quadratic Problem (LQP)

It is well known that LQP method, has been successfully applied to various problems, including some problems of aircraft stability and control. Numerous publications listed as a bibliography can be found in the paper by , Mendel & Gieseking [1971]. These references serve to illustrate the applicability of the LQP method, there have been many more publications, for example see Prasad [1980], AlKhatib [1985].

In flight control work, the optimal control $\mathbf{u}^o$, is obtained by minimising a quadratic performance index of the type,

$$J = \frac{1}{2}\int_0^\infty (x^T Q x + u^T G_o u) dt \ , \qquad 3.34$$

subject to constraint,

$$\dot{x} = A x + B u \ . \qquad 3.35$$

Where x is the state vector $\in \Re^n$, u is the control vector $\in \Re^m$, A is the coefficient matrix of order $[n * n]$, B is the driving matrix of order $[n * m]$, Q is the state weighting matrix of order $[n * n]$ and G_o is the control weighting matrix of order $[m * m]$. It can be shown that the optimal control u^o, which minimises equation 3.34 subject to a number of conditions which will be discussed later, is given by,

$$u^o = - G_o^{-1} B^T S x \ , \qquad 3.36$$

where S is an $[n * n]$ symmetric matrix and is the solution of the algebraic Riccati equation,

$$SA + A^T S - SB\ G_o^{-1} B^T S + Q = 0 \ . \qquad 3.37$$

Equation 3.36 may be expressed alternatively as,

$$u^o = K x \qquad 3.38$$

where, $K = - G_o^{-1} B^T S$.

The detailed solution can be found in Athans & Falb [1966]. It can be seen from equation 3.38 that for a feedback matrix to exist, the inverse of the weighting matrix G_o must exist. The matrix G_o is chosen to be positive definite to ensure invertibility. The conditions on the matrix Q can be evaluated by considering the Hamiltonian associated with the performance index J (equation 3.34). The Hamiltonian is defined as,

$$\mathcal{H} = 1/2\ (\ x^T Q\ x + u^T G_o\ u) + \underline{\Psi}^T (A\ x + B\ u) \qquad 3.39$$

where, $\underline{\Psi}$ is the co-state vector $\in \Re^n$. For equation 3.36 to be true (i.e., for the system to be at least locally optimal), the associated Jacobian matrix of the second variation of J, must be positive definite,viz.,

$$\begin{bmatrix} \dfrac{\partial^2 \mathcal{H}}{\partial x^2} & \dfrac{\partial^2 \mathcal{H}}{\partial x\, \partial u} \\ \dfrac{\partial^2 \mathcal{H}}{\partial u\, \partial x} & \dfrac{\partial^2 \mathcal{H}}{\partial u^2} \end{bmatrix} > 0\ . \qquad 3.40$$

The partial derivatives in equation 3.40 are evaluated by partially differentiating equation 3.39,

$$\frac{\partial \mathcal{H}}{\partial u} = G_o\ u + B^T \underline{\Psi}\ , \qquad 3.41$$

$$\frac{\partial \mathcal{H}}{\partial x} = Q\ x + A^T \underline{\Psi}\ , \qquad 3.42$$

$$\frac{\partial^2 \mathcal{H}}{\partial x^2} = Q\ , \qquad 3.43$$

$$\frac{\partial^2 \mathcal{H}}{\partial u^2} = G_o\ , \qquad 3.44$$

and,

$$\frac{\partial^2 \mathcal{H}}{\partial u \, \partial x} = \frac{\partial^2 \mathcal{H}}{\partial x \, \partial u} = 0 \ . \qquad 3.44a$$

Substitution of equations 3.43, 3.44 and 3.44a in equation 3.40 yields,

$$\begin{bmatrix} Q & 0 \\ 0 & G_o \end{bmatrix} > 0 \ . \qquad 3.45$$

Since G_o is selected to be positive definite[¶], it is seen from equation 3.45, that for the Jacobian matrix to be positive definite, **Q** must be at least positive semi-definite[§].

A variety of methods are available for obtaining numerical solutions of the Riccati equation. In this thesis the solution of Riccati equation was obtained by means of a method based on matrix diagonalisation, proposed by Marshal & Nicholson [1970]. The method is purely algebraic and depends only upon having a good procedure for determining the eigenvalues and eigenvectors of the canonical[‡] matrix. An efficient procedure for inverting a complex matrix is also needed. One disadvantage of the method is that, if the canonical matrix has repeated eigenvalues, then the modal matrix (whose columns are the eigenvectors of the canonical matrix), which is used in the diagonalisation becomes singular, hence its inverse is not defined.

¶ A matrix G_o is said to be positive definite, if for a vector **u** the inner product, $(u, G_o u) > 0$

§ A matrix **Q** is said to be positive semi-definite, if for a vector **x** the inner product, $(x, Qx) \geq 0$

‡ The canonical matrix is defined as,

$$\left[\begin{array}{c|c} A & -B\,G_o^{-1}\,B^T \\ \hline -Q & -A^T \end{array}\right]$$

3.3 Design of Lateral Feedback Controllers for the L-1011

The intention of this section is to demonstrate the effectiveness of the methods discussed in sections 3.1 and 3.2. The GCCF and the LQP methods are used here to obtain two independent feedback controllers. Each lateral feedback controller is to serve the purpose of decoupling the yawing and the rolling motions, and of attaining stability augmentation. The uncontrolled rigid body motion of the L-1011 aircraft, for an initial sideslip angle of 0.02 radians (see figure 2.2), indicated that although the aircraft is stable its damping would need to be augmented. For the aircraft to have desired performance, the eigenvalues associated with its modes must be modified. To meet the design objective, following eigenvalues were specified for the closed-loop.

Eigenvalue	Mode
$-2.0 \pm j\ 1.5$	Roll/Spiral mode
$-1.5 \pm j\ 1.5$	Dutch roll
-20	Rudder mode
-25	Aileron mode
-0.5	Washout filter mode

Table 3.1 : Specified Closed-loop Eigenvalues

Andry et al [1983], specified the same eigenvalue set as given in table 3.1, in the design of a lateral feedback controller for the same model of the L-1011 Tristar aircraft, using their eigenvalue/eigenvector assignment method. To make valid comparisons between the results obtained from the methods described in section 3.1, section 3.2, Andry's eigenvalue/eigenvector assignment and the proposed eigenpair[§] assignment method, eigenvalue set as given in table 3.1 was specified for the closed-loop.

---

§ A method of assigning the closed-loop eigenvalues and the closed-loop eigenvectors is presented in section 3.4. The method is referred in this thesis as eigenpair assignment method(EPAM).

It can be seen from table 3.1, that Andry et al have specified a complex eigenvalue, corresponding to the roll subsidence mode and the spiral mode, roll/spiral modes being tightly coupled, albeit heavily damped. This choice is contrary to the usual flying qualities requirement as typified by discussion of *section 3.3.1.4 , Chalk & Neil et al [1969].* It is plainly stated that coupled roll/spiral mode is not permitted. Nevertheless the designs to be discussed later, adopted Andry's specifications in order that proper comparisons between the methods could be made. However, it was always the intention that any method used must be firmly related to the physical requirements of the aircraft, so that the choice of eigenvalues/eigenvectors could then be related to the flying qualities.

3.3.1 GCCF Method

The method described in section 3.1 is used here to assign the required closed-loop eigenvalues . All the pertinent matrices in the evaluation of the feedback law are presented below. Transformation matrix **T** defined in equation 3.8, is found to be,

$$\mathbf{T} = \begin{bmatrix} 0.0 & 0.0 & -0.44\cdot10^{-4} & 0.46\cdot10^{-2} & -0.13\cdot10^{-3} & 0.1749 & 0.3488 \\ 0.0 & 0.0 & 0.68\cdot10^{-2} & -0.61\cdot10^{-3} & 0.18\cdot10^{-4} & -0.0231 & -0.1744 \\ 0.0 & 0.0 & -0.89\cdot10^{-3} & -0.0641 & 0.67\cdot10^{-2} & 0.313\cdot10^{-2} & 0.8720 \\ 0.05 & -0.0055 & 0.12\cdot10^{-3} & 0.0521 & -0.74\cdot10^{-2} & -0.1343 & -0.0436 \\ 0.0 & 0.0 & -0.035 & 0.43\cdot10^{-3} & -0.12\cdot10^{-4} & 0.0160 & 0.0 \\ 0.0 & 0.0 & 0.62\cdot10^{-3} & -0.016 & -0.035 & -0.21\cdot10^{-2} & 0.0 \\ 0.0 & 0.04 & -0.82\cdot10^{-4} & -0.42\cdot10^{-2} & 0.0359 & 0.159 & 0.0 \end{bmatrix} \qquad 3.46$$

The control invariants were found to be, $\chi_1 = 4$, and $\chi_2 = 3$; the sum of invariants is 7; therefore the system has full state variable controllability. The Transformation matrix **P** (defined in equation 3.11) is found to be,

$$\mathbf{P} = \begin{bmatrix} 1.0 & 0.137 \\ 0.0 & 1.0 \end{bmatrix} \qquad 3.47$$

The feedback matrix which results in the system being in the GCCF , was found to be,

$$K_o = \begin{bmatrix} -20.933 & -46.785 & -20.028 & -20.879 & -8.332 & 1.130 & 0.732 \\ 29.660 & 65.110 & 11.766 & 0.388 & 11.614 & -23.344 & -25.952 \end{bmatrix} \quad 3.48$$

The matrices G and F defined in equations 3.2 and 3.3, with one block as determined by $\chi_1 = 4$ and the other by $\chi_2 = 3$, are,

$$G = \left[\begin{array}{cccc:ccc} 0 & 1 & 0 & 0 & 0 & 0 & 0 \\ 0 & 0 & 1 & 0 & 0 & 0 & 0 \\ 0 & 0 & 0 & 1 & 0 & 0 & 0 \\ 0 & 0 & 0 & 0 & 0 & 0 & 0 \\ \hdashline 0 & 0 & 0 & 0 & 0 & 1 & 0 \\ 0 & 0 & 0 & 0 & 0 & 0 & 1 \\ 0 & 0 & 0 & 0 & 0 & 0 & 0 \end{array}\right] \quad 3.49$$

$$F = \left[\begin{array}{c:c} 0 & 0 \\ 0 & 0 \\ 0 & 0 \\ 1 & 0 \\ \hdashline 0 & 0 \\ 0 & 0 \\ 0 & 1 \end{array}\right] \quad 3.50$$

Since the control invariants are $\chi_1 = 4$ and $\chi_2 = 3$ respectively, a polynomial of order 4 and another of order 3 are constructed from the specified set of eigenvalues, table 3.1. It was found convenient to group the two complex eigenvalues to form a polynomial of order 4 and also the remaining eigenvalues to form a polynomial of order 3. The polynomial of order 4 is given by,

$$(\lambda + 2.0 + j\,1.5)\,(\lambda + 2.0 - j\,1.5)\,(\lambda + 1.5 + j\,1.5)\,(\lambda + 1.5 - j\,1.5) = 0,$$

which after expansion, is :

$$\lambda^4 = -7.0\,\lambda^3 - 22.75\,\lambda^2 - 36.75\,\lambda - 28.125 \ . \quad 3.51$$

The polynomial of order 3 is given by,

$$(\lambda + 20)\,(\lambda + 25)\,(\lambda + 0.5) = 0 \ ,$$

which after expansion, is:

$$\lambda^3 = -45.5\,\lambda^2 - 522.5\,\lambda - 250.0 \ . \qquad 3.52$$

The required closed-loop matrix defined in equation 3.26 is selected to have one companion block of order 4 and the other of order 3; it is constructed from the polynomial coefficients as,

$$A_D = \left[\begin{array}{cccc:ccc} 0 & 1 & 0 & 0 & 0 & 0 & 0 \\ 0 & 0 & 1 & 0 & 0 & 0 & 0 \\ 0 & 0 & 0 & 1 & 0 & 0 & 0 \\ -28.125 & -36.75 & -22.75 & -7.0 & 0 & 0 & 0 \\ \hdashline 0 & 0 & 0 & 0 & 0 & 1 & 0 \\ 0 & 0 & 0 & 0 & 0 & 0 & 1 \\ 0 & 0 & 0 & 0 & -250.0 & -522.5 & -45.5 \end{array}\right] \qquad 3.53$$

Finally, the control law in the original state space using equation 3.32 is,

$$\mathbf{u} = \mathbf{Kx} = \begin{bmatrix} 0.6914 & -0.2130 & 0.9461 & 2.0673 & 2.2095 & -4.7072 & -5.1013 \\ -0.0184 & -0.7799 & 8.4899 & 8.6075 & 16.825 & -9.9131 & 0.0 \end{bmatrix} \mathbf{x} \qquad 3.54$$

The results of using the control law (equation 3.54) are presented in section 3.3.3 and 3.3.4.

3.3.2 LQP Method

A feedback control law, such as equation 3.38 is obtained using the LQP method outlined in section 3.2. A few methods have been proposed for the selection of the weighting matrices, but a disadvantage of these methods is that they do not relate to the time domain characteristics of the system, nor the physical requirements. Hence empirical methods of selection are invariably resorted to. The requirement for $\mathbf{Q}$ to be positive semi-definite, is met by choosing a diagonal matrix such that the elements $Q_{ii} \geq 0$. The requirement for G_o to be positive definite is met by

selecting a diagonal matrix such that the elements $G_{o_{ii}} > 0$. However, this technique cannot guarantee the specified closed-loop eigenvalues are achieved; hence the elements of the weighting matrices have to be arbitrarily adjusted until the specified closed-loop eigenvalues are achieved. Since there is no direct correlation between the choice of the weighting matrices, and the achievable eigenvalues, and thence the time response, the process can be cumbersome and time consuming. The following arbitrary choice of weighting matrices was considered to illustrate the method,

$$Q = \text{diagonal } [1.0,\ 1.0,\ 10.0,\ 10.0,\ 1.0,1.0,\ 1.0] \ , \qquad 3.55$$

$$G_o = \text{diagonal } [5.0,\ 5.0] \cdot \qquad 3.56$$

The control law was determined to be,

$$\mathbf{u = Kx} = \begin{bmatrix} -0.091 & -0.0176 & 0.2993 & 2.0383 & 0.3416 & -1.3427 & 0.0026 \\ -0.0220 & -0.0509 & 0.5642 & 0.8976 & 0.5855 & -1.4804 & -0.0003 \end{bmatrix} x \qquad 3.57$$

3.3.3 Comparison of Feedback Gains

The rudder command δ_{r_c} and aileron command δ_{a_c} for the controlled aircraft, can be expressed by the following equations,viz;

$$\delta_{r_c} = K1_{\delta_r}*\delta_r + K1_{\delta_a}*\delta_a + K1_{\varphi}*\varphi + K1_r*r + K1_p*p + K1_{\beta}*\beta + K1_{x_7}*x_7 \ , \qquad 3.58b$$

$$\delta_{a_c} = K2_{\delta_r}*\delta_r + K2_{\delta_a}*\delta_a + K2_{\varphi}*\varphi + K2_r*r + K2_p*p + K2_{\beta}*\beta + K2_{x_7}*x_7 \ , \qquad 3.58c$$

where the feedback gains ($K1_{\delta_r}$, $K2_{\delta_r}$ etc.,) in the GCCF and LQP control laws are presented in table 3.2.

δ_{r_c}			δ_{a_c}		
Gain	GCCF	LQP	Gain	GCCF	LQP
$K1_{\delta_r}$	0.6914	-0.0919	$K2_{\delta_r}$	-0.0184	-0.0220
$K1_{\delta_a}$	-0.2130	-0.0176	$K2_{\delta_a}$	-0.7799	-0.0509
$K1_{\varphi}$	0.9461	0.2993	$K2_{\varphi}$	8.4899	0.5542
$K1_{r}$	2.0673	2.0383	$K2_{r}$	8.6075	0.8976
$K1_{p}$	2.2095	0.3416	$K2_{p}$	16.8250	0.5855
$K1_{\beta}$	-4.7072	-1.3447	$K2_{\beta}$	-9.9130	-1.4804
$K1_{x_7}$	-5.1013	0.0026	$K2_{x_7}$	0.0000	-0.0003

Table 3.2: Comparison of feedback gains

It is known that the effect of feeding back yaw rate to rudder is to increase the dutch roll damping. From table 3.2 it can be noticed that the feedback gains $K1_r$ for both methods being nearly the same.

The effect of feeding back yaw rate to ailerons is to stabilise the spiral mode. Examination of the gain $K2_r$ in the LQP control law suggests that the stability in the spiral mode would be augmented[§]. Since the specified damping of the roll/spiral mode is much greater, because of the nature of its complex eigenvalue used for the GCCF method, the yaw rate to aileron feedback gain, $K2_r$, in the GCCF control law is much higher (see table 3.2).

Sideslip to aileron feedback has the effect of increasing the damping of the dutch roll mode (N.B. gain $K2_\beta$ is negative in both cases). In order to achieve a high degree of damping in the dutch roll mode, high values of $K2_\beta$ are desirable, McRuer et al [1973].

---

§ Yaw rate to aileron feedback system corresponds to the alteration of the stability L_r. This is an effective method of stabilising the spiral mode by making the augmented value of L_r sufficiently negative. This is achieved by making $K2_r$ positive (this can be confirmed from values given in table 3.2], McRuer et al (1973).

Since the gains $K1_r$ (feedback of yaw rate to rudder) in both control laws are nearly equal, and the gain $K2_\beta$ in the GCCF control law being nearly seven times that in the LQP control law, it is inferred that damping augmented in the dutch roll mode by GCCF control law will be considerably higher compared to the LQP control law (N.B. this can also be inferred form an examination of the closed-loop eigenvalues presented in table 3.3, section 3.3.4). The effect of feeding back both the roll rate and bank angle to ailerons, is to obtain the closure of the roll attitude loop. Both feedback gains $K2_p$ and $K2_\varphi$ are large in the GCCF control law, compared to those in the LQP control law. Such high gains suggest a much tighter control of both the motion variables p and φ i.e., roll rate and bank angle.

3.3.4 Comparison of the Closed-loop Eigenvalues and the Time Response

In table 3.3 are shown the eigenvalues of the controlled aircraft, the block diagram representation of which is shown as figure 3.1. The closed-loop eigenvalues were computed separately for the GCCF and LQP control laws, from the characteristic equation,viz;

$$\det [\lambda I - (A + BK) = 0 . \qquad 3.58a$$

EIGENVALUES			
Mode	Open-loop	Closed-loop	Closed-loop
		GCCF	LQP
Rudder	-20.0	-20.0	-20.48
Aileron	-25.0	-25.0	-25.61
Dutch roll	-0.12±j1.27	-1.5±j1.5	-0.61±j1.44
Spiral	-0.009		-0.89
Roll Subs.	-1.087		-1.236
Roll/Sprial		-2.0±j1.5	
Washout	-0.5	-0.5	-0.5

Table 3.3 : Comparison of the closed-loop eigenvalues

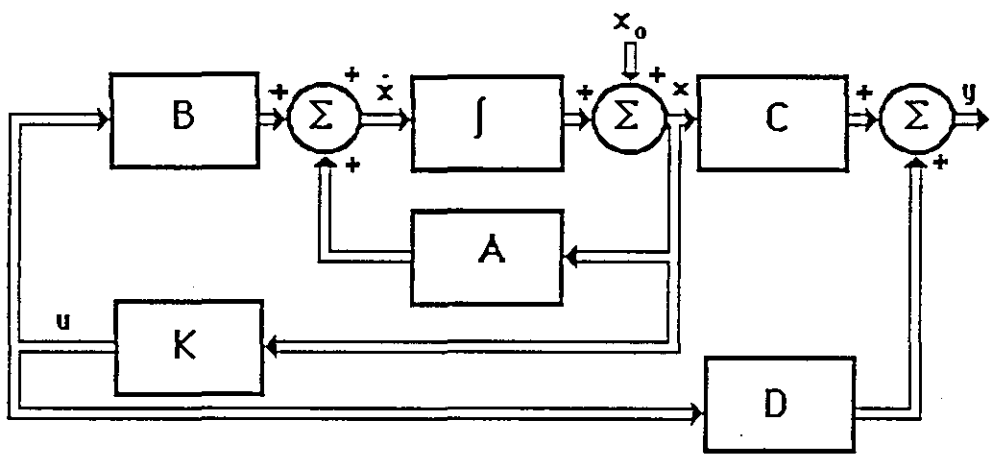

Figure 3.1 Closed-loop System

From table 3.3 it can be seen that, the prescribed closed-loop eigenvalues (shown in table 3.1) have been achieved using the GCCF control law. However, control law based on the solution of the LQP method, computed for an arbitrary choice of weighting matrices, failed to achieve the desired closed-loop eigenvalues. The LQP control law has augmented the stability in both the spiral and the roll subsidence mode. Also, the damping ratio of the dutch roll mode has been increased from 0.09 to 0.39. Eigenvalues corresponding to the rudder and aileron modes are very much the same compared to the open-loop values. A complex eigenvalue for the roll/spiral mode was specified by Andry et al, contrary to the requirements as discussed in section 3.3. It is interesting to note from table 3.3, that the eigenvalues corresponding to the roll subsidence and of the spiral mode, obtained from the use of LQP control law, are both real.

It is seen from table 3.3 that the control law based on GCCF method assigns every specified eigenvalue. The damping of the dutch roll mode has been increased from 0.09 to 0.7. The damping of the rolling motion, i.e., the combination of roll/spiral mode, is augmented by specifying a complex eigenvalue. The damping ratio chosen for the roll/spiral mode was 0.8. Since the GCCF control law assigned every eigenvalue, its closed-loop response will have the desired time domain characteristics.

The response of the controlled aircraft for an initial sideslip angle of 0.02 radians is presented in figures 3.2 and 3.3. By maintaining the same test conditions for each method the effectiveness of the feedback control laws can be demonstrated. An examination of figures 3.2 and 3.3 reveals, that the GCCF control law (equation 3.54) produces a faster response compared with the LQP control law (equation 3.57). Although, the GCCF control law produces a damped system response, peak values of the output variables the washed out yaw rate and lateral acceleration were higher than the corresponding response obtained using LQP control law, see figures 3.1, 3.2. For the GCCF control law, the rolling response was improved while some degradation of the yawing response occurred compared to the uncontrolled response (see figure 2.2). One of the reason for such a loss of response may be the fact that the rolling motion and the yawing motion were coupled, i.e., variables associated with the rolling motion were

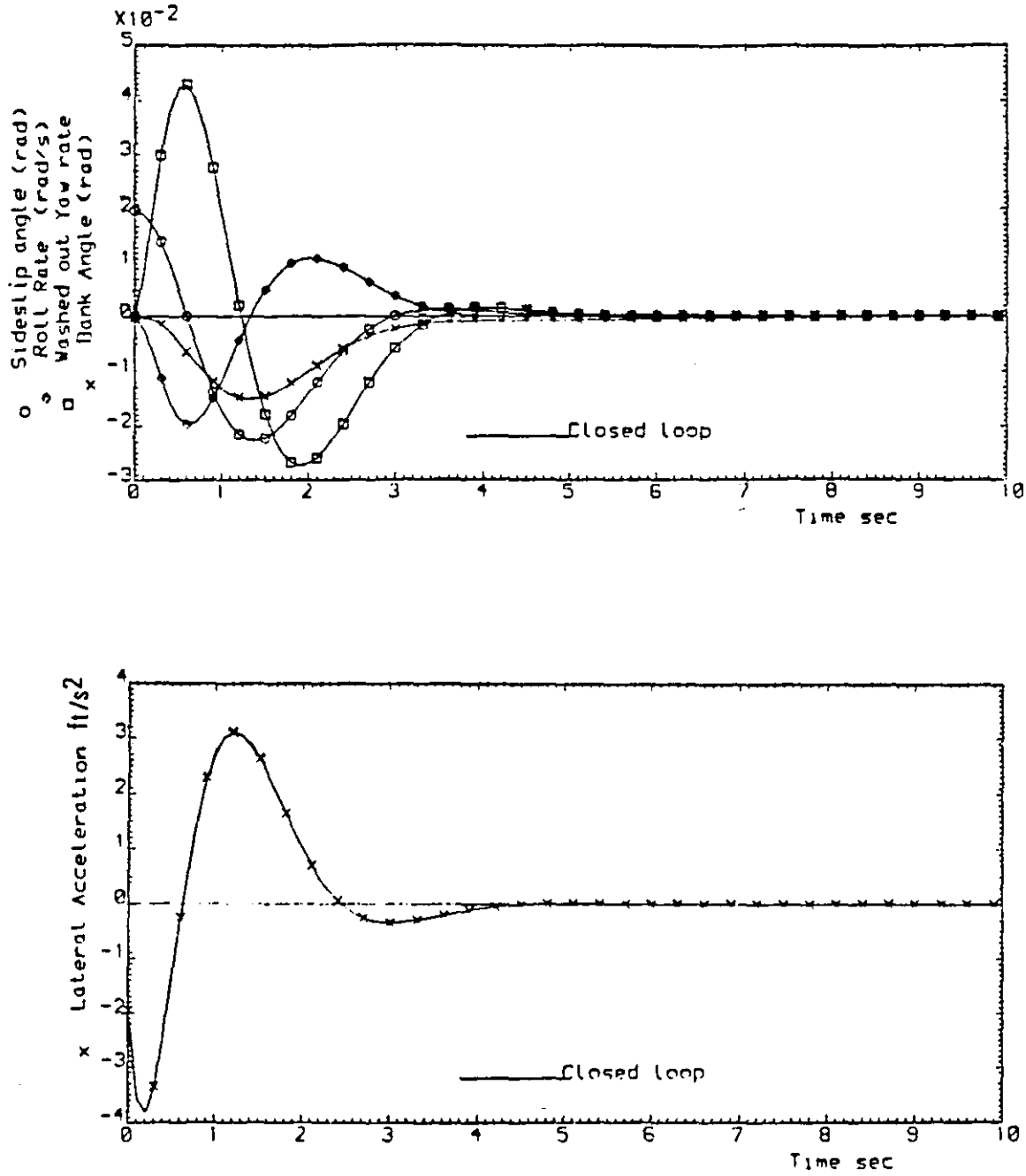

Figure 3.2 :L-1011 controlled response for β_{ic} = 0.02 radians using GCCF control law (equation 3.54)

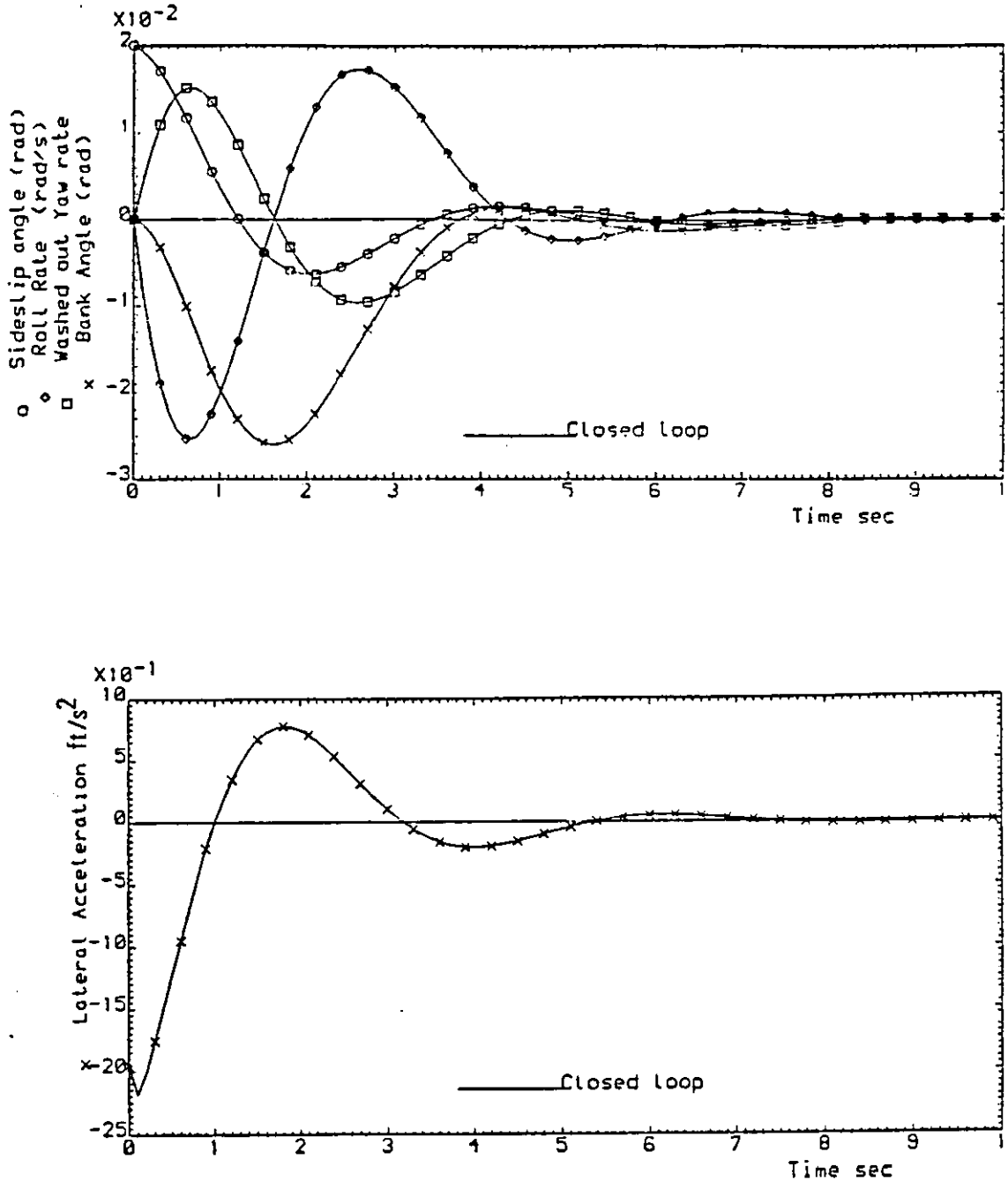

Figure 3.3 : L-1011 controlled response for β_{ic}=0.02 radians using LQP control law (equation 3.57)

influencing the yawing motion variables. The lateral acceleration, largely depends on sideslip velocity and yaw rate, therefore any deterioration in either has a marked effect upon lateral acceleration.

Presented in figures 3.4 and 3.5, are the reductions in percent in the root mean square (RMS) values and the absolute peak values of the output variables. The LQP control law produces a better yawing response, achieving a peak reduction of 42%, of washed out yaw rate and a reduction of 56% in the peak value of sideslip angle, see figure 3.4 and 3.5. Approximately 38% reduction was achieved in the RMS value of lateral acceleration with only a slightly increased peak value, see figure 3.5. The rolling response (roll angle and roll rate) was 65% on average, better than in the open-loop.

Based on a eigenvalue comparison alone, the time domain characteristics, such as the damping and the speed of the response of the system can be inferred. The GCCF control law which assigned every eigenvalue, produced the desired dynamic response. On the other hand, a different set of weighting matrices in the LQP method could have produced a different set of eigenvalues, and hence altered response. It is also feasible that the same feedback law of equation 3.57 could have resulted, for some other choices of weighting matrices. It is shown later that if reductions in the peak and RMS values of the motion variables are required, then the performance of a multivariable control system cannot be judged solely on the examination of eigenvalues, corresponding eigenvectors have to be examined as well.

3.3.5 The Eigenvectors of a Closed-loop System

Although the same set of eigenvalues can be achieved by different control laws, the corresponding eigenvectors will be different. An eigenvector governs not only the amplitude of the response, but also determines the influence of the corresponding eigenvalue on the state variable response. The time response of a closed-loop system,

$$\dot{x} = (A + B\ K)\ x\ , \qquad 3.59$$

to a known initial state vector x(0), is determined to be (see section 2.5, in which the open-loop time response of the state variables to initial conditions on the state variables and control inputs was developed)

$$x(t) = V_c\ e^{\Lambda t}\ V_c^{-1}\ x(0)\ , \qquad 3.60$$

where V_c is the closed-loop modal matrix, whose columns are the eigenvectors of the matrix (A+BK) and is of the order [n * n], Λ is a diagonal matrix whose principal elements are the eigenvalues of the matrix (A+BK). The eigenvalues, λ_i ,and eigenvectors, $\underline{v}_i$, of the closed-loop system satisfy the relation,

$$(A+BK)\ \underline{v}_i = \lambda_i\ \underline{v}_i\ . \qquad 3.61$$

The participation of an eigenvalue associated with a mode, in the state variable response is governed by the elements of the corresponding eigenvector in the modal matrix V_c. It was shown in previous section that, response of yaw rate, sideslip angle and lateral acceleration had deteriorated as a result of using feedback matrix (equation 3.54). In order to identify the cause of degradation, the closed-loop eigenvectors obtained when using the GCCF control law are presented in table 3.4.

An examination of the dutch roll mode and roll/spiral mode eigenvectors, in table 3.4, reveals that the two modes are coupled. The roll/spiral mode is seen to be participating predominantly in yaw rate and rudder deflection. This is inferred from inspecting the magnitude of roll/spiral mode eigenvector components, associated with yaw rate and rudder deflection which are seen to be large . It is also seen from the table 3.4, that the dutch roll mode not only participates in the yawing motion variables, but also in the rolling motion of the aircraft, a small contribution to the rolling response would be expected due to the nature of the dutch roll motion, but it is seen

that magnitude of dutch roll eigenvector components, corresponding to roll rate, bank angle and aileron deflection are fairly large. Since both the dutch roll mode and roll/spiral mode are participating in the yawing response, this observation translates into the degradation of the yawing and lateral acceleration response, figures 3.4 and 3.5. Reductions in the peak and RMS values,particularly of the yaw rate, lateral acceleration and sideslip angle can be obtained if the rolling and yawing motions are decoupled. This can be achieved not only, if the roll/spiral mode eigenvector components, corresponding to the yaw rate,sideslip and rudder deflection are small, but also if the dutch roll mode eigenvector components, corresponding to aileron deflection, roll rate and bank are small. In specific terms, if each mode is only allowed to participate in its constituent motion variables, decoupling of the aircraft motions will then be possible.

	Dutch Roll	Roll / Spiral	Rudder	Aileron	W.O
Eigenvalue	-1.5 + j 1.5	-2.0 + j 1.5	-20.0	-25.0	-0.5
State	E I G E N V E C T O R S*				
δ_r	0.810 + j 0.000	0.895 + j 0.000	0.1118	0.1112	0
δ_a	0.002 - j 0.459	-0.044 - j 0.310	0.9921	0.9928	0
φ	0.018 + j 0.062	0.022 + j 0.044	-0.0028	-0.0018	0
r	0.264 + j 0.129	0.236 + j 0.109	0.0056	0.0046	0
p	-0.122 - j 0.066	-0.110 - j 0.054	0.0564	0.0447	0
β	0.033 + j 0.134	0.042 + j 0.093	0.0002	0.0001	0
x_7	-0.011 - j 0.081	-0.021 - j 0.058	-0.0001	0.0000	1

Table 3.4: Eigenvectors of the closed-loop system, GCCF control Law

It has been shown in previous sections that, although a satisfactory control law could be obtained using either the eigenvalue assignment or the LQP method, they cannot completely satisfy simultaneously every design objective. A method in which not only the eigenvalues but also the eigenvectors were assigned, would be advantageous in the light of the above results.

---

* In the case when an eigenvalue is complex, eigenvector corresponding to only the positive imaginary part is shown in the table.

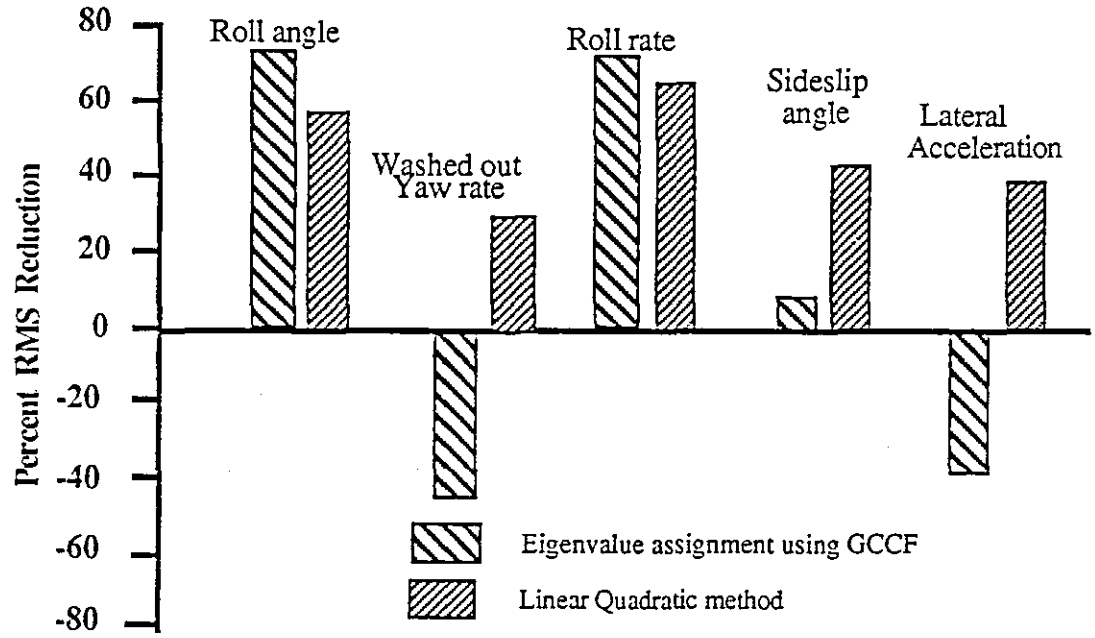

Figure 3.4 : Comparison of responses for different control laws

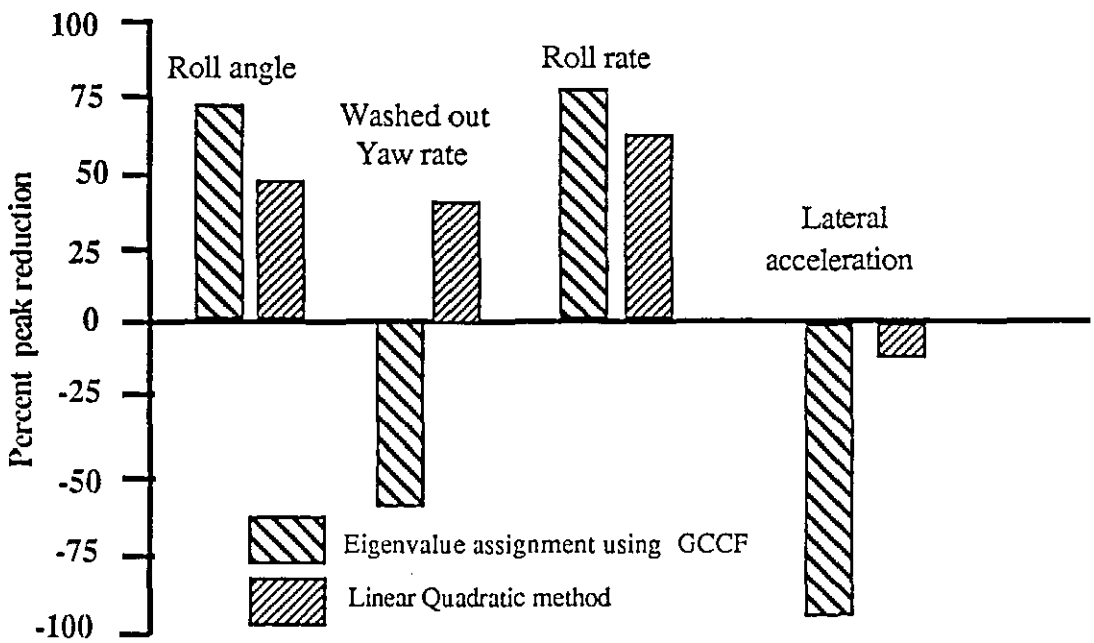

Figure 3.5 : Comparison of responses for different control laws

3.4 Eigenpair Assignment Method (EPAM)

In recent years the design of feedback control systems by eigenvalue/eigenvector assignment has received considerable attention. Moore [1976], Klein & Moore [1977], Porter & D'Azzo [1978], Srinathkumar [1978], Broussard et al [1980], Daywansa & Mukundan [1982], Fahmy & O'Reilly [1982], Andry et al [1983], Shapiro & Chung [1984], Soroka & Shaked [1983], Fahmy & Tantawy [1984] and Mielke & Tung [1985] have presented papers on the subject. The objective of such methods is to assign the closed-loop eigenvalues to desired locations in the complex frequency plane, subject to achieving appropriate corresponding eigenvectors. It has been shown by means of a numerical example in section 3.3.5 how an eigenvector governs the contribution of its corresponding eigenvalues to the state variable response.

It is not feasible to discuss in detail here every published method but a number of features of some of the methods are outlined. Moore [1976] derived the necessary and sufficient conditions for the existence of a real feedback matrix such that the resulting closed-loop system would exhibit the specified eigenvalues and eigenvectors. A necessary condition required the computation of closed-loop eigenvectors such that they spanned the null-space of the matrix $[(\lambda_i \mathbf{I} - \mathbf{A}) \quad \mathbf{B}]$¶ . The method is restricted by the requirement that all the specified closed-loop eigenvalues must be distinct. The closed-loop eigenvectors are calculated as a solution of simultaneous linear equations.

¶ λ_i is the required closed-loop eigenvalue and the matrices A and B are as defined earlier in the equation 2.10, I is an identity matrix of order [n x n]

Porter & D'Azzo[1978][1,2] presented a method of calculating a feedback matrix which assigned not only the closed-loop Jordan canonical form, but also the eigenvectors and the generalised eigenvectors. Such vectors are generated from a sequence of equations, the method being dependent upon selecting appropriate eigenvectors from a computed set of linearly independent eigenvectors and the generalised eigenvectors. Moore's method, however, required the specification of distinct closed-loop eigenvalues; Porter's method is capable of assigning repeated eigenvalues.

The work of Andry et al is a straightforward extension of Moore's work; the closed-loop eigenvectors are required to belong to the sub-space of the matrix $[(\lambda \mathbf{I} - \mathbf{A})^{-1}\mathbf{B}]$. An achievable closed-loop eigenvector is obtained by projecting the desired closed-loop eigenvector on this sub-space. The restriction of the method lies in the fact that the specified closed-loop eigenvalues must be distinct. Clearly if an eigenvalue belonging to the open-loop is specified in the closed-loop, the inverse of the matrix $(\lambda \mathbf{I} - \mathbf{A})$ is not defined.

The method presented in section 3.4.1 uses complex singular valve decomposition to compute the basis for the null space of a matrix. The computed null vector space has its dimension equal to that of the control vector. The method presented is a "direct method", in which a closed-loop eigenvector corresponding to the required eigenvalue is chosen from this null space in a way which chiefly reflects the desired closed-loop system performance. The eigenvectors in this research work were normalised such that their 2-norms equalled unity. The advantages of normalisation are two-fold: first, the distribution of the mode can be represented as a percentage contribution to each of the state variables; second, the magnitude of the eigenvectors can be arranged to be in the range zero to unity.

3.4.1 Theory of Eigenpair Assignment (EPAM)

Consider the following state equation,

$$\dot{x} = A\,x + B\,u \ , \qquad 3.62$$

where, x is the state vector $\in \Re^n$, u is the control vector $\in \Re^n$, A is the coefficient matrix of order[n * n],B is the driving matrix of order [n * m]. Given a set of any conjugate scalars $[\lambda_1 , \lambda_2 , \lambda_3 , .. , \lambda_n]$, the closed-loop eigenvalues, there exists a feedback matrix K of order [m * n] such that,

$$u = K\,x \ , \qquad 3.63$$

and,

$$\dot{x} = (A + BK)\,x \ . \qquad 3.64$$

If λ_i is a closed-loop eigenvalue, then the associated eigenvector $\underline{v}_i$ satisfies the eigenvalue/eigenvector property, Maxwell [1965].

$$(A + BK)\,\underline{v}_i = \lambda_i\ \underline{v}_i \ , \qquad \text{for i = 1,2,..., n .} \qquad 3.65$$

Re-expressing equation 3.65,

$$A\,v_i + BK\,\underline{v}_i - \lambda_i\,\underline{v}_i = 0 \ , \qquad 3.66$$

which can be written as,

$$(\lambda_i I - A)\,\underline{v}_i - BK\,\underline{v}_i = 0 \ . \qquad 3.67$$

Equation 3.67 can be expressed alternatively as,

$$\left[\lambda_i \mathbf{I} - \mathbf{A} \mid \mathbf{B}\right]\begin{bmatrix} \underline{v}_i \\ -\mathbf{K}\underline{v}_i \end{bmatrix} = \mathbf{0} \qquad 3.68$$

Equation 3.68 is a simultaneous matrix linear equation of the form , $\mathbf{H}\,\mathbf{b} = \mathbf{0}$. One interesting point to note from equation 3.68 is that the matrix $[\lambda_i \mathbf{I} - \mathbf{A} \mid \mathbf{B}]$ is rectangular. The system defined by equation 3.68 is under-determined, i.e there are n equations in n+m unknowns. If the rank $[\lambda_i \mathbf{I} - \mathbf{A} \mid \mathbf{B}] = k$, where k=n+m, then obviously the null space is just [0]. However if k<n+m, a basis for the null space of $[\lambda_i \mathbf{I} - \mathbf{A} \mid \mathbf{B}]$ can be constructed from the row echelon form[§] of $[\lambda_i \mathbf{I} - \mathbf{A} \mid \mathbf{B}]$. It can be shown (Noble & Daniel [1977]) that the null space is of dimension n+m-k, and that the vectors which constitute the basis are linearly independent. If it is assumed that A is full rank, i.e n, and that B is also full rank, i.e m (number of independent controls), then it is observed that the dimension of the null-space is also m.

The feedback matrix K which will result in the closed-loop system having the prescribed eigenvalues and the associated eigenvectors can be found as follows. Let,

$$\mathbf{S}_\lambda = [\lambda_i \mathbf{I} - \mathbf{A} \mid \mathbf{B}] \; . \qquad 3.69$$

---

§ The row echelon form is not the only way of computing the null space of $[\lambda_i \mathbf{I} - \mathbf{A} \mid \mathbf{B}]$. For example the algorithm proposed by Porter & D'azzo [1978][1,2] can also be used. In addition to these methods the basis may also be constructed by augmenting the matrix $[\lambda_i \mathbf{I} - \mathbf{A} \mid \mathbf{B}]$ by m rows of zero's, which is then reduced into the Hermite Normal Form (HNF). All the zero's on the leading diagonal are replaced by -1. These columns can be shown to form the basis for the null space of $[\lambda_i \mathbf{I} - \mathbf{A} \mid \mathbf{B}]$. However the method breaks down if the matrix $[\lambda_i \mathbf{I} - \mathbf{A} \mid \mathbf{B}]$ is not reducible to the HNF.

Augmenting equation 3.69 by m rows of zeros to form a square matrix of order $[(n+m)*(n+m)]$, for computational convenience,

$$\hat{S}_{\lambda_i} = \left[\begin{array}{c|c} \lambda_i I - A & B \\ \hline 0 \ldots 0 & 0 \\ 0 \ldots 0 & 0 \end{array}\right] \qquad 3.70$$

and let,

$$R_{\lambda_i} = \begin{bmatrix} N_{\lambda_i} \\ \text{----} \\ M_{\lambda_i} \end{bmatrix} \qquad 3.71$$

where the columns of R_{λ_i} form the basis for the null space of $\hat{S}_{\lambda_i}$. The matrix R_{λ_i} is of the order $[(n+m) * m]$, whereas the order of N_{λ_i} is $[n * m]$ and the order of M_{λ_i} is $[m * m]$. The matrix R_{λ_i} is computed form the singular value decomposition* of the matrix $\hat{S}_{\lambda_i}$. The vectors in N_{λ_i} and M_{λ_i} are defined as,

$$\begin{bmatrix} N_{\lambda_i} \\ M_{\lambda_i} \end{bmatrix} = \begin{bmatrix} \underline{\rho}_{1_i} & \underline{\rho}_{2_i} & \cdots & \underline{\rho}_{\kappa_i} \\ \underline{\omega}_{1_i} & \underline{\omega}_{2_i} & \cdots & \underline{\omega}_{\kappa_i} \end{bmatrix}, \left\{ \text{For } \kappa = 1, \ldots, m \right. . \qquad 3.72$$

---

* Singular Value Decomposition (SVD) is discussed in section 3.4.2. The reason for choosing SVD method for computing the basis for the null-space is that if matrix B is not full rank, then the dimension of the null-space can be determined from the computed singular values. Hence avoiding the necessity for determining the rank of the matrix $[\lambda_i I - A \mid B]$ by a seperate procedure.

If one of the eigenvectors is chosen from R_{λ_i}, to reflect the desired influence of the eigenvalue λ_i, such that,

$$\begin{bmatrix} \underline{\rho}_{\kappa_i} \\ --- \\ \underline{\omega}_{\kappa_i} \end{bmatrix} = \begin{bmatrix} \underline{v}_i \\ --- \\ -K\underline{v}_i \end{bmatrix} , \qquad 3.73$$

where $\kappa = 1$ or 2 or ,..., or m, is an integer specifying the column in R_{λ_i} then,

$$\underline{\rho}_{\kappa_i} = \underline{v}_i \quad , \qquad 3.74a$$

$$\underline{\omega}_{\kappa_i} = -K\,\underline{v}_i \quad . \qquad 3.74b$$

The process of selecting the appropriate column from N_{λ_i} and the corresponding column from M_{λ_i} is repeated for i=1,2,...,n. The feedback matrix K can then be computed as,

$$K = -\left[\underline{\omega}_{\kappa_1}, \underline{\omega}_{\kappa_2}, \ldots, \underline{\omega}_{\kappa_n}\right]\left[\underline{v}_1, \quad \underline{v}_2, \ldots, \underline{v}_n\right]^{-1} . \qquad 3.75$$

To satisfy equations 3.65, 3.68 and 3.75 following must hold,

a) whenever $\lambda_i = \lambda_j{}^*$ then $\underline{v}_i = \underline{v}_j{}^*$ and $\underline{\omega}_i = \underline{\omega}_j{}^*$, (*) denotes complex conjugate,

b) $\underline{v}_i$ must belong to the null-space of $[\,\lambda_i\,\mathbf{I} - \mathbf{A} \mid \mathbf{B}\,]$. Since R_{λ_i} form the basis for the null space of $\hat{S}_{\lambda_i}$, and since the selected vector $\underline{\rho}_{\kappa_i} \in N_{\lambda_i} \in R_{\lambda_i}$ and since $\underline{\rho}_{\kappa_i} = \underline{v}_i$, it follows that $\underline{v}_i$ will belong to the null-space of $[\,\lambda_i\,\mathbf{I} - \mathbf{A} \mid \mathbf{B}\,]$,

c) for an inverse to exist in equation 3.75, $\underline{v}_i$ $i = 1, 2, ..., n$ must be linearly independent.

Equation 3.75 holds if all eigenvalues specified are real. If however a complex eigenvalue is specified, such that $\lambda_1 = \lambda_2^*$, it follows from the requirements above that $\underline{v}_1 = \underline{v}_2^*$ and $\underline{\omega}_{\kappa_1} = \underline{\omega}_{\kappa_2}^*$, therefore for i=1,2,...,n, equation 3.74b can be written as,

$$-K\left[\underline{v}_{1R}+\underline{v}_{1I},\ \underline{v}_{1R}-\underline{v}_{1I},\ \underline{v}_3,\ \cdots,\underline{v}_n\right]=\left[\underline{\omega}_{\kappa_{1R}}+\underline{\omega}_{\kappa_{1I}},\ \underline{\omega}_{\kappa_{1R}}-\underline{\omega}_{\kappa_{1I}},\ \underline{\omega}_{\kappa_3},\ldots,\underline{\omega}_{\kappa_n}\right]. \qquad 3.76$$

In practical implementation of any control law, a feedback gain matrix with complex elements is not admissible. To obtain a feedback gain matrix of real elements, equation 3.76 is multiplied on both sides by a non-singular matrix of order [n * n],

$$\left[\begin{array}{cc|c} 0.5 & -j0.5 & 0 \\ 0.5 & j0.5 & \\ \hline & 0 & I \end{array}\right] . \qquad 3.77$$

In the case when only one complex eigenvalue is specified, the order of the identity matrix I equation 3.77 is [(n-2) * (n-2)]. After multiplication equation 3.76 can be written as,

$$-K\left[\underline{v}_{1R},\underline{v}_{1I},\underline{v}_3,\cdots,\underline{v}_n\right]=\left[\underline{\omega}_{\kappa_{1R}},\underline{\omega}_{\kappa_{1I}},\underline{\omega}_{\kappa_3},\cdots,\underline{\omega}_{\kappa_n}\right] , \qquad 3.78a$$

or,

$$K = -W_o\ V_o^{-1} . \qquad 3.78b$$

The matrix W_o is composed of selected vectors $\underline{\omega}_{\kappa_i}$ and is of the order [m * n] and the matrix V_o is composed of selected vectors $\underline{v}_i$ and is of the order [n * n]. For additional complex eigenvalues equation 3.78a is trivially modified.

3.4.2 Singular Value Decomposition

The singular value decomposition (SVD) method is one of the most powerful and important tools of modern numerical analysis which finds applications in,

- solving a system of linear equations,
- computation of the generalised inverse,
- determination of the numerical rank of a matrix.

However, in recent years, the technique of SVD has been applied in the analysis of control systems. For example, Lehtomaki et al [1981] developed criteria, based on the minimum singular value of the return difference matrix‡, for predicting guaranteed stability margins of multi-loop systems; these were expressed in terms of either gain or phase change in all feedback loops. Mukhopadhyay & Newson [1984] extended Lehtomaki's results to include the simultaneous gain and phase changes in all loops.

---

‡ In general for a system described by the following equations

$$\dot{\mathbf{x}} = \mathbf{A}\,\mathbf{x} + \mathbf{B}\,\mathbf{u} \qquad \text{(i)}$$

$$\mathbf{u} = \mathbf{K}\,\mathbf{x} \qquad \text{(ii)}$$

the return difference matrix is given by

$$\mathbf{T}(s) = \mathbf{I} + \mathbf{G}(s)$$

where

$$\mathbf{G}(s) = \mathbf{K}\,(s\mathbf{I} - \mathbf{A})^{-1}\,\mathbf{B}$$

G(s) is termed the loop-transfer matrix. And a system modelled in a different way from (i) and (ii) above would have a different return difference matrix.

The classical approach in determining the stability margins of a linear system was to use the Nyquist diagrams in which either gain or phase change in any single loop could be examined. However, for a control engineer with a bias towards *classical* methods of synthesis, the use of the minimum singular value of the return difference matrix is invariably an important tool.

The use of SVD for the synthesis of feedback control laws has been outlined in the preceding section. The method denoted EPAM relied upon generating a basis for the null space of a matrix. It will be shown next that such a basis can be constructed from a knowledge of the singular values. The constructed basis has all the necessary properties for successful computation of feedback laws.

3.4.2.1 SVD Theorem‡

Theorem: Let the matrix $\hat{S}_{\lambda_i} \in \mathbb{C}^{n+m,\, n+m}$ have rank k. There exist unitary matrices $U_s \in \mathbb{C}^{n+m,\, n+m}$, and $V_s \in \mathbb{C}^{n+m,\, n+m}$ such that,

$$\Sigma = U_s^H S_\lambda V_s \,, \qquad 3.79\ ¶$$

$$S_\lambda = U_s \Sigma V_s^H \,, \qquad 7.80$$

where,

$$\Sigma = \begin{bmatrix} W & 0 \\ 0 & 0 \end{bmatrix} . \qquad 3.81$$

---

‡ See Noble & Daniel [1977] for a slightly different treatment of the subject

¶ The subscript i on λ and circumflex on S has been dropped here for convenience.

Proof : Since $S_\lambda^H S_\lambda \geq 0$, the singular values[‡] of the matrix $S_\lambda^H S_\lambda$ will lie between 0 and infinity, i.e.,

$$\sigma_s (S_\lambda^H S_\lambda) \subseteq [0, + \infty] \quad , \tag{3.82}$$

denoting $\sigma_s(S_\lambda^H S_\lambda)$ by $\{ \sigma^2_{s_i}, i = 1, 2, \ldots, n+m \}$ the singular values can be arranged in the form,

$$\sigma_{s_1} \geq \sigma_{s_2} \geq \sigma_{s_3} \geq \ldots \geq \sigma_{s_k} \geq 0 \geq \sigma_{s_{k+1}}, \ldots, \sigma_{s_{n+m}} \quad . \tag{3.87}$$

Let $\{ v_1, v_2, \ldots, v_k\}$ be a corresponding set of orthonormal[¶] eigenvectors, and let

$$V_{s_1} = \left[v_1 , v_2, \ldots, v_k \right] \quad ,$$

$$V_{s_2} = \left[v_{k+1}, \ldots, v_{n+m} \right] \quad .$$

If the singular values $\sigma_{s_i}, i = 1, 2, \ldots, k$ are arranged in the form,

$$W = \text{Diag} \left[\sigma_{s_1} , \sigma_{s_2}, \ldots, \sigma_{s_k} \right] \quad .$$

then,

$$S_\lambda^H S_\lambda \, V_{s_1} = V_{s_1} W^2 \quad . \tag{3.84}$$

---

‡ The positive square roots of the eigenvalues of $S_\lambda^H S_\lambda$ are termed the singular values.

¶ Two vectors **u** and **v** are said to be orthogonal when (**u**, **v**) = 0. A set of vectors is said to be orthogonal when every pair of vectors is orthogonal. Moreover, if, in addition each vector satisfies $\| \, . \, \| = 1$, then the set of vectors is said to be orthonormal.

From equation 3.84, it follows that

$$W^{-1} V_{s_1}^H S_\lambda^H S_\lambda V_{s_1} W^{-1} = I \ , \qquad 3.85 \ ‡$$

also,

$$S_\lambda^H S_\lambda V_{s_2} = V_{s_2} . 0 \ , \qquad 3.86$$

so that,

$$V_{s_2}^H S_\lambda^H S_\lambda V_{s_2} = 0 \ , \qquad 3.87$$

thus,

$$S_\lambda V_{s_2} = 0 \ . \qquad 3.88$$

From equation 3.88 it is seen that the matrix V_{s_2} will form the basis for the null space of the matrix S_λ. Let,

$$U_{s_1} = S_\lambda V_{s_1} W^{-1} , \qquad 3.89$$

then from equation 3.85,

$$U_{s_1}^H U_{s_1} = I \ .$$

Choose any matrix U_{s_2} such that,

$$U_s^H = \left[U_{s_1}^H , \ U_{s_2}^H \right] \ \text{ and } \ (U_{s_1} , U_{s_2}) = 0, \ \text{then} ,$$

---

‡ Since

$$S_\lambda^H S_\lambda V_{s_1} = V_{s_1} W^2 ,$$

then the quantity ,

$$W^{-1} V_{s_1}^H (V_{s_1} W^2) W^{-1} = W^{-1} (V_{s_1}^H V_{s_1}) W = I \ .$$

N.B: Since V_{s_1} is unitary the product $V_{s_1}^H V_{s_1} = I$.

$$U_s^H S_\lambda V_s = \left[U_{s_1}^H , U_{s_2}^H \right] S_\lambda \begin{bmatrix} V_{s_1} \\ V_{s_2} \end{bmatrix} , \qquad 3.90$$

$$= \begin{bmatrix} U_{s_1}^H S_\lambda V_{s_1} & U_{s_1}^H S_\lambda V_{s_2} \\ U_{s_2}^H S_\lambda V_{s_1} & U_{s_2}^H S_\lambda V_{s_2} \end{bmatrix} . \qquad 3.91$$

Using equation 3.88 i.e., $S_\lambda V_{s_2} = 0$, equation 3.91 reduces to,

$$= \begin{bmatrix} U_{s_1}^H S_\lambda V_{s_1} & 0 \\ U_{s_2}^H S_\lambda V_{s_1} & 0 \end{bmatrix} . \qquad 3.92$$

Since $S_\lambda V_{s_1} = U_{s_1}^H W$ (from equation 3.89), equation 3.93 becomes,

$$= \begin{bmatrix} U_{s_1}^H S_\lambda V_{s_1} & 0 \\ U_{s_2}^H U_{s_1} W & 0 \end{bmatrix} . \qquad 3.93$$

Since $U_{s_2}^H U_{s_1} = 0$, and by using equation 3.89, equation 3.92 becomes,

$$U_s^H S_\lambda V_s = \begin{bmatrix} U_{s_1}^H S_\lambda V_{s_1} & 0 \\ 0 & 0 \end{bmatrix} = \begin{bmatrix} W & 0 \\ 0 & 0 \end{bmatrix} = \Sigma ,$$

hence,

$$S_\lambda = U_s \Sigma V_s^H ,$$

as desired.

The columns of $\mathbf{U}_s$ are called the left singular eigenvectors of $\mathbf{S}_\lambda$ (or the orthonormal eigenvectors of $\mathbf{S}_\lambda\mathbf{S}_\lambda^H$), while the columns of $\mathbf{V}_s$ are termed the right eigenvectors of $\mathbf{S}_\lambda$ (or the orthonormal eigenvectors of $\mathbf{S}_\lambda^H\mathbf{S}_\lambda$). The matrix $\mathbf{S}_\lambda^H$ has n+m singular values, i.e. the positive square roots of the eigenvalues of the matrix $\mathbf{S}_\lambda\mathbf{S}_\lambda^H$. The choice of $\mathbf{S}_\lambda^H\mathbf{S}_\lambda$ rather than $\mathbf{S}_\lambda\mathbf{S}_\lambda^H$ is arbitrary. Since $\mathbf{S}_\lambda^H\mathbf{S}_\lambda$ can be computed quite easily, which will be shown in the next section, the singular values are always determined from the matrix $\mathbf{S}_\lambda^H\mathbf{S}_\lambda$. The unitary matrices $\mathbf{V}_s$ and $\mathbf{U}_s$ provide information about two fundamental sub-spaces viz:

$$\text{Im}\,\mathbf{V}_{s_2} = \text{Ker}\,(\mathbf{S}_\lambda) \qquad 3.94^{\S}$$

i.e., $\mathbf{V}_{s_2}$ forms a basis for the null space of $\mathbf{S}_\lambda$

$$\text{Im}\,\mathbf{U}_{s_1} = \text{Im}\,\mathbf{S}_\lambda \qquad 3.95$$

i.e., $\mathbf{U}_{s_1}$ forms a basis for the exact range space of $\mathbf{S}_\lambda$

From equation 3.88 it is seen that the matrix $\mathbf{V}_{s_2}$ forms the basis for the null space of $\mathbf{S}_\lambda$. If the eigenvalues and the orthonormal eigenvectors of the matrix $\mathbf{S}_\lambda^H\mathbf{S}_\lambda$ can be computed, the orthonormal eigenvectors corresponding to the singular values which approach zero can then be used to form the matrix $\mathbf{V}_{s_2}$. Hence singular values which are potentially zero are of significance. The computational problems in determining the singular values, and the decision as to when a singular value is zero computationally, are well documented in Kelma & Laub [1980]. The decision about when a singular value is zero affects both the determination of the rank of $\mathbf{S}_\lambda$ and the computation of the sub-spaces defined by equations 3.94 and 3.95.

3.4.2.2 Calculation of $\mathbf{R}_\lambda$

The required basis $\mathbf{R}_\lambda$ (equation 3.71) can be obtained by means of the QR-factorisation (see footnote on the next page) method viz:

$$\mathbf{S}_\lambda = \mathbf{Q}_s\,\mathbf{R}_s \;, \qquad 3.96$$

---

§ Abbreviation Im denotes the *Image* .

where $Q_s \in \mathbb{C}^{n+m,\ n+m}$ is a unitary matrix and R_s is an upper triangular matrix. $S_\lambda^H S_\lambda$ is calculated as follows;

$$\begin{aligned} S_\lambda^H S_\lambda &= Q_s^H R_s^H Q_s R_s \\ &= R_s^H Q_s^H Q_s R_s \\ &= R_s^H R_s \ . \end{aligned} \qquad 3.97$$

Hence from equation 3.97, the singular values (which are the positive square roots of the eigenvalues of $S_\lambda^H S_\lambda$) and the corresponding orthonormal eigenvectors (i.e. matrix , V_s) can be computed directly. The orthonormal eigenvectors corresponding to the zero singular values are then used to construct the matrix V_{s_2}, which also is the required basis R_λ. The matrix U_s can then be calculated using equation 3.89, thus providing the full decomposition of the matrix S_λ as defined by equation 3.80. The algorithm for computing the SVD of a complex matrix based on the QR-factorisation‡ proposed by Bussinger & Golub [1969] was used in this research study.

---

‡ The matrices Q_s and R_s in the QR-factorisation of S_λ are defined as,

$$Q_s = \left[q_{s_1}, \ldots, q_{s_{n+m}} \right] ,$$

and

$$R_s = \begin{bmatrix} r_{1,1} & r_{1,2} & \cdot & \cdot & r_{1,\ n+m} \\ \cdot & r_{2,2} & \cdot & \cdot & r_{2,\ n+m} \\ \cdot & \cdot & \cdot & \cdot & \cdot \\ \cdot & \cdot & \cdot & \cdot & \cdot \\ \cdot & \cdot & \cdot & \cdot & r_{n+m,\ n+m} \end{bmatrix} ,$$

where $r_{1,1} = \| a_1 \|_2$ and $q_{s_1} = a_1 / r_{1,1}$. Vectors a_i are the i^{th} column of S_λ. Subsequently,

$$r_{j,i} = (q_{s_j} , a_i) \quad , \quad \text{for } 1 \le j \le i \ ,$$

and ,

$$r_{i,i}\, q_{s_i} = a_i - r_{1,\,i}\, q_{s_1} - \ldots - r_{i-1,\,i}\, q_{s_{i-1}} \ .$$

3.4.3 Applicability of EPAM

The method of computing, by SVD, the closed-loop eigenvectors which satisfy equation 3.68, avoids the restriction of specifying some open-loop eigenvalues in the closed-loop [§]. Since the control driving matrix **B** is assumed to have full rank, i.e. m, the dimension of the computed null-space is m. Therefore, from m eigenvectors in equation 3.72, a closed-loop eigenvector corresponding to an eigenvalue λ_i can be chosen to reflect the desired mode distribution in the state variable response. Consequently, it is also possible to assign an eigenvalue having a multiplicity of m. The method presented is "direct", since the null-space vector with appropriate mode distribution, is chosen as a closed-loop eigenvector.

If rank(**AB**) < n, i.e., some states are uncontrollable, an eigenvalue associated with a mode identified with the uncontrollable states may also be specified in the closed-loop with the freedom of selecting an appropriate corresponding eigenvector from the computed null space vectors, equation 3.72. An open-loop eigenpair corresponding to an uncontrollable mode may be specified in the closed-loop, because the eigenpair satisfies equation 3.65, and can be assigned in the closed-loop via equation 3.78a, by equating the vector $\underline{\omega}_{\kappa_i}$ equal to zero and by equating the vector $\underline{v}_i$ to the open-loop eigenvector. The feedback matrix thus obtained then results in the closed-loop possessing the open-loop eigenpair. The following steps are observed in the computation of the feedback matrix;

[§] In Andry et al's work a closed-loop eigenvector was obtained by projecting the desired closed-loop eigenvector on to the sub-space of the matrix $(\lambda \mathbf{I} - \mathbf{A})^{-1}\,\mathbf{B}$. Clearly, if an open-loop eigenvalue is specified, then the inverse of the matrix $(\lambda \mathbf{I} - \mathbf{A})$ is not defined. The null-space computed by SVD does not requires the inversion of $(\lambda \mathbf{I} - \mathbf{A})$, making it possible to compute the null-space corresponding to some open-loop eigenvalue, thereby enabling the selection of an appropriate corresponding closed-loop eigenvector.

Step 1: The matrix $\hat{S}_{\lambda_i}$ is formed for the specified eigenvalue λ_i .

Step 2: The SVD of $\hat{S}_{\lambda_i}$ is obtained from equation 3.79. Decomposition for only $\lambda_i = -\sigma + j\,\omega$ is required if eigenvalue is complex.

Step 3: Basis, R_{λ_i}, is constructed, from the matrix V_s, equation 3.79,i.e., vectors in V_s corresponding to the singular values which have a value of zero.

Step 4: The desired eigenvector is selected form the matrix N_{λ_i}, with appropriate column in M_{λ_i}.

Step 5: The selected vectors $\underline{\rho}_{\kappa_i}$ and $\underline{\omega}_{\kappa_i}$, equation 3.72, are stored as the i^{th} column in matrices V_o and W_o. For $\lambda_i = -\sigma + j\,\omega$, the real part of the eigenvector $\underline{\rho}_{\kappa_i}$ is stored in the i^{th} column and the imaginary part in the $(i+1)^{th}$ column of matrix V_o. The vector $\underline{\omega}_{\kappa_i}$ is stored in the matrix W_o in a similar way.

Step 6: The process is repeated for n eigenvalues.

Step 7: Feedback matrix is obtained from equation 3.78b.

3.5 Feedback controller for the L-1011 using EPAM

A model of the Tristar L-1011 aircraft described in Chapter 2 is used to demonstrate the effectiveness of EPAM. It was shown in section 3.3 that the closed-loop lateral acceleration and the yawing motion, arising form the use of the control law based on the GCCF method, had deteriorated because of coupling between the rolling and the yawing motions. Moreover, the control law based on the LQP method failed to achieve the required closed-loop eigenvalues. A feedback controller is now designed to assign the same specified closed-loop eigenvalues as given in table 3.1.

Since the order of the matrix **B** is [7*2], with rank(B)=m=2, the dimension of the null-space is also 2. The vectors $\underline{\rho}_{\kappa_i}$ and $\underline{\omega}_{\kappa_i}$ contained in $\mathbf{R}_{\lambda_i}$, which forms the basis for the null space of $\hat{\mathbf{S}}_{\lambda_i}$, viz equation 3.71, are presented in tables 3.5 through to table 3.8. The physical reasons for the choice of the appropriate eigenvector in $\mathbf{R}_{\lambda_i}$ is presented as a footnote to the tables. Also presented in the tables is the magnitude of the components of the eigenvectors as a percentage, enabling the contribution of the mode to the state variable response to be examined at a glance.

Eigenvalue : -2.0 + j 1.5 (Roll/Spiral Mode) i = 1				
State	Eigenvector $\underline{\rho}_{1_i}$	%	Eigenvector $\underline{\rho}_{2_i}$	%
Rudder Deflection	0.707 + j 0.000	49.9	0.000 + j 0.000	0.0
Aileron Deflection	0.017 - j 0.064	0.4	0.658 - j 0.045	43.3
Bank Angle	0.063 + j 0.026	0.5	0.004 - j 0.164	2.7
Yaw Rate	0.186 + j 0.089	4.3	0.009 + j 0.003	0.0
Roll Rate	-0.165 + j 0.043	2.9	0.237 + j 0.333	16.8
Sideslip Angle	0.032 + j 0.074	0.6	0.000 + j 0.005	0.0
W.O Filter State	-0.016 - j 0.046	0.2	-0.001 - j 0.002	0.0
	$\underline{\omega}_{1_i}$	%	$\underline{\omega}_{2_i}$	%
	-0.636 - j 0.053	40.7	0.000 + j 0.000	0.0
	-0.020 + j 0.058	0.4	-0.608 + j 0.002	37.0

Table 3.5: Assignable Roll/Spiral mode eigenvectors

Footnote : Inspection of vectors $\underline{\rho}_{1_i}$ and $\underline{\rho}_{2_i}$ reveals that if eigenvector $\underline{\rho}_{2_i}$ is chosen then the roll/spiral mode will contribute, as indicated by percentages, minimally to the yawing response variables i.e., the yaw rate and sideslip angle. Since the control of rolling motion is usually accomplished by the ailerons, the roll/spiral mode appears in aileron deflection. The roll/spiral mode is seen to be contributing chiefly to the aileron deflection, bank angle and roll rate. If however, eigenvector $\underline{\rho}_{1_i}$ is chosen then the roll/spiral mode contributes, as indicated by percentages, to the yawing response variables, this has the undesirable effect of coupling the yawing and the rolling motions of the aircraft. Eigenvector $\underline{\rho}_{2_i}$ was deemed to be an appropriate choice for the roll/spiral mode. Vector $\underline{\omega}_{2_i}$ was chosen as required in equation 3.73.

Eigenvalue: -1.5 + j 1.5 (Dutch Roll Mode) i = 3				
State	Eigenvector $\underline{\rho}_{1_i}$	%	Eigenvector $\underline{\rho}_{2_i}$	%
Rudder Deflection	0.660 + 0.000	43.6	0.000 + j 0.000	0.0
Aileron Deflection	0.025 - j0.117	1.4	0.633 - j0.058	40.4
Bank Angle	0.092 + j 0.086	1.6	0.085 - j 0.190	4.3
Yaw Rate	0.213 + j 0.009	5.8	0.012 + j 0.005	0.0
Roll Rate	-0.268 + j 0.009	7.2	0.156 + j 0.412	19.4
Sideslip Angle	0.025 + j 0.109	1.2	0.002 + j 0.007	0.0
W.O Filter State	-0.007 - j 0.068	0.2	-0.001 - j 0.004	0.0
	$\underline{\omega}_{1_i}$	%	$\underline{\omega}_{2_i}$	%
	-0.611 - j 0.050	37.5	0.000 + j 0.000	0.0
	-0.030 + j 0.108	1.3	-0.598 + 0.016	35.8

Table 3.6: Assignable Dutch Roll mode eigenvectors

Footnote : Inspection of eigenvectors $\underline{\rho}_{1_i}$ and $\underline{\rho}_{2_i}$ reveals that if eigenvector $\underline{\rho}_{2_i}$ is chosen, the dutch roll mode, as indicated by percentages, contributes heavily to rolling motion variables i.e., bank angle, roll rate and aileron deflection. The choice of eigenvector $\underline{\rho}_{2_i}$ will result in coupling between the rolling and the yawing motions of the aircraft. It is interesting to note that if eigenvector $\underline{\rho}_{1_i}$ is chosen then, the dutch roll mode contributes mainly to the the rudder deflection, yaw rate and sideslip angle; nevertheless some contribution to the rolling response is noted (the dutch roll motion usually arises as a result of rudder deflection, the aircraft yaws and due to dihedral effects has a tendency to roll). Therefore, the choice of eigenvector $\underline{\rho}_{1_i}$ was made alongwith the choice of vector $\underline{\omega}_{1_i}$ as required in equation 3.73.

Eigenvalue : -25.0 (Aileron mode) i = 5				
State	Eigenvector $\underline{\rho}_{1_i}$	%	Eigenvector $\underline{\rho}_{2_i}$	%
Rudder Deflection	-0.970	94.0	0.000	0.0
Aileron Deflection	-0.001	0.0	-0.979	95.8
Bank Angle	-0.001	0.0	0.002	0.0
Yaw Rate	-0.029	0.1	-0.001	0.0
Roll Rate	0.014	0.0	-0.047	0.2
Sideslip Angle	0.000	0.0	0.000	0.0
W.O Filter State	0.001	0.0	0.000	0.0
	$\underline{\omega}_{1_i}$	%	$\underline{\omega}_{2_i}$	%
	-0.242	5.9	0.000	0.0
	0.000	0.0	0.000	0.0

Table 3.7: Assignable Aileron mode eigenvectors

Footnote : Eigenvector $\underline{\rho}_{2_i}$ is chosen because the aileron mode contributes solely to aileron deflection, from the table above the contribution is seen to be nearly 96% . This enables control decoupling between the ailerons and the rudder. If however eigenvector $\underline{\rho}_{1_i}$ is chosen, then the aileron mode contributes to rudder deflection substantially (from the table above it is seen to be 94%) and will result in a strong coupling of rudder and aileron modes . The choice of vector $\underline{\omega}_{2_i}$ was made, as required in equation 3.73.

Eigenvalue : -20.0 (Rudder mode) i=6				
State	Eigenvector $\underline{\rho}_{1_i}$	%	Eigenvector $\underline{\rho}_{2_i}$	%
Rudder Deflection	0.998	99.8	0.000	0.0
Aileron Deflection	0.001	0.0	0.979	95.8
Bank Angle	0.001	0.0	-0.003	0.0
Yaw Rate	0.037	0.1	0.002	0.0
Roll Rate	-0.018	0.0	0.058	0.3
Sideslip Angle	0.001	0.0	0.000	0.0
W.O Filter State	-0.001	0.0	0.000	0.0
	$\underline{\omega}_{1_i}$	%	$\underline{\omega}_{2_i}$	%
	0.000	0.0	0.000	0.0
	0.000	0.0	-0.196	3.8

Table 3.8 : Assignable Rudder mode eigenvectors

Footnote : Eigenvector $\underline{\rho}_{1_i}$ is chosen because the rudder mode contributes solely to rudder deflection, from the table above the contribution is seen to be nearly 100% . This enables control decoupling to be achieved between the rudder and the ailerons. If however, eigenvector $\underline{\rho}_{2_i}$ is chosen then the rudder mode contributes to aileron deflection substantially (from the table above it is seen to be 96%) and will result in a strong coupling of rudder and aileron modes . The choice of vector $\underline{\omega}_{2_i}$ was made, as required in equation 3.73.

The open-loop eigenvector corresponding to the washout network mode was found to be satisfactory, hence it was specified in the closed-loop. The feedback gains computed using equation 3.78b are presented in table 3.9.

δ_{r_c}	$K1_{\delta_r}$	$K1_{\delta_a}$	$K1_{\varphi}$	$K1_{r}$	$K1_{p}$	$K1_{\beta}$	$K1_{x_7}$
	-0.134	0.001	-0.302	3.582	-2.938	0.131	0.0
δ_{a_c}	$K2_{\delta_r}$	$K2_{\delta_a}$	$K2_{\varphi}$	$K2_{r}$	$K2_{p}$	$K2_{\beta}$	$K2_{x_7}$
	-0.034	-0.120	5.382	2.276	2.731	-7.947	0.0

Table 3.9 : Feedback gains EPAM control law

Inspection of feedback gains $^{K1}\delta_a$ and $^{K2}\delta_r$ reveals that the rudder and the ailerons have been decoupled, whereas an examination of the feedback gains $^{K1}\delta_a$ and $^{K2}\delta_r$ presented in table 3.2 for the GCCF method shows a strong coupling between the ailerons and the rudder. It is noticed from table 3.2 that the gain $^{K1}\delta_a$ corresponding to the feedback of aileron deflection to rudder was -0.213, the same gain from table 3.9 can be seen to be 0.001. It is also noticed from table 3.9 that feedback is not required from the washout filter state. The gains $K1_\beta$ and $K2_\beta$ are of the same order as those of the GCCF control law (table 3.2). As already mentioned, feedback of sideslip especially to ailerons has the effect of increasing the dutch roll damping.

3.6 Comparison between the Feedback Methods

The response for an initial sideslip angle of 0.02 radians is shown in figure 3.6 using the EPAM control law. The response is better damped compared to that obtained using the LQP control law (figure 3.3). The reductions in the RMS values of the output vector are presented in figure 3.7, for the three design methods considered. The reductions obtained from using EPAM were greater for every variable compared with the values obtained from both the GCCF method and

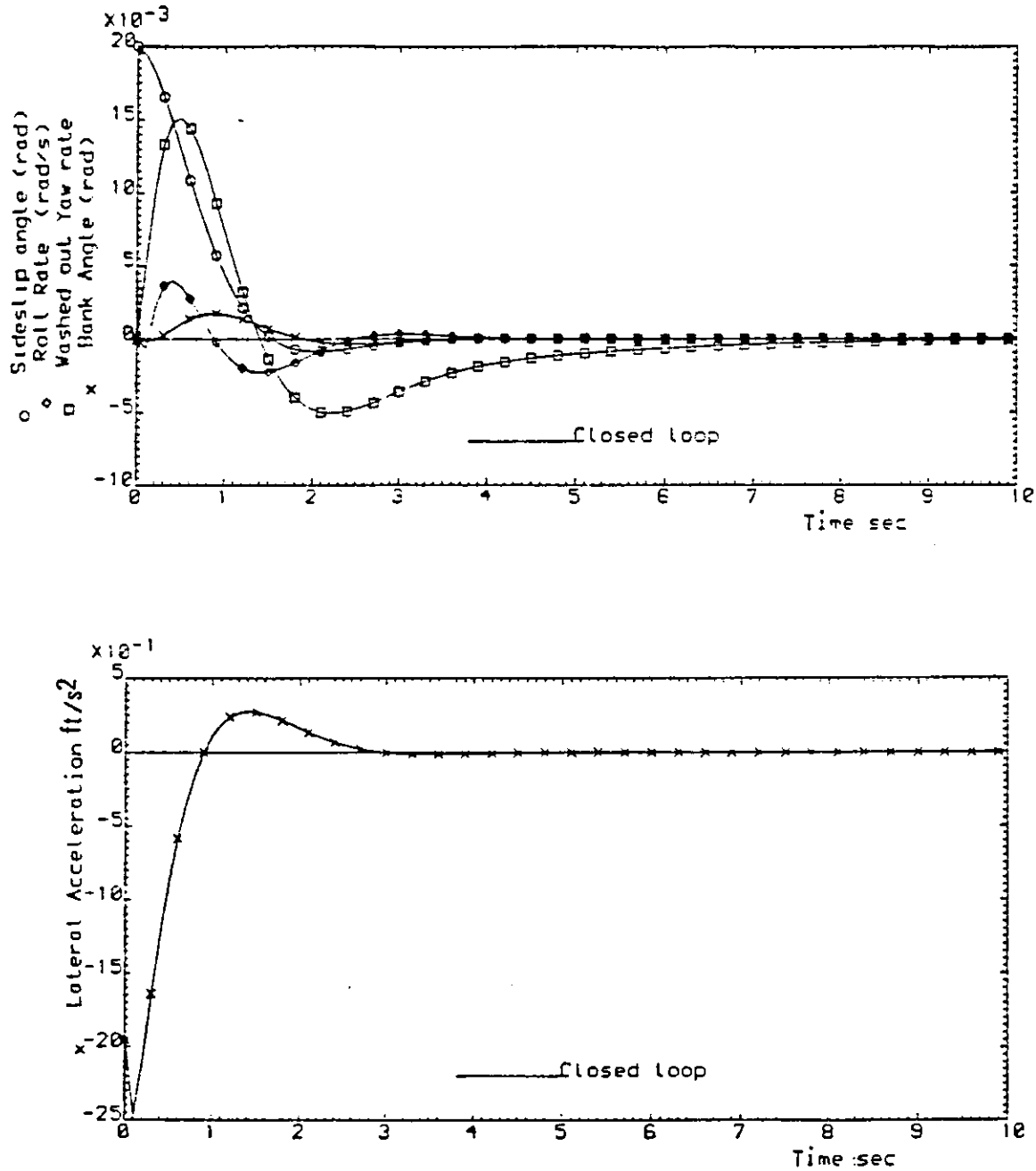

Figure 3.6 : L-1011 closed-loop response for β_{ic}=0.02 radians using EPAM control law.

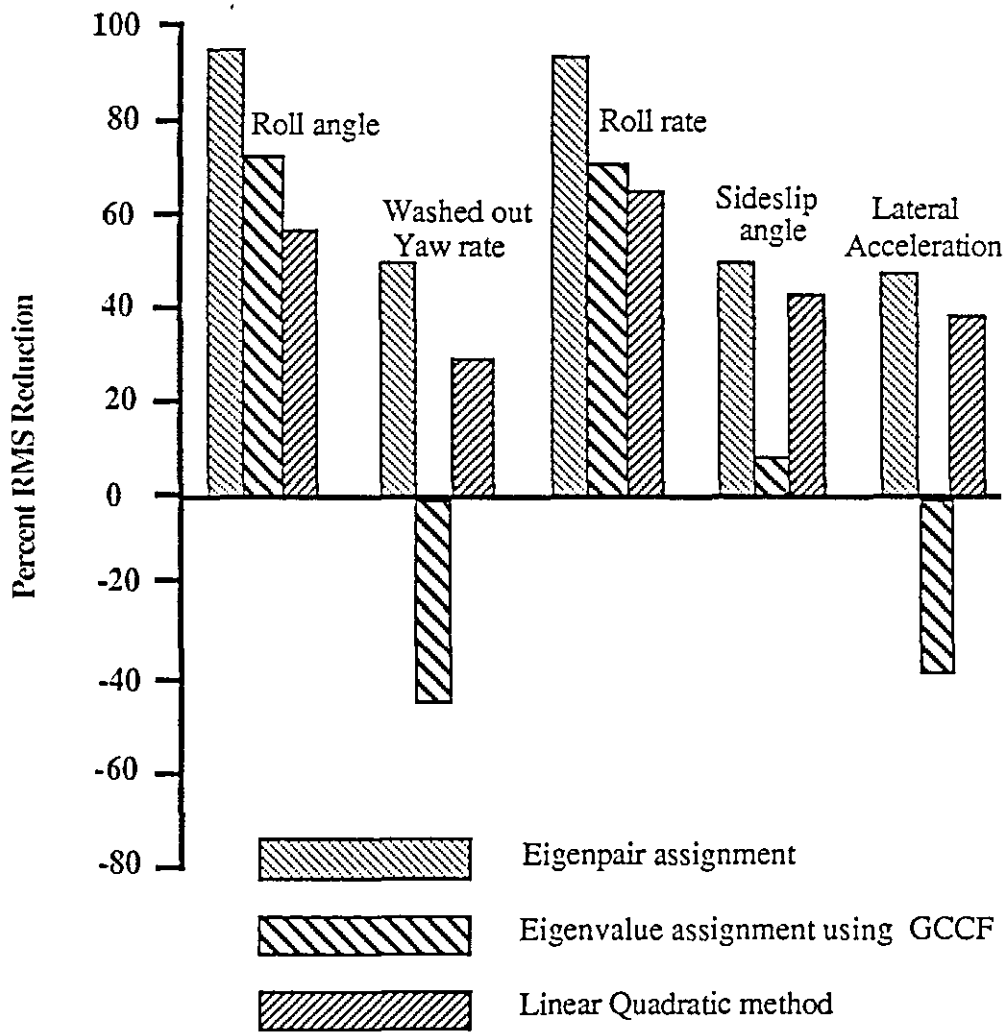

Figure 3.7 : Comparison of responses for different control laws

the LQP method. Reduction of lateral acceleration is significant as persistent levels of acceleration add to the crew and passenger discomfort. A reduction of 48% in the RMS value of the lateral acceleration was achieved by using the EPAM control law.

Presented in figure 3.8 are the reductions in the RMS values for the full state variable feedback (FSVF) control law based on EPAM, and the FSVF control law using the eigenvalue/eigenvector assignment method of Andry, Shapiro &Chung [1983], for the same dynamic model of the L-1011 Tristar aircraft. The results of EPAM compare most favourably with the published results. The rolling response is almost the same for the two methods compared in figure 3.8., with the yawing response being improved by EPAM. The reduction in the RMS level of lateral acceleration by the use of EPAM was greater then that obtained by Andry's method. Also compared in figure 3.8 are the RMS and the absolute peak values values of control deflections. Although the peak and the RMS values of aileron deflection are the same for the two methods, the rudder activity is lower for the EPAM control law.

The closed-loop eigenvectors and eigenvalues associated with roll/spiral mode for the GCCF, LQP and EPAM are presented in table 3.10 for comparison. The closed-loop roll/spiral mode eigenvector resulting from the EPAM control law (table 3.10), however, is not the same numerically as the prescribed vector in table 3.5. This arises because the matrix $\mathbf{R}_{\lambda_i}$, equation. 3.71, which is partitioned into two sub matrices, $\mathbf{M}_{\lambda_i}$ and $\mathbf{N}_{\lambda_i}$ has its columns (the eigenvectors) normalised. To obtain correspondence between the closed-loop roll/spiral eigenvector obtained by EPAM control law(table 3.10) and the prescribed eigenvector $\underline{\rho}_{2_i}$ (table 3.5), eigenvector $\underline{\rho}_{2_i}$ has to be re-normalised such that, $\| \underline{\rho}_{2_i} \|_2=1.0$. This means multiplying the chosen vector $\underline{\rho}_{2_i}$ by a scalar. Multiplication of the chosen vector $\underline{\rho}_{2_i}$ in table 3.5, by 1.26, will result in the EPAM roll/spiral vector in table 3.10 (N.B. the vector in table 3.5 is approximate due to roundoff).

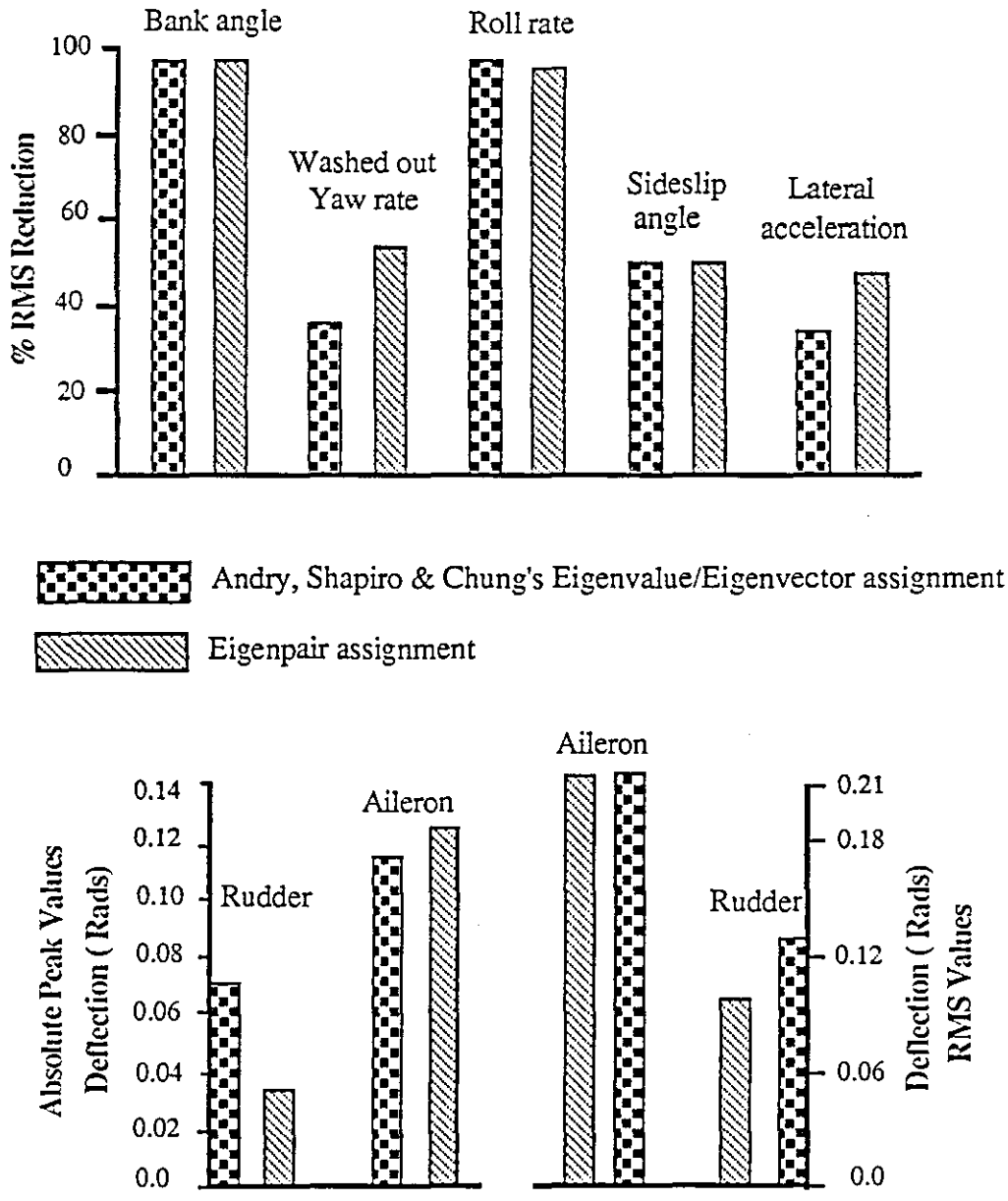

Figure 3.8: Comparison of responses for control laws obtained by using Andry et.al's eigenvalue/eigenvector method and proposed eigenpair assignment method.

	Roll/Spiral	Roll Subs.	Spiral	Roll/Spiral
Eigenvalue	-2.0 +j 1.5	-1.24	-0.89	-2.0 +j 1.5
State Variables	E I G E N V E C T O R S*			
Rudder Deflection	0.89+j0.00	0.046	0.055	0.00+j0.00
Aileron Deflection	-0.04-j0.31	0.065	0.049	0.83+j0.03
Bank Angle	0.02+j0.04	-0.627	0.743	0.02-j0.21
Yaw Rate	0.24+j0.11	0.002	0.036	0.01+j0.00
Roll Rate	-0.11-j0.05	0.775	-0.662	0.27+j0.44
Sideslip Angle	0.04+j0.09	0.024	0.008	0.00+j0.01
W.O Filter State	-0.02-j0.06	-0.002	-0.046	0.00-j0.00
Method	GCCF	LQP		EPAM

Table 3.10: Comparison of roll/spiral mode eigenvectors

It was shown in section 3.3.5, that the roll/spiral mode was influencing the yawing motion. It can be seen from an examination of the eigenvector corresponding to the roll/spiral mode obtained when using the EPAM control law (see table 3.10), that roll/spiral mode's contribution to the yawing variables, i.e. the yaw rate and the sideslip angle has been reduced. This is inferred from examining the eigenvector components corresponding to the yawing variables, which are small when compared to the same components of the GCCF eigenvector. The time response in figure 3.6 shows that the closed-loop system not only has a faster settling time but also produces less peak excursions compared to responses in figures 3.2 and 3.3 respectively. The improvement in the reductions of peak and RMS values of yawing variables was possible due to decoupling of the rolling and yawing motions of the aircraft, through the specification of appropriate roll/spiral mode and dutch roll mode eigenvectors.

3.7 Concluding Remarks

The advantages of designing a feedback controller using the proposed eigenpair assignment, were illustrated in this chapter. It was shown that the prescribed eigenvalues and the corresponding eigenvectors could be achieved by EPAM based on the physical requirements rather than on arbitrary selection. The dynamic model of the L-1011 which was of a relatively low order, was used merely to illustrate the numerical effectiveness and to facilitate the comparison between the various feedback methods.

Incorporation of structural flexibility dynamics and unsteady aerodynamics alongwith the rigid body dynamics, tends to increase the complexity of the model. Such a model of a large transport aircraft, the C5-A Galaxy is presented in chapter 4. The EPAM is used to design feedback controllers, with the aim of reducing structural loads which result from both applied manoeuvre commands and from encountering atmospheric turbulence. The results are presented in chapter 5.

CHAPTER 4

MATHEMATICAL MODEL OF THE C-5A GALAXY

4.1 Introduction

The C-5A is the largest transport aircraft manufactured by the Lockheed Corporation of America. It is a high-wing monoplane with a T-tail, powered by four General Electric TF39 turbofans mounted on pylons under the wings. The first C-5A entered into service with the United States Air Force in september 1969. Just before delivery to the USAF, Lockheed suffered a major technical setback, when there was a structural failure of a wing test specimen in July 1969, at 1.25 times the design load limit, Air International[1984] .

This load figure was significantly below the strength required for demonstration of aircraft's planned structural life. A modification programme to introduce reinforcement at eleven points in the wing was undertaken resulting in a reduction of the payload carrying capacity by 7.5% . Even after the modifications, however, there remained a problem in the wing durability that threatened reduce the operational life to less than 7500 hours rather than the intended 30,000 hours. With some sixty sets of wings already produced, attention was then given to achieving alleviation of wing loads by the means of active control technology.

Methods of reducing, by feedback control, the structural loads on the wing of the C-5A arising as a result of manoeuvre commands or encountering atmospheric turbulence, have been proposed by Stone et al [1972] ,Konar et al [1976], McLean (1976) and McLean & Prasad [1980]. Before any control scheme is implemented to reduce loads on an aircraft structure the theoretical feasibility of a control scheme, using as comprehensive a mathematical description of the aircraft as possible, has to be demonstrated.

4.2 State Variable Representation of the C5-A Galaxy

Numerical data needed to describe the rigid body dynamics, the significant flexural modes of the wing, the actuator dynamics and the approximate functions which account for the unsteady

aerodynamic effects was available in the work presented by Stone et al [1972], Harvey & Pope [1977]. The numerical data available can be used to model the first fifteen flexural modes of the wing of the C5-A. Prasad [1980] showed that for work on automatic flight control systems (AFCS), the first six flexural modes were adequate to represent the significant dynamics of the flexible wing. The data for the model considered in this research, concerns only longitudnal motion and was evaluated at a single flight condition, to which the following parameters relate;

Parameter	Value	Units
Weight	$3.107 * 10^6$	Newtons
Mach Number	0.488	
Altitude	2300	meters (m)
Dynamic Pressure	9150	N/m
C. of G.	31% M.A.C	
Trim angle of attack	0.0515	radians
Load Factor	1.0	
Air speed	143	m/s^2

Table 4.1: Flight condition parameters

The mathematical model of the C5-A , was represented by the following state equation,

$$\dot{x} = A x + B u + G_\eta \eta \ , \qquad 4.1$$

where, x is the state vector $\in \Re^n$, u is the control vector $\in \Re^m$, A is the coefficient matrix of order [n * n], B is the driving matrix of order [n * m], G_η is the noise driving matrix of order [n *1] and η is scaler noise.

Since the aim of the research was to provide a control system to alleviate the structural loads on the wing of the C-5A, an appropriate output vector was defined which included the bending moments and torsional moments at five specific wing stations, which was related to the state

vector and the control vector as shown in equation 4.2,

$$\mathbf{y} = \mathbf{C}\,\mathbf{x} + \mathbf{D}\,\mathbf{u} \ , \qquad 4.2$$

where $\mathbf{y}$ is the output vector $\in \Re^p$, $\mathbf{C}$ is the coefficient matrix of order $[p * n]$, $\mathbf{D}$ is the driving matrix of order $[p * m]$, $\mathbf{x}$ and $\mathbf{u}$ were defined earlier.

The state vector $\mathbf{x}$ used in the study was of dimension 24, and the corresponding control vector $\mathbf{u}$ was of dimension 2 and the the dimension of the output vector defined in equation 4.2, was 38. The matrices A, B, C, D are given in Appendix B. The state and output vectors are described in detail in sections 4.3 and 4.4.

4.3 Definition of the State Vector

The state vector $\mathbf{x}$ was defined as,

$$\mathbf{x} = \begin{bmatrix} x_1 \\ x_2 \\ \cdot \\ \cdot \\ \cdot \\ \cdot \\ x_{23} \\ x_{24} \end{bmatrix} . \qquad 4.3$$

The state variables x_i, $i = 1,2,...,24$ are defined in table 4.2.

Definition	State	Symbol	Units
Vertical Velocity	x_1	w	in/s (0.0254 m/s)
Normalised pitch rate	x_2	q	in/s (0.0254 m/s)
Flexural mode velocity	$x_3,\ldots,x_8$	$\dot{\xi}_\kappa$ $\kappa=1,\ldots,6$	in/s (0.0254 m/s)
Flexural mode displacement	$x_9,\ldots,x_{14}$	ξ_κ $\kappa=1,\ldots,6$	in (0.0254 m)
Aileron deflection	x_{15}	δ_a	radian
Inboard elevator deflection	x_{16}	δ_{e_i}	radian
Outboard elevator deflection	x_{17}	δ_{e_o}	radian
Küssner gust states	$x_{18},\ldots,x_{22}$		
Dryden filter state	x_{23}		
Vertical gust velocity	x_{24}	w_g	in/s (0.0254 m/s)

Table 4.2: State Variable definition

4.3.1 Rigid Body Motion with Flexibility Effects

The rigid body longitudnal motion of the C-5A, which represents the short period small perturbation motion, with the addition of the first six flexural modes of the wing derived in the body-fixed axes , was represented by the following equations,

---

§ The model of the C-5A was in imperial units, whereas in this thesis S.I units are used throughout. Equivalent S.I unit and an appropriate conversion factor is given within the parantheses, to convert Imperial units to S.I units.

$$\dot{w} = Z_w w + U_o q + \sum Z_{\delta_i} \delta_i + \sum Z_{\xi_\kappa} \xi_\kappa + \sum Z_{\dot{\xi}_\kappa} \dot{\xi}_\kappa \quad , \qquad 4.4^{\S}$$

$$\dot{q} = M_w w + M_{\dot{w}} \dot{w} + M_q q + \sum M_{\delta_i} \delta_i + \sum M_{\xi_\kappa} \xi_\kappa + \sum M_{\dot{\xi}_\kappa} \dot{\xi}_\kappa \quad , \qquad 4.5^{\S}$$

where, w is the vertical velocity, q is the normalised pitch rate[¶], $\dot{\xi}_\kappa$ is the flexural mode rate associated with the κ^{th} mode , ξ_κ is the flexural mode displacement associated with the κ^{th} mode, $Z_{(.)}$[‡] is the dimensional stability derivative,which denotes the change in vertical force due to changes in (.). $M_{(.)}$ is the dimensional stability derivative, which denotes the change in pitching moment due to changes in (.). δ_i 's represent the deflections of the control surfaces. Substitution of equation 4.4 in equation 4.5 yields,

$$\dot{q} = (M_w + M_{\dot{w}} Z_w) w + (M_q + M_{\dot{w}} U_o) q + \sum (M_{\delta_i} + M_{\dot{w}} Z_{\delta_i}) \delta_i + \sum (M_{\xi_\kappa} + M_{\dot{w}} Z_{\xi_\kappa}) \xi_\kappa + \sum (M_{\dot{\xi}_\kappa} + M_{\dot{w}} Z_{\dot{\xi}_\kappa}) \dot{\xi}_\kappa \quad . \qquad 4.6$$

$(i = 1, \ldots, 3 \quad \text{and} \quad \kappa = 1, \ldots, 6)$

If equation 4.4 and equation 4.6 are compared with equations representing only the rigid body short period oscillation, viz;

---

§ Inclusion of the unsteady aerodynamics is deferred until section 4.3.4

¶ The normalised pitch rate q is defined as

q = pitch rate in rad per sec/ n_2

where n_2 is a conversion factor equalling $0.6066 * 10^{-3}$ rad/m

‡ The subscript (.) is used to denote any of the variables w, q, δ_i, $\dot{\xi}_i$ and ξ_i

$$\dot{w} = Z_w w + U_o q + \sum Z_{\delta_i} \delta_i \ ,$$

$$\dot{q} = (M_w + M_{\dot{w}} Z_w) w + (M_q + M_{\dot{w}} U_o) q + \sum (M_{\delta_i} + M_{\dot{w}} Z_{\delta_i}) \delta_i \ .$$

It is observed that equations 4.4 and 4.6 are virtually the same as the rigid body equations, except for the addition of the aerodynamic terms coupling them to flexural modes. The state variable x_1 was defined as w, and x_2 was defined as q.

4.3.2 Representation of Flexural Modes

The structural flexibility effects were represented by the equation in terms of dimensional stability derivatives,viz:

$$\ddot{\xi}_j + 2\zeta_j \omega_j \dot{\xi}_j + \omega_j^2 \xi_j = E_{j_{\dot{w}}} \dot{w} + E_{j_w} w + E_{j_q} q + \sum E_{j_{\delta_i}} \delta_i + \sum E_{j_{\xi_\kappa}} \xi_\kappa + \sum E_{j_{\dot{\xi}_\kappa}} \dot{\xi}_\kappa \cdot \begin{cases} \text{for } j=1,\ldots,6 \\ \text{for } i=1,\ldots,3 \\ \text{for } \kappa=1,\ldots,6 \end{cases}$$

Alternatively the equation above can be expressed as,

$$\ddot{\xi}_j = E_{j_{\dot{w}}} \dot{w} + E_{j_w} w + E_{j_q} q + \sum E_{j_{\delta_i}} \delta_i + \{\sum E_{j_{\xi_\kappa}} \xi_\kappa\} + \{\sum E_{j_{\dot{\xi}_\kappa}} \dot{\xi}_\kappa\} - 2\zeta_j \omega_j \dot{\xi}_j - \omega_j^2 \xi_j \ . \quad 4.7$$

Substituting equation 4.4 (expression for $\dot{w}$) in equation 4.7 yields,

$$\ddot{\xi}_j = E_{j_{\dot{w}}} \{Z_w w + U_o q + \sum Z_{\delta_i} \delta_i + \sum Z_{\xi_\kappa} \xi_\kappa + \sum Z_{\dot{\xi}_\kappa} \dot{\xi}_\kappa\} + E_{j_w} w + E_{j_q} q + \sum E_{j_{\delta_i}} \delta_i +$$

$$\{\sum E_{j_{\xi_\kappa}} \xi_\kappa\} + \{\sum E_{j_{\dot{\xi}_\kappa}} \dot{\xi}_\kappa\} - 2\zeta_j \omega_j \dot{\xi}_j - \omega_j^2 \xi_j \ , \quad 4.8$$

which after simplification becomes,

$$\ddot{\xi}_j = \hat{E}_{j_w} w + \hat{E}_{j_q} q + \sum \hat{E}_{j_{\delta_i}} \delta_i + \{\sum \hat{E}_{j_{\xi_\kappa}} \xi_\kappa\} + \{\sum \hat{E}_{j_{\dot{\xi}_\kappa}} \dot{\xi}_\kappa\} - 2\zeta_j \omega_j \dot{\xi}_j - \omega_j^2 \xi_j \quad . \qquad 4.9$$

The circumflexed coefficients $E_{j_{(.)}}$ which appear in equation 4.9 are defined as,

$$\hat{E}_{j_w} = (E_{j_{\dot{w}}} Z_w + E_{j_w}) \,, \quad \hat{E}_{j_{\dot{\xi}_\kappa}} = (E_{j_{\dot{w}}} Z_{\dot{\xi}_\kappa} + E_{j_{\dot{\xi}_\kappa}}) \,, \quad \hat{E}_{j_q} = (E_{j_{\dot{w}}} U_o + E_{j_q})$$

$$\hat{E}_{j_{\xi_\kappa}} = (E_{j_{\dot{w}}} Z_{\xi_\kappa} + E_{j_{\xi_\kappa}}) \,, \quad \hat{E}_{j_{\delta_i}} = (E_{j_{\dot{w}}} Z_{\delta_i} + E_{j_{\delta_i}}) \,.$$

Each circumflexed coefficient $E_{j_{(.)}}$ is a dimensional stability derivative which denotes a change in the vertical force in the j^{th} mode due to changes in (.)[§].

The second order differential equation (equation 4.9) was reduced to two first order differential equations, for implementation in the state variable form, through the substitution of,

$$x_{j+2} = \dot{\xi}_j \,, \quad j = 1, 2, \ldots, 6 \,, \qquad 4.10$$

$$x_{j+8} = \xi_j \,, \quad j = 1, 2, \ldots, 6 \,. \qquad 4.11$$

[§] (.) denotes either of the variables $\dot{\xi}_\kappa$, ξ_κ, δ_i, w, q

The six flexural modes, were represented in the state variable form by the following equation,

$$\begin{bmatrix} \dot{x}_3 \\ \dot{x}_4 \\ \cdot \\ \cdot \\ \cdot \\ \dot{x}_{13} \\ \dot{x}_{14} \end{bmatrix} = \begin{bmatrix} A_1 \\ 0 \end{bmatrix} \begin{bmatrix} x_1 \\ x_2 \end{bmatrix} + \begin{bmatrix} A_2 & A_3 \\ I & 0 \end{bmatrix} \begin{bmatrix} x_3 \\ x_4 \\ \cdot \\ \cdot \\ \cdot \\ x_{13} \\ x_{14} \end{bmatrix} + \begin{bmatrix} A_4 \\ 0 \end{bmatrix} \begin{bmatrix} \delta_1 \\ \delta_2 \\ \delta_3 \end{bmatrix} + \text{Unsteady Aerodyn. effects} \qquad 4.12^{\S}$$

where, I is an identity matrix corresponding to $\xi_j = \int \dot{\xi}_j$, and the matrices A_1, A_2, A_3, and A_4 are given as,

$$A_1 = \begin{bmatrix} \hat{E}_{1_w} & \hat{E}_{1_q} \\ \cdot & \cdot \\ \cdot & \cdot \\ \cdot & \cdot \\ \hat{E}_{6_w} & \hat{E}_{6_q} \end{bmatrix} \qquad 4.13$$

$$A_2 = \begin{bmatrix} \hat{E}_{1_{\dot{\xi}_1}} - 2\zeta_1 \omega_1 & \hat{E}_{1_{\dot{\xi}_2}} & \cdot & \cdot & \hat{E}_{1_{\dot{\xi}_6}} \\ \hat{E}_{2_{\dot{\xi}_1}} & \hat{E}_{2_{\dot{\xi}_2}} - 2\zeta_2 \omega_2 & \cdot & \cdot & \hat{E}_{2_{\dot{\xi}_6}} \\ \cdot & \cdot & \cdot & \cdot & \cdot \\ \cdot & \cdot & \cdot & \cdot & \cdot \\ \hat{E}_{6_{\dot{\xi}_1}} & \cdot & \cdot & \cdot & \hat{E}_{6_{\dot{\xi}_6}} - 2\zeta_6 \omega_6 \end{bmatrix} \qquad 4.14$$

---

§ Unsteady aerodynamic effects are delt with in section 4.3.4.

$$A_3 = \begin{bmatrix} \hat{E}_{1_{\xi_1}} - \omega_1^2 & \hat{E}_{1_{\xi_2}} & \cdot & \cdot & \hat{E}_{1_{\xi_6}} \\ \hat{E}_{2_{\xi_1}} & \hat{E}_{2_{\xi_2}} - \omega_2^2 & \cdot & \cdot & \hat{E}_{2_{\xi_6}} \\ \cdot & \cdot & \cdot & \cdot & \cdot \\ \cdot & \cdot & \cdot & \cdot & \cdot \\ \hat{E}_{6_{\xi_1}} & \cdot & \cdot & \cdot & \hat{E}_{6_{\xi_6}} - \omega_6^2 \end{bmatrix} \qquad 4.15$$

$$A_4 = \begin{bmatrix} \hat{E}_{1_{\delta_1}} & \hat{E}_{1_{\delta_2}} & \hat{E}_{2_{\delta_3}} \\ \cdot & \cdot & \cdot \\ \cdot & \cdot & \cdot \\ \cdot & \cdot & \cdot \\ \hat{E}_{6_{\delta_1}} & \hat{E}_{6_{\delta_2}} & \hat{E}_{6_{\delta_3}} \end{bmatrix} \qquad 4.16$$

4.3.3 Control Surface Deflections

The deflection of the control surfaces were considered to arise as a result of commands being applied to the servo-actuators. The mathematical models of the actuators were considered to be linear and of first order, being represented by simple time lags. The three control surfaces modelled were,

a) symmetrically deflected ailerons,

b) inboard elevator,

c) outboard elevator.

The actuator dynamics associated with the control surfaces were represented by;

Ailerons

$$\frac{\delta_a(s)}{\delta_{a_c}(s)} = \frac{6.0}{s + 6.0} \quad . \tag{4.17}$$

Inboard elevator

$$\frac{\delta_e(s)}{\delta_{e_{i_c}}(s)} = \frac{7.5}{s + 7.5} \quad . \tag{4.18}$$

Outboard elevator

$$\frac{\delta_{e_o}(s)}{\delta_{e_{o_c}}(s)} = \frac{7.5}{s + 7.5} \quad . \tag{4.19}$$

However, in this research only commands to the actuators associated with the ailerons and the inboard elevator were considered , the command input δ_{e_o} was equal to zero, therefore equation 4.19 was written as,

$$\dot{\delta}_{e_o} = -7.5\, \delta_{e_o} \cdot \tag{4.20}$$

x_{15}, x_{16} and x_{17} were defined as δ_a, δ_{e_i} and δ_{e_o} respectively. The dimension of the control vector was 2, and B matrix was of the order [24 * 2].

4.3.4 Küssner Dynamics

Küssner dynamics account for the unsteady aerodynamic effects associated with the change of lift with time, experienced by a lifting surface when it is disturbed by a unit step gust, Bisplinghoff et al [1955]. The Küssner function $\psi_K(t)$ is better approximated by the Sear's function, which for aerofoils of aspect ratio of greater than 6 is given by,

$$J(c) = 1 - 0.5\, e^{-0.13\, c_o} - 0.5\, e^{-c_o}, \qquad 4.21$$

where,

$$c_o = \frac{U_o\, t}{0.5\, \gamma\, \bar{c}} \quad . \qquad 4.22$$

Equation 4.21 is the expression for the output obtained when a unit step input ,such as the edge of a gust, strikes the aerofoil, for the C-5A following data applied;

γ	=	1.38	(mach number correction factor)
$\bar{c}_w$	=	9.429 m	(mean aerodynamic chord of the wing)
$\bar{c}_T$	=	4.660 m	(mean aerodynamic chord of the tail)
U_o	=	143.0 m/s	(forward airspeed)
AR	=	7.75	(aspect ratio of the wing)

After substitution of numerical values for the wing and tail equation 4.21 can be shown to be,

$$J_w(t) = 1.0 - 0.5\, e^{-2.857\, t} - 0.5\, e^{-21.979\, t} \quad . \qquad 4.23$$

$$J_T(t) = 1.0 - 0.5\, e^{-5.781\, t} - 0.5\, e^{-44.470\, t} \quad . \qquad 4.24$$

The transfer function of equations 4.23 and 4.24 for a unit step gust input, can be shown to be:

$$\frac{J_w(s)}{w_g(s)} = \frac{(0.198\,s + 1)}{(0.387\,s + 1)\,(0.0455\,s + 1)}\ , \qquad 4.25$$

similarly,

$$\frac{J_T(s)}{w_g(s)} = \frac{(0.098\,s + 1)}{(0.173\,s + 1)\,(0.022\,s + 1)}\ . \qquad 4.26$$

The frequency response diagrams of the transfer functions in equations 4.25 and 4.26 are shown as figures 4.1 and 4.2 respectively for a unit step gust input. Approximations to the transfer functions of equation 4.25 and 4.26 were made which are also shown on figures 4.1 and 4.2 as dashed curves. The approximate transfer function from figure 4.1 can be seen to be:

$$\bar{G}_w(s) = \frac{1.0}{(1 + s\,T)} = \frac{1.0}{(1 + 0.091\,s)} = \frac{10.98}{(s + 10.98)}\ , \qquad 4.27$$

and from figure 4.2,

$$\bar{G}_T(s) = \frac{1.0}{(1 + s\,T)} = \frac{1.0}{(1 + 0.045\,s)} = \frac{22.2}{(s + 22.2)}\ . \qquad 4.28$$

In state variable form equations 4.27 and 4.28 can be written as,

Tail :

$$\dot{x}_{18} = -22.2\,x_{18} + 22.2\,w_g\ . \qquad 4.29$$

Wing :

$$\dot{x}_{22} = -10.98\,x_{22} + 10.98\,w_g\ . \qquad 4.30$$

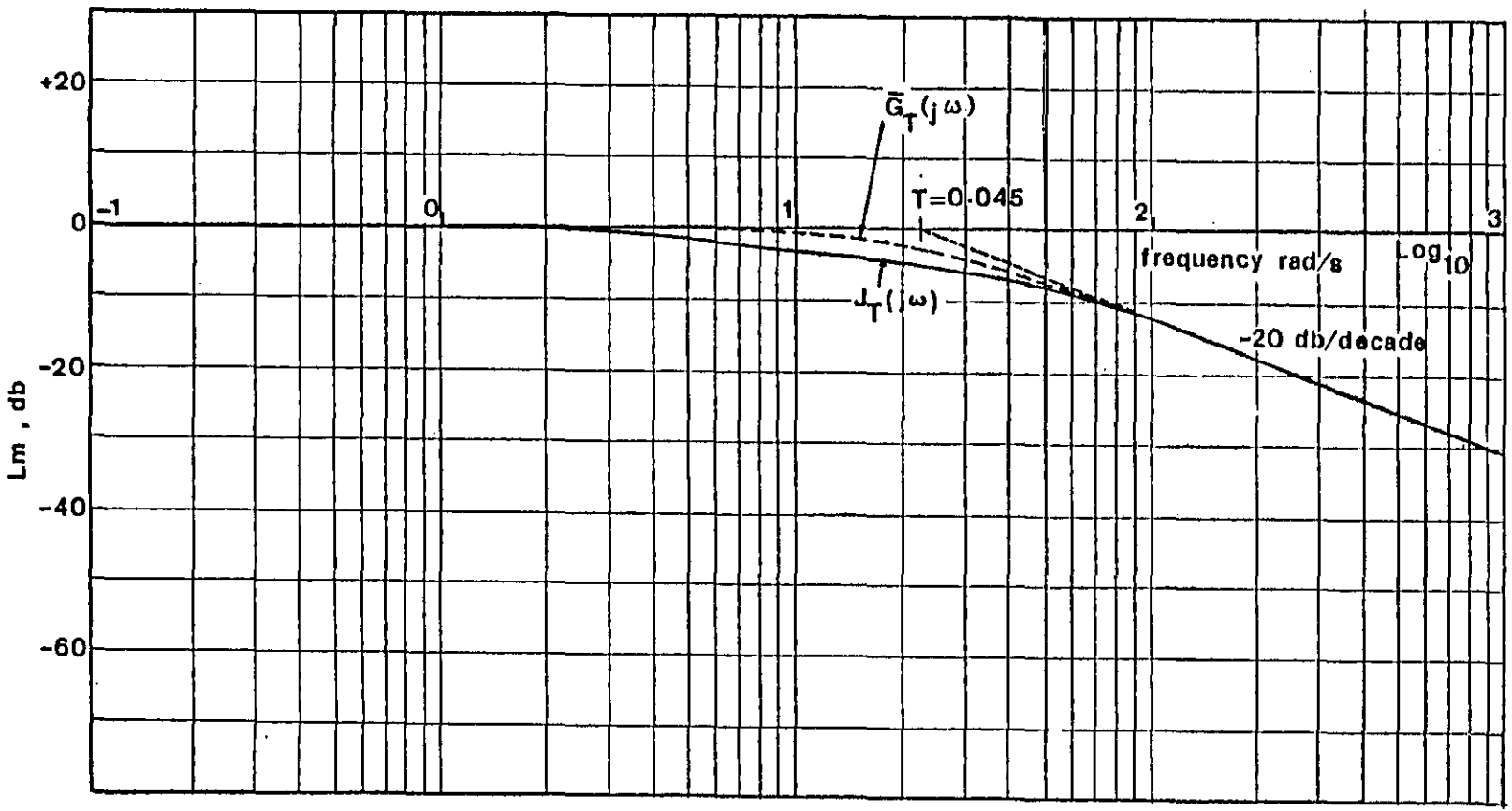

Figure 4.1 : Frequency response diagram of the transfer function representing the Küssner dynamics associated with the tail.

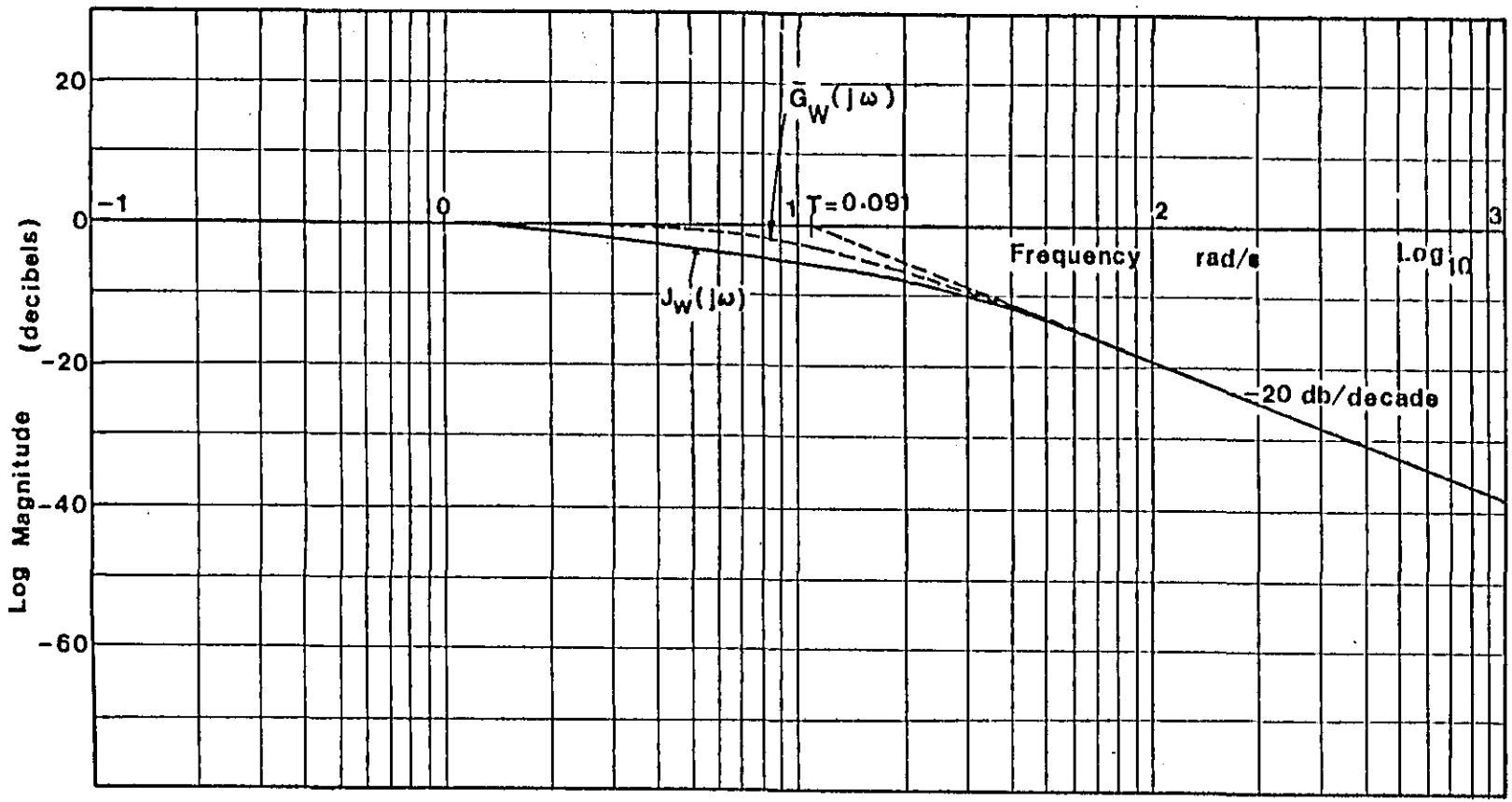

Figure 4.2 : Frequency response diagram of the transfer function representing the Küssner dynamics associated with the wing.

Since the nose of the aircraft penetrates the gust field before its wing or its tail the gust effect will be delayed - a pure transport delay. For the tail,at a distance of 56.1 m behind the nose the time delay, at the given forward airspeed U_o,was:

$$T_T = \frac{56.1}{U_o} = 0.393 \text{ seconds} \quad . \qquad 4.31$$

A pure transport lag is characterised by the transfer function,viz:

$$G_T(s) = e^{-s T_d} \quad . \qquad 4.32^{\S}$$

Equation 4.32 cannot be incorporated in the state equation in its exponential form. The Padé table for e^{-sT_d} furnishes a particularly simple algebraic function(Wall [1948], Truxal [1955]). The Padé approximation is a rational algebraic function, with numerator polynomial of order p_n and a denominator polynomial of order p_m, such that the maximum number of terms in the Taylor series expansion of the approximant agree with similar terms in the expansion of the exponential function of equation 4.32. The choice of the order of the polynomials depends on the required accuracy of the approximation, if T_d is small then the higher order terms in the Taylor series expansion of equation 4.32 can be neglected, and hence a low order Padé approximant may be used.

To represent the time lag T_T (equation 4.31) a first over second order Padé approximant was used, viz:

$$G_{T_T}(s) = \frac{1 - \frac{1}{3} s T_T}{1 + \frac{2}{3} s T_T + \frac{1}{6} s^2 T_T^2} \quad . \qquad 4.33$$

---

§ T_d is the time delay in seconds and s is the Laplace variable.

Equation 4.33 after substitution of T_T, becomes:

$$G_{T_T}(s) = \frac{1 - 0.131\,s}{1 + 0.262\,s + 0.02574\,s^2} \quad , \tag{4.34}$$

division of the numerator by 0.131 and division of the denominator by 0.02574 yields,

$$G_{T_T}(s) = \frac{296.6\,(5.098 - s)}{s^2 + 10.18\,s + 38.85} \quad . \tag{4.35}$$

The Padé approximant to represent the transport lag to the tail as given in Prasad[1980], is,

$$G_{T_T}(s) = \frac{198.5\,(1 + 0.458\,s)}{s^2 + 10.19 + 38.95} \quad . \tag{4.36}$$

Re-expressing equation 4.36,

$$G_{T_T}(s) = \frac{90.913\,(2.184 + s)}{s^2 + 10.19\,s + 38.95} \quad . \tag{4.37}$$

Clearly, the transfer function of equation 4.37 does not agree with the first over second order Padé approximant of equation 4.35 (especially the numerator polynomial). However, in order to validly compare the results obtained by Prasad (i.e,.reduction of bending and torsional moments arising as a result of manoeuvre commands and atmospheric turbulence) and results presented in chapter 5, the transfer function of equation 4.37 was employed to represent the time delay T_T. In state variable form the transfer function can be written as:

$$\dot{x}_{20} = x_{21} - 5.096\,x_{18} \tag{4.38}$$

$$\dot{x}_{21} = 90.891\,x_{18} - 38.95\,x_{20} - 10.19\,x_{21} \tag{4.39}$$

The block diagram of the gust effect on the tail is shown as figure 4.3. Similarly the delay on the gust appearing at the leading edge of the wing, 16.702 m aft of the nose, at the given airspeed, was,

$$T_W = \frac{16.702}{U_o} = 0.1168 \text{ seconds} \quad . \tag{4.40}$$

This delay was represented by a zeroth over first order Padé approximant, whose transfer function was,

$$G_{T_W}(s) = \frac{1.0}{(1 + s\,T_W)} = \frac{1.0}{(1 + 0.1168\,s)} \quad , \tag{4.41}$$

where,

$$G_{T_W}(s) = \frac{x_{19}(s)}{x_{22}(s)} \quad . \tag{4.42}$$

In state variable form, equation 4.39 can be expressed as,

$$\dot{x}_{19} = -8.549\, x_{19} + 8.549\, x_{22} \quad . \tag{4.43}$$

The block diagram of the gust effect striking the leading edge of the wing is shown as figure 4.4. Equations 4.5, 4.6 and 4.12 do not contain the effect of gust delays and the unsteady aerodynamic effects associated with the wing and the tail. State variables x_{18} and x_{19} are added to equation 4.5, 4.6 and 4.12 via the appropriate stability derivatives.

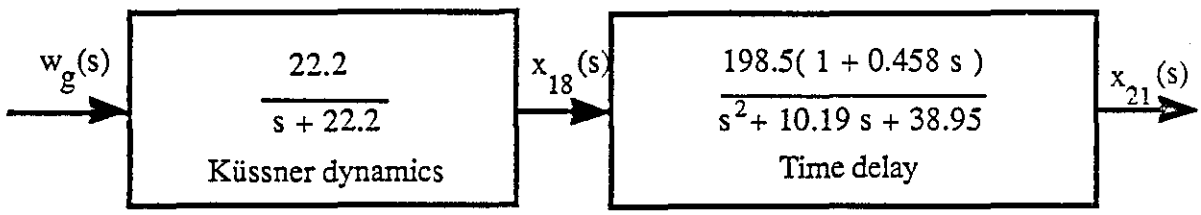

Figure 4.3 : Block diagram representation of the gust effect on the tail.

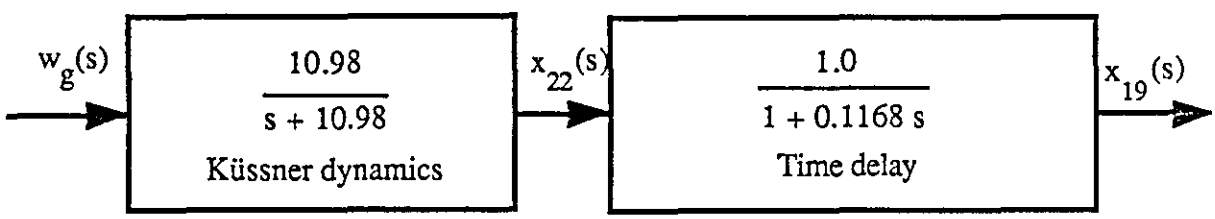

Figure 4.4 : Block diagram representation of the gust effect on the wing.

4.3.5 Mathematical Model of Atmospheric Turbulence

The most widely used models to simulate atmospheric turbulence in aeronautical engineering studies, produce signals with power spectral densities (P.S.D's) which match those obtained from experimental investigations. These models are:

a) The Von Karman model

b) The Dryden model

Since only the vertical component of the gust was used in this research study, the appropriate power spectral density of the vertical gust velocity, for the two models is,

Von Karman

$$\Phi_{w_g}(\omega) = \frac{\sigma^2_{w_g} L \left[1.2667 \left(1.339 L \omega \right)^2 \right]}{\left(1 + 1.339 L \omega \right)^{\frac{11}{6}}} \quad , \qquad 4.44$$

Dryden

$$\Phi_{w_g}(\omega) = \frac{\sigma^2_{w_g} L[1 + 3 (L\omega)^2]}{\left[1 + (L \omega)^2 \right]^2} \quad , \qquad 4.45$$

where $L = L_w/U_o$, $\sigma^2_{w_g}$ is the variance of the gust velocity, L_w is the scale length of turbulence, U_o is the aircraft forward speed, ω is the spatial frequency. Following data applies for the two models,

U_o	143 m/s
L_w	576 m
σ_{w_g}	0.3048 m/s
$L = L_w/U_o$	4.028

The power spectral densities (P.S.D) of the two models are shown as figure 4.5. It is seen from figure 4.5 that the Dryden model produces a P.S.D which closely approximates that produced by the Von Karman model. Inclusion of the Von Karman model in the state equations, to produce a P.S.D such as that of equation 4.44 is very difficult on account of the non integer exponent. As a result of this difficulty it is common practice (and has been followed in this work) to employ the Dryden model.

It is known (Chang [1955]) that the power spectral density of a random signal is completely determined by the filter characteristics and is given by,

$$\Phi_{w_g}(\omega) = \left| G_{w_g}(j\,\omega) \right|^2 \Phi_{\eta}(\omega) \quad , \tag{4.46}$$

where $\sigma_{w_g}(\omega)$ is the power spectral density of the gust velocity, $\Phi_{\eta}(\omega)$ is the power spectral density of the input white noise and $G_{w_g}(j\omega)$ is the filter transfer function. From equations 4.45 and 4.46, it can be shown that,

$$G_{w_g}(s) = \sigma_{w_g} \frac{\sqrt{L}\,(1 + 1.732\,L\,s)}{(1 + L\,s)^2} \quad . \tag{4.48}$$

The appropriate block diagram of the filter is shown as figure 4.6, whose input is white noise and the output is the vertical gust velocity. A model of the Dryden filter was incorporated in the state equation as follows, from figure 4.6

$$\frac{w_g(s)}{\eta(s)} = \sigma_{w_g} \frac{\sqrt{L}\,(1 + 1.732\,L\,s)}{(1 + L\,s)^2} \quad . \tag{4.48}$$

Re-expression of equation 4.48 yields,

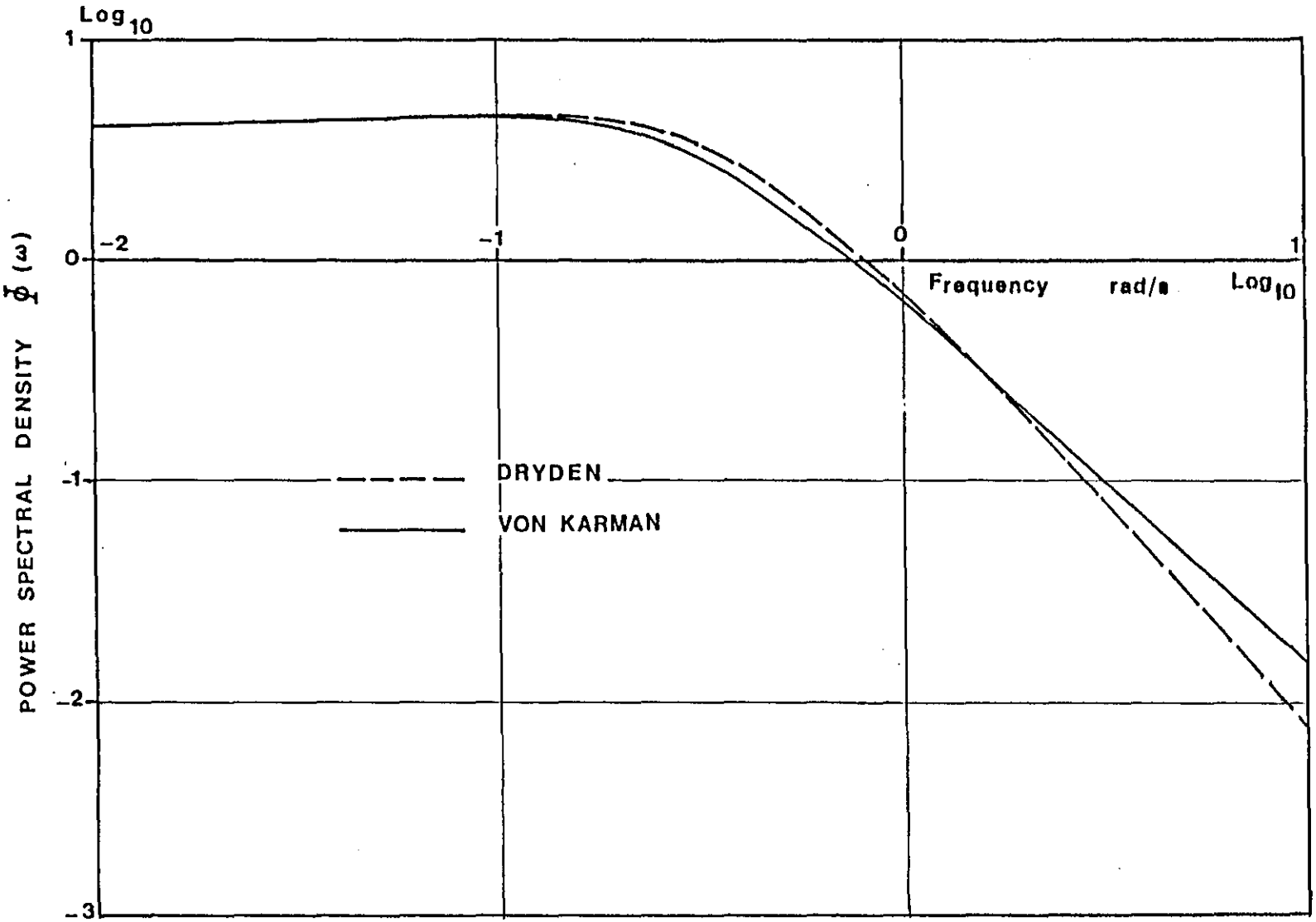

Figure 4.5 : Frequency response diagram of the Dryden and Von Karman models.

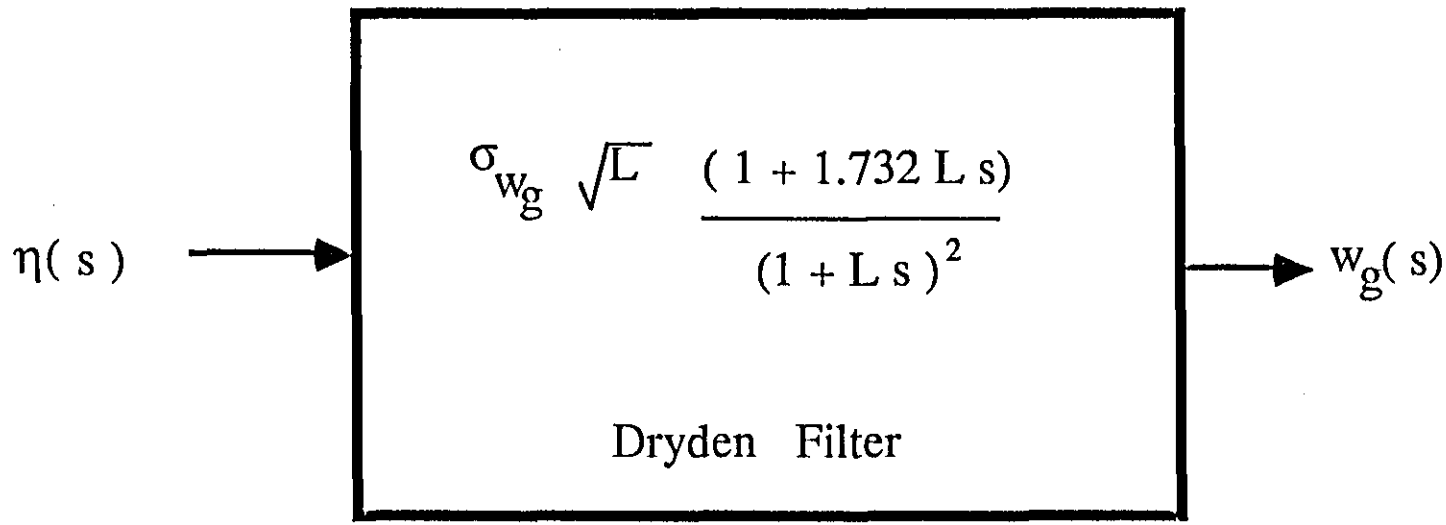

Figure 4.6 : Block diagram representation of the dryden filter.

$$L^2\ddot{w}_g + 2L\dot{w}_g + w_g = \sigma_{w_g}\sqrt{L}\,\eta + \sqrt{3}\,\sigma_{w_g}\sqrt{L^3}\,\dot{\eta} \quad . \tag{4.49}$$

Division of equation 4.49 by L^2 throughout, and re- arrangement yields,

$$\ddot{w}_g = \frac{2}{L}\dot{w}_g - \frac{1}{L^2}w_g + \frac{\sigma_{w_g}}{L^{3/2}}\eta + \frac{\sqrt{3}\,\sigma_{w_g}}{L^{1/2}}\dot{\eta} \quad . \tag{4.50}$$

Let,

$$x_{24} = w_g \quad , \tag{4.51}$$

and ,

$$x_{23} = \dot{w}_g - \frac{\sqrt{3}\,\sigma_{w_g}}{L^{1/2}}\eta \quad . \tag{4.52}$$

Differentiation of equation 4.51 and 4.52 yields,

$$\dot{x}_{24} = \dot{w}_g \quad , \tag{4.53}$$

$$\dot{x}_{23} = \ddot{w}_g - \frac{\sqrt{3}\,\sigma_{w_g}}{L^{1/2}}\dot{\eta} \quad . \tag{4.54}$$

Substitution of equation 4.52 in 4.53 yields,

$$\dot{x}_{24} = x_{23} + \frac{\sqrt{3}\,\sigma_{w_g}}{L^{1/2}}\eta \quad , \tag{4.55}$$

substitution of equation 4.50 (with $x_{24} = w_g$) in 4.54 yields,

$$\dot{x}_{23} = -\frac{2}{L}\dot{x}_{24} - \frac{1}{L^2}x_{24} + \frac{\sigma_{w_g}}{L^{3/2}}\eta \quad , \tag{4.56}$$

substitution of equation 4.55 in 4.56 yields,

$$\dot{x}_{23} = -\frac{2}{L}x_{23} - \frac{1}{L^2}x_{24} + \frac{(1 - 2\sqrt{3})\,\sigma_{w_g}}{L^{3/2}}\eta \quad . \tag{4.57}$$

With $L = 4.028$, and $\sigma_{w_g} = 0.3048$, equation 4.55 and 4.57 can be expressed in the matrix form as:

$$\begin{bmatrix} \dot{x}_{23} \\ \dot{x}_{24} \end{bmatrix} = \begin{bmatrix} -0.497 & -0.062 \\ 1 & 0 \end{bmatrix} \begin{bmatrix} x_{23} \\ x_{24} \end{bmatrix} + \begin{bmatrix} -0.093 \\ 0.262 \end{bmatrix} \eta \quad . \tag{4.58}$$

State variable x_{24} was defined as the vertical gust velocity w_g.

4.4 Definition of the Output Vector

The output vector was defined as,

$$y = \begin{bmatrix} BM_i, TM_i & i = 1,2,3,4,5 \\ \dot{BM}_i, \dot{TM}_i & i = 1,2,3,4,5 \\ \dot{\xi}_\kappa & \kappa = 1, 2, ..., 6 \\ \xi_\kappa & \kappa = 1, 2, ..., 6 \\ \dot{\delta}_a & \\ \dot{\delta}_{e_i} & \\ \delta_a & \\ \delta_{e_i} & \\ w & \\ q & \end{bmatrix} = \begin{bmatrix} y_1, \ldots, y_{10} \\ y_{11}, \ldots, y_{20} \\ y_{21}, \ldots, y_{26} \\ y_{27}, \ldots, y_{32} \\ y_{33} \\ y_{34} \\ y_{35} \\ y_{36} \\ y_{37} \\ y_{38} \end{bmatrix}$$

where BM_i denotes Bending moment at the i^{th} wing station, and TM_i is the torsion moment at the i^{th} wing station, $\dot{\xi}_i$ is the mode rate associated with the ith flexural mode, ξ_i is the mode displacement associated with the ith flexural mode. $\dot{\delta}_a$, $\dot{\delta}_{e_i}$, δ_a,and δ_{e_i} are aileron and inboard elevator deflection rates and displacements respectively. Henceforth the subscript i to denote the inboard elevator is dropped for convenience. w and q are rigid body vertical velocity and the normalised pitch rate .The five specific wing stations at which each of the bending and torsion moments are defined [Stone, Ward, Harvey et al (1972)] are shown as figure 4.7.

4.5 Excitation Cases

In order to evaluate the performance of the uncontrolled aircraft model and the controlled aircraft model artificial test situations were used. Table 4.3 shows the test situations employed. Test

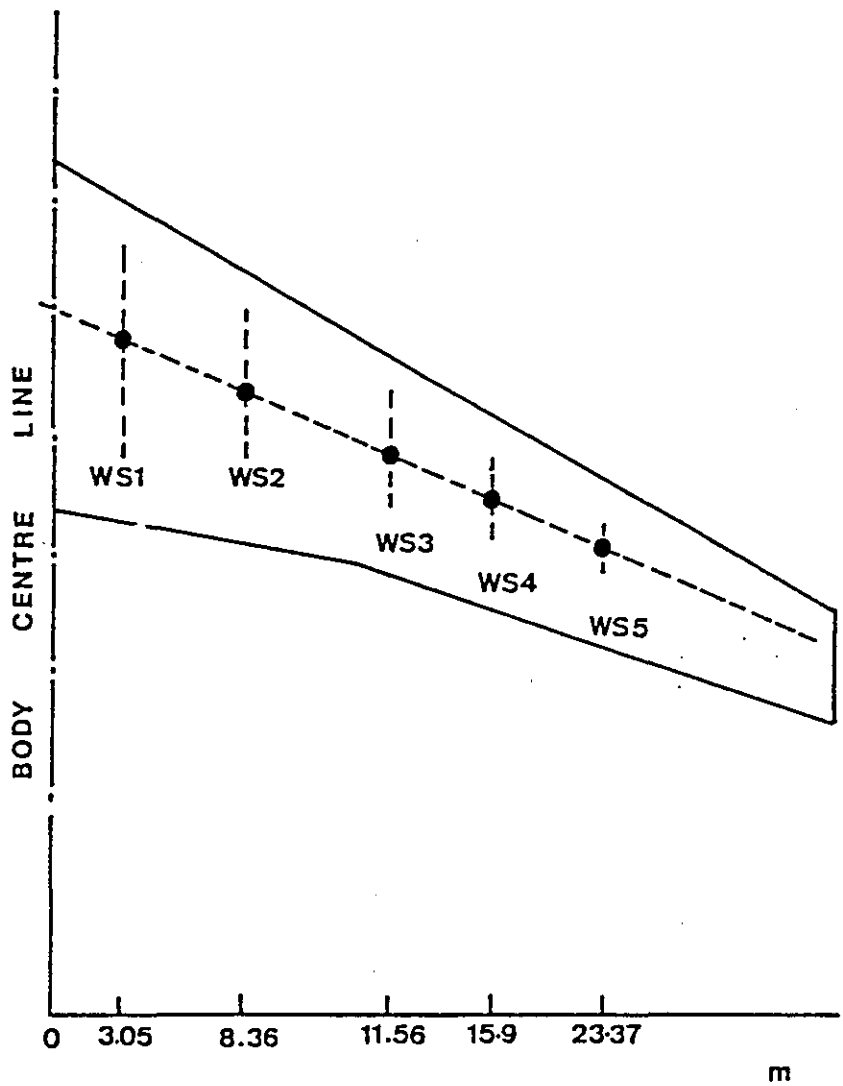

Figure 4.7 : Location of wing stations

case SC1 relates to the case when the model was excited by an initial condition on the perturbation vertical velocity, w(0)=7.15 m/s, whilst initial conditions on other states, the command vector and η (white noise) were zero at t = 0. In test case SC2 the model was disturbed by a step aileron command, δ_{a_c} = 0.025 radians , whilst initial conditions on the states, inboard elevator command, and white noise were zero. Test case SC3 relates to the case when x(0)=0, δ_{a_c} =0.0, η=0, and a step elevator command, δ_{e_c} = 0.01 radians, was applied. For simulation of atmospheric turbulence, test case SC4 was employed, in which white noise of zero mean, having a standard deviation of 0.3048 m/s, was applied at the input of the Dryden filter whose output was the vertical gust velocity. For case SC4 , x(0)=0, u(0)=0 .

CASE	w (m/s)	δ_{a_c} (rad)	δ_{e_c} (rad)	η § (m/s)
SC1	7.15	0	0	0
SC2	0	0.025	0	0
SC3	0	0	0.01	0
SC4	0	0	0	0.3048

Table 4.3: Excitation cases

4.6 Manoeuvre Commands

It was shown in chapter 3 that a feedback control law of the type,

$$\mathbf{u} = \mathbf{K}\,\mathbf{x} \qquad 4.60$$

could be obtained by assigning both the eigenvalues and the eigenvectors. This method was used

§ The standard deviation of white noise of 0.3048 corresponds to moderate levels of turbulence.

in the design of feedback controllers to achieve load reduction on the C-5A, i.e. to achieve a reduction of bending and torsional moments at the five wing stations in response to the test cases described in section 4.5.

In order to make a valid comparison of the performance of the uncontrolled aircraft, with that of the controlled aircraft, the rigid body motion variables namely, vertical velocity, w , and the normalised pitch rate, q, were forced in the closed-loop system to the same steady-state levels as those of the uncontrolled variables w and q, for test cases SC2 and SC3. Since the response of the aircraft due to manoeuvre commands and atmospheric turbulence was considered separately, the state equation representing the dynamics of the C-5A, in the absence of any white noise, was represented by equation ,

$$\dot{\mathbf{x}} = \mathbf{A}\mathbf{x} + \mathbf{B}\mathbf{u} \ , \qquad 4.61$$

at steady state, $\dot{\mathbf{x}} = \mathbf{0}$ and $\mathbf{x} = \mathbf{x}_{ss}$, therefore from equation 4.61, for a command input $\mathbf{u}$,

$$\mathbf{x}_{ss} = -\mathbf{A}^{-1}\,\mathbf{B}\,\mathbf{u} \ . \qquad 4.62$$

Substitution of equation 4.60 in 4.61 yields the closed-loop system,viz:

$$\dot{\mathbf{x}} = (\mathbf{A} + \mathbf{BK})\,\mathbf{x} \ . \qquad 4.63$$

In order to force the closed-loop rigid body variables w and q to the same steady-state open-loop values, equation 4.63 was forced by a command vector $\mathbf{r} \in \Re^m$, $\mathbf{r}^T = [\, r_1\, r_2 \ldots\, r_m]$, acting through a suitable matrix $\mathbf{E}$ of the order $[n * m]$, such that,

$$\dot{\mathbf{x}} = (\mathbf{A} + \mathbf{BK}) + \mathbf{Er} \ . \qquad 4.64$$

At steady state, $\dot{\mathbf{x}} = \mathbf{o}$, $\mathbf{x} = \mathbf{x}_{ssc}$, the controlled steady-state vector, from equation 4.64

therefore is,

$$\mathbf{x}_{ssc} = (\mathbf{A} + \mathbf{BK})^{-1}\,\mathbf{Er} \quad . \tag{4.65}$$

If the steady state values of w & q of the uncontrolled aircraft are to be identical to the values of w & q for the controlled aircraft, then from equation 4.62 and 4.65,

$$\mathbf{r} = \mathbf{E}^{\dagger}(\mathbf{A} + \mathbf{BK})\,\mathbf{A}^{-1}\mathbf{Bu} \quad , \tag{4.66}$$

where $\mathbf{E}^{\dagger}$ is the generalised inverse of E. The matrix E was selected to be,

$$\mathbf{E} = \begin{bmatrix} 1 & 0 \\ 0 & 1 \\ 0 & 0 \\ . & . \\ . & . \\ 0 & 0 \end{bmatrix} .$$

If only one closed-loop variable is required to be forced, then the matrix E is of the order [n * 1] and r is then a scaler. The element e_{i1} in E is set to unity corresponding to the i^{th} state. Since two variables were required to be forced, the dimension of the forcing vector was chosen to be 2, and the choice of the elements in E was made such that, w was forced by command r_1 and q was forced by command r_2. The forcing vector r could be determined for a known command vector u (used for exciting the uncontrolled aircraft) and feedback matrix K. The output vector, equation 4.2, for a control law of the type $\mathbf{u} = \mathbf{K}\,\mathbf{x}$ can be written as,

$$\mathbf{y} = (\mathbf{C} + \mathbf{DK})\mathbf{x} \quad . \tag{4.67}$$

At steady-state, $\mathbf{x} = \mathbf{x}_{ssc}$, therefore substitution of equation 4.65 in 4.67, yields,

$$\mathbf{y} = -(\mathbf{C} + \mathbf{DK})(\mathbf{A} + \mathbf{BK})^{-1}\mathbf{Er} \quad . \qquad 4.68$$

Equation 4.68 was used to calculate the steady-state values of the output vector **y**, enabling a comparison of the uncontrolled steady-state levels of the bending and torsional moments with the steady-state levels of the bending and torsional moments of the controlled aircraft, for test case SC2 and SC3. The block diagram of the forced closed-loop system is presented as figure 4.8

4.7 Analysis of the Dynamic Response of the Uncontrolled Aircraft

In order to determine, in the absence of turbulence, dynamical characteristics of the uncontrolled aircraft, represented by equation 4.61, the eigenvalues of matrix **A**, namely $\lambda_{i\ i=1,2,..,n}$ were found from the characteristic equation, viz:

$$\text{Det}\,[\lambda\mathbf{I} - \mathbf{A}] = 0 \quad . \qquad 4.69$$

The eigenvalues as determined from equation 4.69, are presented in table 4.5. The complex conjugate pair λ_1, λ_2 is associated with the short period rigid body motion of the C-5A; λ_3,.., λ_{14} are associated with the first six flexural modes and are listed in the order of ascending frequency; complex conjugate pair λ_3, λ_4 is associated with the first flexural mode, whereas the complex conjugate pair λ_{13}, λ_{14} is associated with the sixth flexural mode. Eigenvalues λ_{15}, λ_{16} and λ_{17} are associated with the aileron, inboard elevator and outboard elevator modes.Eigenvalue λ_{18} is associated with the Küssner dynamics of the tail. Eigenvalue λ_{19} is associated with the first order Padé approximation, representing the time delay on the gust appearing at the leading edge of the wing. The pair λ_{20}, λ_{21} is associated with the second order Padé approximation, representing the time delay on the gust appearing at the tail. Eigenvalue λ_{22} is associated with the Küssner dynamics of the wing. λ_{23} and λ_{24} are associated with the Dryden filter modes.

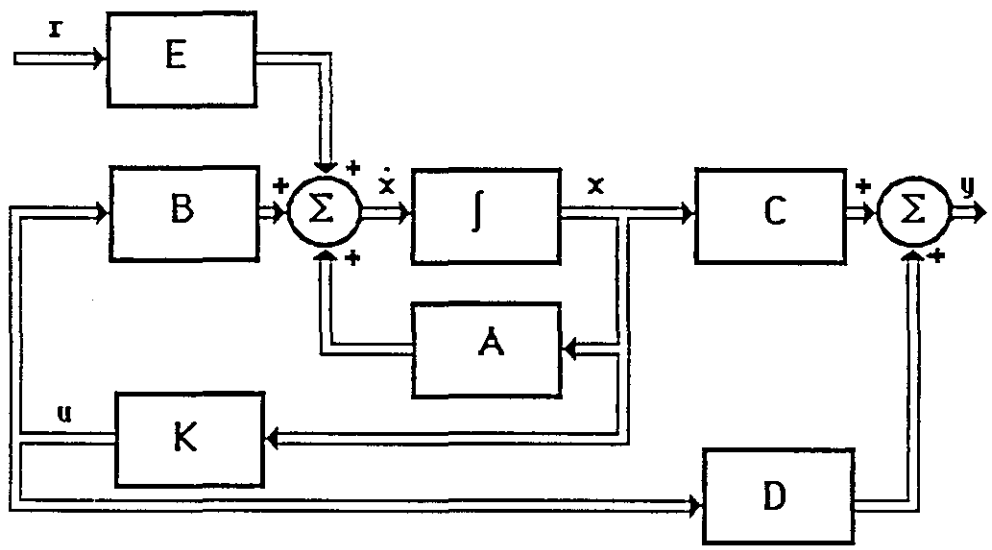

Figure 4.8 : Block diagram representing the closed-loop dynamics of the C-5A Galaxy.

	Eigenvalue $-\sigma \pm j\,\omega$	Natural Frequency ω (rad/s)	Damping Ratio ζ
λ_1 , λ_2	-0.88 ± j 1.27	1.55	0.571
λ_3 , λ_4	-0.51 ± j 5.46	5.48	0.093
λ_5 , λ_8	-0.23 ± j 11.12	11.12	0.021
λ_7 , λ_8	-0.57 ± j 13.80	13.81	0.042
λ_9 , λ_{10}	-0.61 ± j 15.59	15.61	0.039
λ_{11}, λ_{12}	-0.43 ± j 17.48	17.49	0.024
λ_{13}, λ_{14}	-0.62 ± j 18.78	18.79	0.033
λ_{15}	-6.0	-	-
λ_{16}	-7.5	-	-
λ_{17}	-7.5	-	-
λ_{18}	-22.25	-	-
λ_{19}	-8.549	-	-
λ_{20}, λ_{21}	-5.1 ± j 3.6	6.24	0.816
λ_{22}	-10.98	-	-
λ_{23}	-0.247	-	-
λ_{24}	-0.249	-	-

Table 4.4: Eigenvalues of the uncontrolled aircraft

From table 4.5 it is observed that the flexural modes are lightly damped. The damping ratio of the first flexural mode being 0.09 which possessed best damping, all other modes have damping ratio of less than 0.05. It was assumed by Harvey & Pope[1977]¶ that the damping ratios associated with the flexural modes were all equal to 0.1.

¶ On page 217 of Harvey's report the open-loop eigenvalues corresponding to the six flexural modes indicate that the damping ratios associated with the six flexural modes are not all equal to 0.1, contrary to the assumption made by Harvey.

It is evident from table 4.5 that the damping ratios are not all equal to 0.1; these computed values match those given in Harvey and Pope. The damping of the modes can be augmented by state variable feedback, using the eigenpair assignment method described in chapter 3. To examine, which of the modes can be altered by F.S.V.F., the controllability matrix is constructed viz:

$$P_o = U_o^{-1}B \quad , \qquad 4.70$$

where U_o is the modal matrix, whose columns are composed of the eigenvectors of the matrix A. It was found that only the modes associated with eigenvalues $\lambda_1, \ldots, \lambda_{16}$ were controllable i.e, they can be altered by feedback. It has been suggested by McLean [1976], Harvey & Pope[1977] and Prasad[1980] that although the second flexural mode is controllable, the eigenvalue associated with the second flexural mode remains unchanged by feedback. This implies that either the second mode is uncontrollable or the weighting matrices, in the LQP formulation, used by McLean, Harvey and Prasad to compute the feedback control law were inadequate. The later is more likely, because the weighting matrices were choosen by trial and error method. It is shown in chapter 5, that their observation on the controllability of the second flexural mode is not valid. Although the modes associated with eigenvalues $\lambda_{17},\ldots, \lambda_{24}$ are uncontrollable, they are seen to be stable, i.e., all eigenvalues have negative real parts, see table 4.4.

The time response of bending and torsion moments of the uncontrolled aircraft for test case SC1 is shown on figure 4.9 and figure 4.10 respectively. It is observed that the response is oscillatory, which from the fatigue point of view for the subject aircraft is not desirable, Konar et al [1976]. The time responses of the bending and torsion moments for test cases SC2 an SC3 are presented as figures 4.11, 4.12, 4.13 and 4.14 respectively. It is observed from these figures that the time response is oscillatory. Design of full state variable feedback controllers, for structural load alleviation (using the eigenpair assignment method) is presented in the next chapter.

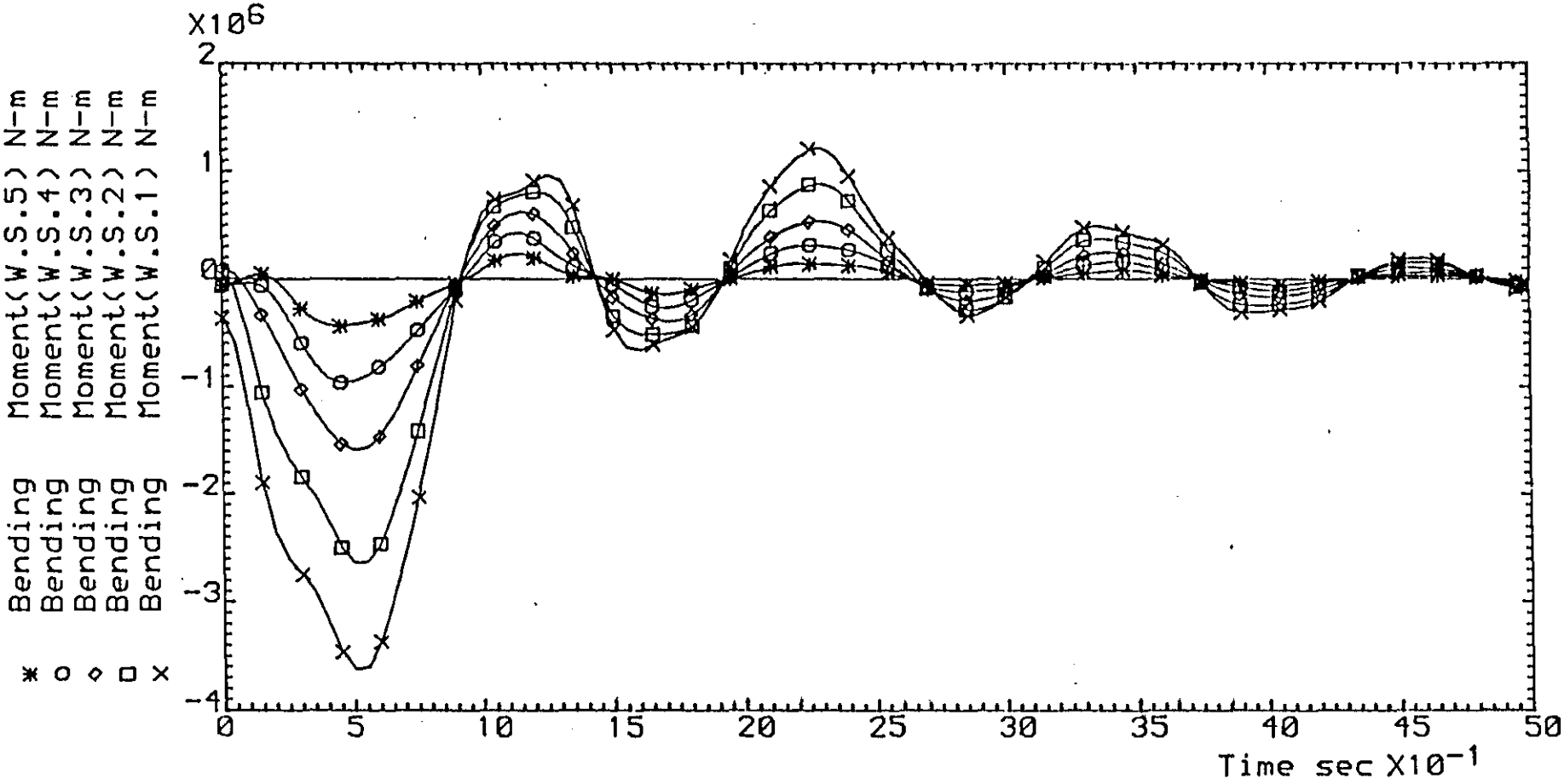

Figure 4.9 : Uncontrolled response, test case SC1

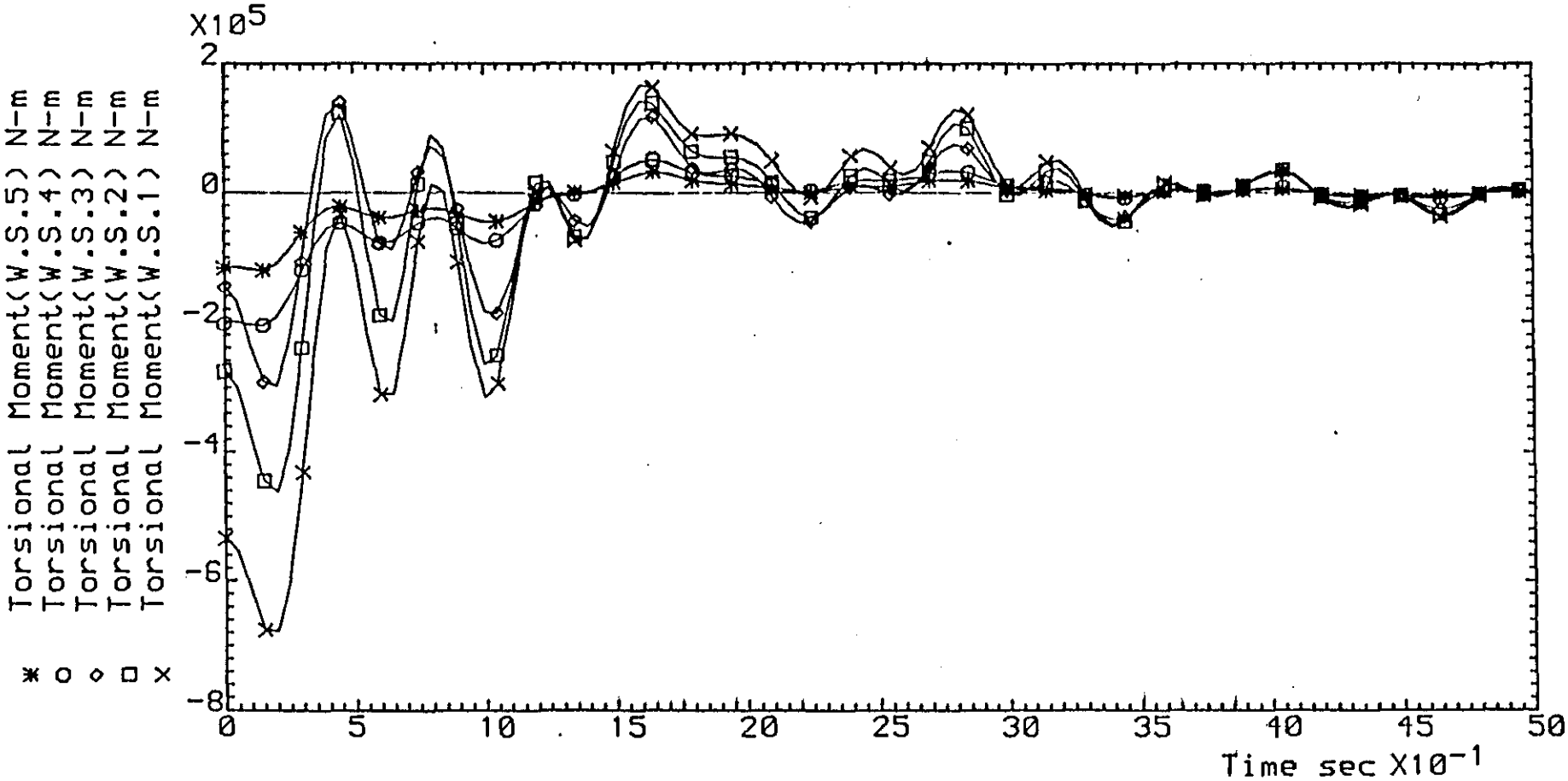

Figure 4.10 : Uncontrolled response, test case SC1

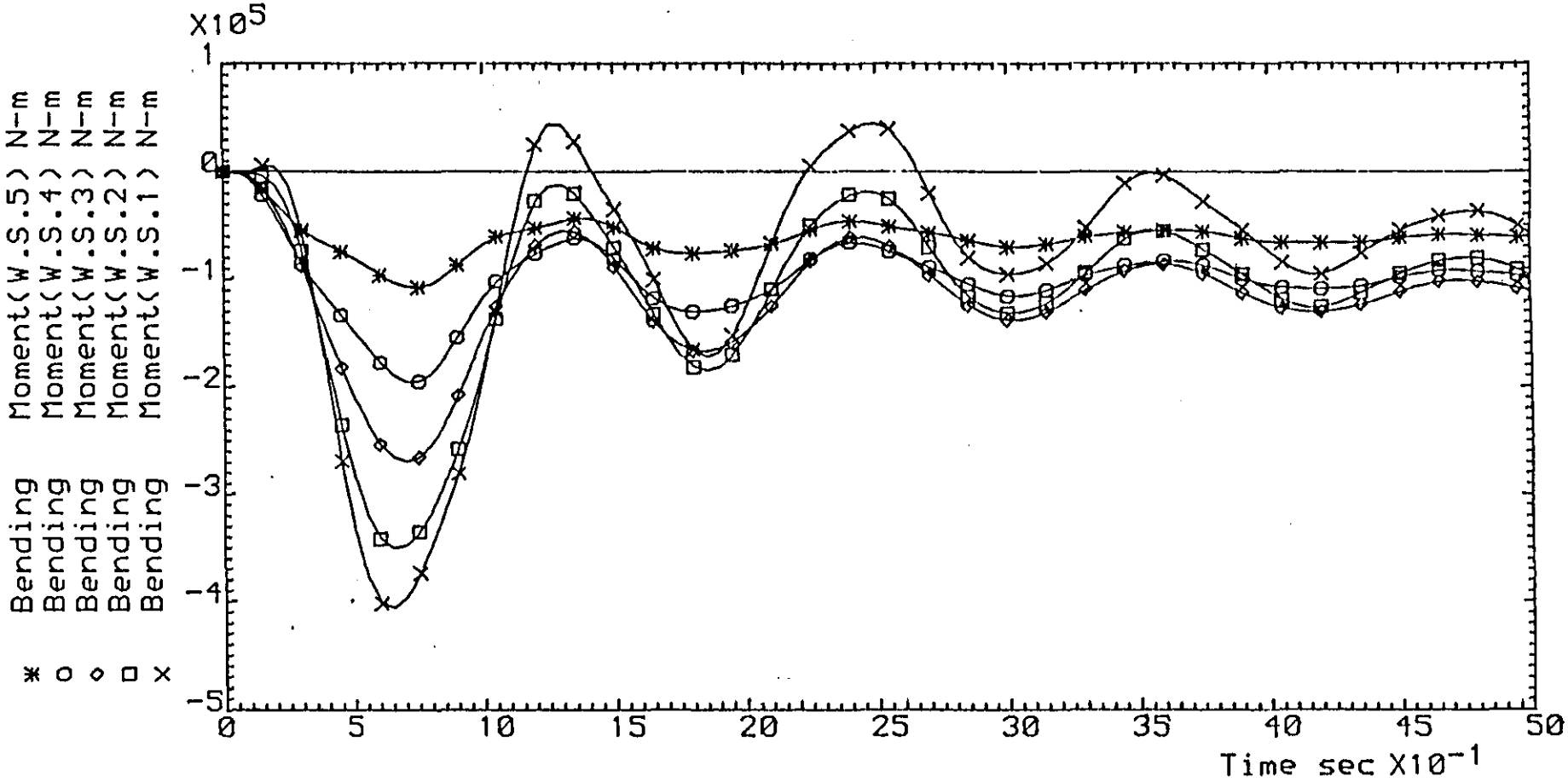

Figure 4.11 : Uncontrolled response, test case SC2

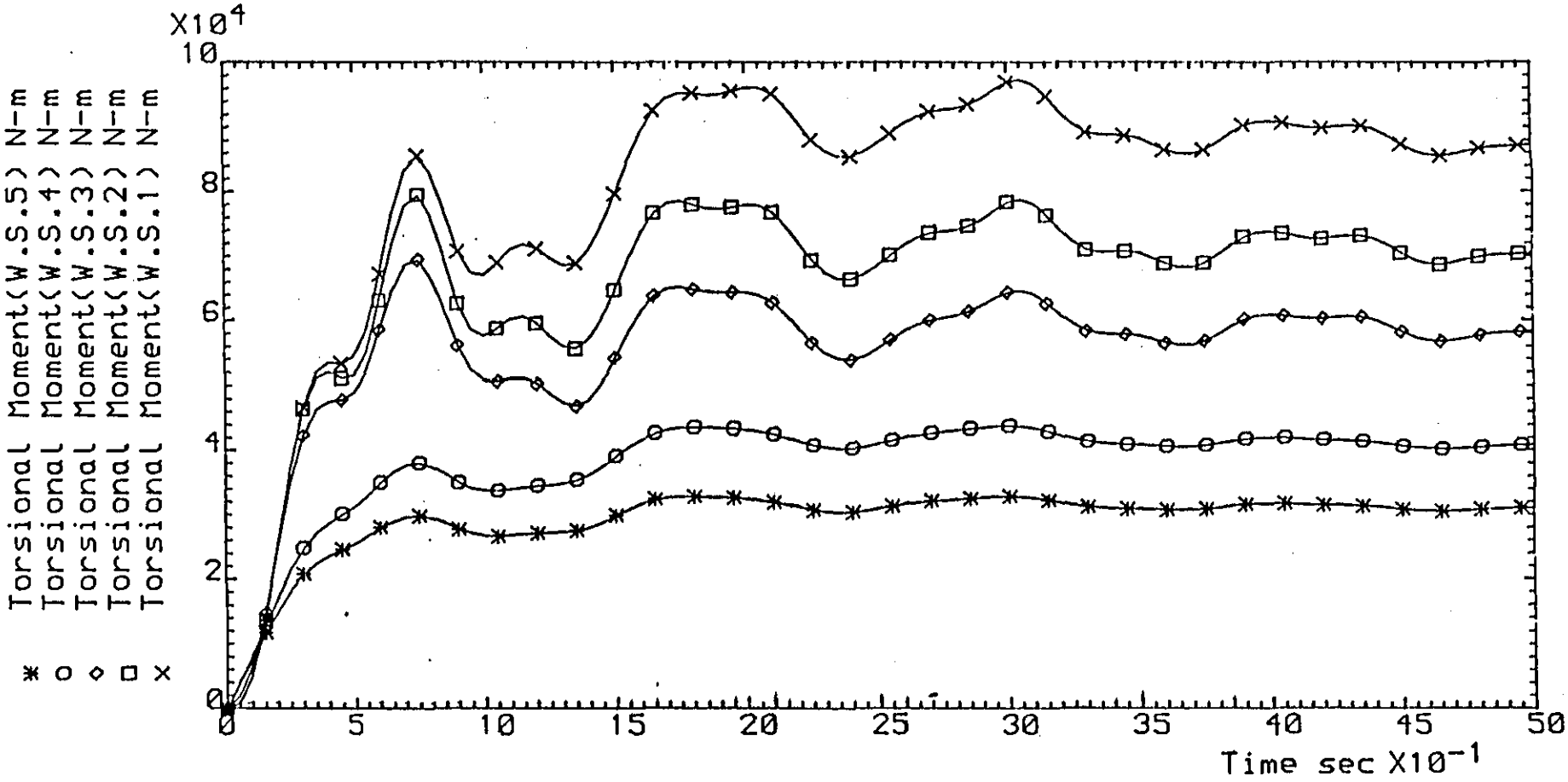

Figure 4.12 : Uncontrolled response, test case SC2

Figure 4.13 : Uncontrolled response, test case SC3

Figure4.14 : Uncontrolled response, test case SC3

CHAPTER 5

STRUCTURAL LOAD ALLEVIATION

5.1 Introduction

Alleviation of structural loads arising as a result of manoeuvre commands or atmospheric turbulence, on aircraft such as the C-5A Galaxy, can be beneficial from both the ultimate strength and fatigue damage standpoint by increasing the structural durability and improvement in the fatigue life of the structural components. A number of methods of synthesising control systems by the use of modern control techniques to achieve such alleviation have been proposed by Stone et al [1972], Konar et al [1976], Harvey & Pope [1977] and Prasad [1980], for example.

Most of the published work has been concerned with the design of control systems for structural load alleviation (SLA), manoeuvre load control (MLC) and gust load alleviation (GLA), using the Linear Quadratic Problem (LQP) method. However, a deficiency of the LQP method for the purposes of SLA lies in the fact that the characteristics of the flexural modes, such as frequency and damping, are arbitrarily assigned and that the selection of the weighting matrices in the LQP design do not relate to the physical requirements; thus a trial and error approach is often adopted for the selection of the weighting matrices. Since the precise specification of the eigenvalues and eigenvectors is not attainable using the LQP design, the effects of altering the flexural mode characteristics, on the structural loads on the C-5A, has not previously been studied in a direct way.

It has been shown by Prasad that for SLA, the feedback control law obtained by the LQP method, required the time constant associated with the inboard elevator dynamics to be $3.0 * 10^{-4}$ seconds, which is too fast for the capabilities of the present day control surface actuators. In the same work it was also noted that the second flexural mode always remained unaffected by feedback. This result may have been due to the choice of weighting matrices considered in that work. It was shown in chapter 3 of this dissertation that, for the L-1011 Tristar, the mathematical model of which consisted solely of the rigid body dynamics, a feedback control law could be realised by the use of an eigenpair assignment method. This method was shown to provide a feedback control superior to any obtained by other design methods.

If structural loads on the aircraft being studied are to be reduced, then the rates and the displacements of the flexural modes must be reduced. Since the bending and torsional moments are related to the aircraft's state variables, any reduction of peak and RMS values reflects in the responses of the bending and torsional moments.

5.2 Specification of the closed-loop eigenstructure

It is well known, (Bisplinghoff, Ashley & Halfman [1955]), that to reduce the displacements of a mode of a vibrating cantilevered slender beam (the wing of the C-5A may be regarded as a slender beam) either Young's modulus should be increased or the moment of inertia should be increased, or both should be increased. The form of open-loop control is to employ hardware modifications, for example by making the wing stiffer (i.e., increasing the moment of inertia). The disadvantage of such changes is the inevitable increase in the weight of the structure, thereby causing a reduction in the payload carrying capacity of the aircraft. The other form of open-loop control is to increase the Young's modulus, which results in increased structural damping. The effect of increase in the stiffness or the Young's modulus is to increase the frequencies or the damping of the flexural modes.

It is known that SLA can only be possible if the frequencies of the flexural modes are well separated from the frequencies of the rigid-body modes or the flexural modes to have sufficient damping. The damping in the flexural modes allows any absorbed energy to be dissipated rapidly. Instead of employing the form of open-loop control (i.e., hardware modifications), the frequencies and the damping of the flexural modes can be altered by the use of feedback control. This surmounts to altering the eigenvalues associated with the flexural modes by feedback control.

It was shown in section 4.7, that the first sixteen state variables of the C-5A Galaxy were controllable. The modes identified with the controllable state variables were,

- rigid body mode (short period pitching oscillation),
- first six flexural modes,
- aileron and inboard elevator modes.

Furthermore, the first twenty state variables are observable (in control sense) in the bending and torsional moments at the five specific wing stations. Hence any shift in the eigenvalues of the controllable modes will reflect in the bending and torsional moment responses.

It was seen from the dynamic response of BM and TM, figures 4.9 to 4.14, that the responses were lightly damped. The oscillatory nature of these responses was attributed to insufficient damping in the flexural modes, the corresponding damping ratios shown in table 4.5 all being low. To increase damping of the TM and BM responses, the damping in the flexural modes had to be increased.

It is also required that the controlled aircraft should have the same handling qualities (usually expressed in terms of the eigenvalues associated with the short period mode) as the uncontrolled aircraft. Therefore, it was specified that the closed-loop system should have the same short period dynamics as the uncontrolled aircraft. Since the eigenvalues associated with the Küssner dynamics, the outboard elevator and those associated with the Dryden filter, were uncontrollable, no attempt was made to alter them. However the possibility of assigning the eigenvectors associated with the uncontrollable eigenvalues was considered. Although the eigenvalues associated with the aileron and the elevator modes could be controlled, they were specified in the closed-loop as having the same numerical values as in the open-loop. Since any changes in the eigenvalues of the closed-loop would have implied the use of actuators with different dynamic properties from those in actual use on the aircraft. Therefore, there only remained the problem of specifying the eigenvalues associated with the six flexural modes.

5.2.1 Specification of the closed-loop eigenvalues

To illustrate the effect of the increase in the damping ratios of the flexural modes on the BM and TM response, the set of eigenvalues as given in table 5.1, was specified for the closed-loop.

Mode	Eigenvalue	Frequency	Damping Ratio
1	-2.54±j 4.86	5.48	0.465
2	-1.16±j 11.06	11.12	0.104
3	-2.86±j 13.51	13.81	0.207
4	-3.03±j 15.31	15.61	0.194
5	-2.13±j 17.36	17.49	0.122
6	-3.10±j 18.53	18.79	0.165

Table 5.1: Specified closed-loop eigenvalues

It can be seen from table 5.1, that while specifying the closed-loop damping ratios associated with the six flexural modes, the frequencies are the same as they were in the open-loop (see table 4.5). An arbitrary increase in the values of the damping ratios, of five times that of the uncontrolled values is specified¶. The damping ratio of the first flexural mode is required to be augmented from 0.093 (the uncontrolled value) to 0.465 (controlled value) , see table 5.1. An arbitrary increase of five times the computed value in the damping ratio, especially that of the first flexural mode, will result in a favourable bending moment response. It is shown later that the first flexural mode has a dominant influence on the bending moment response.

¶ If excessive damping is required, then not only will the control activity be high but the corresponding control deflections will be high as well. Therefore, an increase of five times in the values of the damping ratio was considered to be adequate.

5.2.2 Specification of the closed-loop eigenvectors

Case A : The equations which determine the influence of eigenvectors on the state variable response, due to initial conditions on the states and due to control inputs were developed in section 2.5. Although the equations for zero input and zero state response i.e., equation 2.28 and 2.32 were developed for the open-loop case, similar expressions can be obtained for the closed-loop response, by replacing matrix A with the matrix (A + BK) which is the closed-loop matrix. It has been pointed out (see section 5.1) that if structural loads are to be reduced, then the amplitude of the flexural modes must be reduced. An eigenvector selection scheme which enabled some reductions in the amplitude of motion variables, pertinent to the lateral dynamics of the L-1011 Tristar, was presented in section 3.5 of this thesis. The eigenvectors (chosen from the computed null space vectors) corresponding to the specified eigenvalues allowed the participation of each mode in the dominant mode variables.

For example, for the C-5A, the short period mode is mainly composed of the vertical velocity and the normalised pitch rate (state variables x_1 and x_2); some contribution from flexural modes will also result as the rigid body motion is seen to be coupled to the elastic motion, see equations 4.4 and 4.6. State variable x_1 and x_2 are termed as the dominant mode variables of the short period mode. The overall amplitude of the variables x_1 and x_2 can be reduced if the specified eigenvectors inhibit the participation of the remaining modes in the response of x_1 and x_2. Similarly the amplitude of the variables x_3 and x_9 i.e., 1^{st} flexural mode rate and displacement; (Note that for this mode x_3 and x_9 are termed as the dominant mode variables) can be reduced if the specified eigenvectors inhibit the participation of the short period mode, the second flexural mode , the third flexural mode, the fourth flexural mode, the fifth flexural mode and the sixth flexural mode to the response of the motion variable x_3 and x_9. This would imply that the specified eigenvectors allow only the 1^{st} flexural mode to participate in the response of x_3 and x_9. If the eigenvectors corresponding to the remaining flexural modes are specified in a similar way, decoupling of the flexural modes will result.

The null space eigenvectors of equation 3.72 are presented in table 5.2 to 5.8 corresponding to the short period eigenvalue and the specified eigenvalue set of table 5.1. The contribution of a specific mode to the motion variables is presented as a percentage in these tables, enabling the choice of an appropriate eigenvector from the computed null space eigenvectors , even though the eigenvector components may be complex. This is possible due to normalisation of eigenvectors, as discussed in section 2.5 and 3.6.

From Table 5.2 $\underline{\rho}_{1_i}$ is chosen, because the short period mode is seen to be contributing predominantly to the vertical velocity and the pitch rate (the percent contributions being 86.5 and 13.3 respectively). From table 5.3 $\underline{\rho}_{2_i}$ is chosen because the 1st flexural mode is seen to be contributing mainly to the 1st flexural mode rate and displacement (the percent contributions are seen to be 96.0 and 3.2, respectively). For the 2nd flexural mode eigenvector $\underline{\rho}_{1_i}$ was chosen from table 5.4 , although it is seen that the second flexural mode is contributing heavily to the third flexural mode rate, some contribution to the rigid body variables and higher frequency flexural modes is also noted. Nevertheless, if eigenvector $\underline{\rho}_{2_i}$ were chosen then it would seem that the second mode would certainly contribute to the first flexural mode rate. As most of the bending energy is thought be contained in the first flexural mode rate and displacement, any contributions from the higher frequency modes to these variables is not desirable. Hence the choice of $\underline{\rho}_{1_i}$ would decouple the first and the second flexural modes. From table 5.5 the third mode is seen to be contributing mainly to the third flexural mode rate, therefore $\underline{\rho}_{1_i}$ was chosen. From table 5.6 $\underline{\rho}_{2_i}$ is chosen. It is seen that the contribution of the fourth mode to the 4th flexural mode rate is 49%. Some contribution to other motion variables is also noted. From tables 5.7 and 5.8 eigenvectors $\underline{\rho}_{2_i}$ was chosen for the fifth and $\underline{\rho}_{2_i}$ was chosen for the sixth flexural mode. The open-loop eigenvectors corresponding to the remaining uncontrollable eigenvalues were specified in the closed-loop. Also presented in tables 5.2-5.8 are the vectors $\underline{\omega}_{\kappa_i}$. Since κ is either 1 or 2 (because the dimension of the control vector is 2), whenever eigenvector $\underline{\rho}_{1_i}$ is selected eigenvector $\underline{\omega}_{1_i}$ is also chosen. Similarly, whenever eigenvector $\underline{\rho}_{2_i}$ is selected eigenvector $\underline{\omega}_{2_i}$ is selected as well. This enables definition of equation 3.73.

EIGENVALUE λ_1 = -0.88 + j 1.273 Short Period Mode $i = 1$

State variable	Eigenvector $\underline{p}_{1_i}$	%	Eigenvector $\underline{p}_{2_i}$	%
Vertical Vel	0.930 , 0.000	86.5	0.000 , 0.000	0.0
Pitch rate	-0.073 , 0.358	13.3	0.116 , -0.018	1.4
Flexural mode 1, rate	-0.020 , -0.031	0.1	0.487 , -0.675	69.2
Flexural mode 2, rate	-0.001 , 0.001	0.0	0.003 , -0.005	0.0
Flexural mode 3, rate	-0.002 , 0.004	0.0	0.022 , -0.034	0.2
Flexural mode 4, rate	0.009 , -0.006	0.0	-0.023 , 0.033	0.2
Flexural mode 5, rate	0.001 , -0.001	0.0	-0.001 , 0.002	0.0
Flexural mode 6, rate	-0.003 , 0.002	0.0	0.007 , -0.010	0.0
Flexural mode 1, disp	-0.009 , 0.022	0.1	-0.537 , -0.011	28.9
Flexural mode 2, disp	0.001 , 0.000	0.0	-0.004 , 0.000	0.0
Flexural mode 3, disp	0.003 , -0.001	0.0	-0.026 , 0.001	0.1
Flexural mode 4, disp	-0.006 , -0.003	0.0	0.026 , 0.000	0.1
Flexural mode 5, disp	-0.001 , 0.000	0.0	0.001 , 0.000	0.0
Flexural mode 6, disp	0.002 , 0.001	0.0	-0.008 , 0.000	0.0
Aileron Dfln	0.000 , 0.000	0.0	0.005 , 0.000	0.0
Inb. Elev Dfln	0.000 , 0.000	0.0	-0.001 , 0.000	0.0
Otb. Elev Dfln	0.000 , 0.000	0.0	0.000 , 0.000	0.0
Küssner Dyn	0.000 , 0.000	0.0	0.000 , 0.000	0.0
Küssner Dyn	0.000 , 0.000	0.0	0.000 , 0.000	0.0
Küssner Dyn	0.000 , 0.000	0.0	0.000 , 0.000	0.0
Küssner Dyn	0.000 , 0.000	0.0	0.000 , 0.000	0.0
Küssner Dyn	0.000 , 0.000	0.0	0.000 , 0.000	0.0
Dryden state	0.000 , 0.000	0.0	0.000 , 0.000	0.0
Gust Velocity	0.000 , 0.000	0.0	0.000 , 0.000	0.0

$\underline{\omega}_{1_i}$	$\underline{\omega}_{1_i}$
0.000 , 0.000 0.0	-0.004 , -0.001 0.0
0.000 , 0.000 0.0	0.001 , 0.000 0.0

Table 5.2: Assignable eigenvectors

EIGENVALUE $\lambda_3 = -2.537 + j\ 1.486$ First Flexural Mode $i = 3$

State variable	Eigenvector $\underline{\rho 1_i}$	%	Eigenvector $\underline{\rho 2_i}$	%
Vertical Vel	0.506 , 0.000	25.6	0.000 , 0.000	0.0
Pitch rate	-0.177 , 0.820	70.4	0.062 , -0.013	0.4
Flexural mode 1, rate	0.043 , -0.033	0.3	0.850 , 0.485	96.0
Flexural mode 2, rate	0.025 , -0.005	0.1	0.004 , -0.001	0.0
Flexural mode 3, rate	0.147 , -0.043	2.4	0.030 , -0.018	0.1
Flexural mode 4, rate	0.096 , -0.038	1.1	-0.042 , 0.013	0.2
Flexural mode 5, rate	0.020 , -0.008	0.0	-0.003 , 0.001	0.0
Flexural mode 6, rate	-0.028 , 0.012	0.1	0.013 , -0.006	0.0
Flexural mode 1, disp	-0.009 , -0.004	0.0	0.007 , -0.179	3.2
Flexural mode 2, disp	-0.003 , -0.004	0.0	-0.001 , -0.001	0.0
Flexural mode 3, disp	-0.019 , -0.020	0.1	-0.005 , -0.003	0.0
Flexural mode 4, disp	-0.014 , -0.012	0.0	0.006 , 0.006	0.0
Flexural mode 5, disp	-0.003 , -0.003	0.0	0.000 , 0.000	0.0
Flexural mode 6, disp	0.004 , 0.003	0.0	-0.002 , -0.002	0.0
Aileron Dfln	0.000 , 0.000	0.0	0.001 , 0.001	0.0
Inb. Elev Dfln	0.001 , 0.001	0.0	0.000 , 0.000	0.0
Otb. Elev Dfln	0.000 , 0.000	0.0	0.000 , 0.000	0.0
Küssner Dyn	0.000 , 0.000	0.0	0.000 , 0.000	0.0
Küssner Dyn	0.000 , 0.000	0.0	0.000 , 0.000	0.0
Küssner Dyn	0.000 , 0.000	0.0	0.000 , 0.000	0.0
Küssner Dyn	0.000 , 0.000	0.0	0.000 , 0.000	0.0
Küssner Dyn	0.000 , 0.000	0.0	0.000 , 0.000	0.0
Dryden state	0.000 , 0.000	0.0	0.000 , 0.000	0.0
Gust Velocity	0.000 , 0.000	0.0	0.000 , 0.000	0.0

$\underline{\omega 1_i}$		$\underline{\omega 1_i}$	
0.000 , 0.000	0.0	0.000 , -0.001	0.0
0.000 , -0.001	0.0	0.000 , 0.000	0.0

Table 5.3: Assignable eigenvectors

EIGENVALUE $\lambda_5 = -1.156 + j\ 11.06$ Second Flexural Mode $i = 5$

State variable	Eigenvector $\underline{\rho}_{1_i}$	%	Eigenvector $\underline{\rho}_{2_i}$	%
Vertical Vel	-0.121 , 0.000	1.5	0.000 , 0.000	0.0
Pitch rate	-0.104 , -0.353	13.6	-0.058 , -0.081	1.0
Flexural mode 1, rate	-0.155 , 0.187	5.9	0.815 , -0.251	72.8
Flexural mode 2, rate	-0.249 , 0.090	7.0	-0.082 , -0.052	0.9
Flexural mode 3, rate	-0.024 , 0.759	57.6	-0.315 , 0.143	12.0
Flexural mode 4, rate	-0.088 , 0.345	12.7	0.329 , 0.101	11.8
Flexural mode 5, rate	-0.008 , 0.061	0.4	0.019 , 0.013	0.1
Flexural mode 6, rate	0.016 , -0.084	0.7	-0.079 , -0.018	0.7
Flexural mode 1, disp	0.018 , 0.012	0.0	-0.030 , -0.071	0.6
Flexural mode 2, disp	0.010 , 0.021	0.1	-0.004 , 0.008	0.0
Flexural mode 3, disp	0.068 , -0.005	0.5	0.016 , 0.027	0.1
Flexural mode 4, disp	0.032 , 0.005	0.1	0.006 , -0.030	0.1
Flexural mode 5, disp	0.006 , 0.000	0.0	0.001 , -0.002	0.0
Flexural mode 6, disp	-0.008 , -0.001	0.0	-0.001 , 0.007	0.0
Aileron Dfln	0.000 , 0.001	0.0	-0.001 , -0.002	0.0
Inb. Elev Dfln	-0.002 , 0.000	0.0	0.000 , 0.001	0.0
Otb. Elev Dfln	0.000 , 0.000	0.0	0.000 , 0.000	0.0
Küssner Dyn	0.000 , 0.000	0.0	0.000 , 0.000	0.0
Küssner Dyn	0.000 , 0.000	0.0	0.000 , 0.000	0.0
Küssner Dyn	0.000 , 0.000	0.0	0.000 , 0.000	0.0
Küssner Dyn	0.000 , 0.000	0.0	0.000 , 0.000	0.0
Küssner Dyn	0.000 , 0.000	0.0	0.000 , 0.000	0.0
Dryden state	0.000 , 0.000	0.0	0.000 , 0.000	0.0
Gust Velocity	0.000 , 0.000	0.0	0.000 , 0.000	0.0

$\underline{\omega}_{1_i}$		$\underline{\omega}_{1_i}$	
0.001 , 0.000	0.0	-0.004 , 0.003	0.0
0.002 , 0.003	0.0	0.001 , 0.000	0.0

Table 5.4: Assignable eigenvectors

EIGENVALUE $\lambda_7 = -2.858 + j\ 13.511$ Third Flexural Mode $i = 7$

State variable	Eigenvector $\underline{\rho}_{1_i}$	%	Eigenvector $\underline{\rho}_{2i}$	%
Vertical Vel	-0.066 , 0.000	0.4	0.000 , 0.000	0.0
Pitch rate	-0.071 , -0.224	5.5	0.060 , -0.113	1.6
Flexural mode 1, rate	-0.282 , -0.017	8.0	0.395 , 0.553	46.2
Flexural mode 2, rate	-0.058 , -0.039	0.5	0.015 , -0.014	0.0
Flexural mode 3, rate	-0.826 , 0.161	70.8	0.118 , -0.260	8.1
Flexural mode 4, rate	-0.359 , 0.068	13.4	-0.574 , 0.285	41.0
Flexural mode 5, rate	-0.042 , 0.044	0.4	-0.042 , 0.038	0.3
Flexural mode 6, rate	0.070 , -0.039	0.6	0.080 , -0.124	2.2
Flexural mode 1, disp	0.003 , 0.020	0.0	0.033 , -0.036	0.2
Flexural mode 2, disp	-0.002 , 0.005	0.0	-0.001 , -0.001	0.0
Flexural mode 3, disp	0.024 , 0.056	0.4	-0.020 , -0.004	0.0
Flexural mode 4, disp	0.010 , 0.024	0.1	0.029 , 0.036	0.2
Flexural mode 5, disp	0.004 , 0.002	0.0	0.003 , 0.002	0.0
Flexural mode 6, disp	-0.004 , -0.004	0.0	-0.010 , -0.004	0.0
Aileron Dfln	-0.001 , 0.001	0.0	0.002 , -0.001	0.0
Inb. Elev Dfln	-0.001 , 0.000	0.0	-0.001 , 0.000	0.0
Otb. Elev Dfln	0.000 , 0.000	0.0	0.000 , 0.000	0.0
Küssner Dyn	0.000 , 0.000	0.0	0.000 , 0.000	0.0
Küssner Dyn	0.000 , 0.000	0.0	0.000 , 0.000	0.0
Küssner Dyn	0.000 , 0.000	0.0	0.000 , 0.000	0.0
Küssner Dyn	0.000 , 0.000	0.0	0.000 , 0.000	0.0
Küssner Dyn	0.000 , 0.000	0.0	0.000 , 0.000	0.0
Dryden state	0.000 , 0.000	0.0	0.000 , 0.000	0.0
Gust Velocity	0.000 , 0.000	0.0	0.000 , 0.000	0.0

$\underline{\omega}_{1_i}$	$\underline{\omega}_{1_i}$
0.002 , 0.001 0.0	-0.002 , -0.004 0.0
0.000 , 0.002 0.0	0.000 , 0.002 0.0

Table 5.5: Assignable eigenvectors

EIGENVALUE λ_9 = -3.03 + j 15.61 Fourth Flexural Mode $i = 9$

State variable	Eigenvector $\underline{\rho}_{1_i}$	%	Eigenvector $\underline{\rho}_{2_i}$	%
Vertical Vel	0.065 , 0.000	0.4	0.000 , 0.000	0.0
Pitch rate	0.098 , 0.197	4.9	0.089 , -0.122	2.3
Flexural mode 1, rate	0.441 , 0.171	22.4	0.288 , 0.463	29.8
Flexural mode 2, rate	0.041 , 0.039	0.3	0.016 , -0.019	0.1
Flexural mode 3, rate	0.693 , 0.331	59.0	0.183 , -0.273	10.8
Flexural mode 4, rate	0.142 , 0.292	10.5	-0.572 , -0.043	48.9
Flexural mode 5, rate	0.092 , -0.037	1.0	-0.120 , -0.006	1.4
Flexural mode 6, rate	-0.099 , -0.043	1.2	0.226 , -0.111	6.4
Flexural mode 1, disp	0.005 , -0.028	0.1	0.024 , -0.022	0.1
Flexural mode 2, disp	0.002 , -0.003	0.0	-0.001 , -0.001	0.0
Flexural mode 3, disp	0.011 , -0.045	0.2	-0.018 , -0.008	0.0
Flexural mode 4, disp	0.016 , -0.012	0.0	-0.017 , 0.038	0.2
Flexural mode 5, disp	-0.003 , -0.005	0.0	0.001 , 0.007	0.0
Flexural mode 6, disp	-0.001 , 0.006	0.0	-0.009 , -0.012	0.0
Aileron Dfln	0.002 , -0.002	0.0	0.002 , -0.001	0.0
Inb. Elev Dfln	0.001 , 0.000	0.0	-0.001 , -0.001	0.0
Otb. Elev Dfln	0.000 , 0.000	0.0	0.000 , 0.000	0.0
Küssner Dyn	0.000 , 0.000	0.0	0.000 , 0.000	0.0
Küssner Dyn	0.000 , 0.000	0.0	0.000 , 0.000	0.0
Küssner Dyn	0.000 , 0.000	0.0	0.000 , 0.000	0.0
Küssner Dyn	0.000 , 0.000	0.0	0.000 , 0.000	0.0
Küssner Dyn	0.000 , 0.000	0.0	0.000 , 0.000	0.0
Dryden state	0.000 , 0.000	0.0	0.000 , 0.000	0.0
Gust Velocity	0.000 , 0.000	0.0	0.000 , 0.000	0.0

$\underline{\omega}_{1_i}$		$\underline{\omega}_{1_i}$	
-0.005 , -0.003	0.0	-0.003 , -0.004	0.0
0.000 , -0.002	0.0	-0.001 , 0.002	0.0

Table 5.6: Assignable eigenvectors

EIGENVALUE λ_{11} = -2.134 + j 17.359 Fifth Flexural Mode $i = 11$

State variable	Eigenvector $\underline{\rho}_{1_i}$	%	Eigenvector $\underline{\rho}_{2_i}$	%
Vertical Vel	-0.065 , 0.000	0.4	0.000 , 0.000	0.0
Pitch rate	-0.112 , -0.172	4.2	0.110 , -0.075	1.8
Flexural mode 1, rate	-0.463 , -0.195	25.3	0.120 , 0.446	21.3
Flexural mode 2, rate	-0.037 , -0.037	0.3	0.023 , -0.010	0.1
Flexural mode 3, rate	-0.595 , -0.431	54.0	0.325 , -0.155	13.0
Flexural mode 4, rate	0.008 , -0.316	10.0	-0.182 , -0.645	45.0
Flexural mode 5, rate	-0.161 , 0.053	2.9	-0.166 , -0.105	3.9
Flexural mode 6, rate	0.143 , 0.074	2.6	0.372 , -0.096	14.7
Flexural mode 1, disp	-0.008 , 0.028	0.1	0.024 , -0.010	0.1
Flexural mode 2, disp	-0.002 , 0.002	0.0	-0.001 , -0.001	0.0
Flexural mode 3, disp	-0.020 , 0.037	0.2	-0.011 , -0.017	0.0
Flexural mode 4, disp	-0.018 , 0.002	0.0	-0.035 , 0.015	0.1
Flexural mode 5, disp	0.004 , 0.009	0.0	-0.005 , 0.010	0.0
Flexural mode 6, disp	0.003 , -0.009	0.0	-0.008 , -0.020	0.0
Aileron Dfln	-0.001 , 0.002	0.0	0.001 , 0.000	0.0
Inb. Elev Dfln	-0.001 , 0.000	0.0	-0.001 , -0.001	0.0
Otb. Elev Dfln	0.000 , 0.000	0.0	0.000 , 0.000	0.0
Küssner Dyn	0.000 , 0.000	0.0	0.000 , 0.000	0.0
Küssner Dyn	0.000 , 0.000	0.0	0.000 , 0.000	0.0
Küssner Dyn	0.000 , 0.000	0.0	0.000 , 0.000	0.0
Küssner Dyn	0.000 , 0.000	0.0	0.000 , 0.000	0.0
Küssner Dyn	0.000 , 0.000	0.0	0.000 , 0.000	0.0
Dryden state	0.000 , 0.000	0.0	0.000 , 0.000	0.0
Gust Velocity	0.000 , 0.000	0.0	0.000 , 0.000	0.0

$\underline{\omega}_{1_i}$	$\underline{\omega}_{1_i}$
0.007 , 0.003 0.0	-0.002 , -0.004 0.0
0.001 , 0.001 0.0	-0.001 , 0.002 0.0

Table 5.7: Assignable eigenvectors

EIGENVALUE λ_{13} = -3.10 + j 18.53 Sixth Flexural Mode $i = 13$

State variable	Eigenvector $\underline{p}_{1_i}$	%	Eigenvector $\underline{p}_{2_i}$	%
Vertical Vel	-0.072 , 0.000	0.5	0.000 , 0.000	0.0
Pitch rate	-0.136 , -0.222	6.8	0.084 , -0.129	2.4
Flexural mode 1, rate	-0.459 , -0.171	24.0	0.320 , 0.440	29.6
Flexural mode 2, rate	-0.041 , -0.041	0.3	0.018 , -0.018	0.1
Flexural mode 3, rate	-0.581 , -0.423	51.7	0.249 , -0.211	10.7
Flexural mode 4, rate	-0.059 , -0.315	10.2	-0.345 , -0.496	36.5
Flexural mode 5, rate	-0.158 , -0.033	2.6	-0.126 , 0.104	2.7
Flexural mode 6, rate	0.139 , 0.128	3.6	0.422 , 0.020	17.8
Flexural mode 1, disp	-0.005 , 0.026	0.1	0.020 , -0.021	0.1
Flexural mode 2, disp	-0.002 , 0.002	0.0	-0.001 , -0.001	0.0
Flexural mode 3, disp	-0.017 , 0.034	0.1	-0.013 , -0.011	0.0
Flexural mode 4, disp	-0.016 , 0.006	0.0	-0.023 , 0.022	0.1
Flexural mode 5, disp	0.000 , 0.009	0.0	-0.004 , 0.008	0.0
Flexural mode 6, disp	0.006 , -0.008	0.0	-0.003 , -0.022	0.1
Aileron Dfln	-0.002 , 0.002	0.0	0.002 , -0.001	0.0
Inb. Elev Dfln	-0.001 , 0.000	0.0	-0.001 , 0.000	0.0
Otb. Elev Dfln	0.000 , 0.000	0.0	0.000 , 0.000	0.0
Küssner Dyn	0.000 , 0.000	0.0	0.000 , 0.000	0.0
Küssner Dyn	0.000 , 0.000	0.0	0.000 , 0.000	0.0
Küssner Dyn	0.000 , 0.000	0.0	0.000 , 0.000	0.0
Küssner Dyn	0.000 , 0.000	0.0	0.000 , 0.000	0.0
Küssner Dyn	0.000 , 0.000	0.0	0.000 , 0.000	0.0
Dryden state	0.000 , 0.000	0.0	0.000 , 0.000	0.0
Gust Velocity	0.000 , 0.000	0.0	0.000 , 0.000	0.0

$\underline{\omega}_{1_i}$	$\underline{\omega}_{1_i}$
0.007 , 0.004 0.0	-0.005 , -0.005 0.0
0.001 , 0.003 0.0	0.000 , 0.003 0.0

Table 5.8: Assignable eigenvectors

CASE B : From the computed null space eigenvectors, corresponding to the short period eigenvalues and the specified eigenvalue set of table 5.1 (tables 5.2-5.8), appropriate eigenvectors were chosen such that the short period mode was allowed to contribute to the vertical velocity and pitch rate response, the contribution from the six flexural modes to vertical velocity and pitch rate being small. The eigenvectors thus specified should completely decouple the rigid body motions and the elastic motions. Eigenvectors shown in table 5.9 were chosen for this case.

Table Number	Mode	Eigenvector
5.2	Short Period mode	$\underline{\rho}_{1_i}$ i = 1
5.3	First Flexural mode	$\underline{\rho}_{2_i}$ i = 3
5.4	Second Flexural mode	$\underline{\rho}_{2_i}$ i = 5
5.5	Third Flexural mode	$\underline{\rho}_{2_i}$ i = 7
5.6	Fourth Flexural mode	$\underline{\rho}_{2_i}$ i = 9
5.7	Fifth Flexural mode	$\underline{\rho}_{2_i}$ i = 11
5.8	Sixth Flexural mode	$\underline{\rho}_{2_i}$ i = 13

Table 5.9 : Specified closed-loop eigenvectors : Case B

The eigenvector choice of case B differs from case A on two counts: firstly eigenvector $\underline{\rho}_{2_i}$ has been specified for 2nd flexural mode, secondly eigenvector $\underline{\rho}_{2_i}$ has been specified for 3rd flexural mode. The choice of the eigenvectors corresponding to the short period mode and other flexural modes is same for both cases. As in case A, the eigenvectors corresponding to the uncontrollable eigenvalues were specified for the closed-loop.

The aileron command δ_{a_c} and inboard elevator command δ_{e_c} for the controlled aircraft, can be expressed by the following equations,viz:

$$\delta_{a_c} = K1_{x_1} * x_1 + K1_{x_2} * x_2 + \ldots + K1_{x_{24}} * x_{24} \quad , \qquad 5.1$$

$$\delta_{e_c} = K2_{x_1} * x_1 + K2_{x_2} * x_2 + \ldots + K2_{x_{24}} * x_{24} \quad . \qquad 5.2$$

The feedback gains $K1_{x_1}$ $K2_{x_1}$:tc., are given in table 5.9, and the state variables x_1, x_2 etc., have been defined in table 4.2.

	CASE A	CASE B		CASE A	CASE B
$K1_{x_1}$	-0.00065	-0.00063	$K2_{x_1}$	-0.00027	-0.00004
$K1_{x_2}$	-0.00082	-0.00179	$K2_{x_2}$	-0.00045	-0.00024
$K1_{x_3}$	0.00134	0.00092	$K2_{x_3}$	-0.00006	-0.00011
$K1_{x_4}$	0.01381	-0.05776	$K2_{x_4}$	-0.00828	0.01271
$K1_{x_5}$	0.00883	-0.00617	$K2_{x_5}$	-0.00159	0.00840
$K1_{x_6}$	-0.00858	-0.00242	$K2_{x_6}$	-0.00140	-0.00088
$K1_{x_7}$	-0.11414	-0.05241	$K2_{x_7}$	0.03754	0.03929
$K1_{x_8}$	-0.00468	-0.00685	$K2_{x_8}$	-0.00814	-0.00474
$K1_{x_9}$	-0.01054	-0.00259	$K2_{x_9}$	0.00337	0.00196
$K1_{x_{10}}$	0.03067	-0.08797	$K2_{x_{10}}$	-0.12186	-0.24687
$K1_{x_{11}}$	0.02194	-0.24107	$K2_{x_{11}}$	-0.02153	0.02095
$K1_{x_{12}}$	0.30891	0.09128	$K2_{x_{12}}$	-0.12755	-0.07652
$K1_{x_{13}}$	-0.19803	-0.66197	$K2_{x_{13}}$	-0.47339	-0.19664
$K1_{x_{14}}$	0.71917	0.31820	$K2_{x_{14}}$	-0.23943	-0.20997
$K1_{x_{15}}$	-1.40000	-1.42180	$K2_{x_{15}}$	0.17116	-0.39238
$K1_{x_{16}}$	2.33750	-1.48620	$K2_{x_{16}}$	-2.09120	-2.07370
$K1_{x_{17}}$	0.48027	-0.43605	$K2_{x_{17}}$	-0.51838	-0.47782
$K1_{x_{18}}$	-0.00015	0.00144	$K2_{x_{18}}$	0.00089	0.00087
$K1_{x_{19}}$	0.00143	0.00276	$K2_{x_{19}}$	0.00051	0.00543
$K1_{x_{20}}$	0.01117	-0.01776	$K2_{x_{20}}$	-0.01152	-0.00658
$K1_{x_{21}}$	0.00006	-0.00153	$K2_{x_{21}}$	-0.00024	0.00051
$K1_{x_{22}}$	-0.00487	0.00599	$K2_{x_{22}}$	0.00182	0.00001
$K1_{x_{23}}$	0.00530	0.00146	$K2_{x_{23}}$	-0.00103	-0.00027
$K1_{x_{24}}$	-0.01678	0.00083	$K2_{x_{24}}$	0.00379	-0.00405

Table 5.9 : Feedback gains of Law A and Law B[§]

§ The gains have been rounded off to 5 decimal places. However double precision (14 significant decimal places) was used throughout in the computer programs.

5.2.3 Effect of feedback on Flexural modes

The rates and displacements of the first three flexural modes for control law A, test case SC1 are presented in figures 5.1 to 5.6. From inspection of figures 5.1 and 5.2 it can be seen that the controlled response is damped, and has smaller peak values, than the uncontrolled response. The desired damping ratio for the first mode of 0.463 being assigned exactly (see table 5.11). From figure 5.3 and 5.4 it can be seen that, a slight increase in the peak values of the second flexural mode has occurred, although the damping ratio has increased from 0.021 to 0.104, this represents an increase of five times the uncontrolled damping ratio (see table 5.11). It is obvious from figures 5.3 and 5.4 that the second mode has been controlled. Figures 5.5 and 5.6 indicate an increase in the peak values of the rate and displacement associated with the third flexural mode; nevertheless, the RMS values of the controlled response were much lower.

The dominance of the first bending mode can be inferred from an examination of figure 5.1 and 5.2. The peak values of the mode rate and displacement of this mode are much higher than the peak values of the second and third flexural modes. For example, the peak bending displacement of the first mode is seen to be 0.4 m, whereas, that of the second and the third modes are 0.0071 m and 0.021 m respectively. Therefore, the first flexural mode is likely to affect the bending moment response more than the second and third flexural modes (the deduction is based on an examination of the matrix [**C**+ **DK**] i.e., the closed-loop output matrix, in conjunction with peak values of mode rates and displacements).

Although the responses of the other high frequency flexural modes are not shown, the peak values of the 4^{th}, 5^{th} and 6^{th} flexural modes were found to be 0.04 m, 0.005 m and 0.003 m respectively. The specified damping ratios of 4^{th}, 5^{th} and 6^{th} flexural modes were assigned exactly (see table 5.11).

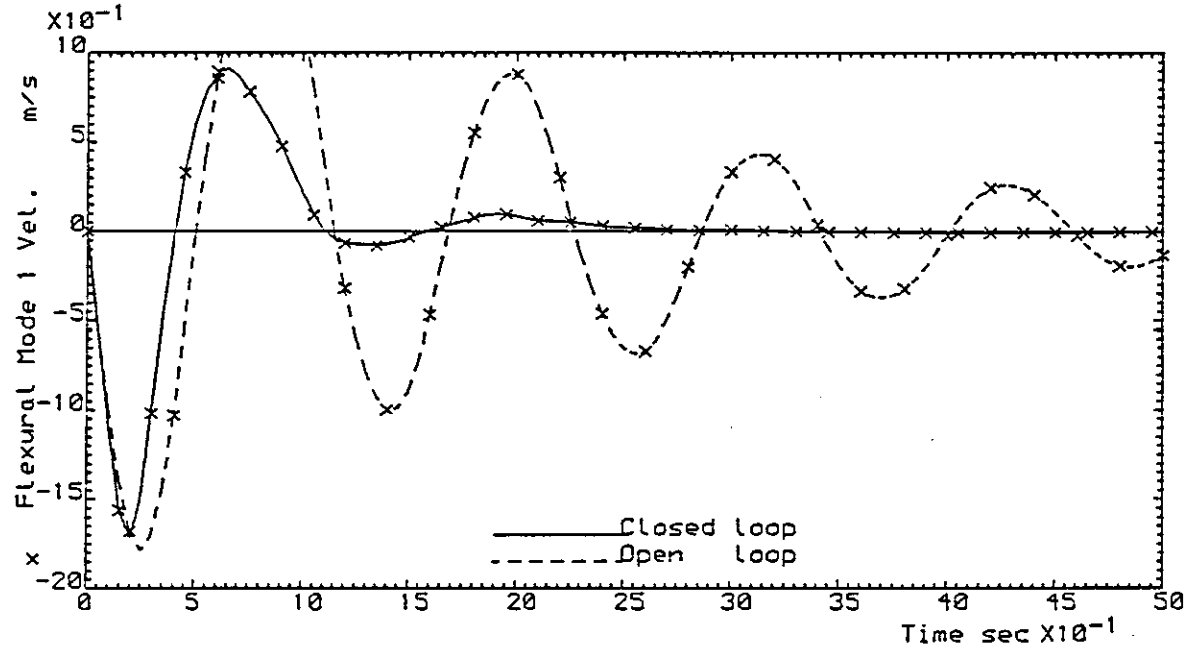

Figure 5.1: C5-A controlled response, control law A, test case SC1

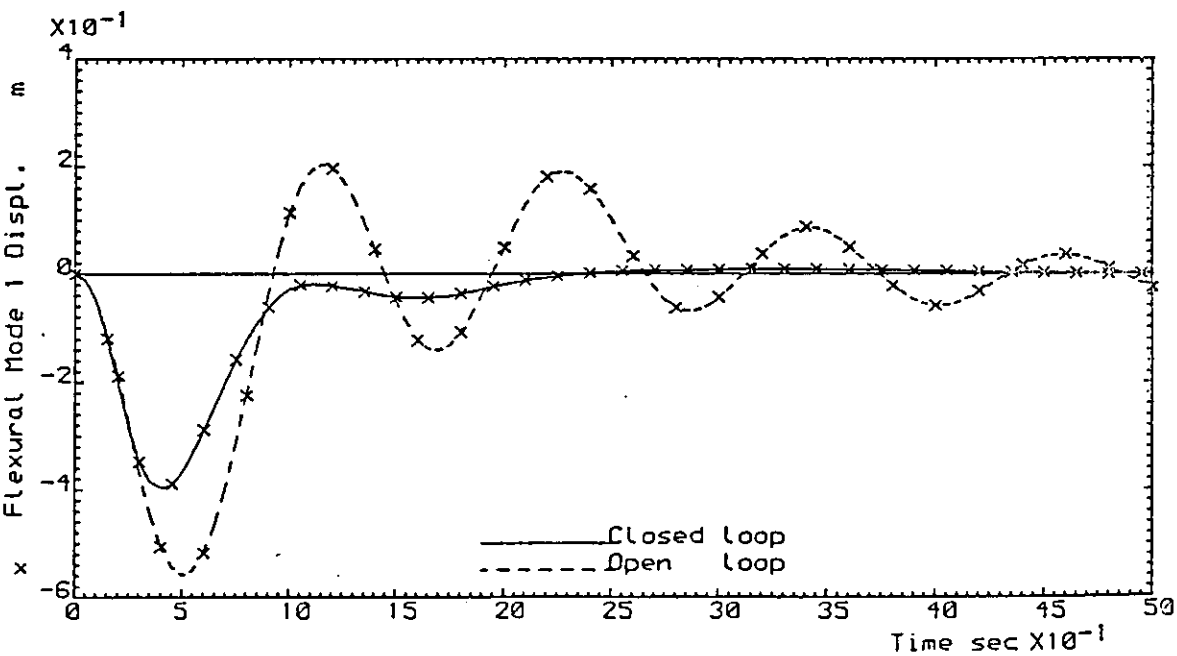

Figure 5.2: C5-A controlled response, control law A, test case SC1

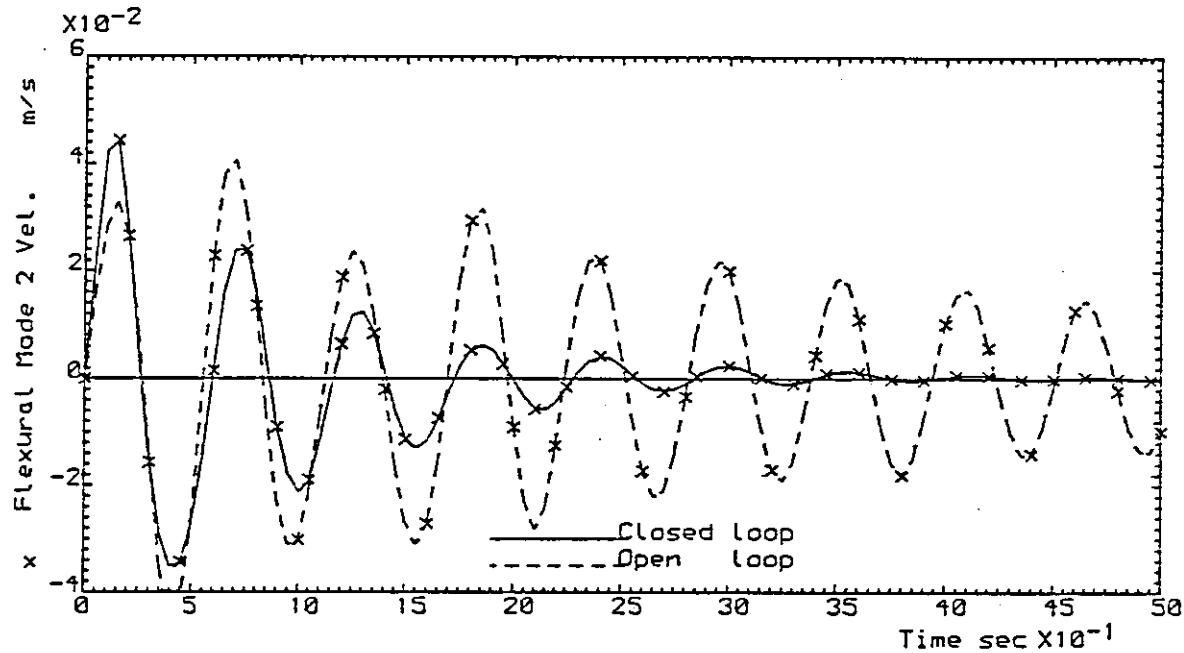

Figure 5.3 : C5-A controlled response, control law A, test case SC1

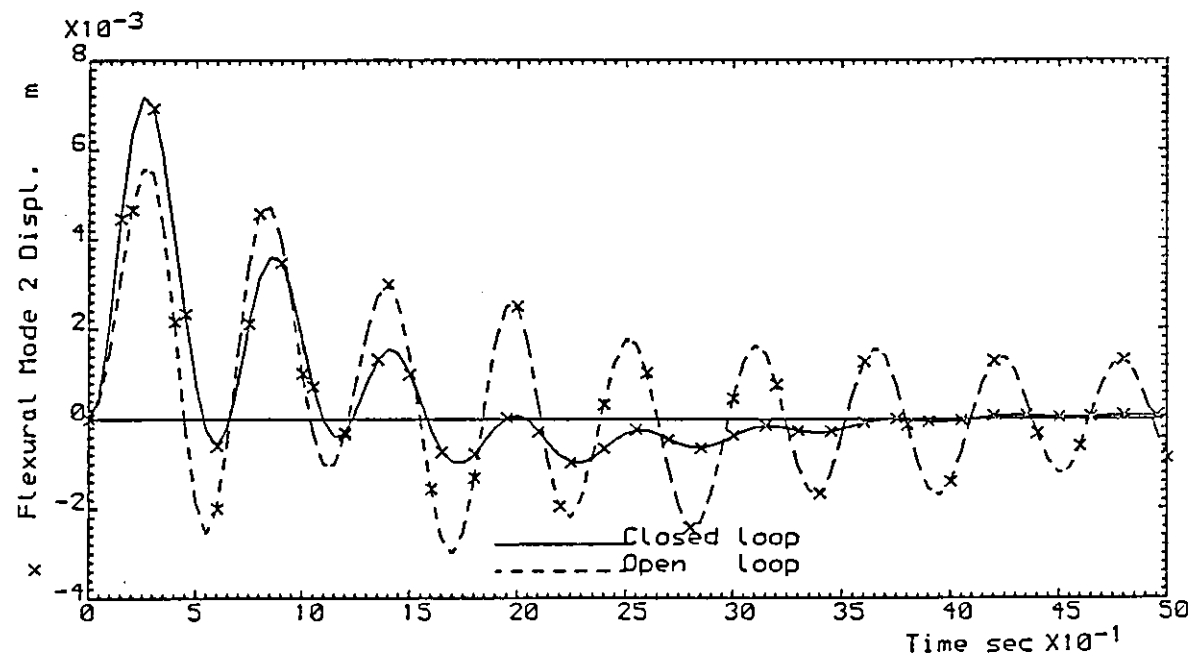

Figure 5.4 : C5-A controlled response, control law A, test case SC1

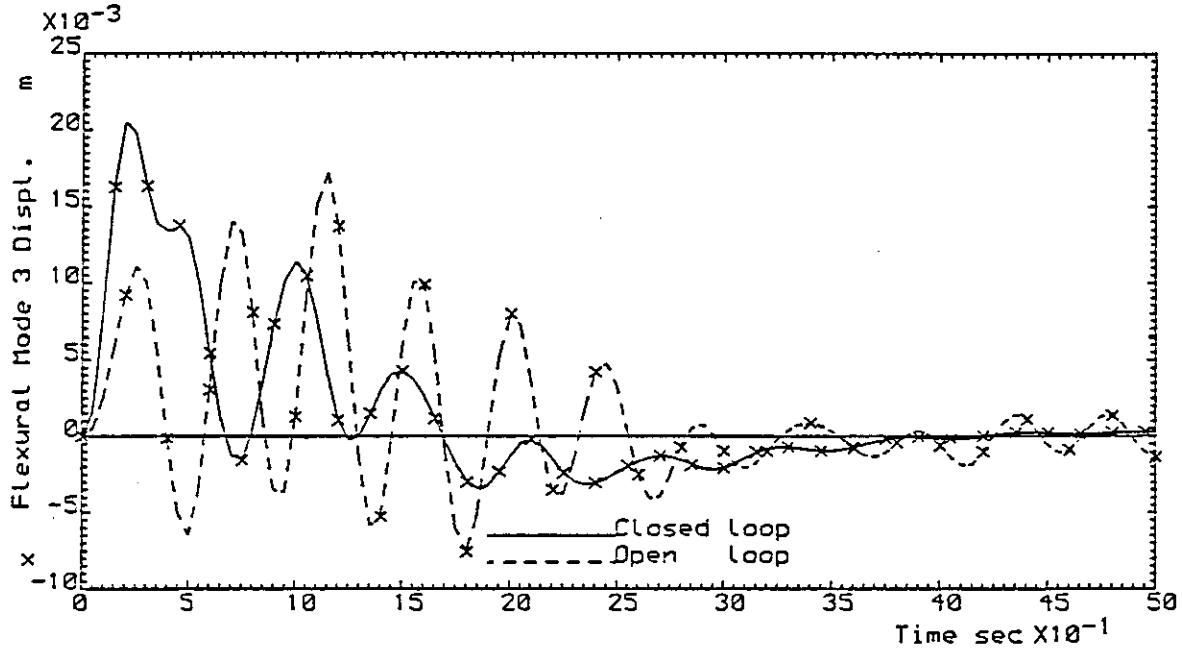

Figure 5.5 : CS-A controlled response, control law A, test case SC1

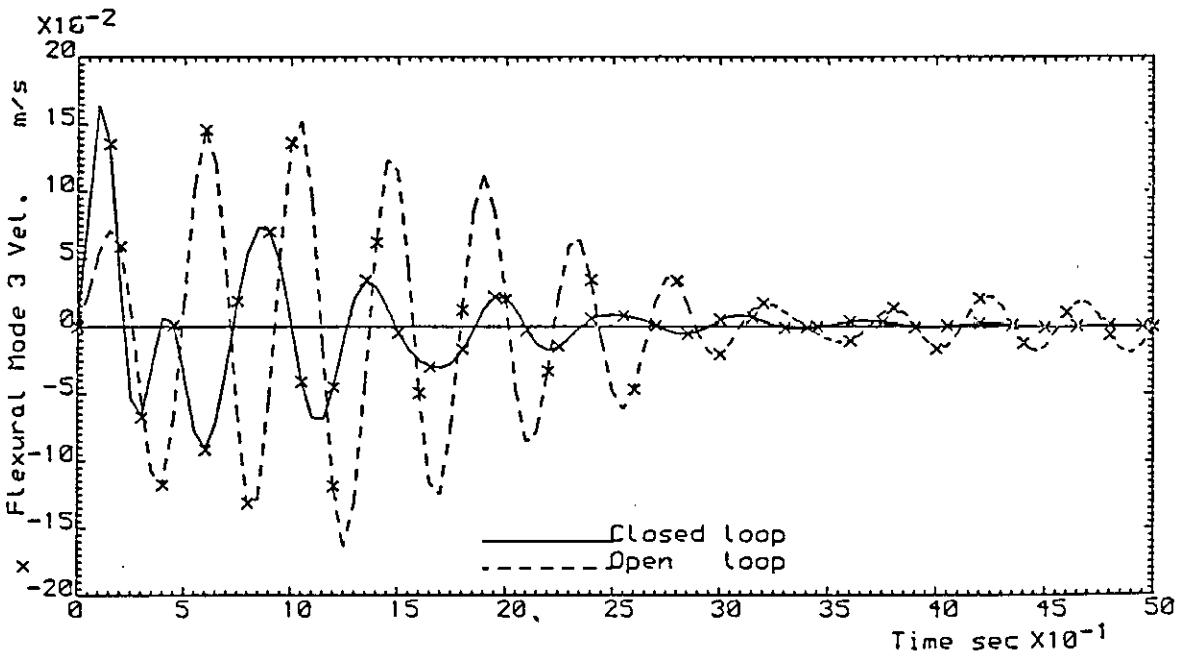

Figure 5.6 : CS-A controlled response, control law A, test case SC1

Mode	Eigenvalue	Frequency	Damping Ratio
Short Period	-0.88 ± j 1.27	1.55	0.569
First Flexural mode	-2.53 ± j 4.86	5.48	0.463
Second Flexural mode	-1.16 ± j 11.06	11.12	0.104
Third Flexural mode	-2.86 ± j 13.51	13.81	0.207
Fourth Flexural mode	-3.02 ± j 15.31	15.61	0.194
Fifth Flexural mode	-2.13 ± j 17.36	17.49	0.122
Sixth Flexural mode	-3.10 ± j 18.53	18.79	0.165
Aileron	-6.0	-	-
Inboard Elevator	-7.5	-	-
Outboard Elevator	-7.5	-	-
Küssner Dynamics : Tail	-22.25	-	-
Küssner Dynamics : Wing	-10.98	-	-
First Order Padé approx.	-8.54	-	-
Second Order Padé approx.	-5.10 ± j 3.60	6.24	0.816
Dryden Filter	-0.247	-	-
Dryden Filter	-0.249	-	-

Table 5.11: Eigenvalues of the closed-loop system, using Law A

5.3 Comparison between feedback laws A and B

These feedback control laws were obtained primarily to establish the validity of the eigenpair assignment method for structural load alleviation in particular the eigenvector selection scheme of case A (as discussed in section 5.2.2 of this thesis). The BM responses at W.S.1, W.S.2 and W.S.3 for control laws A and B, for test case SC1, are shown as figures 5.7 and 5.8. Comparison of figures 5.7 and 5.8 shows that the application of control law B results in a greater reduction of bending moments compared to the reductions obtained by using control law A, from consideration of both the peak and the RMS values. The TM responses for control laws A and B (for test case SC1), are shown as figures 5.9 and 5.10, it is evident from these figures that the peak values of TM responses for law A are lower then those obtained by law B. The controlled responses for both laws are more damped than the uncontrolled response, which is highly oscillatory. The controlled response is satisfactory from the consideration of fatigue

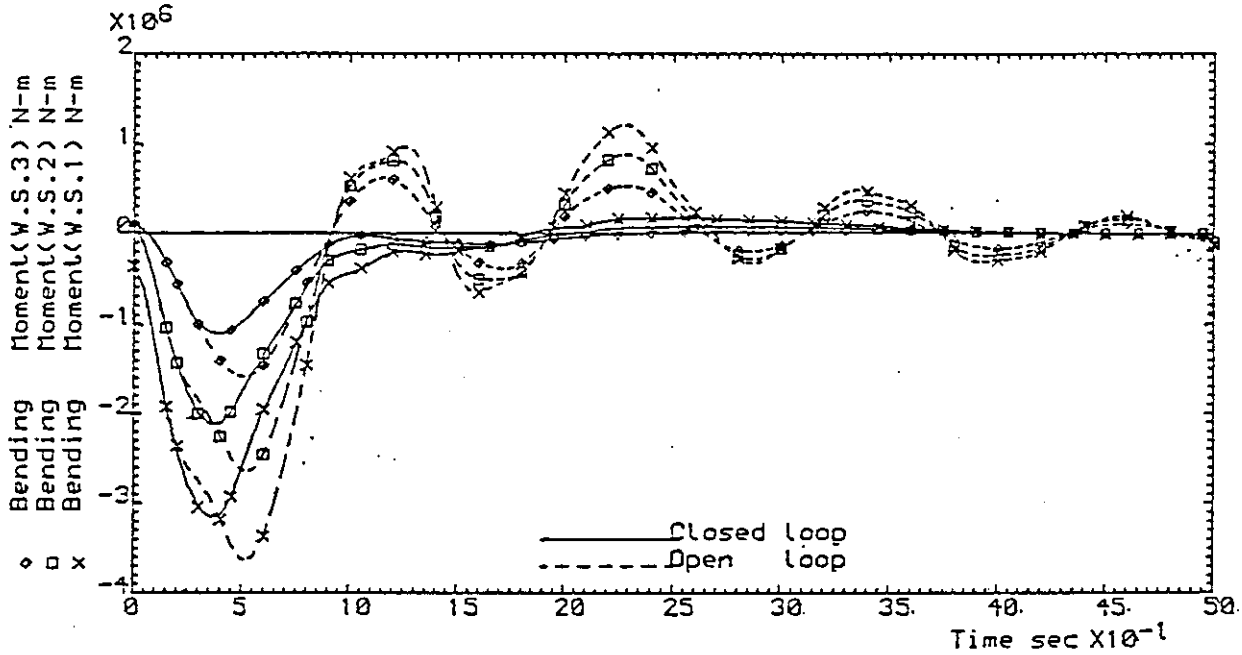

Figure 5.7 : CS-A controlled response, control law A, test case SC1

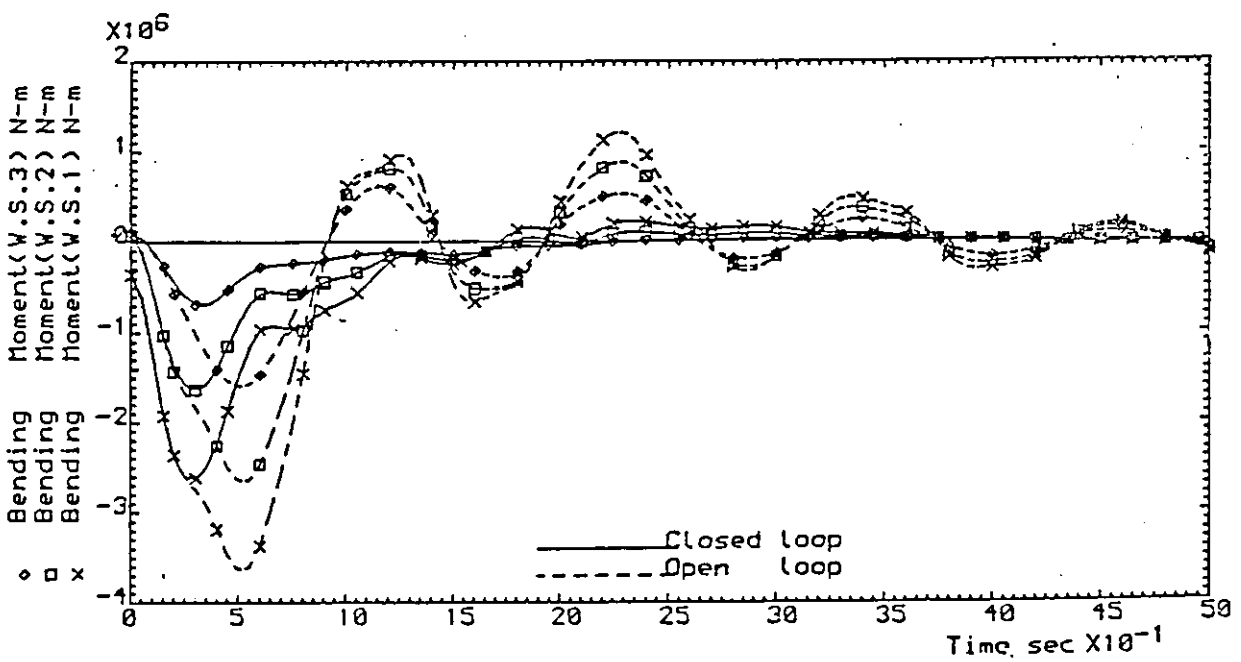

Figure 5.8 : CS-A controlled response, control law B, test case SC1

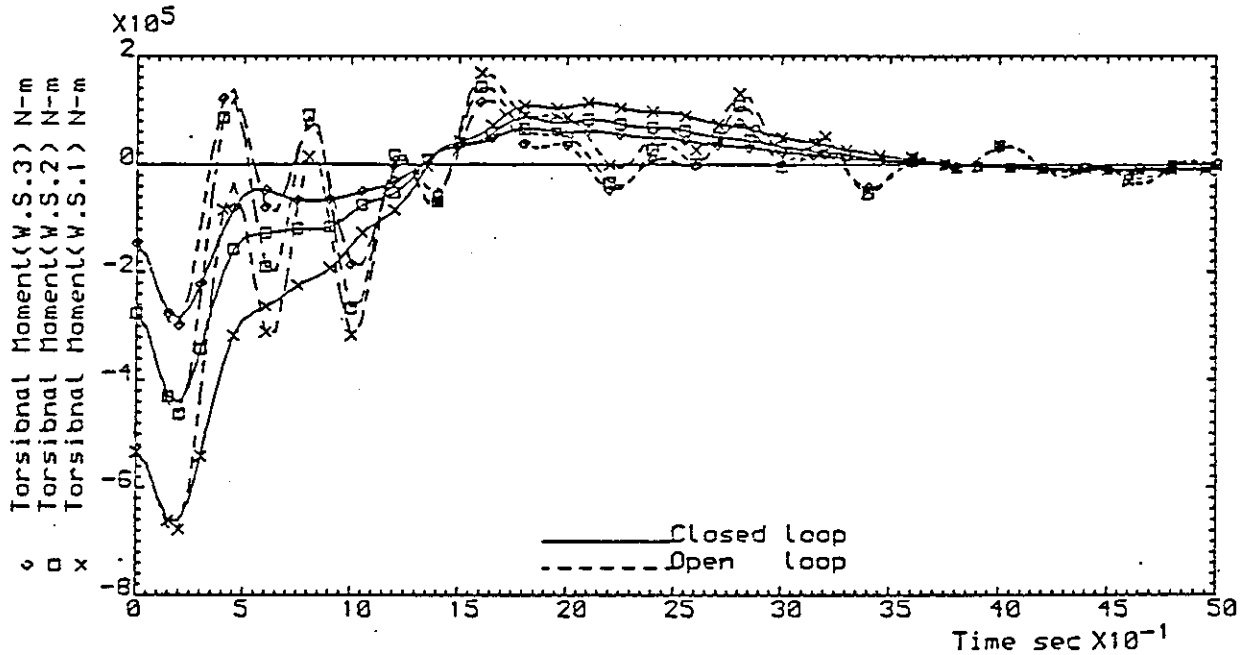

Figure 5.9 : CS-A controlled response, control law A, test case SC1

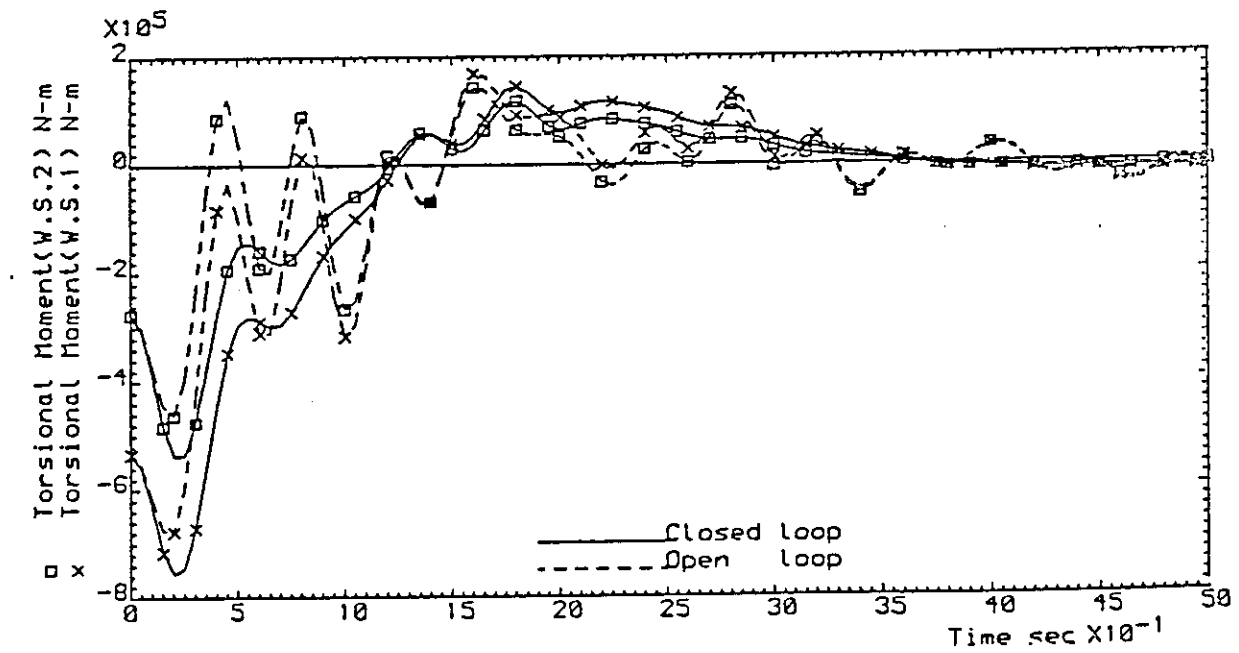

Figure 5.10 :CS-A controlled response, control law B, test case SC1

standpoint, since only low frequency components are present with high frequency components having being reduced.

The reductions, expressed as percentages in the RMS values of the BM and TM at the five wing stations for both control laws, are presented as figures 5.11 and 5.12. From figure 5.11 it may be noted that the bending moment reduction is greatest near the wing tip, whereas the corresponding torsional moment at W.S.5 has increased. The increase in TM is due largely to the fact that the ailerons are situated near the wing tip; the symmetric deflection of ailerons which helps to decrease the bending moments, results in an increase in the torsional moments. A reduction of 22% in the RMS value of the BM, together with an increase of 7.5% in the RMS value of the TM at W.S.1 was achieved for control law A. From figure 5.12 it is seen that control law B results in greater RMS reductions of the bending moments when compared to the reductions obtained for control law A.

Presented as figures 5.13 and 5.14 are the peak values of the bending and torsional moments for laws A and B respectively. It is seen from figure 5.13 that the reductions in the peak values of the bending moments for law B are much greater than for law A. Nevertheless, from figure 5.14 it is seen that the peak torsional moments are considerably greater for law B compared to the values resulting in the uncontrolled case.

One noteworthy feature of the BM response presented in figure 5.7 is its similarity to the shape of the displacement response of the first flexural mode (see figure 5.2), which confirms the dominance of the influence of the first flexural mode upon the bending moment response.

From the results presented so far, the use of control law A produced better results than obtained by using control law B. It has been shown that although the use of law B can produce the desired reductions in bending moments, an associated increase in the torsional moments is always observed.It was decided therefore to use control law A in the further studies relating to manoeuvre load control (MLC) and gust load alleviation (GLA).

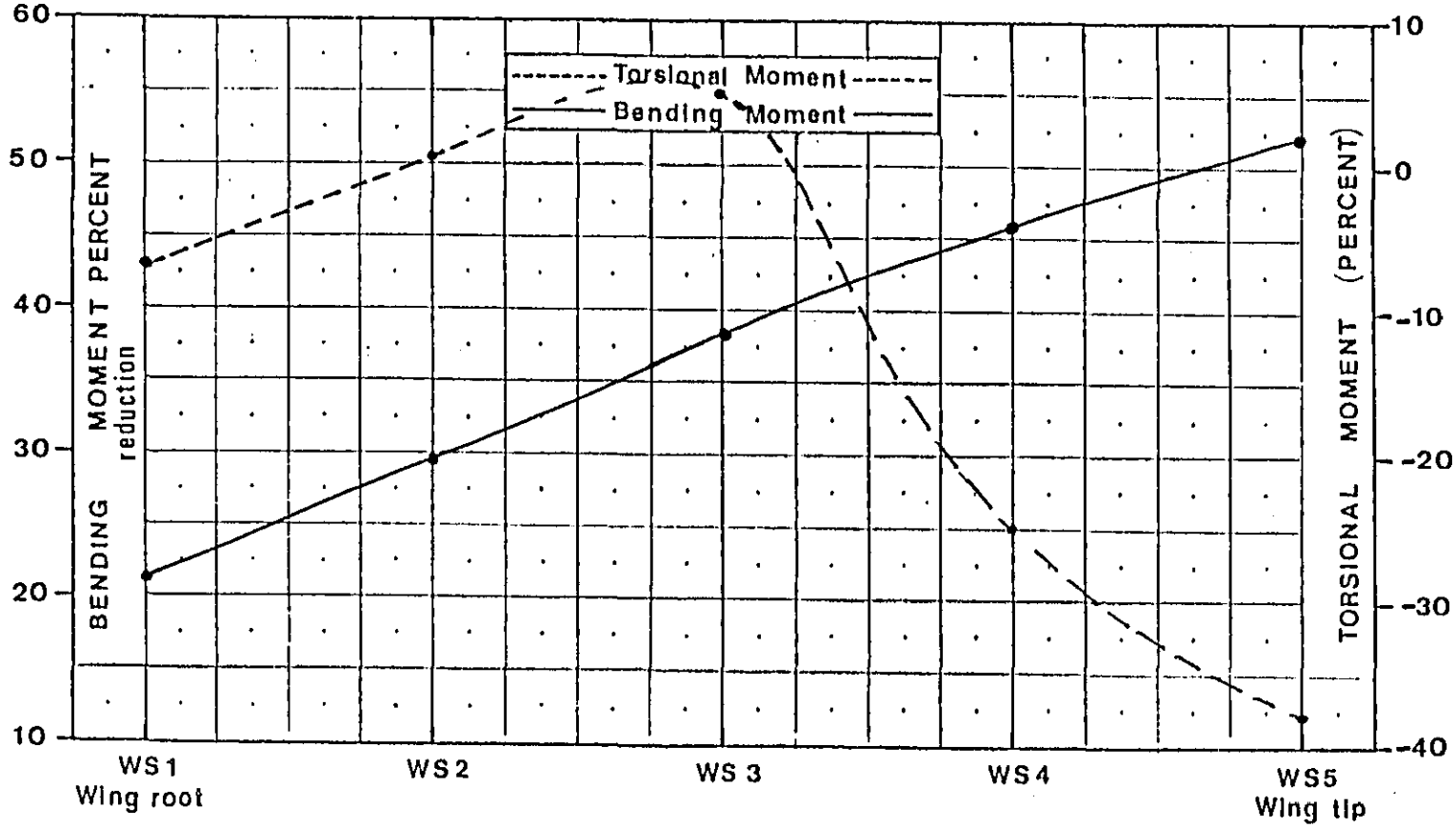

Figure5.11 : Percent reduction of Bending and Torsional moments, control law A, test case SC1

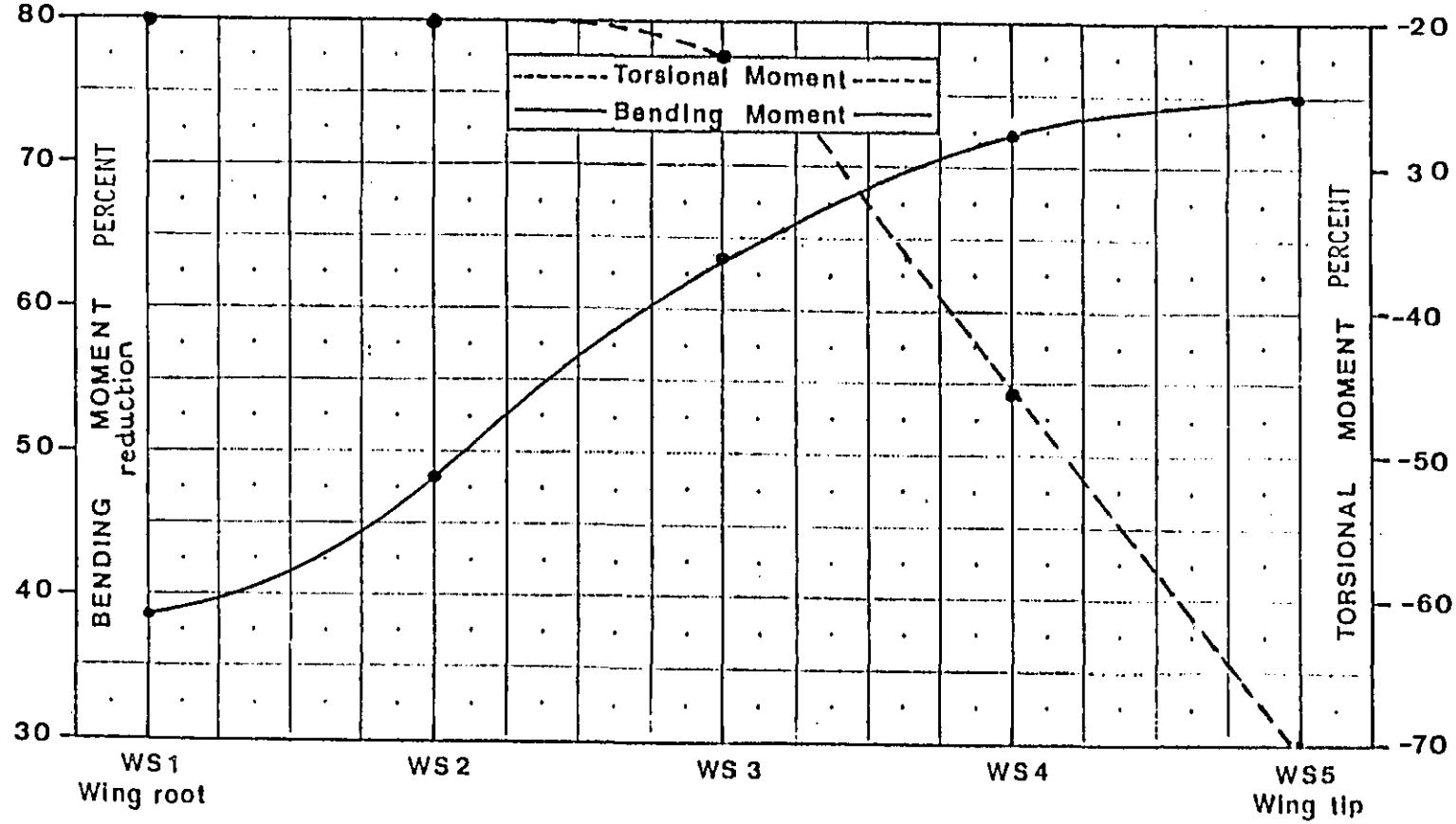

Figure 5.12 : Percent reduction of Bending and Torsional moments, control law B, test case SC1

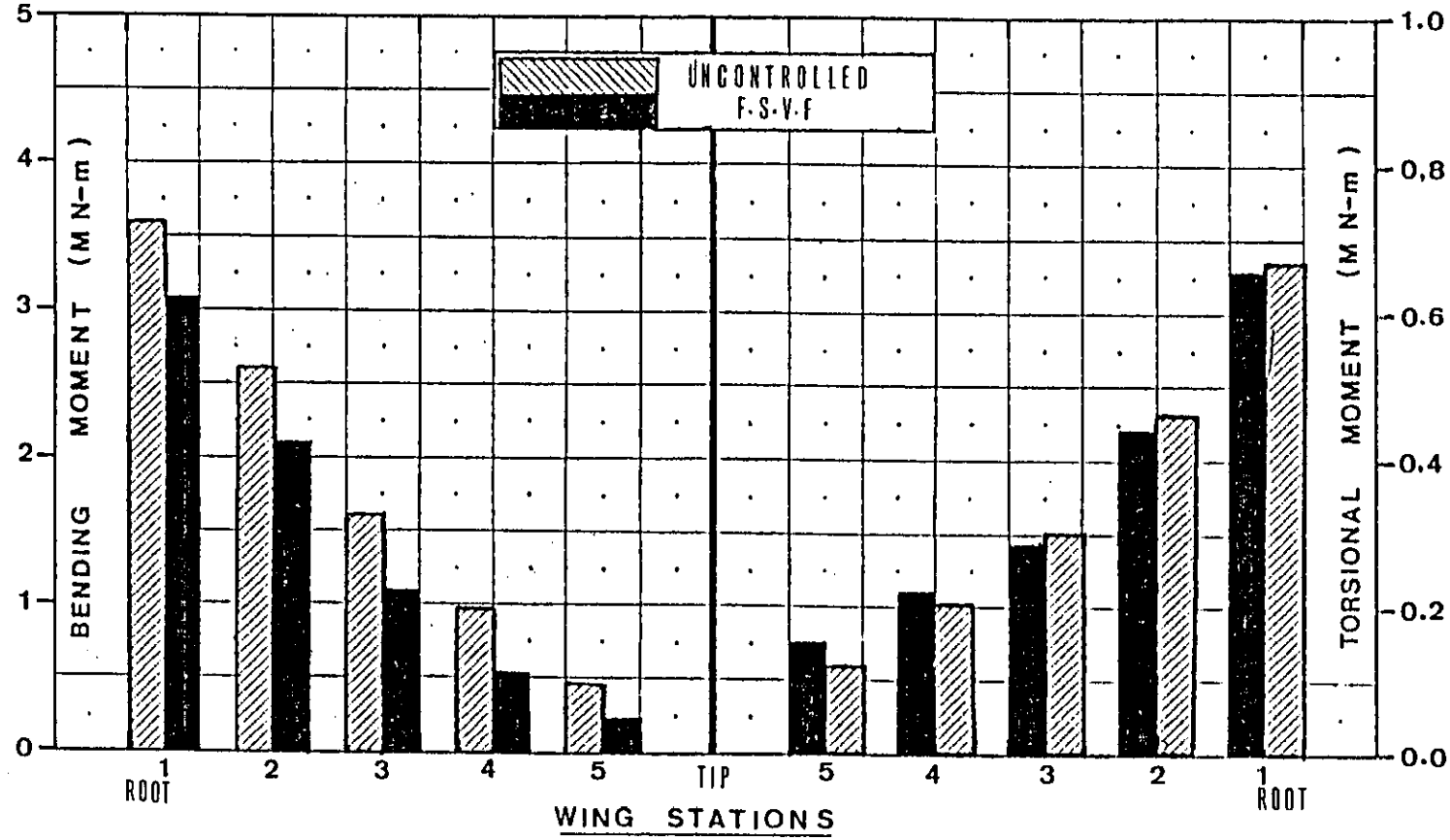

Figure 5.13 : Absolute peak values of Bending and Torsional moments, Law A, case SC1

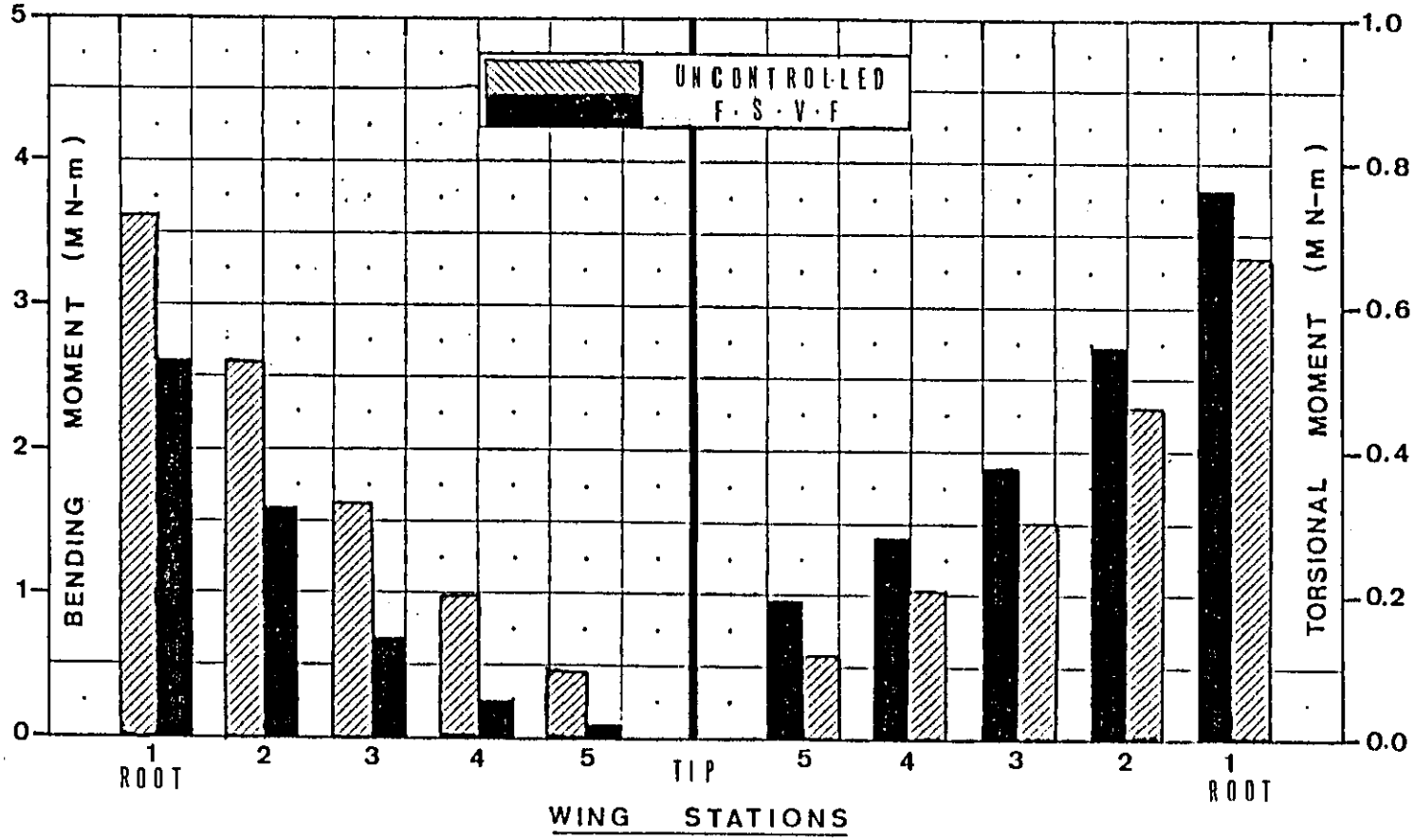

Figure 5.14 : Absolute peak values of Bending and Torsional moments, Law B, csae SC1

5.4 Manoeuvre Load Control

The method described in section 4.6 was used to force the closed-loop system. The effect of commands to both the ailerons and the inboard elevator is studied. The forcing vector (equation 4.66) computed for test cases SC2 and SC3 was found to be,

Test case SC2

$$r = \begin{bmatrix} -2.24 \\ -11.21 \end{bmatrix} . \qquad 5.3$$

Test case SC3

$$r = \begin{bmatrix} 1.667 \\ -22.11 \end{bmatrix} . \qquad 5.4$$

The steady-state values for test case SC2 and SC3, of the vertical velocity (w) were found to be -0.48 m/s and -0.83 m/s respectively these values are comparable to the values for the uncontrolled aircraft, being within 0.2% of the uncontrolled values. The steady-state values of the normalised pitch rate (q), for test case SC2 and SC3 were found to be -0.075 m/s and -0.146 m/s respectively, which are within 5.0% of the uncontrolled values.

The controlled responses of the normalised pitch rate and the vertical velocity are shown as figures 5.15a and 5.15b respectively. It is seen from these figures that the controlled response closely follows the uncontrolled response. Since a pilot's motion cues are based on the rigid body motion variables, by forcing the controlled rigid body variables to the same steady-state values as in the open-loop system, it is then possible to assess any reductions in the bending and torsional moments which may arise due to command inputs.

From figure 5.15a and 5.15b it is also seen that the dynamic response of the controlled variables w and q are almost identical to those of the uncontrolled variables. This is because the short period eigenvalues have not been altered in the closed-loop. Minor differences occur due to

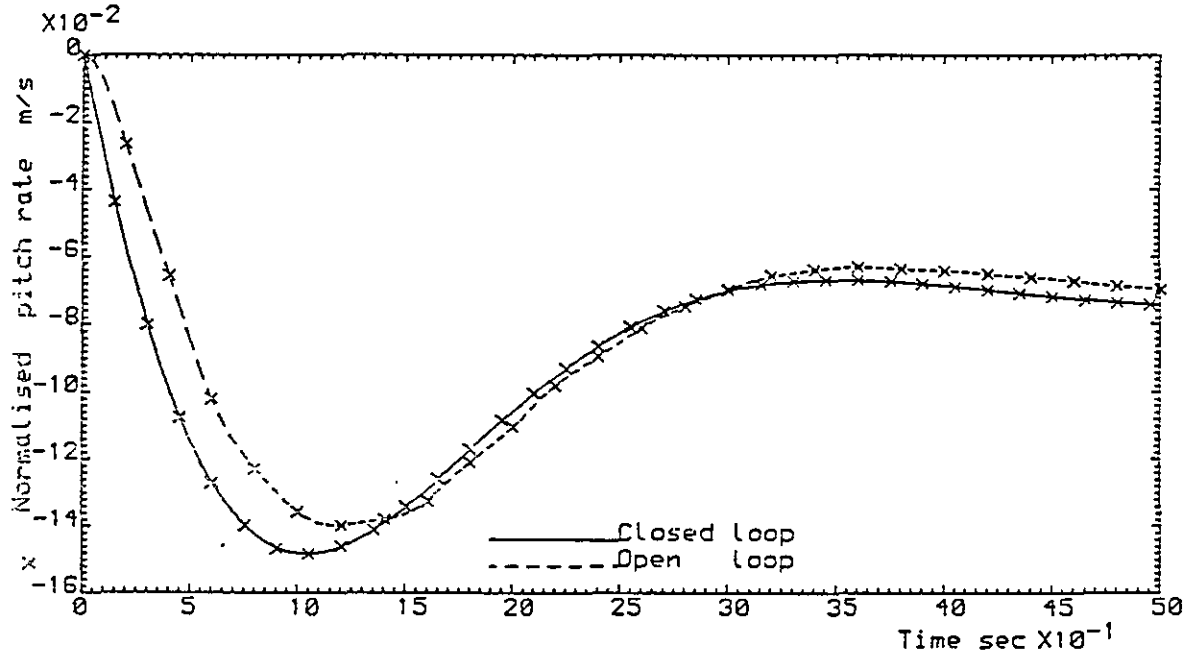

Figure 5.15a: C5-A controlled response, control law A, test case SC2

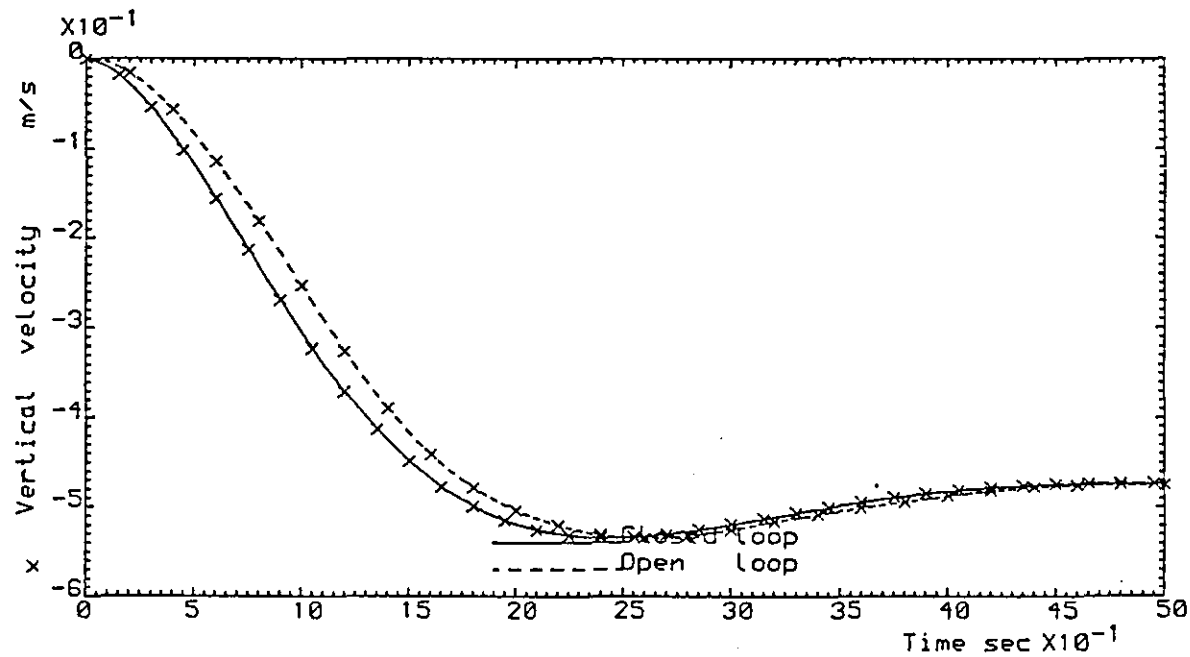

Figure 5.15b: C5-A controlled response, control law A, test case SC2

difference in the closed-loop eigenvectors corresponding to the short period eigenvalues.

The assessment of bending and torsional moments is based on the peak values and the RMS values. For the controlled aircraft (control law A, test case SC2), the responses of the bending and torsional moments at the five wing stations, are presented in figure 5.16 and 5.17. From both these figures it is seen that the settling time is small when compared to the uncontrolled response. The oscillatory nature of the uncontrolled response is not evident in the controlled response. The reductions in the RMS and peak values, in percentages are presented in table 5.12.

Variable	RMS	Peak
BM W.S.1	19.7	67.8
BM W.S.2	61.0	81.2
BM W.S.3	91.0	94.0
BM W.S.4	96.4	99.3
BM W.S.5	89.1	94.0
TM W.S.1	38.6	36.8
TM W.S.2	48.8	47.0
TM W.S.3	56.8	57.0
TM W.S.4	47.4	43.5
TM W.S.5	53.4	48.9

Table 5.12: Percent reduction in RMS and peak values

From table 5.12 it is evident that, by using control law A, substantial reductions have been achieved in both the bending and torsional moments. The bending and torsional moments (control law A, test case SC3) are presented as figures 5.18 and 5.19. It is interesting to note that for test case SC3, although the bending moment response has been greatly improved, the torsional moment response has deteriorated both in terms of peak values and as well as steady-state values. Nevertheless, the absence of oscillatory motion from the responses of the bending and torsional moments indicates the suitability of the control law from the structural fatigue standpoint. Although steady-state values of the torsional moments for the controlled

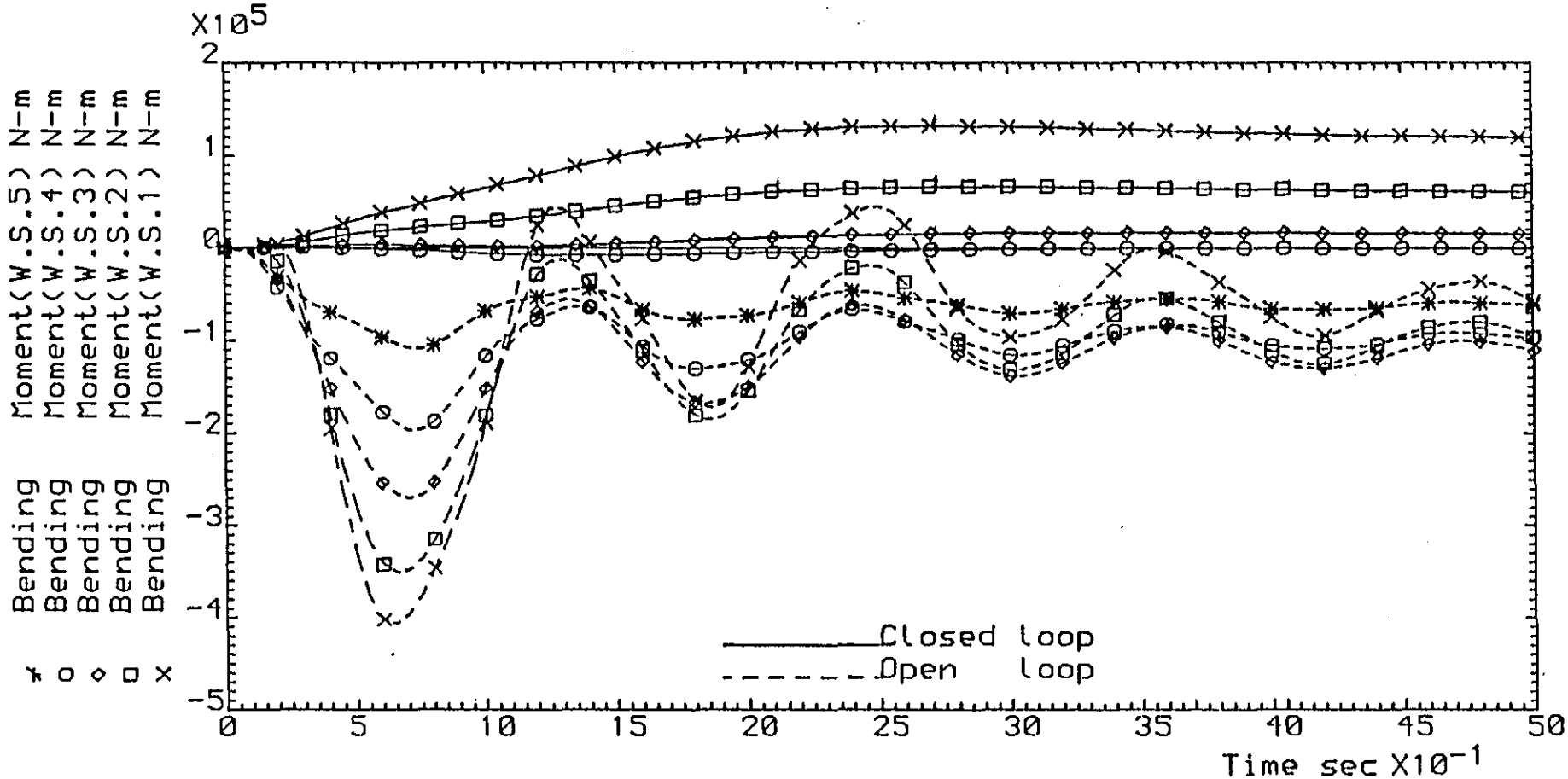

Figure 5.16 :C5-A controlled response, control law A, test case SC2

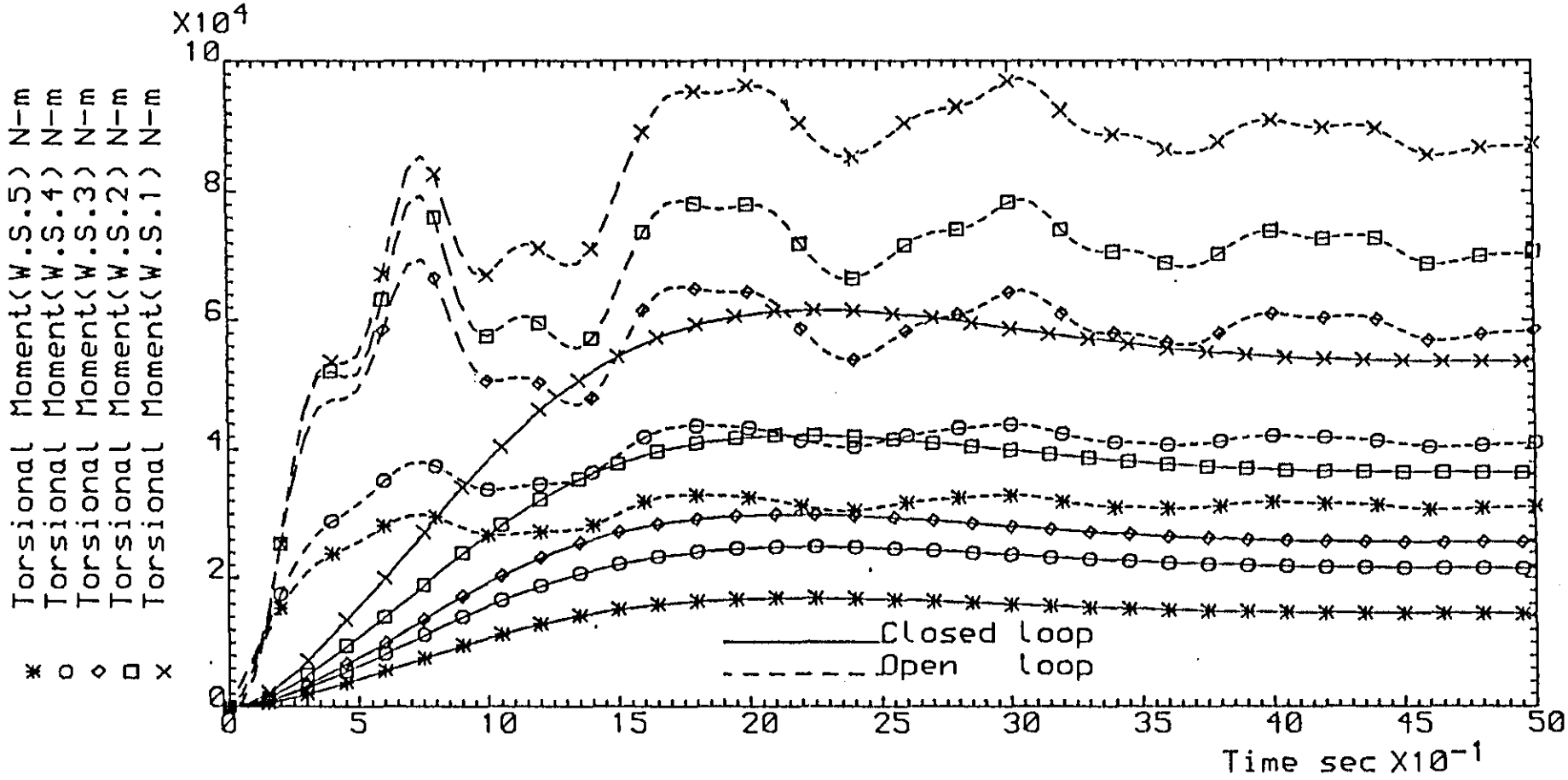

Figure 5.17 :C5-A controlled response, control law A, test case SC2

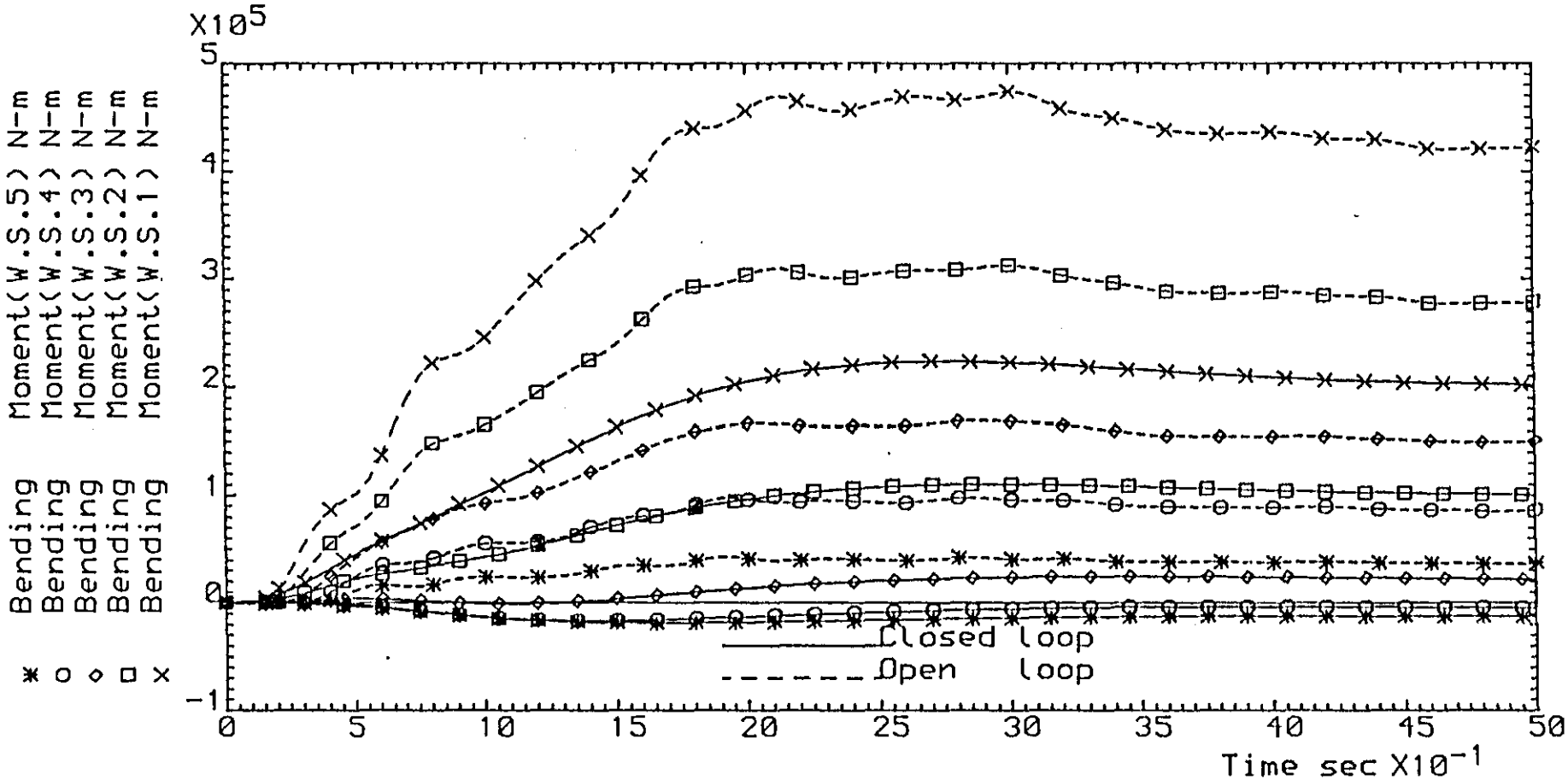

Figure 5.18 : C5-A controlled response, control law A, test case SC3

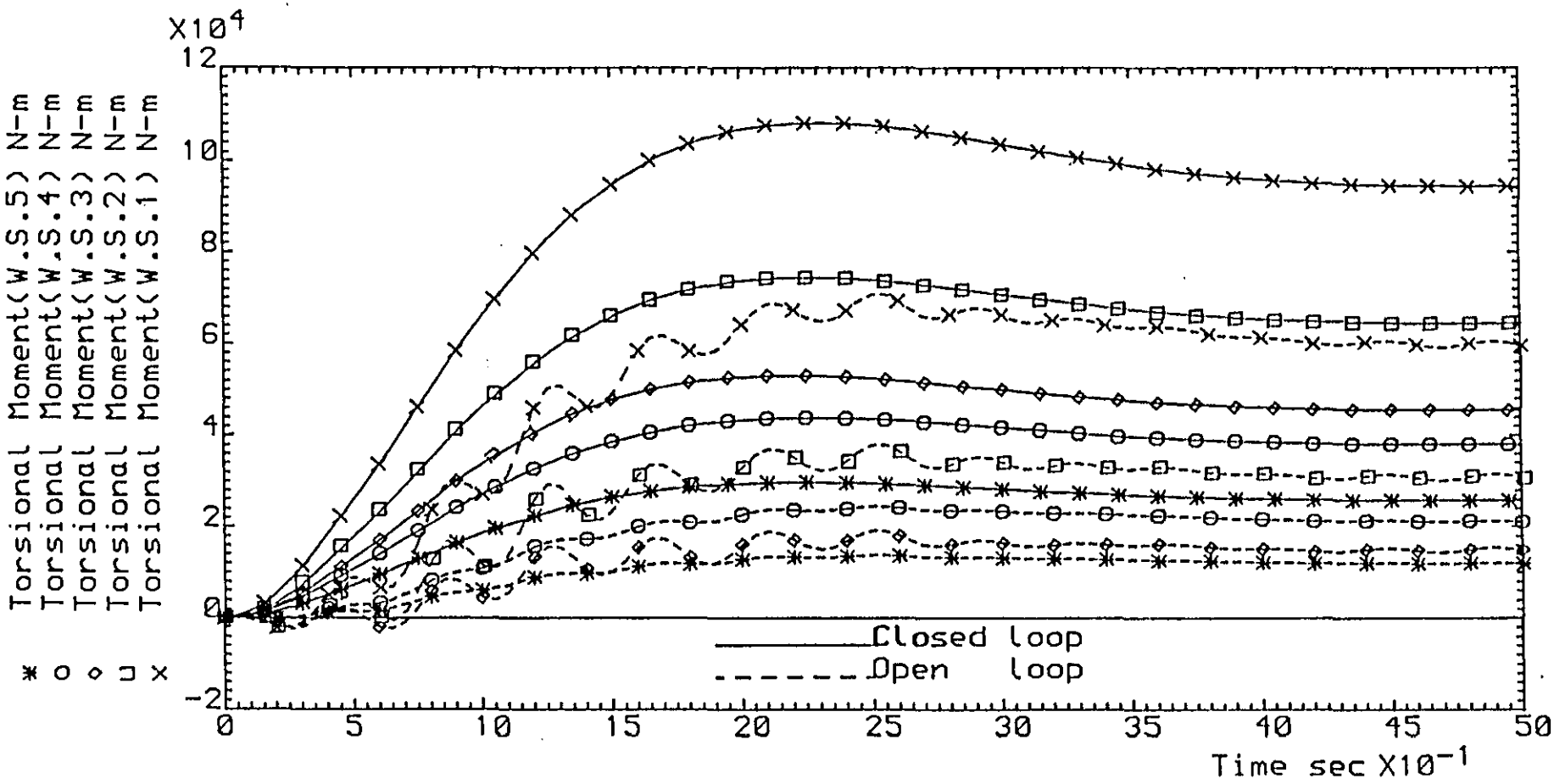

Figure 5.19 : C5-A controlled response, control law A, test case SC3

aircraft for case SC3 are higher than the uncontrolled values, the peak TM at W.S.1 is almost identical to the peak TM at W.S.1 for test case SC2 for the uncontrolled aircraft (see figures 5.17 and 5.19). If the ultimate torsional strength at various wing stations is known, only then can a quantitative assessment can be made of whether the controlled peak or the steady-state TM's are within the ultimate strength requirements.

The steady-state value of 0.094 MN-m of TM at W.S.1 (figure 5.19), compares favourably with the controlled steady-state value of 0.106 MN-m of TM at W.S.1 obtained by Prasad [1980], for the same test conditions, using a full state variable feedback control law obtained from the use of LQP. The control law devised by Prasad was based on the optimal output regulator, in which all the quantities in the output vector (see section 4.4) were weighted. Since the objective was to cause reductions in the torsional and bending moments, optimal output regulator has advantages over the optimal state regulator, in that the moments can be weighted directly in the performance index. It known (Newberry [1969]) that to effect reductions in the TM and BM, the peak amplitudes of the flexural modes have to be reduced, and such reductions can be accomplished by use of the eigenvector specification scheme discussed earlier (see section 5.2.2). The results presented so far are better in every respect, than those presented before by other authors using optimal control. Therefore it can be said that the control law synthesised by EPAM has all the features required for SLA: it achieves the desired load reduction without causing any deterioration in the basic handling qualities of the aircraft and it is still possible to manoeuvre the aircraft to any desired operating point.

5.4.1 Requirements for MLC

The deflection rates and angular deflections of a control surface are important parameters in judging the effectiveness of any control scheme, for securing reductions in structural loads. If the required rates and deflections exceed the capabilities of the existing hardware (servos, actuators etc), then either the existing hardware has to be changed or some new control law has to be found to conform to the specifications. For the MLC (using control law A) the rates and

deflections associated with the ailerons and the inboard elevator were found to be within the capabilities of existing actuators. Presented in figure 5.20 to 5.27 are the rates and deflections associated with the ailerons and the elevator for the two test cases SC2 and SC3. It is observed from these figures that the values of these the rates and deflections are not excessive. For example, a maximum aileron deflection of $9.0*10^{-3}$ rads and maximum elevator deflection of $1.7*10^{-3}$ rads are required for test case SC1 (figure 5.21 and 5.23). For test case SC3 peak aileron and elevator deflections were $1.6*10^{-2}$ and $0.3*10^{-2}$ rads respectively (see figures 5.25 and 5.27). The eigenvalues associated with the actuator modes, in the closed-loop were chosen to be identical to those in the open-loop (see table 5.11). Since the time constants of the actuator modes are the same, the alleviation of structural loads was achieved without the need for the use of faster acting actuators than those already used on the aircraft.

5.5 Gust Load Alleviation

The digital simulation language, Advanced Continuous Simulation Language (ACSL), was used to simulate atmospheric turbulence, primarily because of the availability within the package of MACROS which facilitated the generation of white noise, which is required as the input to a Dryden filter. The standard deviation of the white noise was selected to be 0.3048 m/s with a zero mean value. This choice corresponds to moderate levels of turbulence. Test case SC4 represented the situation of an aircraft traveling in its trimmed flight state and suddenly encountering atmospheric turbulence. Some selected responses are presented as figures 5.28 to 5.34. It can be seen from figure 5.28, that test case SC4 produces a larger value of bending moment at W.S.1 compared to the levels produced for the deterministic cases SC2 and SC3. The selected responses presented are for the uncontrolled aircraft (curves marked A), and for the FSVF control law A (curves marked B). The bending moment response at W.S.1, W.S.2 and W.S.3 are presented as figures 5.28 , 5.30 and 5.32. It is evident that the peak values of the controlled response are much lower than the uncontrolled values, and the controlled response is better damped. From the response of the torsion moment shown in figures 5.29 and 5.31 it is evident that the peak values are almost the same for both the controlled and the uncontrolled

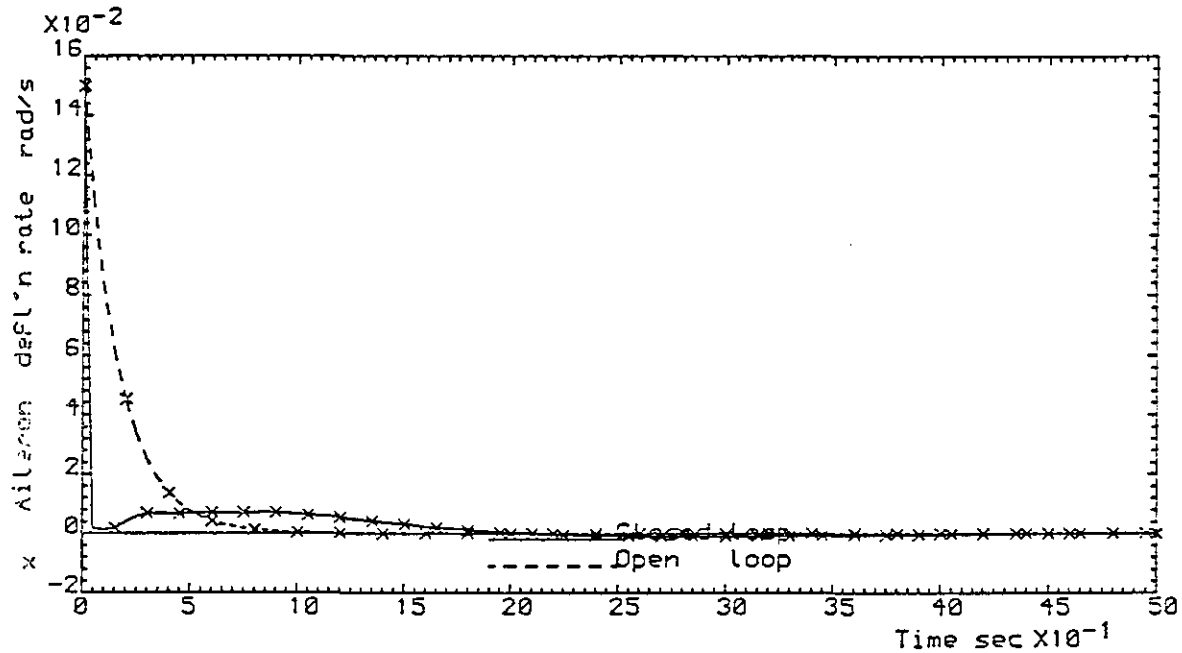

Figure 5.20 :CS-A controlled response, control law A, test case SC2

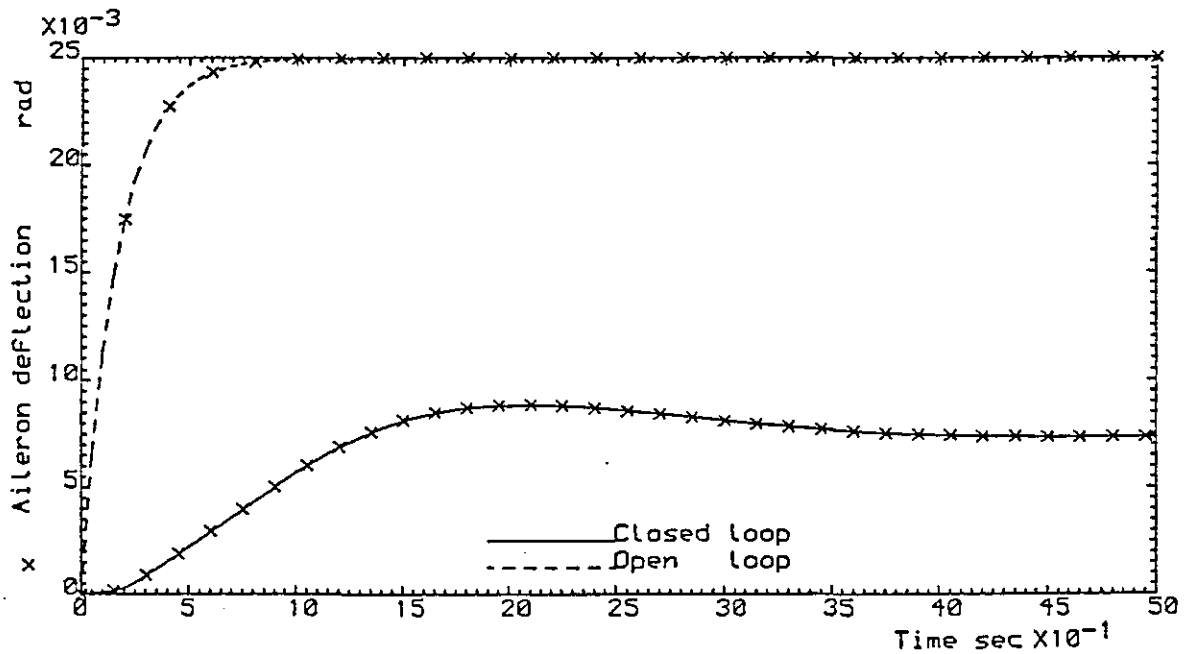

Figure 5.21 : CS-A controlled response, control law A, test case SC2

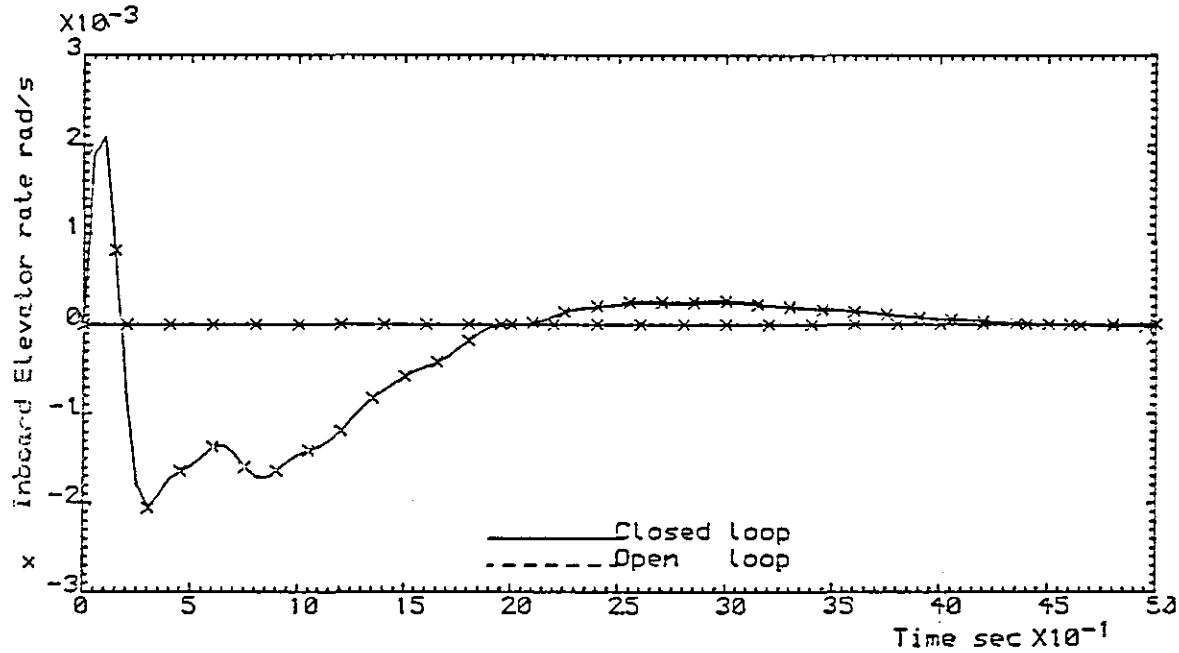

Figure 5.22 : C5-A controlled response, control law A, test case SC2

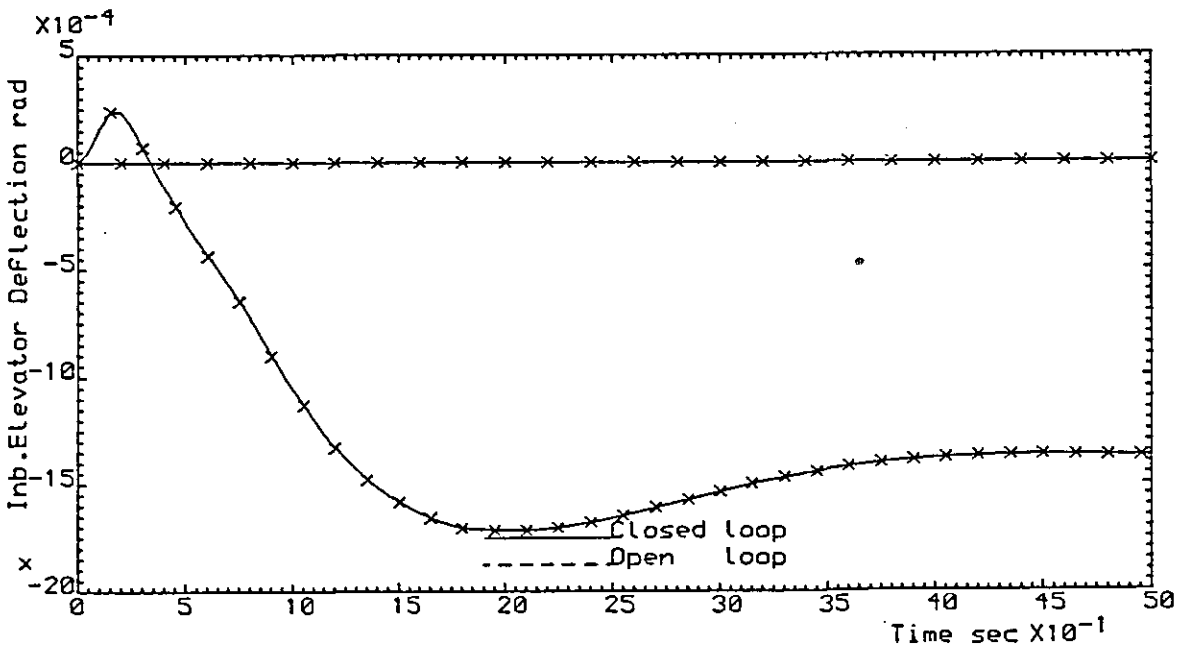

Figure 5.23 : C5-A controlled response, control law A, test case SC2

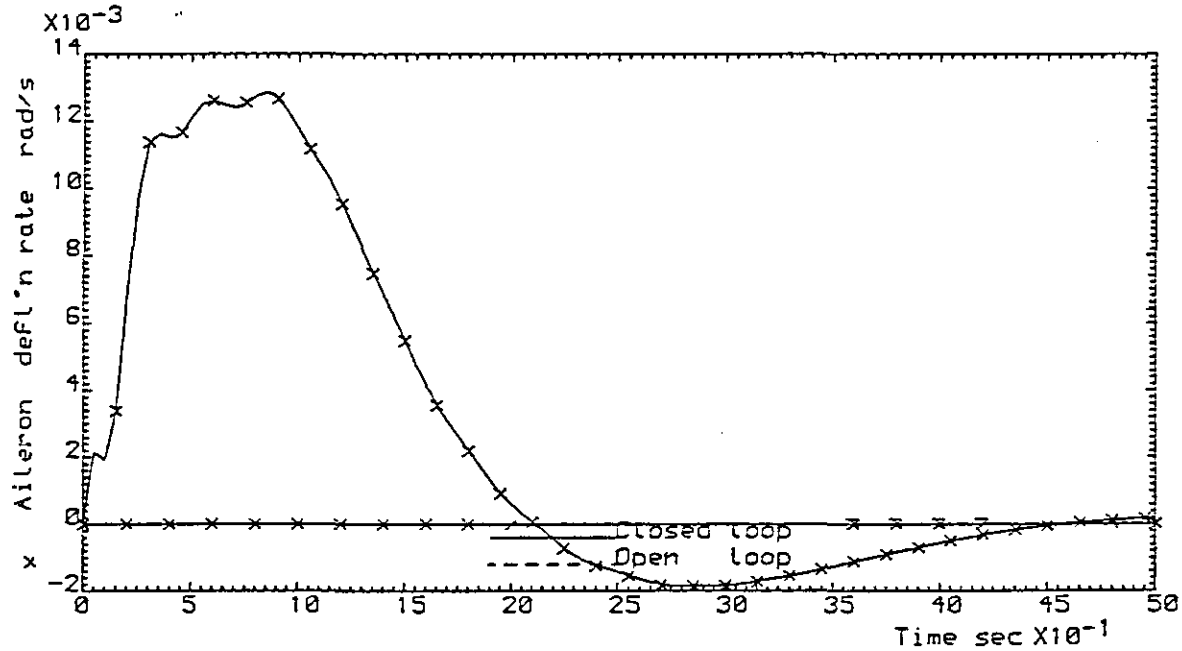

Figure 5.24 : C5-A controlled response, control law A, test case SC3

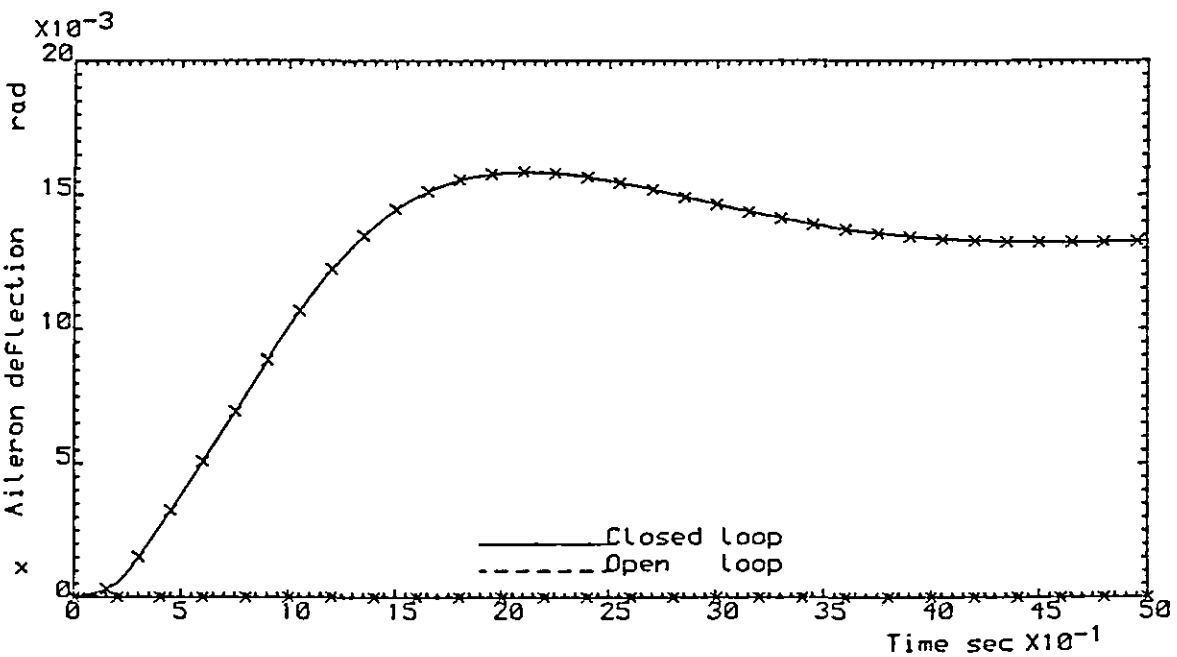

Figure 5.25 : C5-A controlled response, control law A, test case SC3

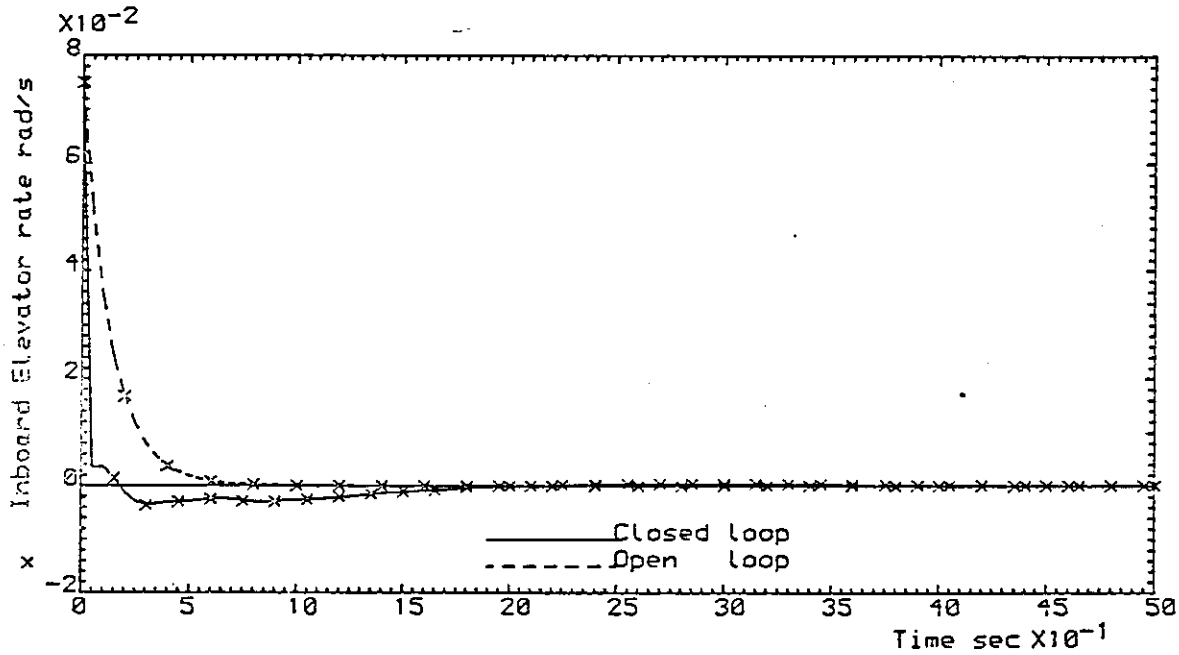

Figure 5.26:C5-A controlled response, control law A, test case SC3

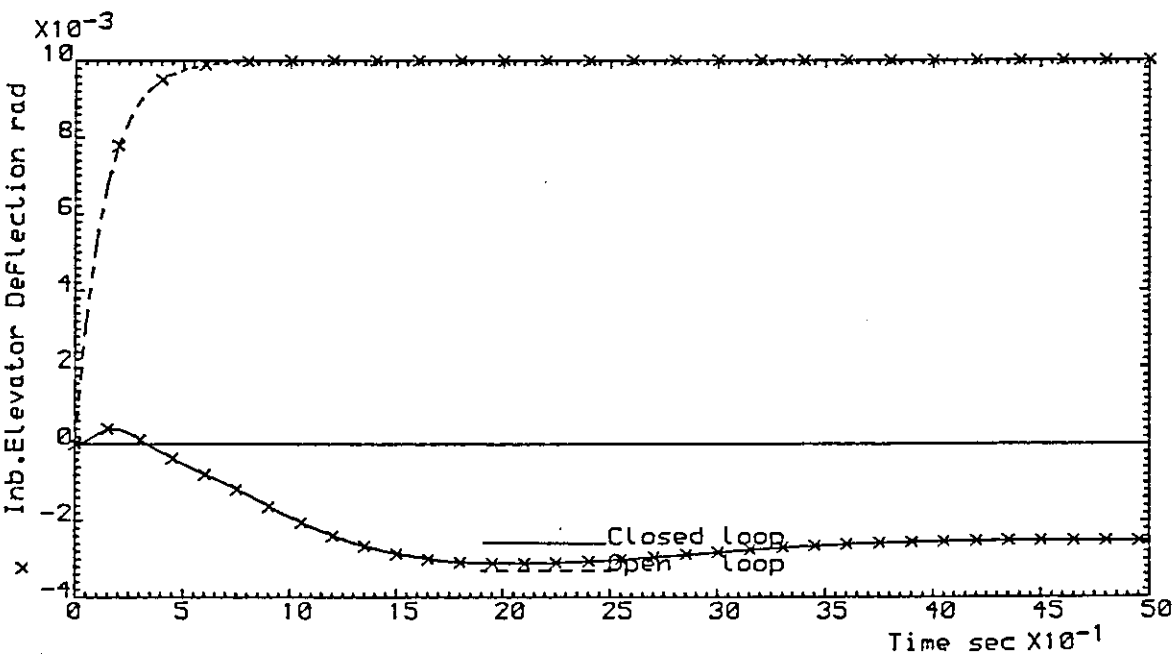

Figure 5.27 C5-A controlled response, control law A, test case SC3

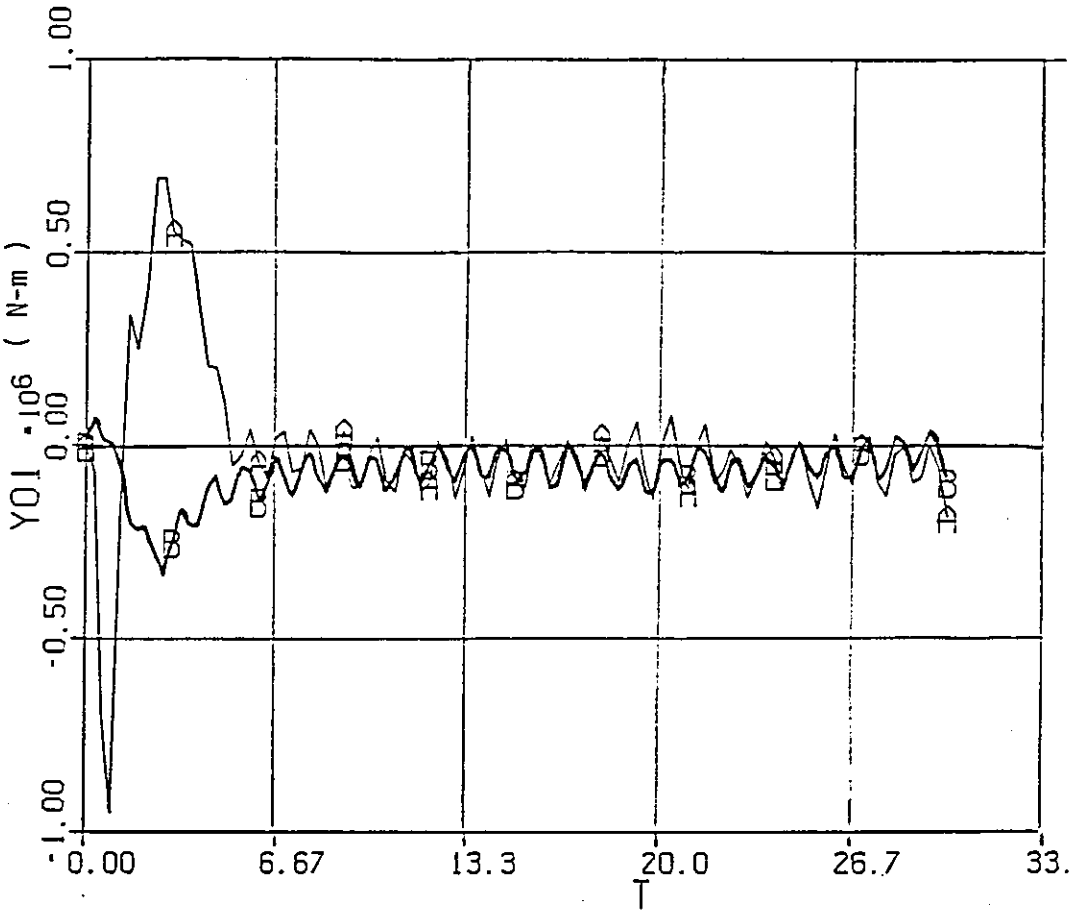

Figure 5.28 : Bending moment W.S.1, control law A, test case SC4

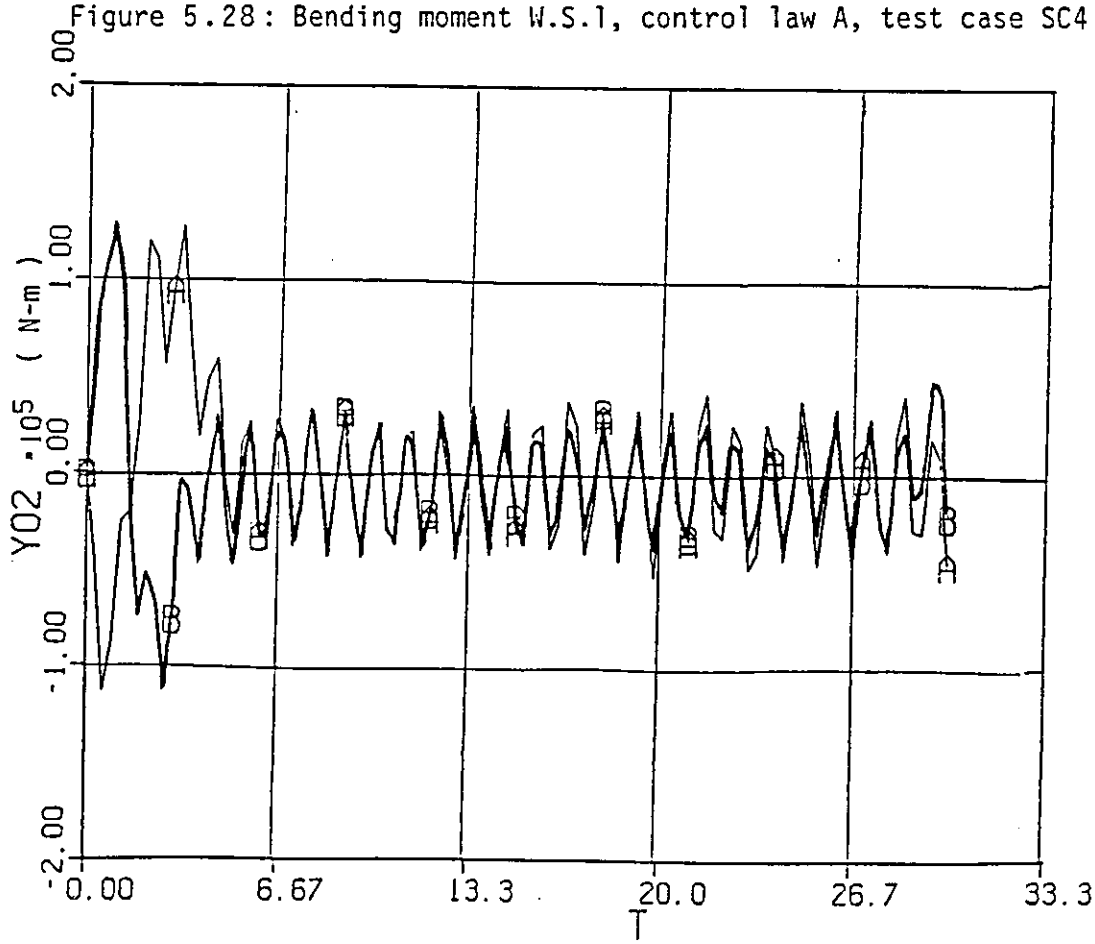

Figure 5.29 : Torsion moment W.S.1, control law A, test case SC4

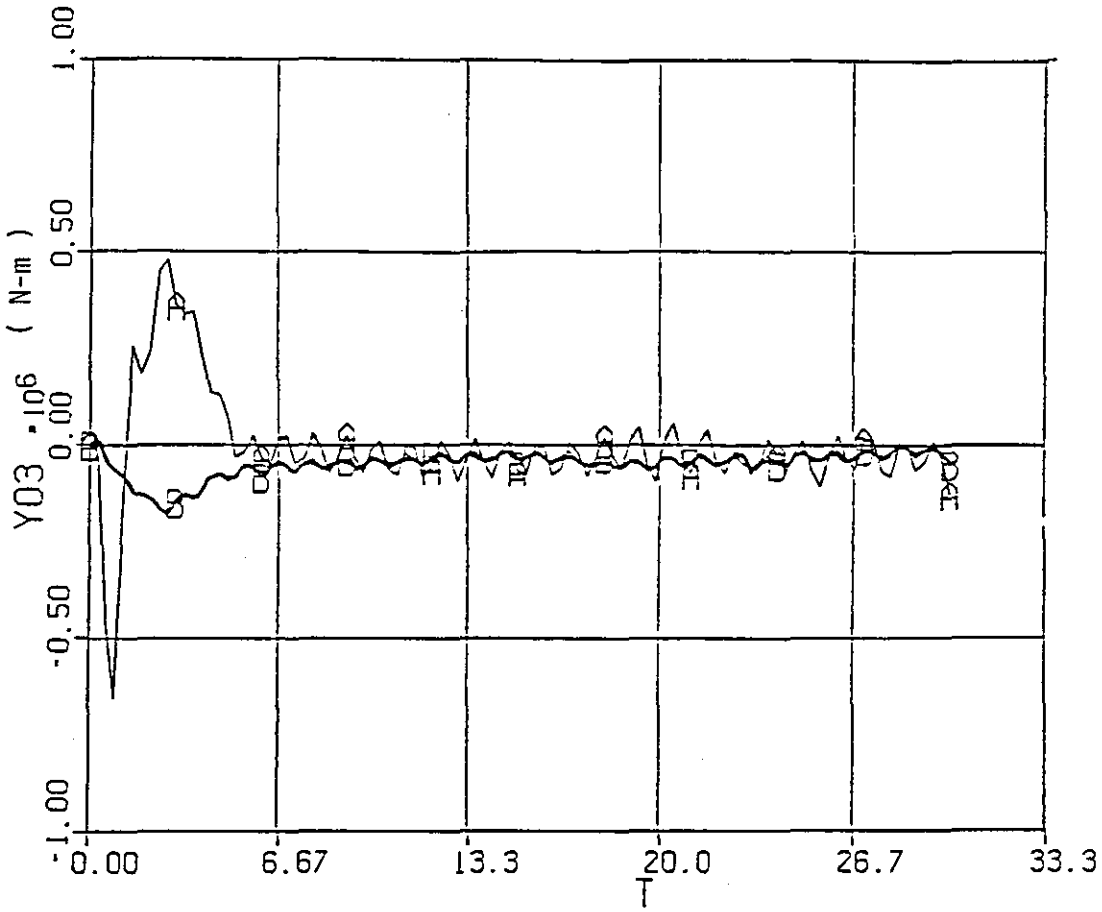

Figure 5.30 : Bending moment W.S.2, control law A, test case SC4

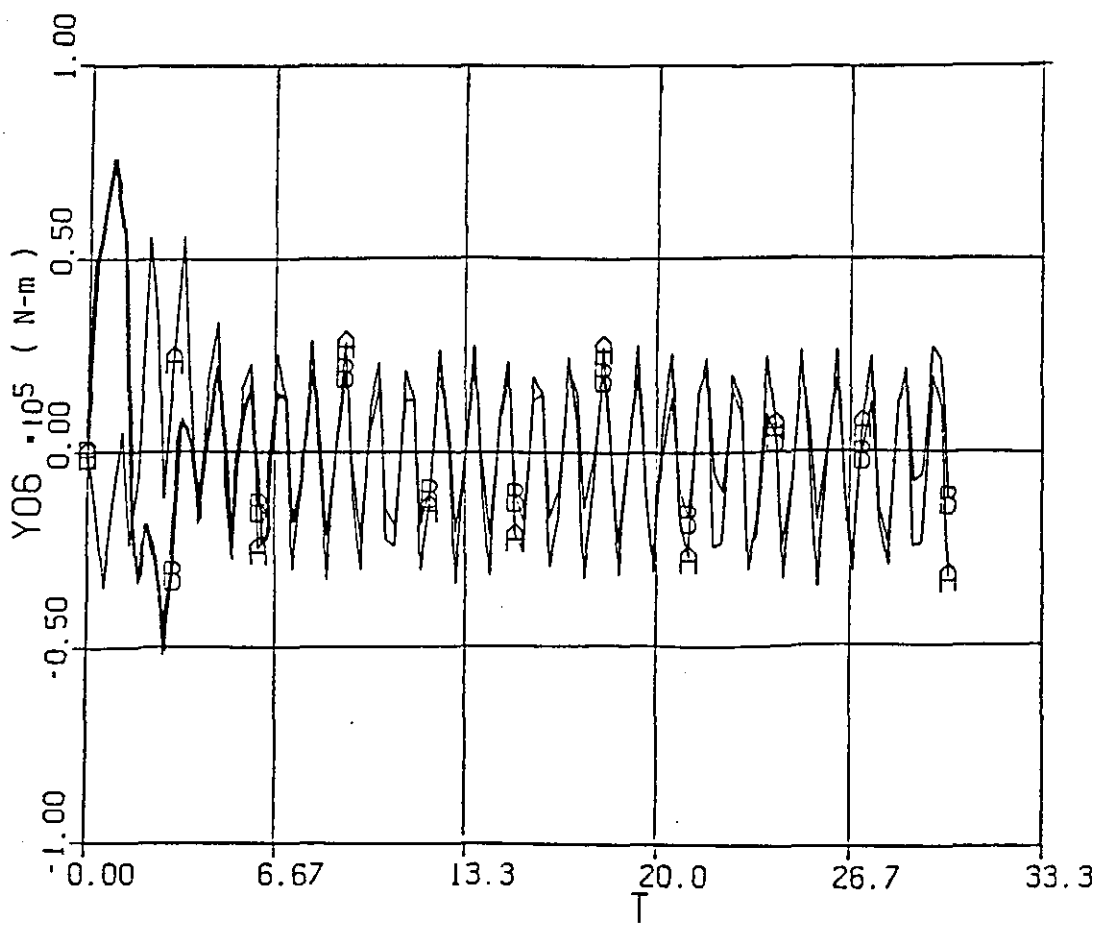

Figure 5.31 : Torsion moment W.S.3, control law A, test case SC4

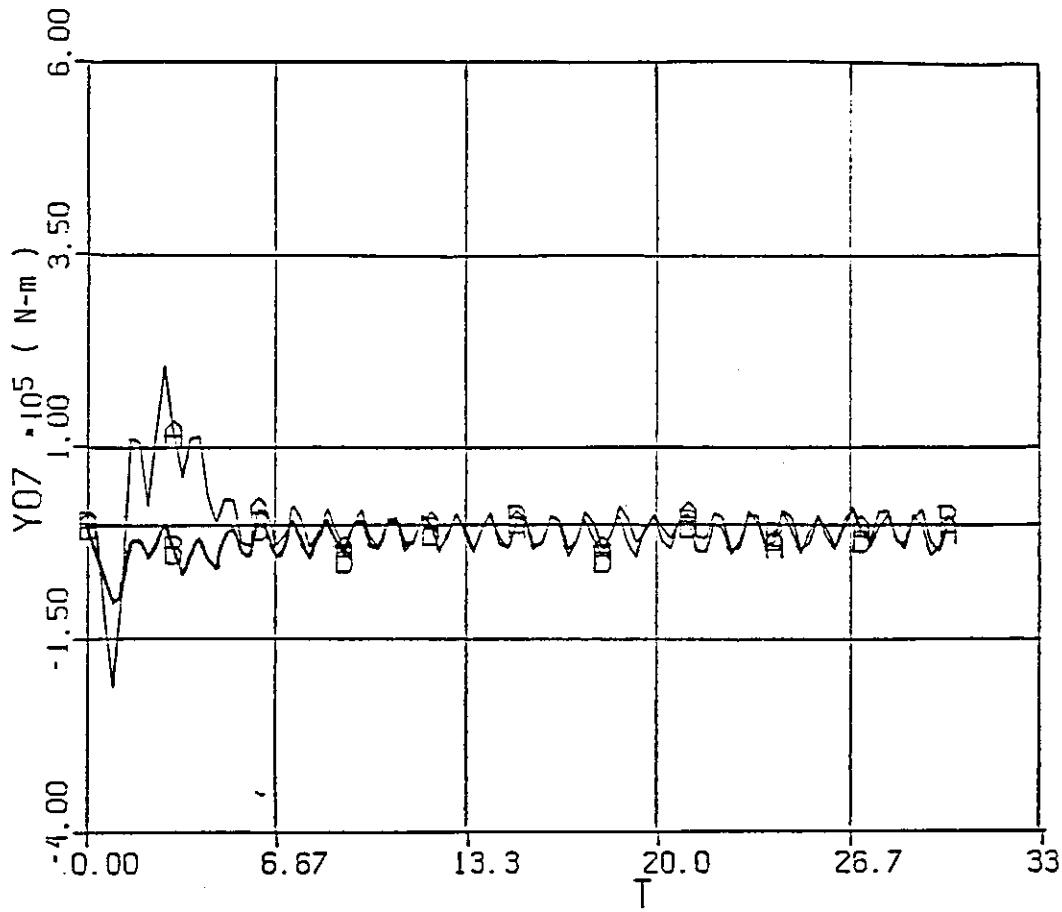

Figure 5.32 : Bending moment W.S.4, control law A, test case SC4

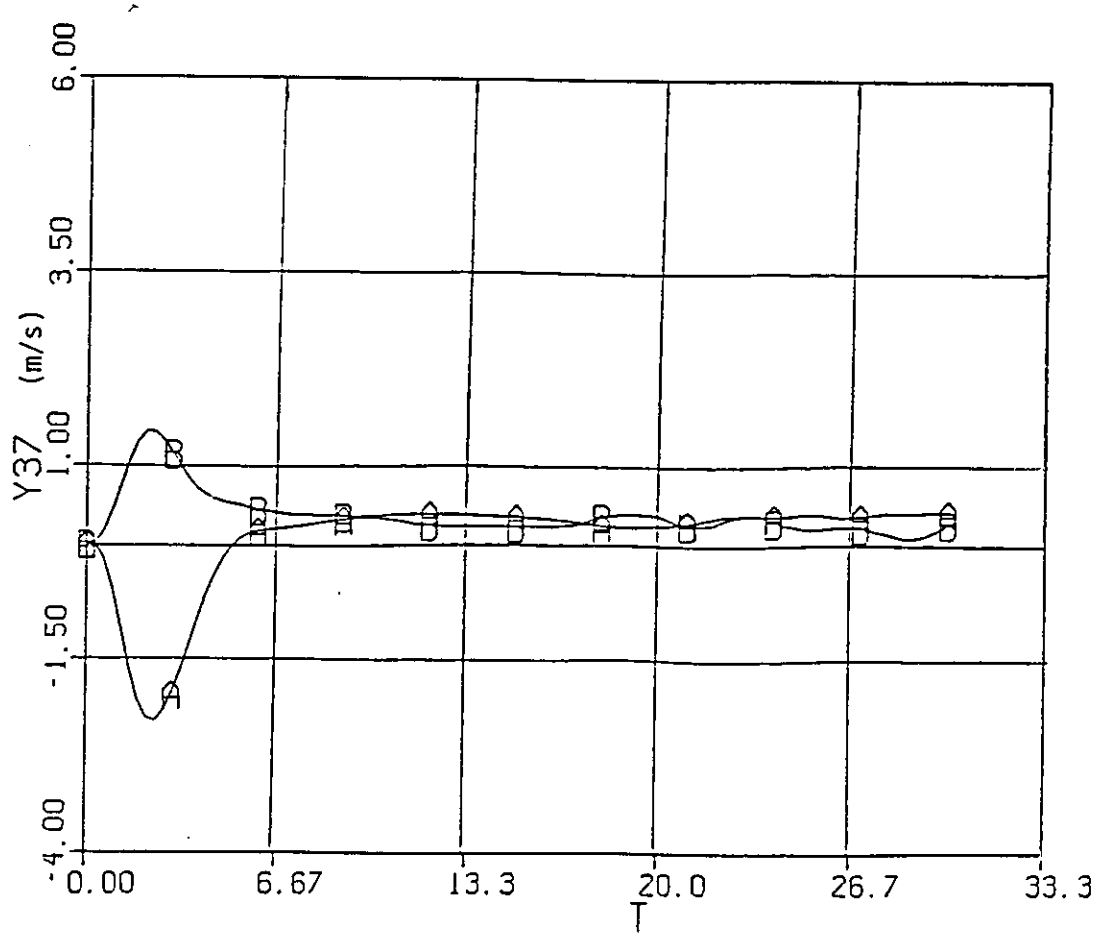

Figure 5.33: Vertical velocity(Rigid body), control law A, test case SC4

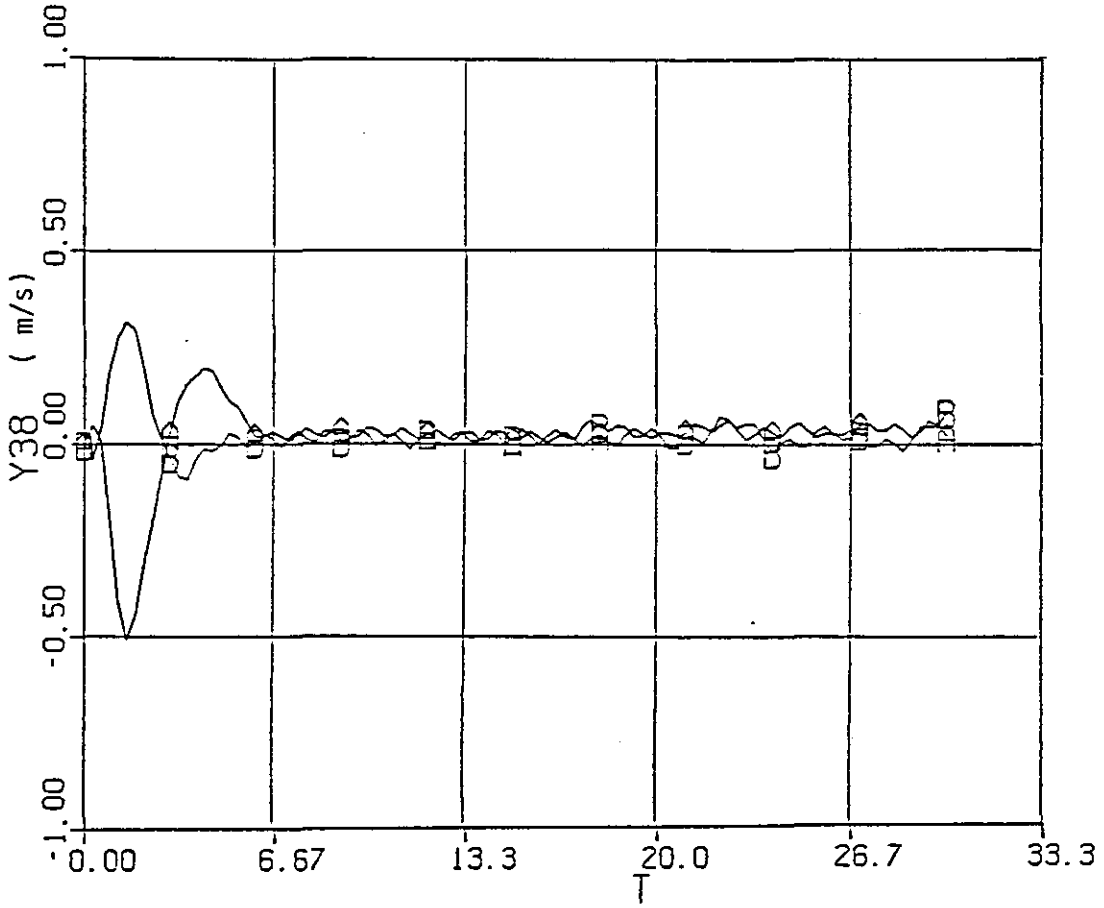

Figure 5.34: Normalised pitch rate(Rigid body), control law A, test case SC4

response.In the design specifications, however, it was required that at W.S.1 at least 30% reduction of the bending moment with no more than 5% increase in the torsional moment, should result. A reduction in the RMS value of the BM at W.S.1 of 63.5 % was achieved using control law A. The reduction in TM at W.S.1 was 17.2 % . From figures 5.33 and 5.34 it is seen that the controlled rigid body motion variables have lower peak values compared to the uncontrolled rigid body variables.

5.7 Concluding remarks

Although no attempt was made to augment the rigid body stability, by altering the eigenvalues associated with the short period mode, it was shown that the effect of reducing mode displacements resulted in reduction of structural loads. Part of the reduction being due possibly to the decoupling of the modes of motion effected by the eigenvector selection scheme of case A. It is also known that structural loading and fatigue damage rates are reduced with stability augmentation by reducing the peak loads and the number of cycles of loading, Newberry [1969]. It was shown that not only were the peak loads effectively reduced by using control law A but the absence of any high frequency oscillations in the dynamic response of bending and torsional moments, in the case of MLC, indicates the quality of control law A from structural fatigue standpoint.

It was shown that the influence of the first flexural mode on the bending moment response is dominant. And that the shape of the bending moment response matches that of the first flexural mode displacement. The displacements of the first flexural mode were an order of magnitude higher than those of the other high frequency structural modes.

It was also shown that the choice of eigenvectors for SLA, for the two cases considered, produced radically different responses and very different degrees of load alleviation. The eigenvector choice of case A which allowed each mode to participate in the dominant mode variables proved to be more effective method for SLA.

It was also shown that all the specified goals (required reductions in the BM and TM observed at W.S.1, appropriate to MLC and GLA) were achieved without impairing the response of the rigid body motion variables and the handling qualities of the aircraft. It is also known that a gust alleviation system that uses only elevator control is not completely effective, Oehman [1973]. An elevator is primarily a device for controlling the pitch rate and the angle of attack and does not provide adequately the changes of force in the z-direction that are necessary for good gust load alleviation. The reductions in the bending and torsional moments due to manoeuvre commands and atmospheric turbulence, were as a result of using a combination of both the elevator deflection and symmetrically deflected ailerons to provide direct lift.

The results presented in this chapter apply only to one flight condition. The suitability of law A when changes in the stability derivatives occur due to changes in the flight conditions are investigated in the next chapter. Moreover, the requirement of measuring all of the state variables required for the feedback of law A is dispensed with, by considering reduced order feedback derived by using the reduced order models. The design of a full order observer by using the EPAM to estimate the unavailable signals, and the digital implementation of the observed system is delt with in chapter 6.

CHAPTER 6

REDUCED ORDER ROBUST CONTROLLERS

6.1 Effects of Changes in the Stability Derivatives of the C-5A

The 24th order model of the C-5A presented in chapter 4 applies only to a single flight condition. No other information is available in the open literature concerning any variations which arise as the flight condition changes. Nevertheless, it is well known that the stability derivatives of the rigid-body motion of any aircraft are profoundly influenced by the speed and height at which the aircraft travels. The effects of elastic motion of the wings and the fuselage are no less important. To ensure that the proposed control laws, such as Law A, remain effective at off-nominal conditions, an investigation was carried out to consider the effects upon the dynamic performance of the aircraft due to the changes in the elements of the A matrix.

It is intended to demonstrate in the next section that even if the coefficients in the A matrix describing the structural dynamics are changed, to take into account the modelling inaccuracies, the aircraft remains stable and that SLA is still possible using control Law A.

6.1.1 Changes in the Frequencies of the Flexural Modes.

From appendix B, and equations 4.14 and 4.15, the elements $A_{3,3}$ and $A_{3,9}$, are seen to be

$$A_{3,3} = \hat{E}_{1_{\xi_1}} - 2\zeta_1 \omega_1 = -0.98741 \quad , \tag{6.1a}$$

$$A_{3,9} = \hat{E}_{1_{\xi_1}} - \omega_1^2 = -29.851 \quad . \tag{6.1b}$$

The values of $A_{3,3}$, $A_{3,9}$ corresponds to the nominal uncontrolled system; ~~for which~~ the frequency and the damping ratio of the first flexural mode being 5.48 rad/s, 0.093 respectively. The new value of the element $A_{3,3}$ can be calculated as:

$$A_{3,3_{(new)}} = \hat{E}_{1_{\xi_1}} - 2\,\zeta_1\,\omega_{1_{(new)}} \quad , \qquad 6.1c$$

where (new) signifies the new value. Similar expression can be obtained for the element $A_{3,9}$ by using equation 6.1b. The new value of the frequency of the first flexural mode is calculated by the expression viz;

$$\omega_{1_{(new)}} = \omega_{1_{(original)}} - \omega_{1_{(change)}} \quad , \qquad 6.1d$$

where (change) signifies the required change in the frequency of the flexural mode. Note that this change is being subtracted. If the change is additive, it would imply that there will be a greater frequency separation between the rigid-body and the first flexural mode. Whereas a subtractive change brings the frequencies of the two modes closer together, hence making the flexural mode prone to being excited by the rigid-body motion. If the control Law can cope with this situation it will cope with the additive change[§]. If it is assumed that the frequency of the 1st flexural mode is in error by say -15% (while the damping ratio is correct) , then by using equations 6.1a, 6.1b, 6.1c, and 6.1d the new values of $A_{3,3}$ and $A_{3,9}$ are found to be,

$$A_{3,3} = -0.835 \quad ,$$
$$A_{3,9} = -21.536 \quad .$$

These new elements represent a frequency of 4.66 rad/s and a damping ratio of 0.093 associated with the first flexural mode.

---

§ Separation between the frequency of the rigid-body mode and of the first flexural mode will result due to the additive change, hence making the flexural mode less prone to being excited by the rigid-body motion

The eigenvalues of the coefficient matrix (i.e., the open-loop eigenvalues of the off-nominal system) and the closed-loop eigenvalues, when using control Law A, associated with the rigid-body mode and the six flexural modes are presented as table 6.1. From which it may be seen that the damping ratios associated with all the flexural modes (except the first flexural mode) are approximately the specified values (see table 5.3). The damping ratio of the first flexural mode has been increased to 0.75, an increase in its frequency is also noted. With the damping ratio and frequency of the rigid-body mode essentially fixed at the specified values, the increase in the damping ratios associated with the first flexural mode and the remaining modes will reflect very favourably in the bending moment response.

	Nominal Uncontrolled		Off-Nominal Uncontrolled		Off-Nominal Controlled	
Mode	ζ	ω	ζ	ω	ζ	ω
Short Period	1.55	0.57	1.54	0.57	1.61	0.58
Flexural Mode 1	5.48	0.09	4.6	0.09	4.89	0.75
Flexural Mode 2	11.12	0.02	11.12	0.02	11.12	0.10
Flexural Mode 3	13.81	0.04	13.84	0.04	13.82	0.21
Flexural Mode 4	15.61	0.04	15.60	0.04	16.59	0.19
Flexural Mode 5	17.49	0.02	17.49	0.02	17.47	0.12
Flexural Mode 6	18.79	0.03	18.79	0.03	18.81	0.16

Table 6.1: Comparison of the open and closed-loop eigenvalues of the nominal and off-nominal system.

The bending and torsion moment response observed at W.S.1 for test case SC2 (which relates to an step aileron command of 0.025 radians) are shown as figure 6.1 and 6.2. It is not surprising that the responses presented are better damped than those presented for the same test condition in figure 5.16 and 5.17, this is mainly due to the additional damping in first flexural mode. From a comparison of figure 5.16 and 6.1 it is noted that the peak value of the uncontrolled bending moment response at W.S.1 has been increased from 4.0 MN-m to 6.0 MN-m. This increase is mostly due to the fact that the frequency of the first flexural mode and the rigid-body mode are much closer together, and that the two modes have been much more tightly coupled.

Another test in which the frequency of the first flexural mode was changed by -15% and the frequency of the second flexural mode by -10% simultaneously, showed very little difference from the results discussed previously. For example, the percent reductions in the peak values of the bending and torsion moment at W.S.1 are shown in table 6.2. Tests of a similar nature were carried out to determine by how much the frequency of the first flexural mode could be changed before the response was affected. A change of -50% (i.e., lowering the frequency by 50%) proved to be disastrous in that the closed-loop system became unstable.

	*	+
BM W.S.1	75.3	75.7
TM W.S.1	45.4	46.9

* Change of -15% in the frequency of the first flexural mode

+ Change of -15% and -10% in the frequency of the first and second flexural modes respectively.

Table 6.2: Percent reductions in peak values of BM and TM at W.S.1

It is noted from table 6.2 that the percentage reduction obtained in the peak values of bending and torsion moments at W.S.1 are greater to those obtained when using Law A on the nominal system (see table 5.12). However, the peak value of bending moment observed at W.S.1 of the nominal controlled system of 1.3 MN-m is lower than the corresponding value of the off-nominal controlled system of 2.5 MN-m (see figures 5.16 and 6.1). It is evident from the results presented so far that there must be adequate frequency separation between the rigid-body motion and that of flexural dynamics, otherwise excessive peak loads will result due to the coupling of the rigid-body mode with the flexural modes. The reduction in peak values of the bending moments is a matter of specification. For example, if the frequency and damping ratio associated with the first flexural mode of the controlled off-nominal system (see table 6.1) were specified for the controlled nominal system instead of the values given in table 5.3, reductions tabulated in table 6.2 resulted.

6.2 Reduced Order Feedback

In the previous section it was shown that control Law A (24^{th} order FSVF control Law) performed very well even when some of the coefficients in the A matrix were changed. These changes represented modelling inaccuracies or changes in the flight condition. One of the disadvantage in synthesising Law A for MLC is that all the states associated with Küssner dynamics, Padé approximations and the Dryden filter have to be measured. Since in the absence of turbulence for example, when demonstrating MLC i.e., load alleviation due to pilot commands only, these states remain zero, then feedback from these states is not essential. In order to study the effect of excluding feedback from these states, reduced order models are defined in the next section. The reduced order feedback laws derived from these reduced order models are then subsequently applied to the full order 24^{th} order model of the C-5A.

6.2.1 Definition of the Reduced Order Models

Three reduced order models derived from the original 24^{th} order model (see chapter 4) are presented in this section. Each model is derived from reducing the 24^{th} order model by the method of modal truncation. The retained modes in each of the models are not represented by any aeroelastic correction factors which relate to the deleted modes of vibration. The three models are designated Alpha, Beta and Gamma respectively.

The model Alpha comprises of the rigid-body dynamics the dynamics of the six flexural modes and the aileron and the elevator dynamics. The model Beta was the same as the model Alpha, except that only the first two flexural modes were included. The model Gamma differed from the model Beta in that only the first flexural mode was included. Consequently the dimension of the state vector of models Alpha, Beta and Gamma is 16, 8, and 6 respectively. The definition of the state vectors for each models are shown in table 6.3. The composition of the output vector corresponding to each model shown in table 6.4.

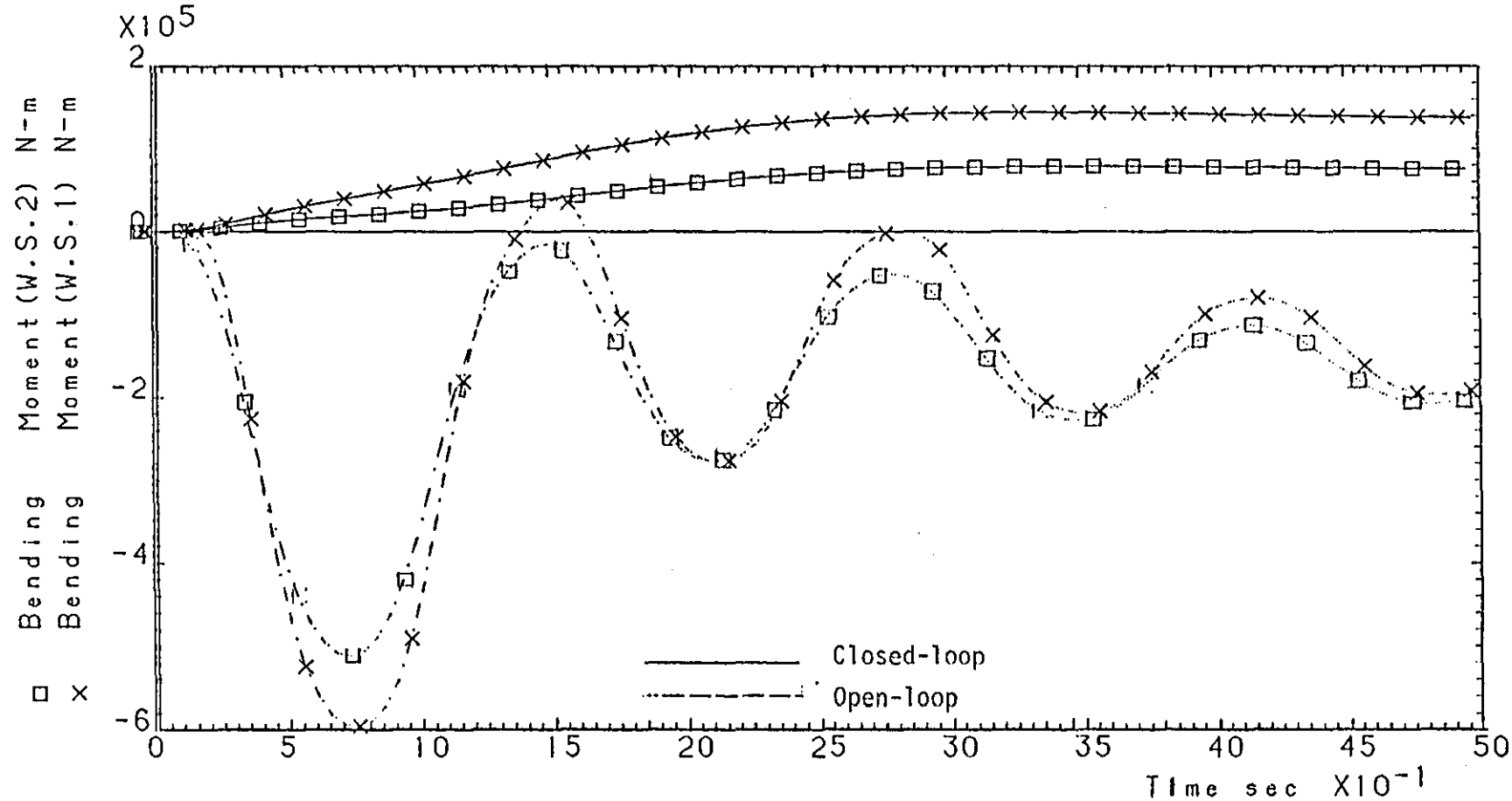

Figure 6.1 : Bending moment response at W.S.1 & W.S.2 of the off-nominal closed-loop control system using Law A, test case SC_2

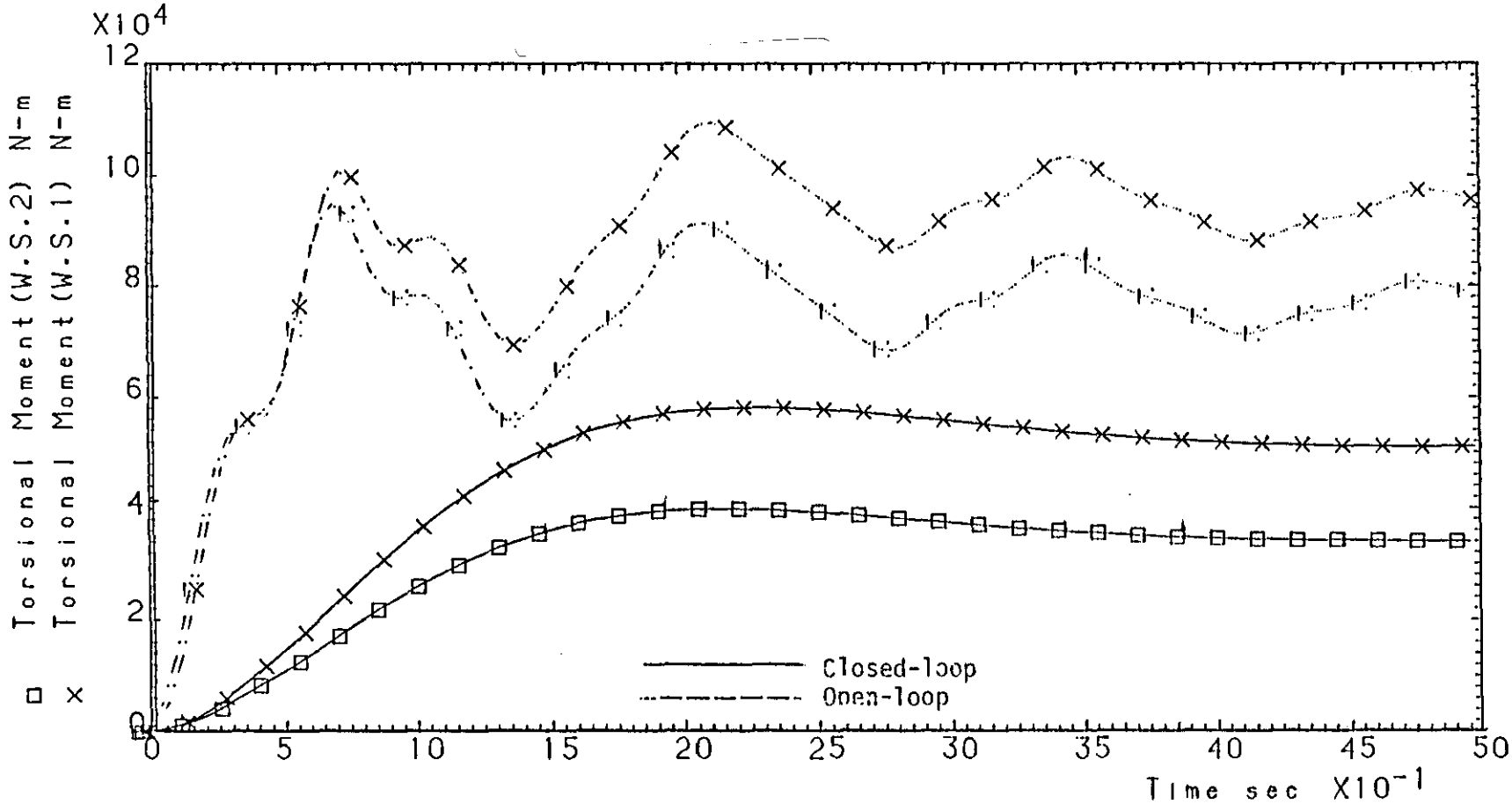

Figure 6.2 : Torsional moment response at W.S.1 & W.S.2 of the off-nominal closed-loop control system using Law A, test case SC2.

	Alpha	Beta	Gamma
Vertical Velocity	w	w	w
Pitch Rate	q	q	q
Rate & Disp. 1st FM	$\dot{\xi}_1, \xi_1$	$\dot{\xi}_1, \xi_1$	$\dot{\xi}_1, \xi_1$
Rate & Disp. 2nd FM	$\dot{\xi}_2, \xi_2$	$\dot{\xi}_2, \xi_2$	–
Rate & Disp. 3rd FM	$\dot{\xi}_3, \xi_3$	–	–
Rate & Disp. 4th FM	$\dot{\xi}_4, \xi_4$	–	–
Rate & Disp. 5th FM	$\dot{\xi}_5, \xi_5$	–	–
Rate & Disp. 6th FM	$\dot{\xi}_6, \xi_6$	–	–
Aileron Deflection	δ_a	δ_a	δ_a
Elevator Deflection	δ_e	δ_e	δ_e

Table 6.3 : Variables included in the state vector for each of the models

Alpha	Beta	Gamma
BM_i , TM_i $i = 1,...,5$	BM_i , TM_i $i = 1,...,5$	BM_i , TM_i $i = 1,...,5$
$\dot{BM}_i$, $\dot{TM}_i$ $i = 1,...,5$	$\dot{BM}_i$, $\dot{TM}_i$ $i = 1,...,5$	$\dot{BM}_i$, $\dot{TM}_i$ $i = 1,...,5$
$\dot{\xi}_\kappa$ $\kappa = 1,...,6$	$\dot{\xi}_\kappa$ $\kappa = 1,...,2$	$\dot{\xi}_\kappa$ $\kappa = 1$
ξ_κ $\kappa = 1,...,6$	ξ_κ $\kappa = 1,...,2$	ξ_κ $\kappa = 1$
$\dot{\delta}_a$	$\dot{\delta}_a$	$\dot{\delta}_a$
$\dot{\delta}_e$	$\dot{\delta}_e$	$\dot{\delta}_e$
δ_a	δ_a	δ_a
δ_e	δ_e	δ_e
w	w	w
q	q	q

Table 6.4 : Output vector definition for the reduced order models

6.2.2 Reduced Order Feedback Laws

Reduced order feedback control laws are derived in this section using the reduced order models described in section 6.2.1. The objective is to demonstrate that when the feedback controllers derived from the reduced order models are applied to the 24^{th} order model, the degree of alleviation achieved is comparable to the alleviation achieved when using the FSVF control Law A. The feedback controllers were designed by the EPAM method presented in chapter 3.

The eigenvalues specified for the closed-loop for each of the models are shown in table 6.5.

MODE	Alpha	Beta	Gamma
Short Period	-0.88 ± j 1.27	-0.88 ± j 1.27	-0.88 ± j 1.27
First FM	-2.54 ± j 4.86	-2.54 ± j 4.86	-2.54 ± j 4.86
Second FM	-1.16 ± j 11.06	-1.16 ± j 11.06	_
Third FM	-2.86 ± j 13.51	_	_
Fourth FM	-3.03 ± j 15.31	_	_
Fifth FM	-2.13 ± j 17.36	_	_
Sixth FM	-3.10 ± j 18.53	_	_

Table 6.5 : Specified closed-loop Eigenvalues.

From Table 6.5 it is seen that the closed-loop eigenvalue set specified for the flexural modes of the model Alpha is the same as the set specified for the 24 th order model (see table 5.1). It is also noted from table 6.5 that the eigenvalues corresponding to the short period mode are identical to the uncontrolled values. Since it is desired that the handling qualities, normally expressed in terms of the short-period eigenvalues, remain unaffected by feedback it is essential that the same eigenvalues are specified for the closed-loop.

The eigenvectors corresponding to the short-period and the flexural modes are chosen from the null-space vectors (equation 3.72) such that the chosen eigenvector corresponding to the mode resulted in the mode to contribute mainly to the dominant motion variables. Such a method of eigenvector selection has already been discussed in section 5.2.2, where it was shown that such an eigenvector selection scheme results in load alleviation and also in the decoupling of the modes of motion. However, in the present section only the consequences of using the reduced order control laws are discussed. The control laws were determined in exactly the same manner as previously outlined (see sections 3.4.3 for the computational steps involved and section 5.2.2 for the eigenvector selection scheme). The three control laws designated as Law Alpha, Law Beta and Law Gamma are presented below §;

Law Alpha

$$u = \begin{bmatrix} -0.0003 & -0.0005 & 0.0012 & 0.0168 & 0.0091 & -0.0024 & -0.1286 & 0.0058 \\ -0.0106 & -0.0176 & 0.0183 & 0.3236 & 0.5073 & 0.8822 & -1.2584 & 3.0125 \\ 0 & 0 & 0 & 0 & 0 & 0 & 0 & 0 \\ -0.0004 & -0.0005 & -0.0000 & -0.0082 & -0.0016 & -0.0033 & 0.0316 & -0.0127 \\ 0.0033 & -0.0951 & -0.0180 & -0.1087 & -0.7131 & -0.2344 & 0.1402 & -2.1569 \\ 0 & 0 & 0 & 0 & 0 & 0 & 0 & 0 \end{bmatrix} x$$

Law Beta

$$u = \begin{bmatrix} -0.0005 & -0.0005 & 0.0010 & 0.0021 & 0 & 0 & 0 & 0 \\ -0.0051 & -0.0409 & 0 & 0 & 0 & 0 & -0.6234 & 0.2964 \\ 0 & 0 & 0 & 0 & 0 & 0 & 0 & 0 \\ 0.0001 & 0.0000 & -0.0001 & 0.0053 & 0 & 0 & 0 & 0 \\ 0.0017 & -0.0895 & 0 & 0 & 0 & 0 & 0.0336 & -0.2814 \\ 0 & 0 & 0 & 0 & 0 & 0 & 0 & 0 \end{bmatrix} x$$

---

§ The feedback matrices are presented by rows. For example, in law Alpha the feedback gain element $K_{1,1}$=-0.0003, $K_{1,2}$ = -0.0005, $K_{1,9}$= -0.0106 etc. The elements $K_{2,1}$, $K_{2,2}$, $K_{2,9}$ are seen to be -0.0004, -0.0005, 0.0033 respectively.

Law Gamma[§]

$$u = \begin{bmatrix} -0.0005 & -0.0005 & 0.0010 & 0 & 0 & 0 & 0 & 0 \\ -0.0052 & 0 & 0 & 0 & 0 & 0 & -0.5841 & 0.3883 \\ 0 & 0 & 0 & 0 & 0 & 0 & 0 & 0 \\ 0.0001 & 0.0001 & -0.0001 & 0 & 0 & 0 & 0 & 0 \\ 0.0015 & 0 & 0 & 0 & 0 & 0 & 0.1305 & -0.0691 \\ 0 & 0 & 0 & 0 & 0 & 0 & 0 & 0 \end{bmatrix} x$$

The order of the feedback matrices in each case was [2 * 24]. In each of the feedback matrices the gains have been rounded to four significant decimal places. From the laws presented above it is noted that there have been inserted in the various laws zeros which correspond to the variables not included in the reduced order models. This has been done to ensure dimensional compatibility when applying these laws to the 24th order model. Moreover, the presence of zeros in the gain matrices indicate the non-availability of the corresponding variables for feedback. This corresponds to sensor failure conditions. The frequencies and the damping ratios of the various modes obtained when using the reduced order feedback laws are presented in table 6.6. Note from this table that, when Law Alpha is used, the frequencies and damping ratios of the rigid-body and the flexural modes are almost the same as those obtained when using Law A. However, it is noted from table 6.6 that there is a marked change in the closed-loop damping ratios associated with the second, third, fourth, fifth and the sixth flexural modes when Law Gamma is used. These values are seen to approach the uncontrolled values. It is inferred that the Law Gamma has little or no effect on the high frequency modes. However, the frequency and the damping ratios of the short-period and of the first flexural mode are nearly the same as the specified values.

---

§ The feedback matrix is presented by rows. For example, in law Gamma the feedback gain element $K_{1,1}$=-0.0005, $K_{1,2}$ = -0.0005, $K_{1,9}$= -0.0052 etc. The elements $K_{2,1}$, $K_{2,2}$, $K_{2,9}$ are seen to be 0.0001, 0.0001, 0.0015 respectively.

MODE	Open-Loop		Law A		Law Alpha		Law Beta		Law Gamma	
	ω	ζ	ω	ζ	ω	ζ	ω	ζ	ω	ζ
Short Period	1.55	0.57	1.55	0.57	1.55	0.57	1.45	0.58	1.49	0.57
First FM	5.48	0.09	5.48	0.47	5.48	0.47	5.48	0.41	5.47	0.41
Second FM	11.12	0.02	11.12	0.12	11.12	0.10	11.25	0.08	11.12	0.02
Third FM	13.81	0.04	13.81	0.20	13.81	0.21	13.77	0.05	13.81	0.04
Fourth FM	15.61	0.04	15.61	0.19	15.61	0.19	15.58	0.04	15.62	0.04
Fifth FM	17.49	0.02	17.49	0.12	17.49	0.12	17.49	0.02	17.49	0.02
Sixth FM	18.79	0.03	18.79	0.17	18.79	0.17	18.79	0.03	18.79	0.03

Table 6.6 : Comaprison of the closed-loop eigenvalues obtained for various control laws.

It was shown in chapter 5 that the first flexural mode has a predominant effect on the bending and torsion moment response. Hence, provided the damping in the first flexural mode is significantly augmented (this can be seen from table 6.6) load alleviation must be possible (N.B. This is shown graphically in the next section).

6.2.3 MLC using Reduced Order Feedback Controllers

In order to make a valid comparison of the reductions obtained in the values of the bending and torsional moments as a result of using Law A and using the reduced order feedback laws, test case SC2 was employed. This test case involves an aileron step command of 0.025 radians. The method described in section 4.6 of forcing the loop was used to force the closed-loop rigid-body variables to the same steady-state values as in the open-loop case. Since reductions in the bending and torsional moments are required, without impairing the rigid-body dynamics, the method of forcing the loop proved to be very useful in assessing the reductions obtained.

Presented in figure 6.3 and 6.4 are the closed-loop bending and torsional moment responses at five wing stations using Law Alpha. It should be noted from these figures that the bending and torsional moment responses are almost the same as those obtained with Law A. This is owing to the fact that Law Alpha assigned the same eigenstructure as that assigned by Law A. It is noted from figure 6.5 and figure 6.6 that the use of Law Gamma does not produce a bending and torsional moment response which is radically different to the response obtained by either Law A or Law Alpha. It is inferred from these figures that provided Law Gamma is at least available for feedback, then MLC will always be possible.

The percentage reduction in the RMS and peak values of the bending and torsional moments at various wing stations for Law A and reduced order feedback laws are given in table 6.7. From which it is seen that the reduction in the bending and torsional moments for Law A and Law Alpha are almost the same. However, reductions caused in the bending moments by the use of Law Gamma are somewhat reduced, but a corresponding increase in the reduction of the torsional moments is also to be observed. The slight increase in the reduction of the torsion moments is at the expense of the decreased reduction in the bending moments.

The use of Law Beta produces approximately the same levels of reduction as those obtained by the Law Gamma. This merely implies that feedback of the displacement and the rate of the second flexural mode is unnecessary ***provided*** the variables associated with the first flexural mode are available for feedback. The degree of reduction in the bending and torsional moment response obtained when using Law Beta or Gamma indicate that the first flexural mode indeed has a dominant effect on the structural loads.

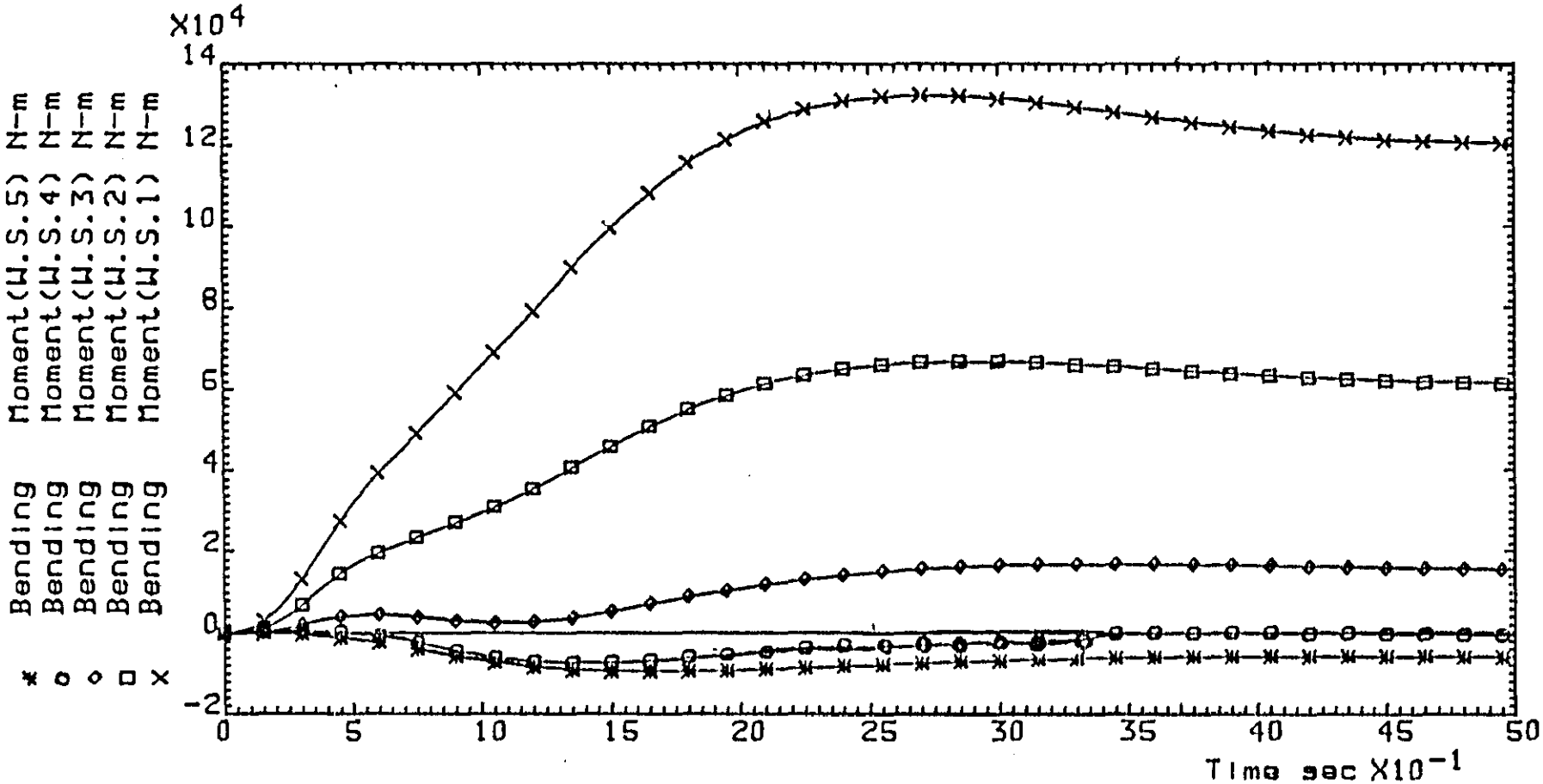

Figure 6.3 : C-5A controlled response, control law Alpha, test case SC2, showing bending moment response at W.S.1 - W.S.5.

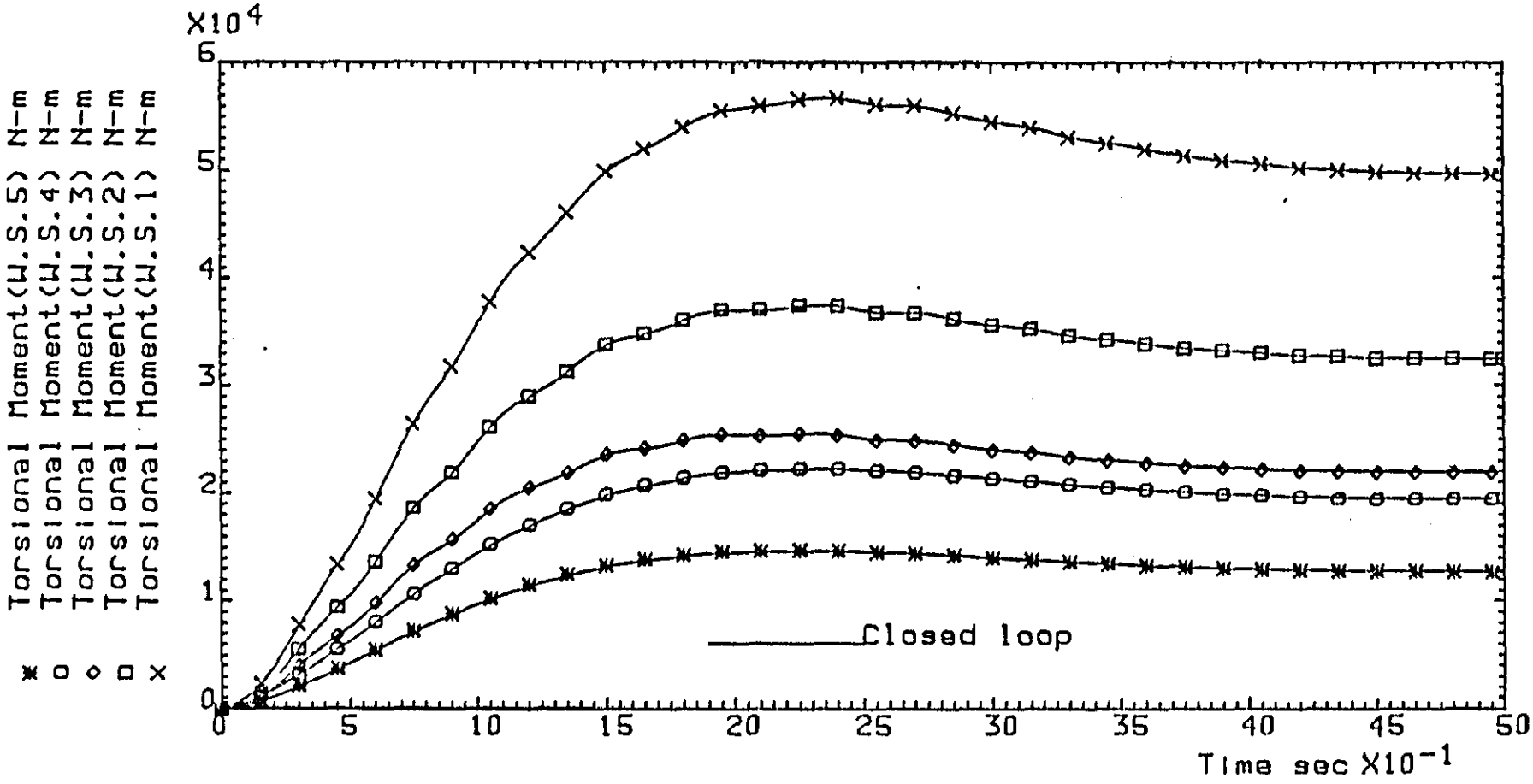

Figure 6.4 : C-5A controlled response, control law Alpha, test case SC2, showing torsional moment response at W.S.1 - W.S.5.

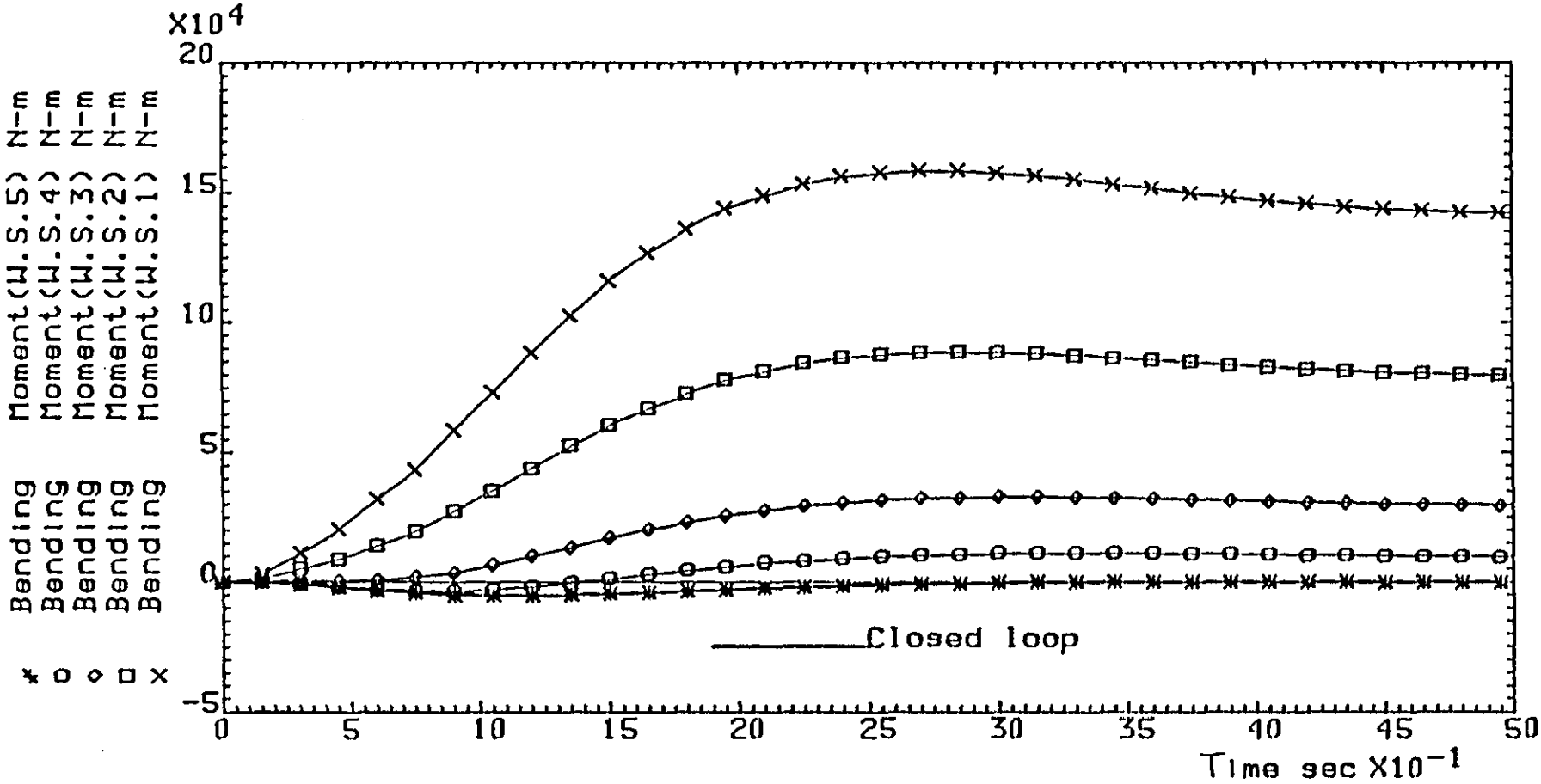

Figure 6.5 : C-5A controlled response, control law Gamma, test case SC2, showing bending moment response at W.S.1 - W.S.5.

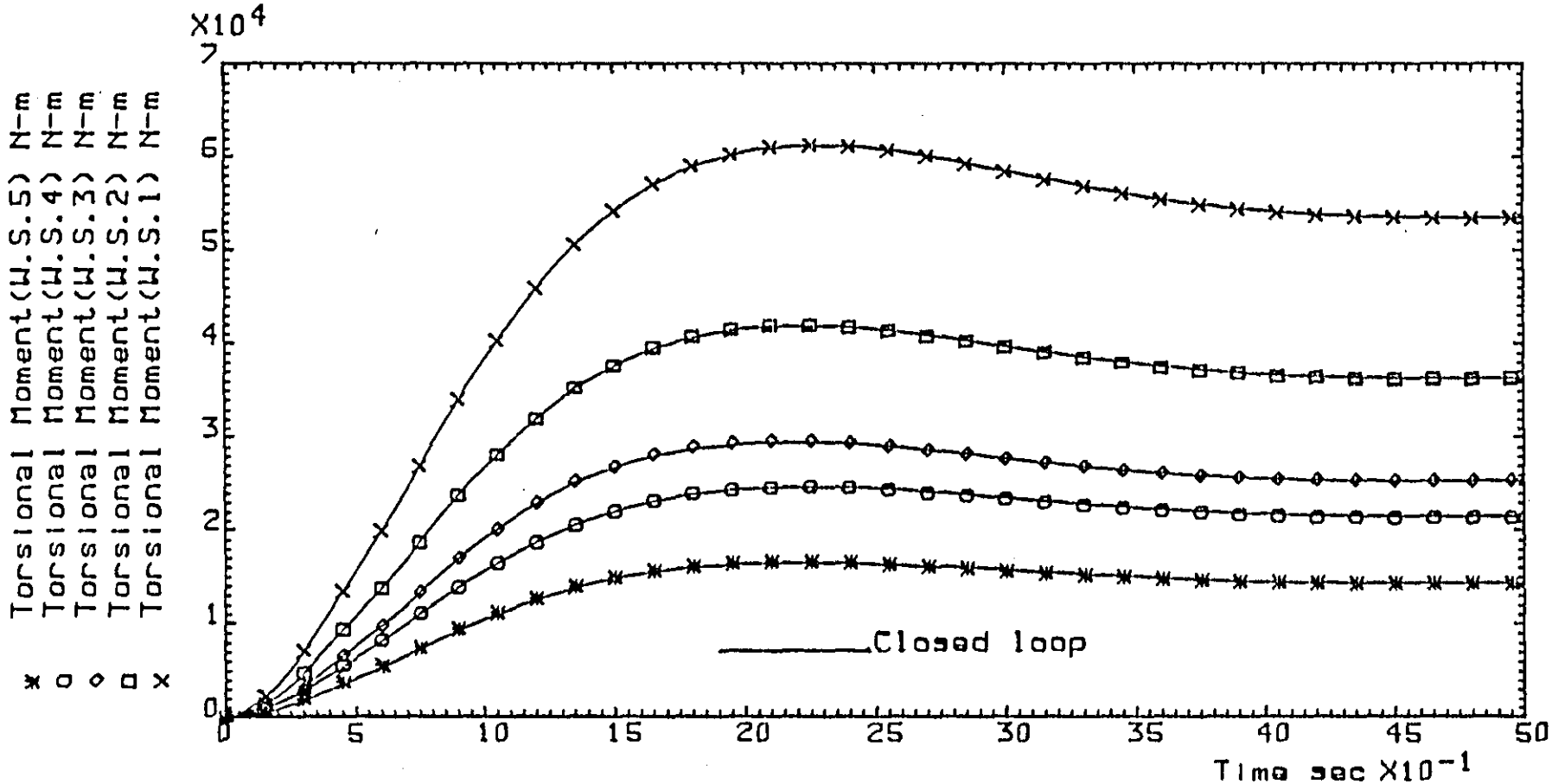

Figure 6.6: C-5A controlled response, control law Gamma, test case SC2, showing torsional moment response at W.S.1 - W.S.5.

VARIABLE	Law A		Law Alpha		Law Beta		Law Gamma	
	RMS	Peak	RMS	Peak	RMS	Peak	RMS	Peak
Bending Moment W.S.1	19.7	67.8	19.2	67.4	5.3	61.2	5.3	61.2
Bending Moment W.S.2	61.0	81.2	60.5	80.9	49.0	75.0	49.0	75.0
Bending Moment W.S.3	91.0	94.0	90.3	93.8	81.1	88.2	81.1	88.2
Bending Moment W.S.4	96.4	99.3	96.7	96.1	93.0	94.7	93.0	94.7
Bending Moment W.S.5	89.1	94.0	89.6	91.2	95.8	95.0	95.8	95.0
Torsion Moment W.S.1	38.6	36.8	38.8	37.1	43.1	41.7	43.1	41.7
Torsion Moment W.S.2	48.8	47.0	49.0	47.3	54.0	52.7	54.0	52.7
Torsion Moment W.S.3	56.8	57.0	57.0	57.3	62.5	63.0	62.5	63.0
Torsion Moment W.S.4	47.4	43.5	47.7	43.8	52.3	49.1	52.3	49.1
Torsion Moment W.S.5	53.4	48.9	53.7	49.3	58.6	55.1	58.6	55.1

Table 6.7 : Percent reductions in the RMS and peak values of moments observed at various wing stations, using FSVF law A and reduced order feedback.

It is worth emphasising that the control laws proposed are extremely effective for the purpose of MLC and SLA. For example the entry in table 6.7 relating to bending moment at W.S.1 shows that when Law A is used the reduction in the RMS value of bending moment was about 20% with an associated reduction in the peak value of nearly 70%. It should be also noted that when Law Gamma or Beta have to be used, although the reduction in the peak values remain about the same the reduction achieved in the RMS values is significantly reduced. Nevertheless, from a flying point of view, the reduction in the peak values for structural loads is what a SLA control system has to achieve to provide the degree of safety required. The loss of RMS performance simply reflects in the fatigue life of the airframe which it is stressed is not lessened, for some reduction in the RMS values has been achieved.

The entry in table 6.7 relating to torsional moment at W.S.1 shows that when Law A is used the reduction in the RMS value of torsional moment was about 39% with an associated reduction in the peak value of nearly 37%. The reductions obtained in the bending and torsional moments when using Law Gamma or Beta are 43% and 42% respectively, it is noted that these values are slightly higher than the corresponding values obtained when using Law A. These results are not in the least surprising; for reduction in the bending moments is caused by symmetric deflection of ailerons. Achievement of higher levels of reduction in the bending moments must inevitably involve large aileron deflections. This in turn will cause increased torsional moments about the wing center line. Hence, a decrease in the reduction of bending moments would invariably result in a increased reduction of the torsional moments, which is exactly what the results presented above suggest.

6.2.4 GLA Using Reduced Order Feedback Control Law Gamma

It was shown in chapter 5 that GLA was possible when using the FSVF Law A. Required reductions in the RMS values of the bending moment at W.S.1 were achieved. Law A required the measurement of all the states associated with the 24^{th} order model. Reduced order feedback control laws which did not required feedback of the states associated with the unsteady aerodynamics were sucessfully applied to achieve MLC. It is shown in this section that even when the reduced order feedback control Law Gamma is used in the presence of atmospheric turbulence, GLA can be achieved. To demonstrate GLA test case SC4 (see table 4.3) was employed. The response of the bending moment observed at W.S.1 (y-axix annotated YY1) is shown as figure 6.6a. Also shown on the same figure is the RMS response of the bending moment at W.S.1 (y-axis annotated RMSBM). The curves labelled A are for the open-loop and curves labelled B are for the closed-loop. From the bending moment response presented in figure 6.6a it can be seen that not only is the controlled response more damped, it produces lower peak values when compared to the uncontrolled response. Substantial RMS reductions are also seen to result.

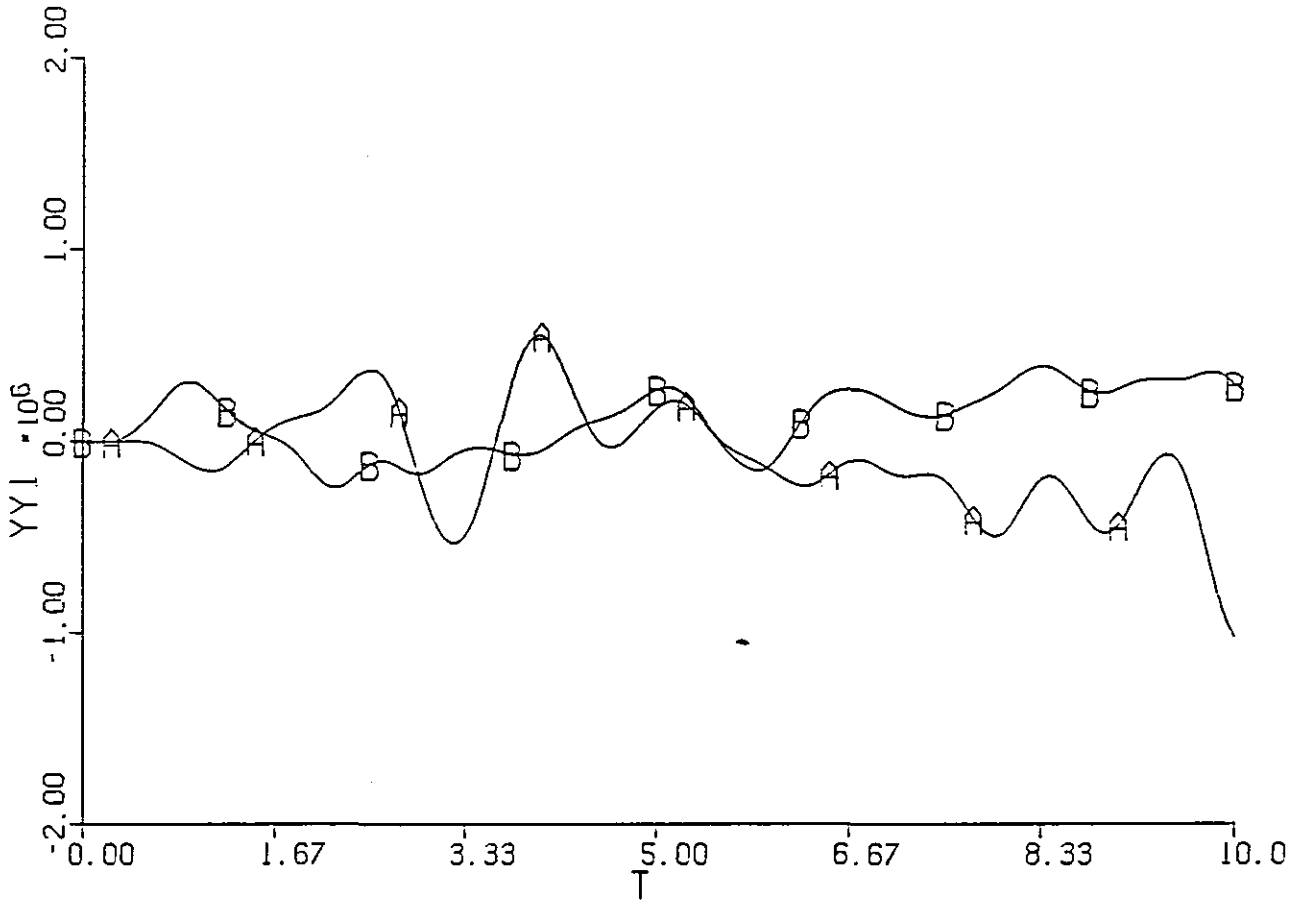

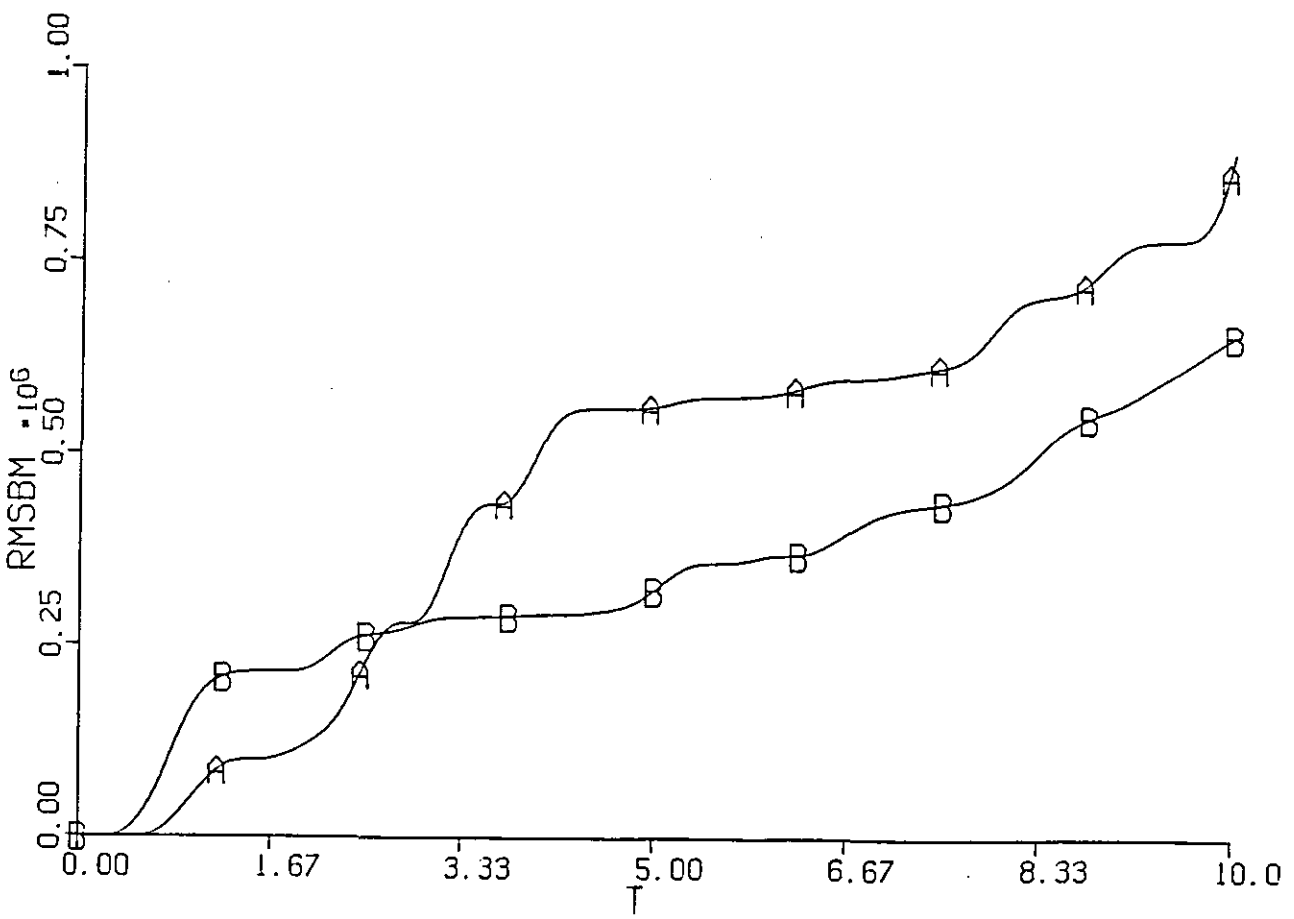

Figure 6.6a : Wing root bending moment response in moderate levels of turbulence (standard deviation of gust velocity of 0.3048)

6.3 Full Order Observers

In the preceding section it has been demonstrated that structural loads, arising due to manoeuvre commands or owing to atmospheric turbulence, can be effectively reduced by using reduced order feedback controllers designed by means of EPAM. It was shown that SLA could still be achieved when using the Law Gamma. The basic requirement for SLA is that every aircraft state variable is simultaneously available for measurement. However, even when reduced order feedback is employed, Law Gamma for example, there remains a difficulty of measuring directly the rate and displacement associated with the first flexural mode. The state vector describing the model Gamma was defined as,

$$x^T = [\, w, q, \dot{\xi}_1, \xi_1, \delta_a, \delta_e \,]$$

For implementation of a feedback control such as Law Gamma, variables associated with the flexural modes, for example, could be constructed from the knowledge of the measurable state and control variables.

A method for obtaining an estimate of the state vector is by means of the Kalman-Bucy filter. The design of such a filter takes explicit account of measurement noise in sensors in addition to any noise arising as a result of atmospheric turbulence, and is obtained as a solution of the Linear Quadratic Gaussian (LQG) problem. Another method of state estimation is to use a full-order observer, the theory of which is due to Luenberger [1966, 1971]. The proposed EPAM, described in chapter 3, can also be used to design such full order observers. The methods of state estimation are well documented, and the feasibility of their being applied to SLA has already been demonstrated by Prasad [1980].

6.3.1 Theory of Observers

Consider the following state equation

$$\dot{x} = A\,x + B\,u\ , \tag{6.1e}$$

where x, u, A, B have been defined earlier. Let the measurable outputs be defined by the relationship,

$$y_m = C_m\,x\ , \tag{6.2}$$

where y_m is the measurement vector $\in \mathcal{R}^{\ell}$, and C_m is an $[\ell * n]$ output matrix which, if Law Gamma is to be implemented, has the following form,

$$C_m = \begin{bmatrix} 1 & 0 & 0 & 0 & 0 & 0 \\ 0 & 1 & 0 & 0 & 0 & 0 \\ 0 & 0 & 0 & 0 & 1 & 0 \\ 0 & 0 & 0 & 0 & 0 & 1 \end{bmatrix} . \tag{6.3}$$

Equation 6.3 assumes that the variables w, q, δ_a and δ_e associated with the model Gamma are available for measurement. Let the dynamic equation of the observer be defined by,

$$\dot{x}_e = F_e\,x_e + G_e\,y_m + B\,u\ , \tag{6.4}$$

where F_e is a coefficient matrix of order $[n * n]$, G_e is of order $[n * \ell]$ and is termed the observer gain matrix. Let the difference between the actual state vector and the estimated state vector be defined by,

$$e = x - x_e \ , \qquad 6.5$$

differentiation of 6.5 yields,

$$\dot{e} = \dot{x} - \dot{x}_e \ . \qquad 6.6$$

Substitution of 6.1e and 6.4 in equation 6.6 yields,

$$\dot{e} = \dot{x} - \dot{x}_e = A\,x + B\,u - F_e\,x_e - G_e\,y_m - B\,u \ . \qquad 6.7$$

Substitution of equation 6.2 in 6.7 yields,

$$\begin{aligned} \dot{e} = \dot{x} - \dot{x}_e &= A\,x + B\,u - F_e\,x_e - G_e\,C_m\,x - B\,u \\ &= (A - G_eC_m)\,x - F_e\,x_e \ . \end{aligned} \qquad 6.8$$

At steady state the vector e must equal to the null vector, consequently from equation 6.8

$$(A - G_eC_m)\,x = F_e\,x_e \ . \qquad 6.9$$

The actual state vector and the estimated state vectors can be equal if and only if

$$F_e = A - G_eC_m \ , \qquad 6.10$$

then from equation 6.8 and equation 6.10

$$\begin{aligned} \dot{x} - \dot{x}_e = \dot{e} &= (A - G_e\,C_m)\,x - (A - G_eC_m)\,x_e \\ &= (A - G_eC_m)\,(x - x_e) \\ \dot{e} &= (A - G_eC_m)\,e \ . \end{aligned} \qquad 6.11$$

For a stable observer to exist the real parts of the eigenvalues of the matrix $(A - G_e C_m)$ must be negative. The observer gain matrix G_e can be found by a number of ways. Such as, from the solution of the Linear Quadratic Problem (LQP), Prasad [1980] or by using the eigenvalue assignment method based on the GCCF (see section 3.1).

For example, since the eigenvalues determine how the error modes will decay, it is essential that any method used must assign the specified eigenvalues. If LQP method is used then the choice of the weighting matrices eventually determine what the observer eigenvalues will be. Since the choice of weighting matrices and the eventual observer eigenvalues are not directly related the observer design can be very cumbersome. Moreover, complex observer eigenvalues may result as a result of choosing inappropriate weighting matrices. Consider the following figure,

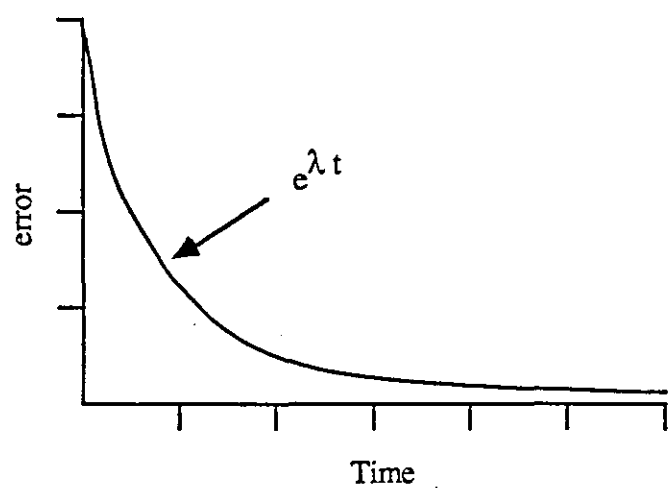

the figure shows the error plotted against time. Since the error is defined as being the difference between the actual state and the estimated state, it is greatest at t=0. If the error is required to decay monotonically, then, obviously, a real and negative eigenvalue has to be specified, the rate of decay being determined by how far it is located to the left from the origin in the s-plane. Obviously if some of the error states are required to decay monotonically at the same rate, then repeated eigenvalues must be specified. However, it is the intention to use the EPAM described in chapter 3 to determine the observer gain matrix.

The eigenvalues and the eigenvectors of the matrix $(A - G_e C_m)$ satisfy the relationship viz:

$$(A - G_e C_m)\,\underline{v}_i = \lambda_i \underline{v}_i \quad , \text{ for } i = 1, 2, \ldots, n \,, \tag{6.12}$$

where λ_i is an observer eigenvalue and v_i is an associated eigenvector. Equation 6.12 can be alternatively expressed as,

$$\left[\lambda_i I - A^T \mid C_m^T\right]\begin{bmatrix} \underline{v}_i \\ G_e^T \underline{v}_i \end{bmatrix} = 0 \,. \tag{6.13}$$

Since the eigenvalues of the matrix $(A - G_e C_m)$ are the same as of $(A^T - C_m{}^T G_e{}^T)$ equation 6.13 can be written in the form as shown. Let,

$$S_\lambda = [\,\lambda_i\, I - A^T \mid C_m{}^T\,] \,, \tag{6.13a}$$

where I is an identity matrix of the order $[n * n]$. Augmenting equation 6.13a by ℓ rows of zeros (for computational ease) to form a square matrix of order $[(n+\ell) * (n+\ell)]$,

$$\hat{S}_{\lambda_i} = \left[\begin{array}{c|c} \lambda_i I - A^T & C_m^T \\ \hline 0 \ldots 0 & 0 \\ 0 \ldots 0 & 0 \end{array}\right] \,, \tag{6.14}$$

and let,

$$R_{\lambda_i} = \begin{bmatrix} N_{\lambda_i} \\ \hline M_{\lambda_i} \end{bmatrix} \,. \tag{6.15}$$

The columns of R_{λ_i} form the basis for the null space of $\hat{S}_{\lambda_i}$. The matrix R_{λ_i} is of the order [(n + ℓ) * ℓ] , whereas the order of N_{λ_i} is [n * ℓ] and the order of M_{λ_i} is [ℓ * ℓ] . The matrix R_{λ_i} is computed form the singular value decomposition of the matrix $\hat{S}_{\lambda_i}$ (see section 3.4.2). The vectors in N_{λ_i} and M_{λ_i} are defined as,

$$\begin{bmatrix} N_{\lambda_i} \\ M_{\lambda_i} \end{bmatrix} = \begin{bmatrix} \underline{\rho}_{1_i} & \underline{\rho}_{2_i} & \cdots & \underline{\rho}_{\kappa_i} \\ -- & -- & -- & -- \\ \underline{\omega}_{1_i} & \underline{\omega}_{2_i} & \cdots & \underline{\omega}_{\kappa_i} \end{bmatrix} \begin{cases} \text{For } i = 1,2,\ldots,n \\ \text{For } \kappa = 1,2,\ldots,\ell \end{cases} . \qquad 6.16$$

If one of the eigenvectors is chosen from R_{λ_i} , to reflect the desired influence of the eigenvalue λ_i (on the dynamic response of the error states), such that,

$$\begin{bmatrix} \underline{\rho}_{\kappa_i} \\ --- \\ \underline{\omega}_{\kappa_i} \end{bmatrix} = \begin{bmatrix} \underline{v}_i \\ --- \\ G_e^T \underline{v}_i \end{bmatrix} , \quad \text{For } \kappa = 1 \text{ or } 2 \text{ or } \ldots \ell , \qquad 6.17$$

where $\kappa = 1$ or 2 or ... or ℓ, is an integer specifying the column in R_{λ_i} then,

$$\underline{\rho}_{\kappa_i} = \underline{v}_i , \qquad 6.18$$

$$\underline{\omega}_{\kappa_i} = G_e^T \underline{v}_i . \qquad 6.19$$

From equation 6.18 and 6.19 the feedback matrix can be computed as,

$$G_e^T = \left[\underline{\omega}_{\kappa_1}, \underline{\omega}_{\kappa_2}, \ldots, \underline{\omega}_{\kappa_n} \right] \left[\underline{v}_1, \underline{v}_2, \ldots, \underline{v}_n \right]^{-1} . \qquad 6.20$$

To satisfy equations 6.12, 6.13 and 6.20 following must hold,

a) whenever $\lambda_i = \lambda_j{}^*$ then $\underline{v}_i = \underline{v}_j{}^*$ and $\underline{\omega}_i = \underline{\omega}_j{}^*$, (*) denotes complex conjugate.

b) $\underline{v}_i$ must belong to the null-space of $[\lambda_i \mathbf{I} - \mathbf{A}^T \mid \mathbf{C}_m{}^T]$.

c) For an inverse to exist in equation 6.20, $\underline{v}_{i\ i=1,2,...,n}$ must be linearly independent.

If the specified eigenvalues are real then equation 6.20 must hold. Equation 6.11 is a vector differential equation whose solution to an initial error vector can be shown to be,

$$e(t) = \mathbf{V}\, e^{\Lambda t}\, \mathbf{V}^{-1}\, e(0) \ , \qquad 6.21$$

where $\mathbf{V}$ is the modal matrix whose columns are the eigenvectors of the matrix $(\mathbf{A} - \mathbf{G}_e\mathbf{C}_m)$. Equation 6.21 can be expanded in the form,

$$e(t) = \left[\underline{v}_1, \underline{v}_2, \ldots, \underline{v}_n\right] \begin{bmatrix} e^{\lambda_1 t} & . & . & 0 \\ . & . & . & . \\ . & . & . & . \\ 0 & . & . & e^{\lambda_n t} \end{bmatrix} \left[\underline{v}_1, \underline{v}_2, \ldots, \underline{v}_n\right]^{1} e(0) \ . \qquad 6.21a$$

Equation 6.21 can be simplified by defining,

$$\underline{\alpha} = [\underline{v}_1 , \underline{v}_2 , \ldots, \underline{v}_n \ ]^{-1}\, e(0) \ . \qquad 6.22$$

Expansion of equation 6.21a after substitution of equation 6.22 yields,

$$\begin{aligned} e_1(t) &= v_{11} e^{\lambda_1 t} \alpha_1 + v_{12} e^{\lambda_2 t} \alpha_2 + \ldots + v_{1n} e^{\lambda_n t} \alpha_n \\ &\ \ . \qquad\quad . \qquad\quad . \qquad\quad . \\ &\ \ . \qquad\quad . \qquad\quad . \qquad\quad . \\ e_n(t) &= v_{n1} e^{\lambda_1 t} \alpha_1 + v_{n2} e^{\lambda_2 t} \alpha_2 + \ldots + v_{nn} e^{\lambda_n t} \alpha_n \end{aligned} \qquad 6.23$$

It is seen from equation 6.23 that the error e(t) will converge to zero if and only if the error modes converge. This implies that the eigenvalues must have negative real parts. Furthermore the error states will decay monotonically provided only that the specified eigenvalues are real and negative. A rapid convergence of the error vector can be obtained by specifying the observer eigenvalues to be located far to the left of the origin of the s-plane.

Assuming that suitable observer eigenvalues can be specified, however, there remains a problem of specifying appropriate corresponding eigenvectors which will distribute the error modes in the response of the error states. It has been shown in chapter 3, and also in chapter 5, that the amplitude of the response is governed by the eigenvectors. It was also shown in section 5.3 that different choice of eigenvectors produces a radically different control system.

From a choice of ℓ computed null-space vectors (equation 6.16) it would be possible to select an appropriate eigenvector so as to distribute the mode in the response of the error vector. One possible method of specifying the eigenvectors for the observer would be to ensure that a specific mode participates only in the constituent mode variables. For example, if in equation 6.23, λ_1 is chosen to be sufficiently negative and if the eigenvector components $v_{12}, \ldots, v_{1n}$ are arranged to be zero, then only the mode $e^{\lambda_1 t}$ participates in the response of the error state $e_1(t)$, the extent of such mode participation being controlled by v_{11} and the overall amplitude being governed by α_1.

6.3.2 Specification of Observer Eigenvalues and Eigenvectors

It is assumed that variables w, q, δ_a, δ_e of the model Gamma are available for measurement. Therefore the matrix C_m was chosen to be,

$$C_m = \begin{bmatrix} 1 & 0 & 0 & 0 & 0 & 0 \\ 0 & 1 & 0 & 0 & 0 & 0 \\ 0 & 0 & 0 & 0 & 1 & 0 \\ 0 & 0 & 0 & 0 & 0 & 1 \end{bmatrix}$$

To determine the effect of the observer dynamics on the resulting structural loads, the following three sets of eigenvalues were specified for the observer.

	Set 1	Set 2	Set 3
λ_1	-1	-5	-25
λ_2	-1	-5	-25
λ_3	-1	-5	-25
λ_4	-1	-5	-25
λ_5	-6.0	-6.0	-6.0
λ_6	-7.5	-7.5	-7.5

Table 6.8 : Eigenvalues specified for the observer

Note particularly from table 6.8 that repeated eigenvalues have been specified. Since four states are available for measurement, the dimension of the null-space is four. Hence, the four linearly independent null-space eigenvectors can be assigned corresponding to the repeated eigenvalues (λ_1, λ_2, λ_3, λ_4). It is worth noting that if the method proposed by Shapiro et al [1983] was used to synthesise the observer gain matrix, the assignment of repeated eigenvalues would not have been possible. However, eigenvalue/eigenvector method proposed by Porter [1978] does enable such repeated eigenvalues to be assigned.

Eigenvalues corresponding to the aileron and elevator error modes are specified as having the same values for the three sets. Since an observer eigenvalue merely determines the speed of convergence of the mode it is associated with, the choice may be arbitrary. The obvious limitation is that an eigenvalue of multiplicity greater than t may not be specified, because the inverse in equation 6.20 does not then exists. The eigenvectors corresponding to λ_5 and λ_6 can be chosen from the respective null-spaces such that $e^{\lambda_5 t}$ and $e^{\lambda_6 t}$ participate only in the response of e_5 and e_6. The observer gain matrix for each of the specified sets was calculated as,

$$G_e^T = \left[\underline{\omega}_{1_1}, \underline{\omega}_{2_1}, \underline{\omega}_{3_1}, \underline{\omega}_{4_1}, \underline{\omega}_{4_5}, \underline{\omega}_{4_6} \right] \left[\underline{\rho}_{1_1}, \underline{\rho}_{2_1}, \underline{\rho}_{3_1}, \underline{\rho}_{4_1}, \underline{\rho}_{4_5}, \underline{\rho}_{4_6} \right]^{-1} . \qquad 6.24$$

6.3.3 Modelling the Observed System

The system of equations describing the observer, the aircraft and the control Law are:

$$\dot{x}_e = F_e x_e + G_e C_m x + B u \ , \qquad 6.25$$

$$\dot{x} = A x + B u \ , \qquad 6.26$$

$$u = K x_e \ , \qquad 6.27$$

where the feedback matrix K is the same as in the control Law Gamma. The matrix F_e is defined by equation 6.10. Substitution of equation 6.27 in 6.26 and 6.25 results in,

$$\dot{x}_e = F_e x_e + G_e C_m x + B K x_e \ , \qquad 6.28$$

$$\dot{x} = A x + B K x_e \ . \qquad 6.29$$

The vector differential equations 6.28 and 6.29 can be written in the compact form, viz:

$$\begin{bmatrix} \dot{x} \\ \dot{x}_e \end{bmatrix} = \begin{bmatrix} A & BK \\ G_e C_m & F_e + BK \end{bmatrix} \begin{bmatrix} x \\ x_e \end{bmatrix} . \qquad 6.30$$

In order to access the reductions in the bending and torsional moments at various wing stations when using estimated full state variable feedback (EFSVF), the output equation was defined as,

$$y = C\,x + D\,K\,x_e . \qquad 6.31$$

The block diagram representing equation 6.30 and 6.31 is shown as figure 6.7.

6.3.4 Dynamic Response of the Observed System

Test case SC1which represents an initial condition on the vertical velocity was used to excite the controlled system. Time histories of bending moment at W.S.1., torsion moment at W.S.1, displacement of the first flexural mode and vertical velocity are presented in figures 6.8, 6.9, 6.10 and 6.11 respectively. Presented on each figure is the uncontrolled response, controlled response when using full state variable feedback (FSVF) and controlled response using EFSVF.

From these figures it should be noted that as the observer dynamics is made faster (i.e., the eigenvalues are increased negatively) x_e approaches x much more quickly. Even with an observer having comparatively slow dynamics, i.e., eigenvalue Set 1, some reduction in the peak values of the bending and torsional moment at W.S.1 are still achieved. However, if the same degree of of alleviation is required as that obtained when using the FSVF Law Gamma, the observer dynamics have to be very fast, i.e., eigenvalue Set 3. It is worth noticing from the figures corresponding to Set 3 that the EFSVF responses closely follow the FSVF responses.

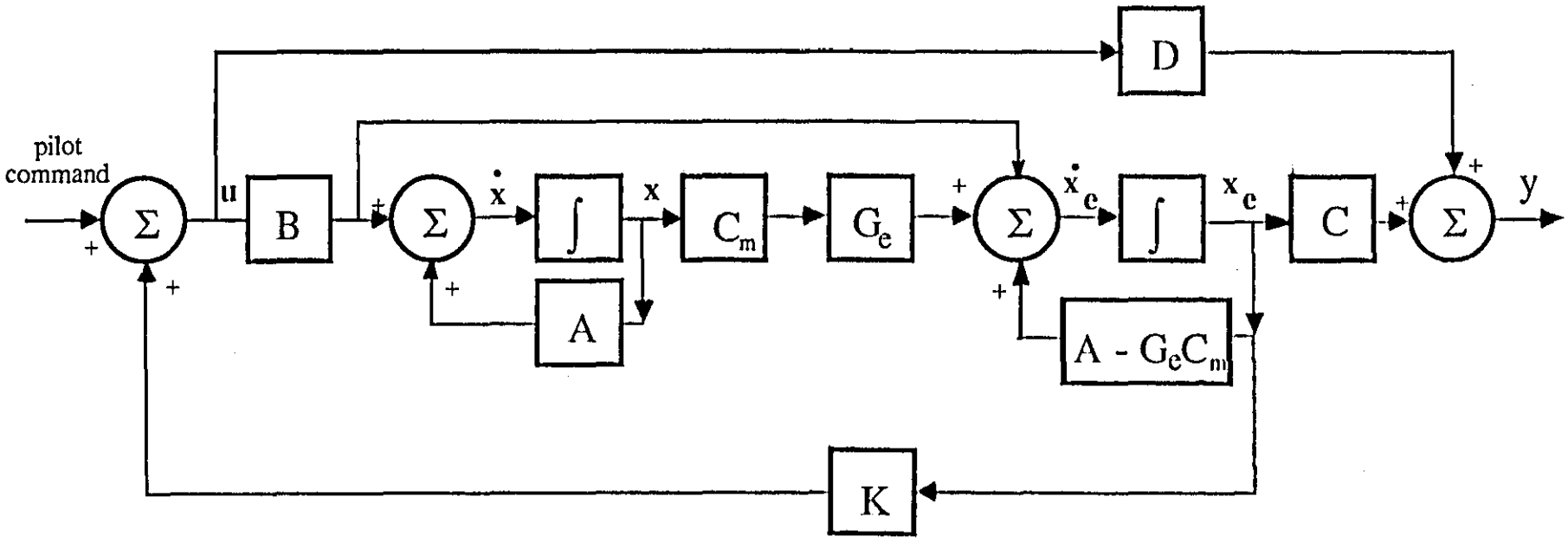

Figure 6.7 : Block diagram representing the observed closed-loop control system

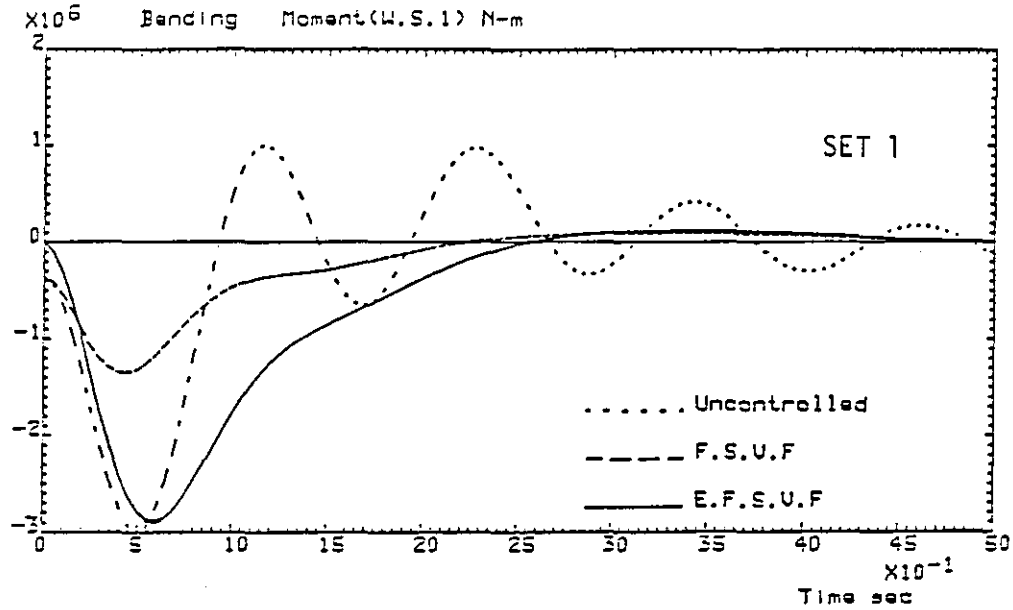

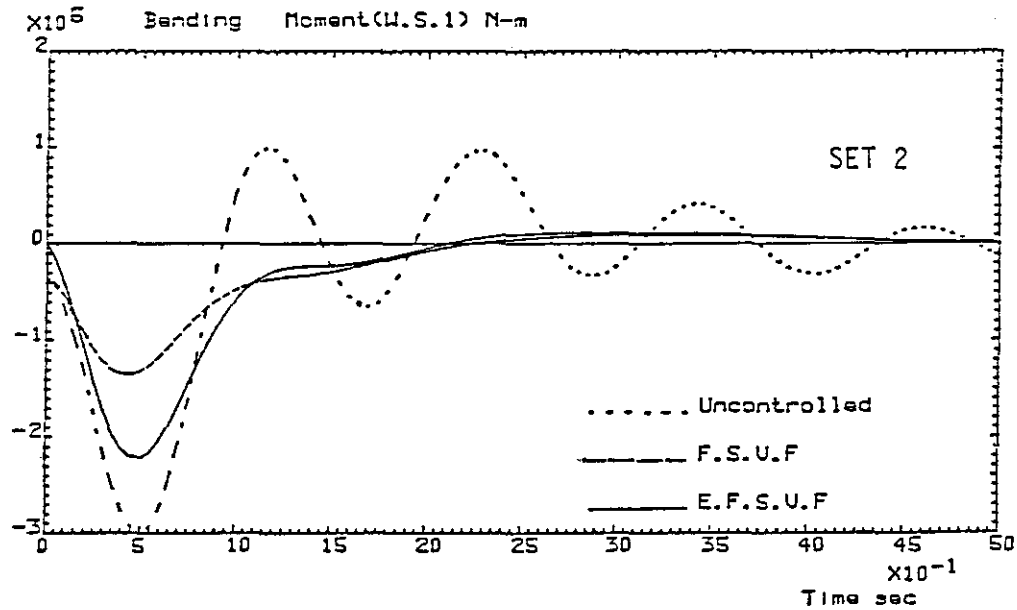

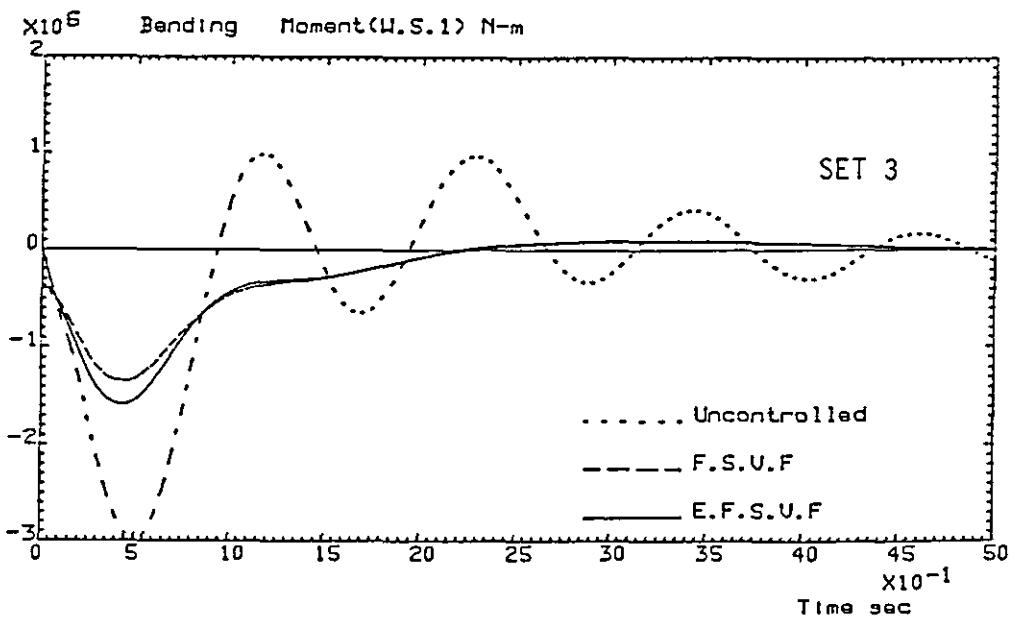

Figure 6.8 : The effect of observer dynamics on bending moment response at W.S.1 using EFSVF, control law Gamma test case SC1.

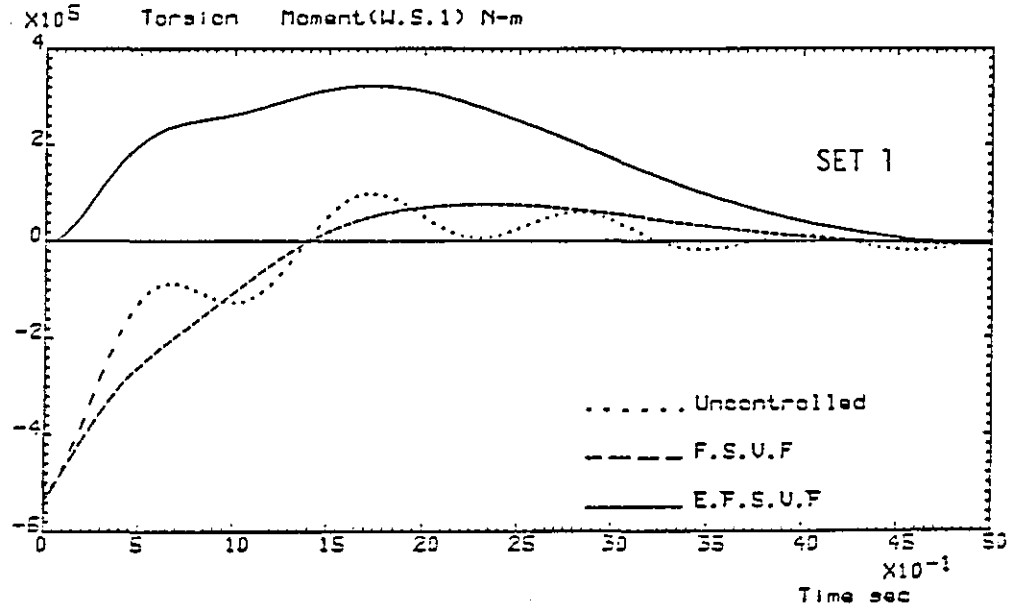

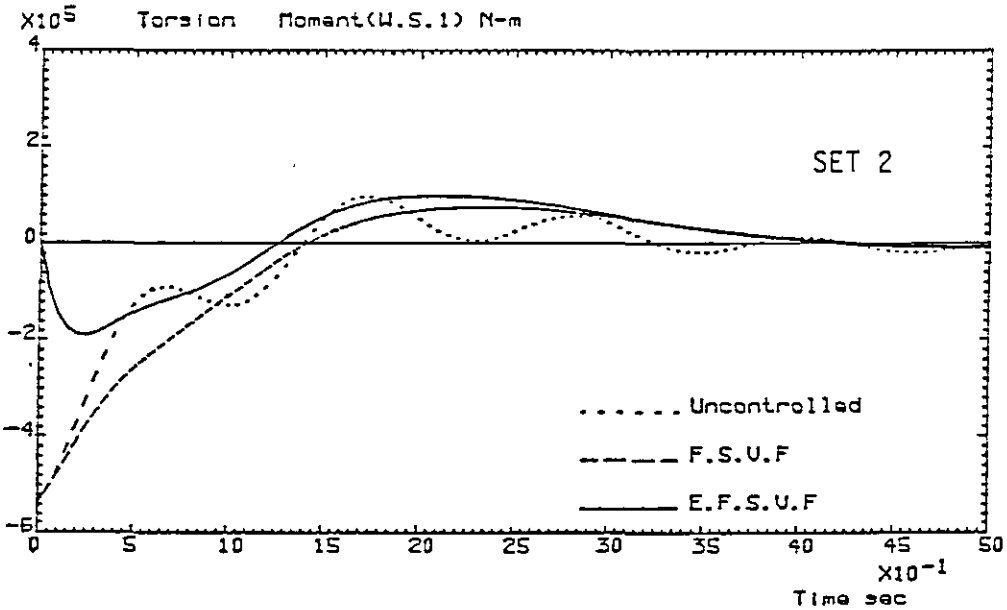

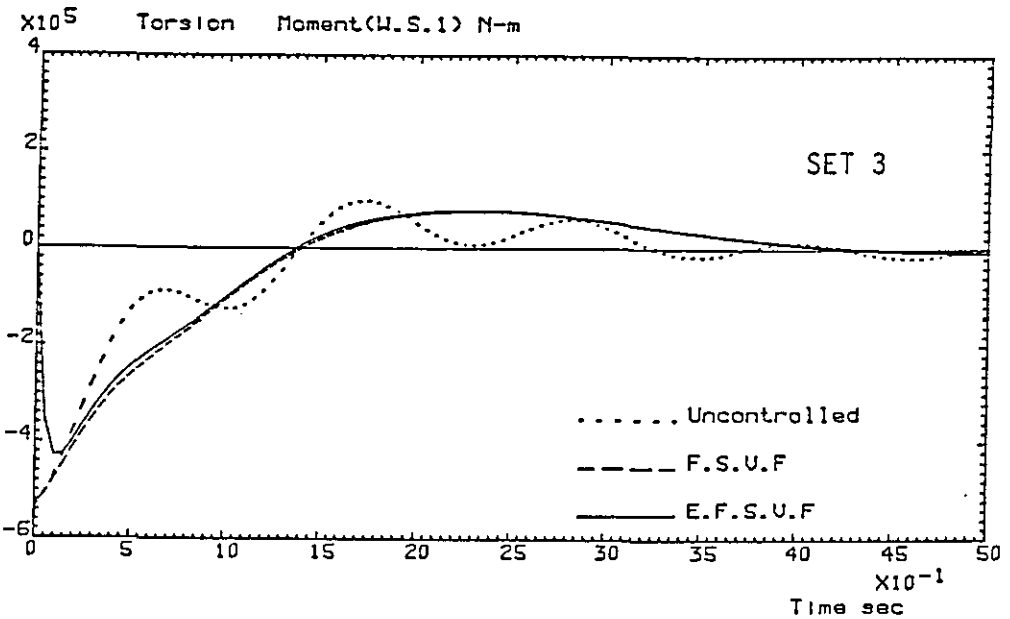

Figure 6.9 : The effect of observer dynamics on torsional moment response at W.S.1 using EFSVF, control law Gamma, test case SC1.

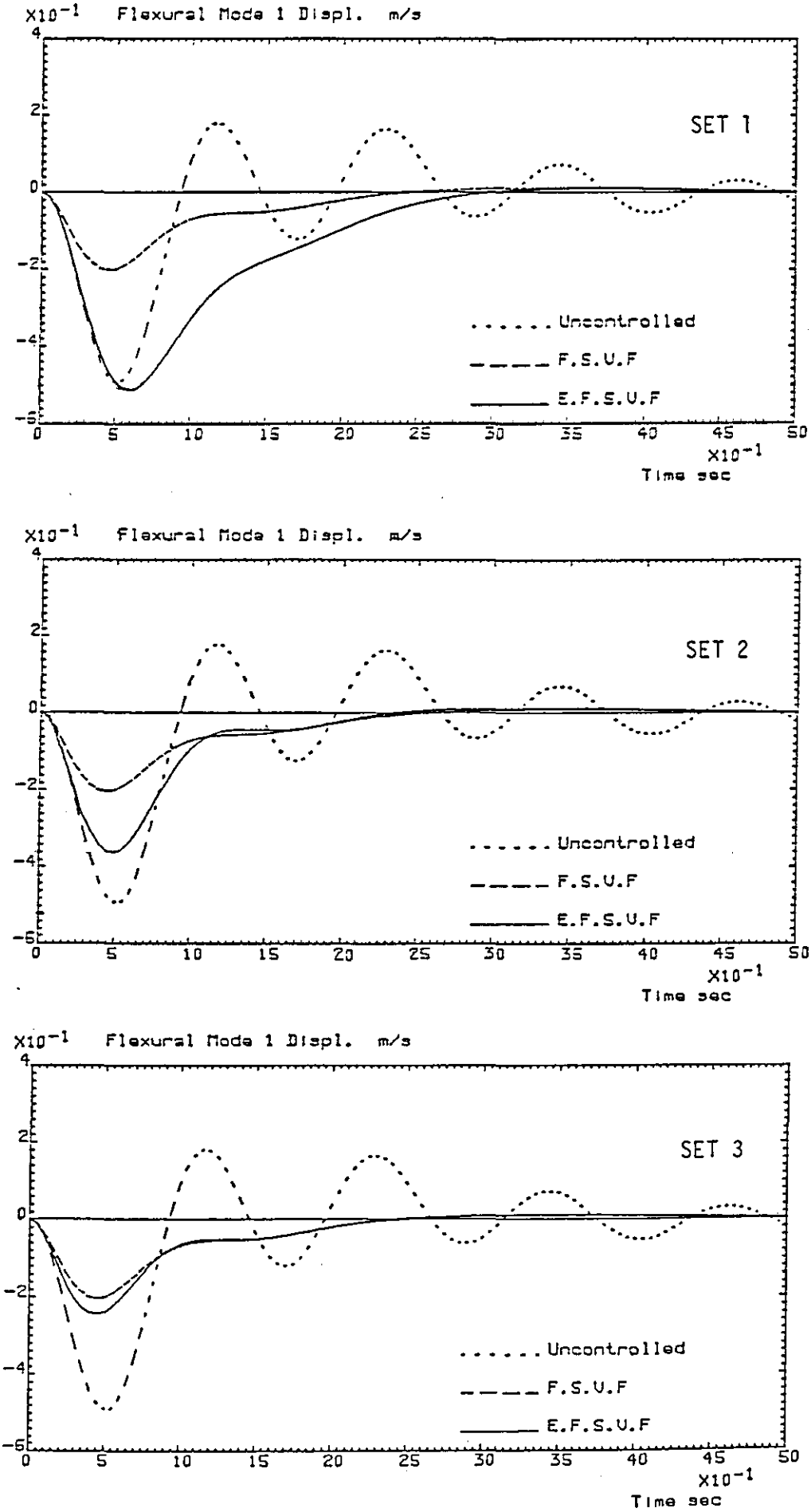

Figure 6.10 : The effect of observer dynamics on displacement of the first flexural mode using EFSVF, control law Gamma, test case SC1.

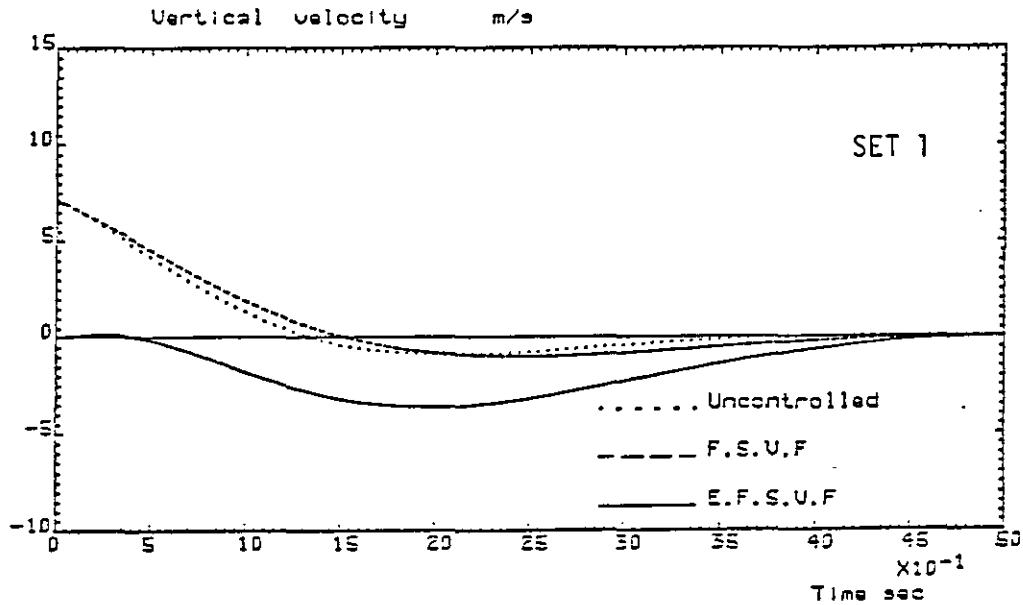

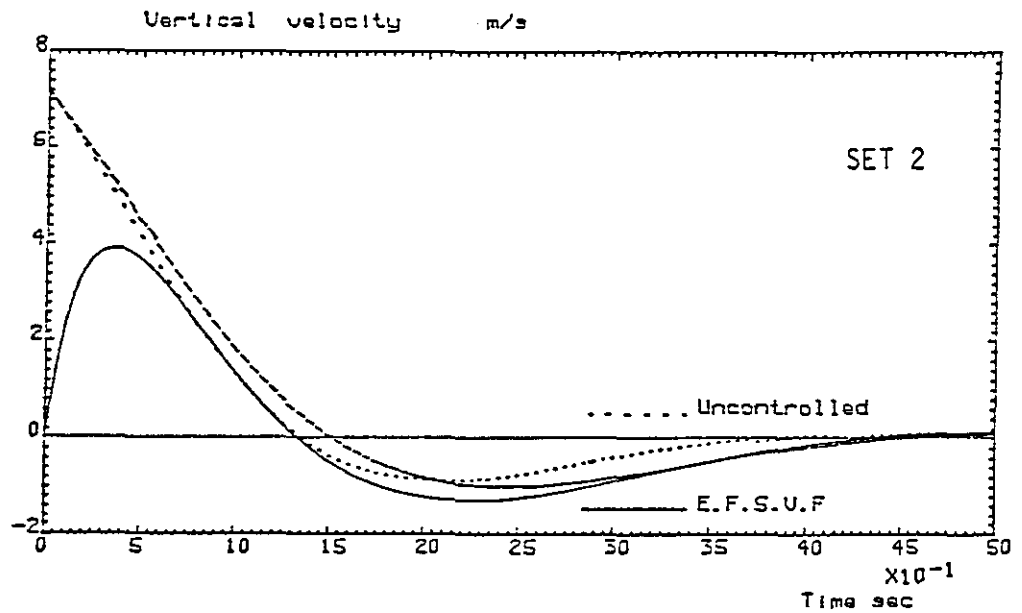

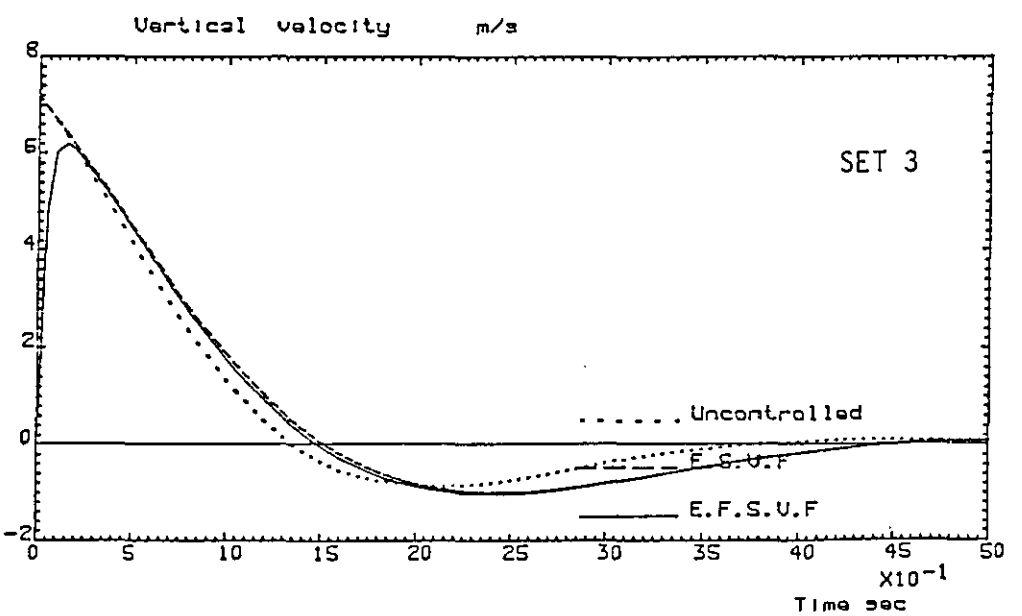

Figure 6.11 : The effect of observer dynamics on the vertical velocity using EFSVF, control law Gamma, test case SC1.

6.4 Digital Synthesis of the Observed System

It was shown in the previous section that the states required for feedback of Law Gamma could be constructed by using a full order observer. It was also shown that provided the estimator dynamics are fast, load alleviation could be achieved by using EFSVF. The levels of reduction obtained were the same as those obtained when using FSVF Law Gamma. If it is assumed that all of the states required for feedback of Law Gamma are available for measurement, then, by observing these states, redundancy can be demonstrated. Digital systems provide an advantage, from the point of view of the design of redundant systems, in that logical and arithmetic comparisons can be made.

However, the information upon which a digital flight control system operates is derived from the sensors which are essentially analogue devices. Moreover, the actuating elements in an AFCS are also analogue. Hence, in order to pass information to the computer and obtain from it the control signals, an analogue-to-digital converter (ADC) and an digital-to-analogue converter (DAC) are required. Advanced Continuous Simulation Language (ACSL) was used to simulate the three elements i.e. the ADC, computer and the DAC . The block diagram representing the digital estimated state variable feedback control system is shown as figure 6.12. It is seen from the figure that the available states are being fed to an sample and zero order hold circuit. The sampled signals are then used to obtain the full state vector, essentially by solving equation 6.30.

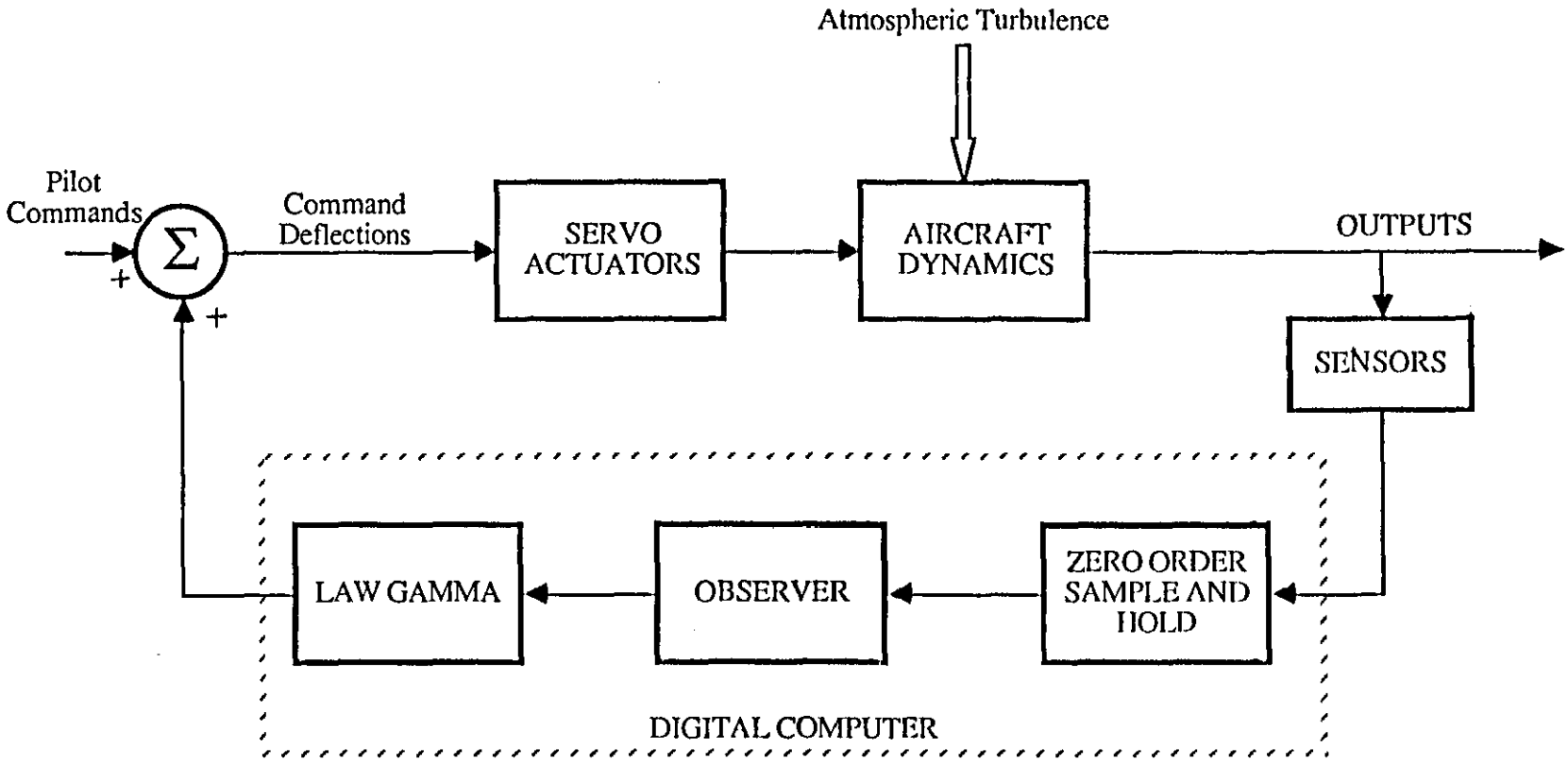

Figure 6.12: Block diagram representation of the digital EFSVF control system

6.4.1 Effect of Sampling on Structural Loads

It is well known that sampling frequency adversely affects the performance of a digital control system. Some selected responses, which highlight the effect of sampling on the dynamic response of the aircraft, are presented in figures 6.13, 6.14 and 6.15. The observer gain matrix corresponding to set 3 and Law Gamma were used. The responses presented on each figure are the bending moment at W.S.1 (y-axis annotated YY1), the torsional moment at W.S.1 (y-axis annotated YY2) and the rigid-body vertical velocity (y-axis annotated YY37). The responses are for test case SC1 which relates to an initial condition on the vertical velocity of 7.15 m/s (281 in/s).

Shown in figure 6.13 are some selected responses when using EFSVF. The measurable states w, q, δ_a and δ_e were sampled at the same rate of 14 Hz. It can be noticed from this figure that the response of vertical velocity is almost the same as the response obtained for the equivalent analogue situation (see figure 6.11). It is noticed that the bending moment and the torsion moment response have become oscillatory and the peak values are much higher compared to those in figures 6.8 and 6.9.

Presented next is the response obtained for a sampling frequency of 100 Hz. From figure 6.14 it is noticed that the responses obtained at the sampling frequency of 100 Hz are almost the same as the uncontrolled case. It appears that EFSVF has little or no influence on structural loads. This can only imply that sampling has a degrading effect on the observer dynamics, and hence on the alleviation of the structural loads being achieved.

Tests carried out at the same sampling frequency without the observer, i.e., the basic FSVF control system using Law Gamma, indicated no difference between the comparable analogue case. This test proved beyond doubt that the observer was sensitive to the sampling frequency.

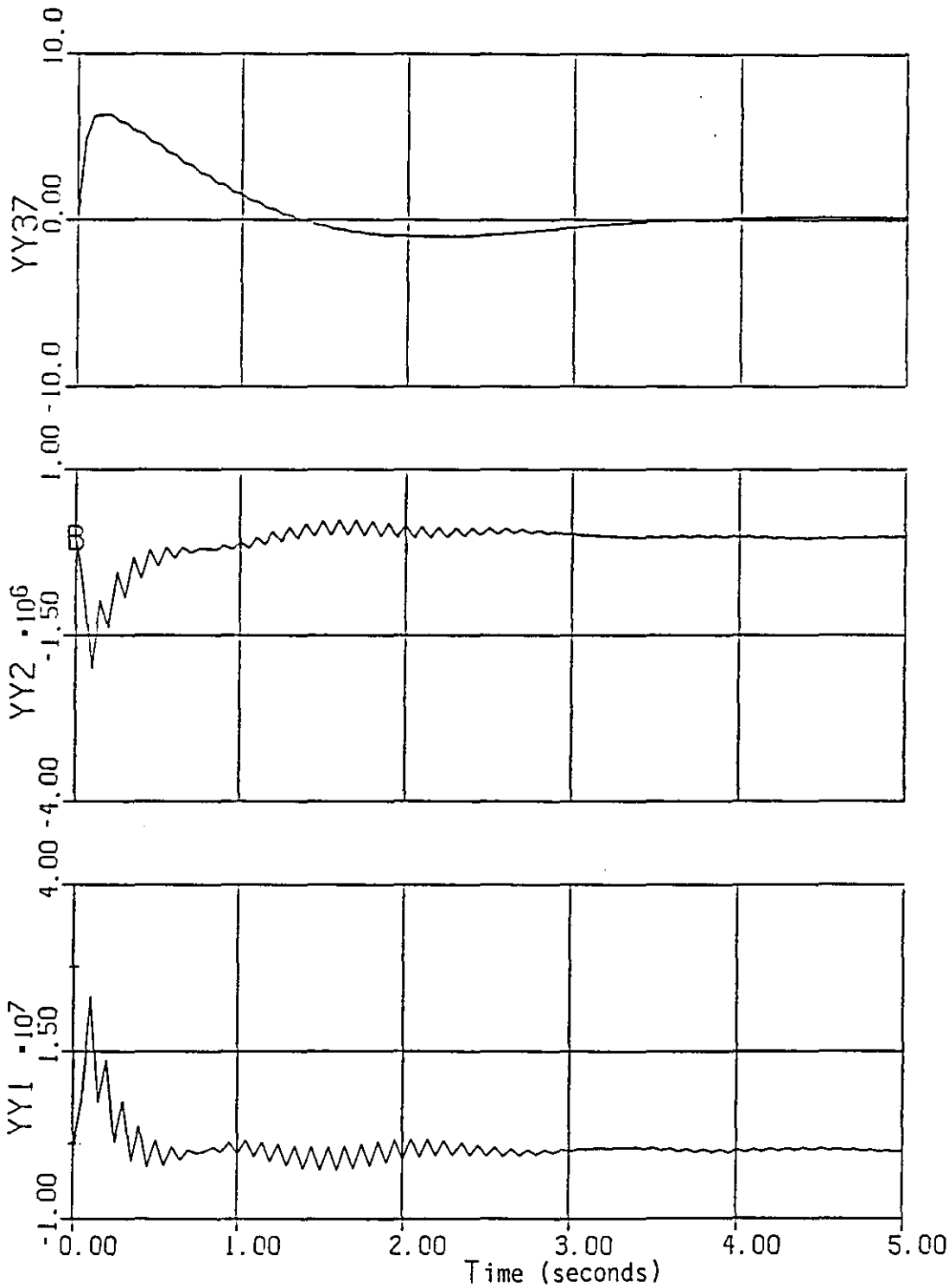

Figure 6.13 : Selected responses of the digital EFSVF control system obtained for a sampling frequency of 14 Hz, control law Gamma, test case SC1.

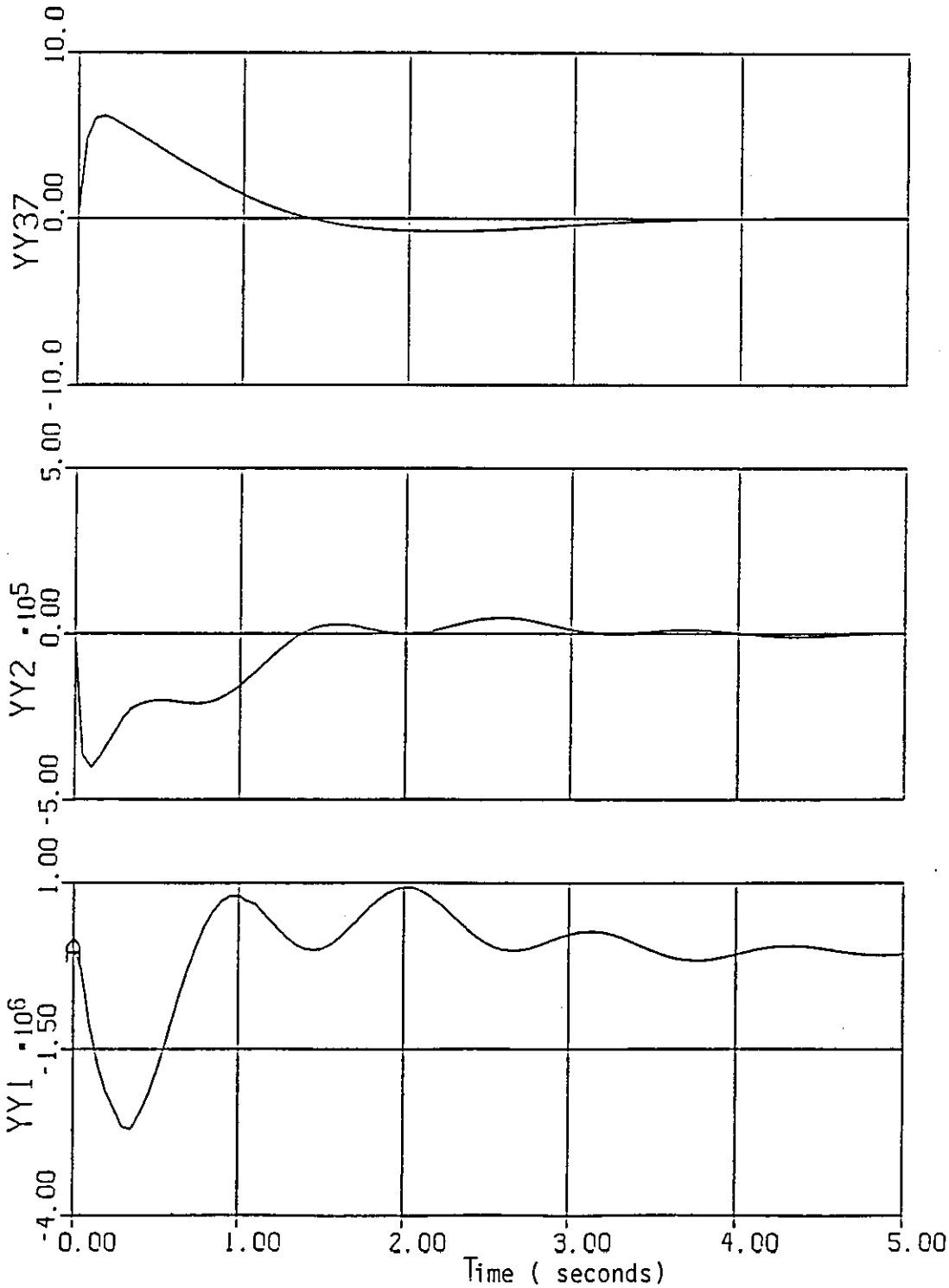

Figure 6.14 : Selected responses of the digital EFSVF control system obtained for a sampling frequency of 10 Hz, control law Gamma, test case SC1.

Presented in figure 6.15 are the responses obtained for sampling frequency of 1000 Hz. It can be seen from this figure that the BM and TM responses are essentially the same as those for the analogue situation (see figure 6.8 and 6.9). It is clearly evident from figures 6.13, 6.14, and 6.15 that the observer is very sensitive to the sampling frequency. In order to demonstrate SLA a minimum sampling frequency of 1000 Hz would be required.

6.4.2 Gust Load Alleviation

To demonstrate that gust load alleviation would be possible when using the EFSVF Law Gamma, the ACSL simulation program which modelled the observed control system was modified to include the dynamics of the Dryden filter, the Küssner dynamics and the gust delays. The gust effects were then injected in the equations of motion via appropriate stability derivatives. The program was run using an initial condition on w of 7.15m/s (281in/s) and with white noise (which is the input to the Dryden filter) having a standard deviation of 0.3m/s. The wing root bending moment and the RMS bending moment response is shown as figure 6.16. The curves marked A are for the uncontrolled case and the curves marked B are for the controlled case when using EFSVF. It can be noted from this figure that even when EFSVF is employed GLA can be achieved. Substantial reductions in the RMS values are seen to result. An RMS reduction of 58% was achieved. Although this value is somewhat lower when compared to FSVF control Law A (63% reduction was achieved), nevertheless is above the required value of 30% at wing station 1.

6.4.3. Hardware Requirements

The simulation results presented in section 6.4.2 indicated that sampling frequency 1kHz was required to achieve SLA and GLA. The conversion of analogue signals at this rate would obviously require a fast ADC. The required sampling frequency is by no means beyond the

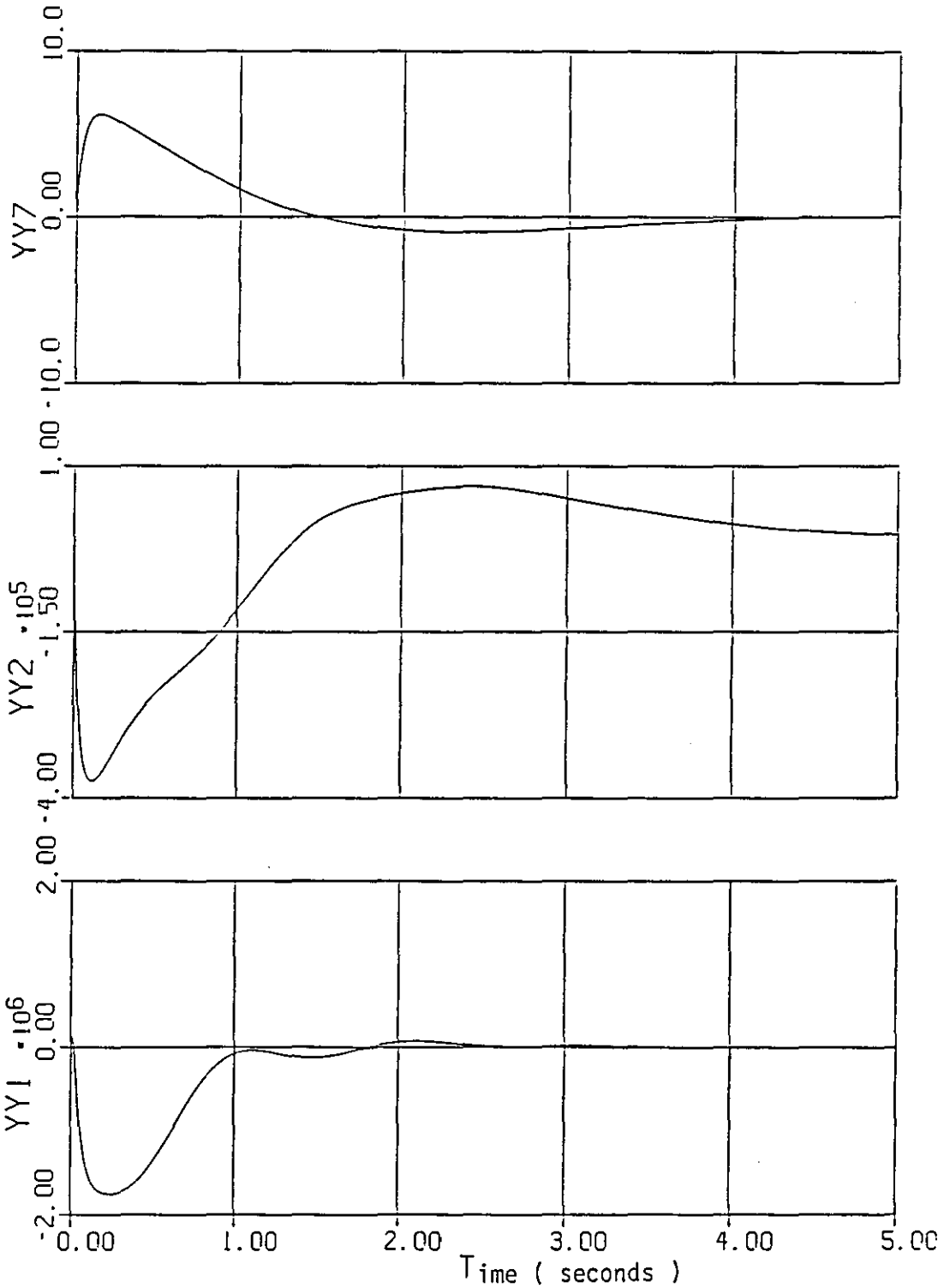

Figure 6.15 : Selected responses of the digital EFSVF control system obtained for a sampling frequency of 1000 Hz, control law Gamma, test case SC1.

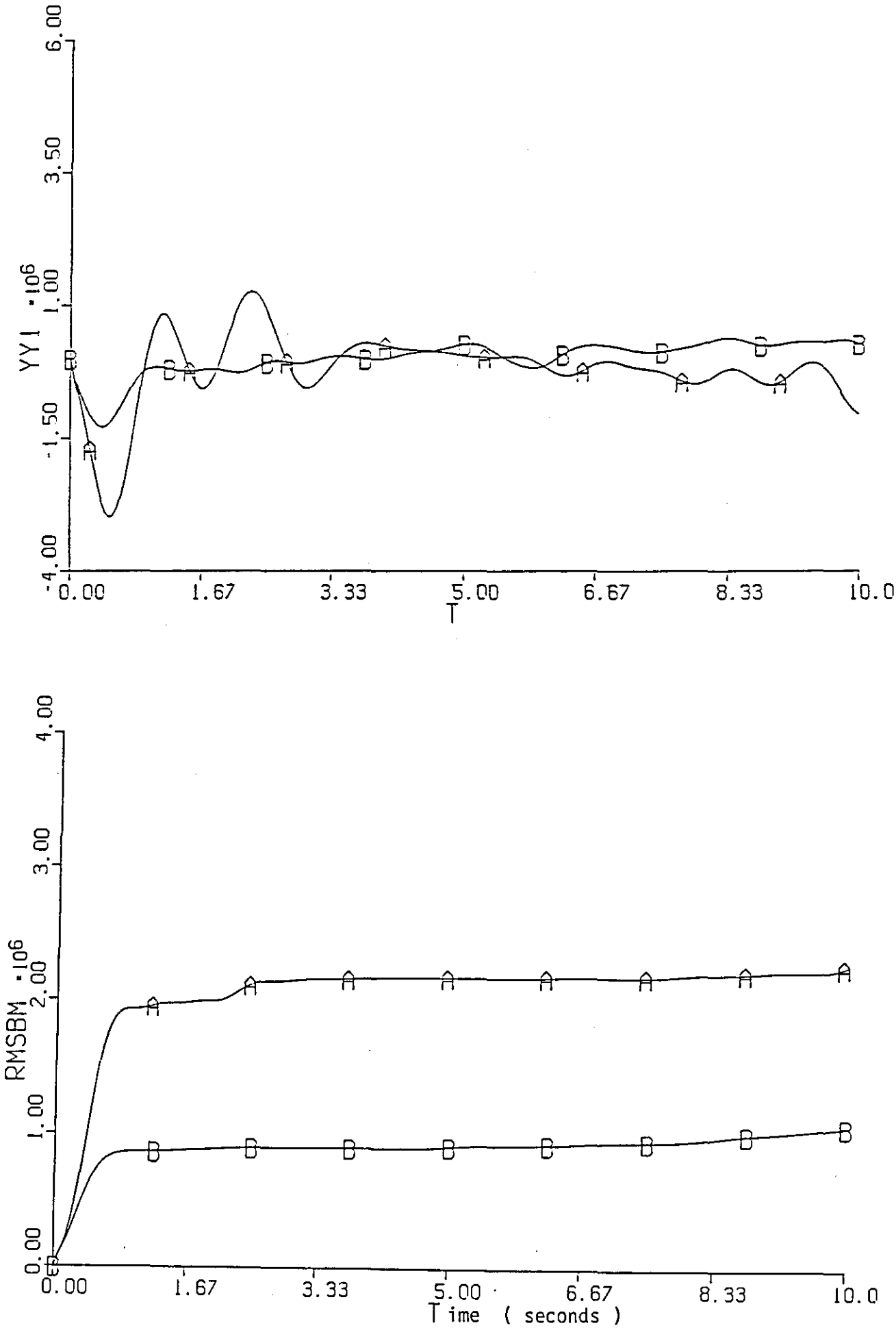

Figure 6.16 : Wing root bending moment response in moderate levels of turbulence, test case SC1 and SC4,

capabilities of the present day ADC's, which can provide sampling frequencies of up to 100 k Hz. Synthesis of digital control systems requires three discrete components, i.e. an ADC, microprocessor and a DAC. The design of such a control computer is expensive. It is now feasible to employ a single chip microcontroller which essentially encompass the three basic elements as indicated earlier.

Unlike microprocessors, microcontrollers are generally optimal for specific application. The MCS™ - 96 range of microcontrollers has been designed for high speed/high performance control applications. INTEL's 8097 microcontroller is a member of MCS™ - 96 family which uses a 16-bit Arithmetic Logic unit (ALU) and operates on a 256 byte register file instead of an acculmulator. Any of the locations in the register file can be used as a sources or destinations. This is called the register to register architecture. In the lower 24 bytes of the register file are the register-mapped input/output (I/O) control locations, also called the special function registers (SFR's). These registers are used to control the on chip I/O features. The remaining 232 bytes are general purpose RAM. Some other features of the 8097 microcontroller are outlined next:

- **16 Bit architecture, 64K addressable space**
- **Clock frequency 12MHz**
- **8 bit wide digital Port (quasi-bidirectional)**

  This port can be used either as an input port or an output port.
- **hardware serial channel**

  The hardware serial channel can be configured to the RS-232 or RS-422 specifications.
- **Two 16-Bit hardware counters/timers**
- **Eight multiplexed analogue channels, 10-Bit ADC (with sample and hold)**
- **One variable duty Pulse Width Modulated output (PWM)**
- **6 or 4 high speed outputs (HSO)**

  By using the hardware timer PWM outputs can be generated on the HSO pins by setting the on-times and the off-times. Integration of the PWM signals by using an

active or a passive RC filter will provide analogue outputs. Analogue voltage can also be obtained by generating a 50% duty cycle PWM signal of variable frequency on the HSO pin, which can be converted by using a frequency to voltage converter.

- **2 or 4 High speed inputs (HSI)**

  HSI are provided for measurement of pulses of 2 ms duration or greater.

- **6.25 μs 16-bit x 16-bit multiply, 6.25 μs 32-bit / 16-bit divide**
- **1 to 2 μs average instruction time**

A single board computer (SBC) based on the 8097 microcontroller has been designed by the author for dedicated control applications¶. The 8097 has a single 10-bit ADC with sample and hold, convertions on a single channel take 22μs. If the SBC based on the 8097 is used to synthesise the EFSVF control system, then the requirement of sampling the four measurements at a frequency of 1 kHz can be met easily. If all the eight channels were being sampled then a maximum sampling frequency of 5.7 kHz on each channel would be possible. It was merely an intention here to indicate that SBC based on an microcontroller can be used for the digital synthesis of EFSVF control systems to provide SLA, MLC and GLA. However much work still needs to be done as far as practical implementation is concerned.

¶ The design of a single board computer (SBC) based on the INTEL 8097 microcontroller was started in January 1986 and was completed in November 1986. The work was sponsored by the Department of Transport Technology, Loughborough University. The SBC is intended to be used in aerospace and automotive applications. Typical areas of usage are likely to be;

- flight control
- engine management systems
- drive train control
- data acquisition

Software development is done on the INTEL Series IV and Series III 16-bit microprocessor development systems (MDS), in conjunction with the in circuit emulation (ICE) facility.

6.5 Concluding Remarks

The robust nature of the proposed feedback laws was demonstrated by considering reduced order feedback laws derived from the reduced order models. It was shown that if Law Gamma at least is available for feedback then SLA would be possible. Load alleviation in manoeuvres and in turbulence was demonstrated. It was shown that if some of the aircraft's states are unavailable for measurement then a full order observer could be designed by using the EPAM. The effect of observer dynamics on the observed states and hence on load alleviation was demonstrated by considering three separate observers. It was also shown that the error between the actual states and the estimated states converged to zero more rapidly as the dynamics of the observer are made fast. The EFSVF control system was synthesised digitally by using the simulation language ACSL. The effect of different sampling frequencies on the observer dynamics was demonstrated. Finally it was indicated that a microcontroller may be used to implement the EFSVF control system digitally.

CHAPTER 7

CONCLUSIONS AND RECOMMENDATIONS

7.1 Concluding remarks

Reduction of the aerodynamic loads which arise on the aircraft owing to responding to manoeuvre commands or when encountering atmospheric turbulence, is an important problem in flight control. The reductions can be beneficial from both the ultimate structural strength and the fatigue life of the airframe. Such reductions increase the structural durability and improvement in the fatigue life of structural components. The eigenpair assignment method (EPAM) described in chapter 3, was successfully applied to design feedback controllers, which resulted in the reduction of the loads on the wing of the C5-A. All design objectives were met i.e. there was achieved the required alleviation of the steady state and RMS values of bending and torsional moments at W.S.1. These reductions were caused by effectively controlling the first flexural mode. The EPAM was used to augment the damping in the first flexural mode from an uncontrolled value of 0.093 to 0.465. Another factor for such reductions was the choice of eigenvector selection scheme, which enabled the reduction of the peak and RMS values of the displacement and rate of the first flexural mode.

The robust nature of the proposed feedback laws was demonstrated by considering reduced order feedback laws derived from the reduced order models. It was shown that if at least Law Gamma is available for feedback then SLA would be possible. It was shown that if some of the aircrafts states are unavailable for measurement then a full order observer could be designed by using the EPAM. The effect of observer dynamics on the observed states and hence on load alleviation was demonstrated by considering three separate observers. It was also shown that the error between the actual states and the estimated states converged to zero more rapidly as the dynamics of the observer are made fast. The EFSVF control system was synthesised digitally by using the simulation language ACSL. The effect of different sampling frequencies on the observer dynamics was also demonstrated.

It was shown in chapter 2 that the dynamic response of the aircraft, owing to control inputs or due to disturbances on the aircraft's state variables, can be determined by using the eigenvalues and the eigenvectors of the coefficient matrix **A**. It was shown that the eigenvalues determine the rate of decay of the modes, whereas the associated eigenvectors determine the extent of mode participation in the state variable response and the amplitude of the response.

A mathematical model describing the dynamics of the L-1011 Tristar aircraft was presented in chapter 2. The lack of damping and the coupling between the modes of motion of the L-1011 , was explained in terms of the eigenvectors of the uncontrolled aircraft. The dutch roll mode was found to be very lightly damped, and the time constant associated with the spiral mode was found to be very large. It was also noted that the rolling and yawing motions of the aircraft were coupled. The lack of damping in the Dutch roll mode is due to the coupling of the rolling and yawing motions of the aircraft. It was suggested that in order to augment the damping and possibly to decouple the modes of motion, feedback would be required.

Three feedback methods for obtaining full state variable feedback control laws were presented in chapter 3. The first method presented assigned the specified eigenvalues. A generalised control canonical form derived from the canonical forms for multivariable systems, such as those presented by Luenberger[1967] was used in the eigenvalue assignment technique and it was shown that by using state variable feedback, the eigenvalues of such linear multivariable systems can be arbitrarily assigned. The specified eigenvalues for the L-1011 Tristar, being achieved exactly. The method presented is purely algebraic, and offered features such as;

a) The indication of the controllability of the pair (**A**, **B**).

b) Computation of a feedback matrix using real arithmetic, even if the specified eigenvalues are complex.

c) The procedure of determining the feedback matrix does not require inversion of the modal matrix (a matrix whose columns are composed of eigenvectors), therefore making it possible to assign repeated eigenvalues, or eigenvalues which also belong to the open-loop spectrum of A.

The second method briefly outlined in chapter 3 was solution of the LQP. The method is based on obtaining a control which minimises a chosen performance index. The feedback gains are obtained as a solution of the algebraic Riccati equation. It was shown in chapter 3, that although a satisfactory control law could be obtained using the LQP method (a lateral feedback controller for the L-1011 was designed by using LQP method), exact assignment of the specified eigenvalues and eigenvectors, which translate into the dynamic performance of the system, could not be achieved. It was also shown that the choice of weighting matrices could not be related to the attainable dynamic characteristics of the aircraft.

Based on an eigenvalue comparison alone, the time domain characteristics, such as damping and the speed of response of the system could be inferred. In the case when the eigenvalue is real, the time constant of a monotonic mode associated with it can be inferred. Whereas if the eigenvalues occur as complex conjugate pair then the frequency and the damping of a mode associated with the eigenvalues could be obtained. Although the GCCF control law assigned every specified eigenvalue, some degradation of the yawing response of the L-1011 was observed. The degradation of the yawing motion was explained from an examination of the closed-loop eigenvectors resulting from the use of GCCF control law. The coupling of the

yawing and rolling motions of the aircraft still persisted, even under the influence of the control law using the GCCF control law. The coupling of the modes of motion (yawing/rolling arising due to the use of GCCF control law) and the arbitrariness associated with the selection of the weighting matrices in the LQP method was overcome by the use of eigenpair assignment method (EPAM), in which the required closed-loop eigenvalues and the eigenvectors were assigned.

It was shown in chapter 3 that the lateral feedback controller for the L-1011 designed by using the EPAM improved the dynamic response of the aircraft. The controller was shown to be superior to the controllers designed by the GCCF, the solution to the LQP and the method proposed by Andry et al[1983]. It was also shown that the performance of a multivariable control system cannot be solely judged on the examination of eigenvalues alone: corresponding eigenvectors have to be examined. The results presented in chapter 3 indicate the suitability of the EPAM for the design of stability augmentation systems and for improving the handling qualities .

A requirement of Andry's method of eigenvalue/eigenvector assignment is that the specified closed-loop eigenvectors must belong to a sub-space of the matrix $(\lambda I - A)^{-1}B$. The desired closed-loop eigenvector is projected on to this sub-space and an achievable closed-loop eigenvector is obtained by minimising the least squared error between the achievable and the desired closed-loop eigenvector. It is quite obvious, that, if the desired closed-loop eigenvector is orthogonal to the sub-space, it can never be made to span it. From this basic consideration a suitable choice of the closed-loop eigenvector has to be made in the first instance. Moreover, the projected eigenvector may not span the sub-space exactly, it will do so in the least squared error sense. Another disadvantage of the method is that if an eigenvalue which belongs to the open-loop spectrum is specified in the closed-loop the inverse of the matrix $(\lambda I - A)$ is not defined hence the appropriate sub-space corresponding to the specified open-loop eigenvalue cannot be formed. The method of computing by SVD the closed-loop eigenvectors which satisfy equation 3.68 in the EPAM, has following features:

a) The method does not depend on the inversion of the matrix $(\lambda I - A)$. Therefore a controllable open-loop eigenvalue can be specified for the closed-loop.

b) The eigenvectors in the computed null-space are linearly independent, and from this set of eigenvectors a suitable eigenvector could be chosen to reflect the desired distribution of the mode in the state variable response. Since EPAM assigns an null-space eigenvector in the closed-loop, the method of ' eigenvector projection' in common practice can be avoided.

c) If the rank(A B) $< n$, i.e., some modes are uncontrollable, eigenvalues identified with the uncontrollable modes may be also specified in the closed-loop There is freedom to select appropriate corresponding eigenvectors from the computed null-space.

d) An eigenvalue having a multiplicity of m can be specified for the closed-loop system. Since the dimension of each null-space is m, it is possible to select m eigenvectors corresponding to m eigenvalues which do not to make the modal matrix singular.

It was shown in chapter 3, that the peak values of the dynamic response, of the L-1011 Tristar were substantially reduced by the use of feedback controller designed by the eigenpair assignment method. The specified eigenstructure (which consisted of some open-loop eigenpairs, and the dutch roll and roll/spiral eigenpairs) was assigned exactly in the closed-loop, resulting in the L-1011 having the desired dynamic response.

Methods of reducing by feedback control, the structural loads on the wing of the C-5A, arising as a result of manoeuvre commands and atmospheric turbulence, have been proposed by many authors, see for example Stone et al[1972], Konar et al[1976], McLean[1976] and Prasad[1980].

Before any control scheme is implemented on an aircraft, the theoretical feasibility of a control scheme, using as comprehensive a mathematical description of the aircraft as possible, has to be demonstrated. For this purpose a model of the C-5A was presented in chapter 4. The model included the longitudinal rigid body dynamics, the description of the first six flexural modes of the wing, the unsteady aerodynamics associated with the lifting surfaces namely the wing and the tail was modeled by Küssner functions. Transportation lags (pure delay associated with the aircraft penetrating the gust field, in which the edge of the gust strikes the wing first before striking the tail some finite time later) were modeled by Páde approximations. Actuator dynamics were modeled by linear first order time lags and atmospheric turbulence modelled by a Dryden filter. This total model was represented by a state variable equation. The main objective of this research study was the reduction of the wing loads. For this purpose bending and torsional moments related to the aircraft's state and control variables were defined at five specific wing stations.

It was shown in chapter 4, that when the aircraft was excited from initial conditions on the vertical velocity the uncontrolled response of the bending moments and the torsional moments was highly oscillatory, which is highly undesirable from the fatigue life standpoint. The oscillatory nature of the BM and TM response was attributed to the insufficient damping of the flexural modes. Furthermore, it was shown that the eigenvalues associated with the rigid body mode (the short period mode), the first six flexural modes, the inboard elevator and aileron modes were controllable. Most of the published work concerned with the design of control systems for structural load alleviation (SLA), manoeuvre load control (MLC), and gust load alleviation (GLA), has made use of the LQP method. However, a particular deficiency of the LQP method for structural load alleviation lies in the fact that the characteristics of the flexural modes such as damping and frequency are arbitrarily assigned in the closed-loop.

The arbitrary assignment of the closed-loop eigenstructure can be related to the selection of the weighting matrices. However, with an intuitive knowledge of the SLA problem it is possible to select appropriate weighting matrices which will result in a suitable control law for the purposes of SLA. Since it is known that most of the bending energy is contained in the first flexural mode, control of this mode will result in the reduction of the bending moments. For example, the SLA control system proposed by Prasad [1980] assigns the frequency and the damping ratio associated with the first flexural mode in the closed-loop to be 15.4 rad/s and 0.25 respectively. The frequency of the first flexural mode is effectively separated from the rigid-body mode ($\omega_{n_{sppo}} = 1.55$ rad/s) by a factor of approximately 10, and the damping ratio of this mode was augmented from the uncontrolled value of 0.093 to 0.25. From a knowledge of the system dynamics it is known that SLA can only be possible; if either the frequencies of the flexural modes are separated from the frequencies of the rigid-body modes, or the flexural modes have sufficient damping to dissipate any absorbed energy rapidly. Since the frequency and the damping ratio associated with the first flexural mode assigned by the SLA control system proposed by Prasad, reflected these requirements, load alleviation was possible. However, the computation of feedback laws which result from a choice of weighting matrices determined by intuition or by trial and error approach, can be both cumbersome and time consuming.

From these considerations a method of synthesising feedback controllers which assigns the frequencies and the damping ratios of the flexural modes in the closed-loop and affects the distribution of the modes in the dynamic response would be advantageous. The design of the controller for the purposes of SLA can thus be accomplished in a single design iteration. The effectiveness of full state variable feedback controllers designed by the EPAM, for SLA, MLC and GLA was demonstrated in chapter 5.

It was shown in chapter 5 that, although no attempt was made to augment the rigid body stability by altering the eigenvalues associated with the short period mode, the effect of reducing the

displacements and rates associated with the flexural modes resulted in reduction of structural loads. Part of the reduction being due possibly to the decoupling of the modes of motion, effected by the eigenvector selection scheme of case A. It is also known that structural loading and fatigue damage rates are reduced with stability augmentation, by reducing the peak loads and the number of cycles of loading, Newberry[1969]. It was shown that not only were the peak loads effectively reduced by using control law A, but the absence of any high frequency oscillations in the dynamic response of bending and torsional moments indicates the quality of control law A from structural fatigue consideration.

It was shown in chapter 5 that the second flexural mode is controllable, and that both the damping ratio and the frequency of this mode could be altered by feedback. It was also shown that the choice of eigenvectors for SLA, for the two cases considered, produced radically different responses and very different degrees of load alleviation. The eigenvector choice of scheme A relates to the case in which the eigenvectors are chosen from the null-space such that they allow each mode to contribute to the dominant mode variables. For example, the rigid-body mode mainly consists of the rigid-body vertical velocity and the rigid-body pitch rate, the eigenvector for this mode was chosen such that it allowed the short period mode to contribute mainly to the rigid-body variables. Similarly, the eigenvectors chosen corresponding to the flexural modes allowed the flexural modes to contribute mainly to the dominant variables associated with the flexural modes. Such a choice results in the decoupling of the rigid-body and the flexural modes. The eigenvector choice of scheme A provides a design procedure for structural load alleviation.

It was also shown that all the specified goals (required reductions in the BM and TM observed at W.S.1 appropriate to MLC and GLA) were achieved without impairing the response of the rigid body motion variables and the handling qualities of the aircraft. It is also known that a gust alleviation system that uses only elevator control is not completely effective, Oehman [1973]. An

elevator is primarily a device for controlling the pitch rate and the angle of attack and does not provide adequately the changes of force in the z-direction that are necessary for good gust load alleviation. The reductions in the bending and torsional moments due to manoeuvre commands and atmospheric turbulence were as a result of using a combination of both the elevator deflection and symmetrically deflected ailerons to provide direct lift.

It was shown in chapter 5, that the influence of the first flexural mode on the bending moment response is dominant and that the shape of the bending moment response matches that of the first flexural mode displacement. The displacements of the first flexural mode were an order of magnitude higher than those of the high frequency modes. Since the first flexural mode has a pronounced effect on the bending and torsional moment response, the effects higher frequency flexural modes can be neglected from the dynamic representation of the aircraft. Moreover provided the variables associated with the short period mode, the first flexural mode and the control surface deflections are available for feedback SLA will be possible. Results to this effect, using reduced order models, were presented in chapter 6.

It was shown in section 6.1 that the proposed control laws, such as Law A, remain effective at off-nominal conditions. The off-nominal conditions were simulated by altering the elements of the A matrix. These changes represented changes that would occur due to varying flight conditions or due to modelling inaccuracies. A change of -10% in the frequency of the first flexural mode was made. The new elements in the A matrix represented a frequency of 4.66 rad/s and a damping ratio of 0.093 associated with the first flexural mode. The eigenvalues of the off-nominal closed-loop system when using control Law A, associated with the rigid-body mode and the six flexural modes, indicated that the damping ratios associated with all the flexural modes (except the first flexural mode) were approximately the specified values (see table 5.3). The damping ratio of the first flexural mode had increased to 0.75. Since the damping ratio and frequency of the rigid-body mode were essentially fixed at the specified values, the increase in

the damping ratios associated with the first flexural mode and the remaining modes reflected very favourably in the bending moment response.

From a comparison of figure 5.16 and 6.1 it was noted that the peak value of the uncontrolled bending moment response at W.S.1 had increased from 4.0 MN-m to 6.0 MN-m. This increase was mostly due to the fact that the frequency of the first flexural mode and the rigid-body mode are much closer together, and that the two modes have been much more tightly coupled. It can be inferred from the results presented in section 6.1 that there must be adequate frequency separation between the rigid-body motion and that of flexural dynamics, otherwise excessive peak loads will result due to the coupling of the rigid-body mode with the flexural modes. The reduction in peak values of the bending moments, is a matter of specification. For example if the frequency and damping ratio associated with the first flexural mode of the controlled off-nominal system (see table 6.1) were specified for the controlled nominal system instead of the values given in table 5.3, reductions tabulated in table 6.2 will result.

In section 6.2 three reduced order models were derived from the original 24^{th} order model (see chapter 4). Each model was derived from reducing the 24^{th} order model by the method of modal truncation. The retained modes in each of the models were not represented by any aeroelastic correction factors which relate to the deleted modes of vibration. The three models were designated Alpha, Beta and Gamma respectively. The model Alpha comprises of the rigid-body dynamics the dynamics of the six flexural modes and the aileron and the elevator dynamics. The model Beta was the same as the model Alpha, except that only the first two flexural modes were included. The model Gamma differed from the model Beta in that only the first flexural mode was included. Consequently the dimension of the state vector of models Alpha, Beta and Gamma was 16, 8, and 6 respectively.

The reduction in bending and torsional moments at five wing stations using Law Alpha were almost the same as those obtained with Law A. This was owing to the fact that Law Alpha assigned the same eigenstructure as that assigned by Law A. It was noted that the use of Law Gamma does not produce a bending and torsional moment response which is radically different to the response obtained by either Law A or Law Alpha. It was inferred from results obtained that provided Law Gamma is at least available for feedback, then MLC will always be possible.

The percentage reduction in the RMS and peak values of the bending and torsional moments at various wing stations for Law A and Law Alpha were almost the same. However, reductions caused in the bending moments by the use of Law Gamma were somewhat reduced, but a corresponding increase in the reduction of the torsional moments was observed. The slight increase in the reduction of the torsion moments was at the expense of the decreased reduction in the bending moments. The use of Law Beta produced approximately the same levels of reduction as those obtained by the Law Gamma. This merely implies that feedback of the displacement and the rate of the second flexural mode is unnecessary if the variables associated with the first flexural mode are available for feedback. The degree of reduction in the bending and torsional moment response obtained when using Law Beta or Gamma indicated that the first flexural mode indeed has a dominant effect on the structural loads.

It is worth emphasising that the control laws proposed are extremely effective for the purpose of MLC and SLA. For example, it was shown that when using Law A the reduction in the RMS value of bending moment was about 20% with an associated reduction in the peak value of nearly 70%. When Law Gamma or Beta have to be used, although the reduction in the peak values remained about the same, the reduction achieved in the RMS values was significantly reduced. Nevertheless from a flying point of view the reduction in the peak values for structural loads is what a SLA control system has to achieve to provide the degree of safety required. The loss of RMS performance simply reflects in the fatigue life of the airframe which it is stressed was not

lessened, for some reduction in the RMS values had been achieved.

It was shown in the same section that when using Law A, reduction in the RMS value of torsional moment was about 39% with an associated reduction in the peak value of nearly 37%. The reductions obtained in the bending and torsional moments when using Law Gamma or Beta were 43% and 42% respectively, it was noted that these values were slightly higher than the corresponding values obtained when using Law A. These results are not in the least surprising; for reduction in the bending moments is caused by symmetric deflection of ailerons. Achievement of higher levels of reduction in the bending moments must inevitably involve large aileron deflections. This in turn will cause increased torsional moments about the wing center line. Hence, a decrease in the reduction of bending moments would invariably result in a increased reduction of the torsional moments, which is exactly what the results suggest.

In section 6.3 it was shown that the state vector required for the feedback of Law Gamma could be reconstructed from the knowledge of the measurable state and control variables. The proposed EPAM was used to design such full order observers. It was shown that provided the observer dynamics are fast, load alleviation could be achieved by using EFSVF. The levels of reduction obtained were the same as those obtained when using FSVF Law Gamma. If it is assumed that all of the states required for feedback of Law Gamma are available for measurement, then by observing these states redundancy can be demonstrated.

In section 6.4 the observed control system was digitally synthesised using the advanced simulation language (ACSL). The effects of sampling on the dynamics of the observer were investigated in this section, where it was shown that when the measurable states w, q, δ_a and δ_e were sampled at a frequency 14 Hz the bending moment and the torsion moment response became oscillatory and the peak values were much higher compared to analogous analogue case. The responses obtained for a sampling frequency of 100 Hz were almost the same as the

uncontrolled case. It was inferred that at this frequency EFSVF has little or no influence on structural loads. In order to demonstrate SLA a minimum sampling frequency of 1000 Hz was required. It was shown that at a sampling frequency of 1000 Hz, GLA can be achieved when using EFSVF. Substantial reductions in the RMS values were seen to result. An RMS reduction of 58% was achieved. Although this value was somewhat lower when compared to FSVF control Law A (63% reduction was achieved), nevertheless was above the required value of 30% at wing station 1. Finally, it was indicated that a single chip microcontroller which essentially encompasses the three basic elements i.e, an ADC , microprocessor and an DAC could be used to synthesise the EFSVF control system for load alleviation. However much work still needs to be done as far as practical implementation is concerned.

7.2 Recommendations

1. For the purposes of structural load alleviation, there remains a clear need for designing feedback controllers using the eigenpair assignment method described in chapter 3, for flight conditions other than investigated in this work. Furthermore, the theoretical results should be verified by the practical implementation of the proposed reduced order feedback laws, such as law Gamma on the aircraft or, at second best, a flight simulator.

2. In this study (the only model available to the author) only the longitudinal dynamics were considered[§]. However, there is a need to demonstrate the effectiveness of the EPAM on a model which incorporates, the longitudinal and lateral dynamics of both the rigid-body and the structural modes of the wing and fuselage (only the fundamental flexural modes need be considered).

---

§ It is the most comprehensive model available. No other models could be obtained, relating to flight conditions other than investigated in this work, in spite of exhaustive searching.

3. For the purposes of SLA, in the specification of the eigenstructure (which resulted in the reduction of structural loads) no attempt was made to alter the frequencies of the six flexural modes. The effect of changing the frequencies by feedback is the same as having a wing of higher stiffness. The effect of altering the frequencies of the flexural modes must be investigated. But note that some preliminary consideration of the problem is discussed in chapter 6 in relation to the robustness properties of the reduced order feedback controllers.

4. An attempt should also be made to synthesise a reduced order observer by using the EPAM (in a full order observer not only the unavailable state variables are estimated the available state variables are estimated as well, whereas in a reduced order observer only the unavailable state variables are reconstructed and are fed back alongwith the available state variables). The advantage of synthesising such reduced order observers, would be to reduce the computational burden.

5. To demonstrate SLA only state variable feedback was considered in this thesis. However, SLA using output feedback has been demonstrated in this thesis indirectly by the studies connected with reduced order feedback, which may be regarded as an form of output feedback. From the benificial results obtained with this technique it is worth proposing that an investigation into SLA on the complete mathematical description using output feedback directly should be undertaken. Algorithms which assign the complete eigenstructure by using output feedback, such as, proposed by Srinathkumar [1978] or Porter and Bradshaw [1978] may be used. Alternatively the proposed EPAM could be appropriately modified to realise control laws using output feedback.

6. The effectiveness of the estimated full state variable feedback (EFSVF) control system should be verified, on a flight simulator, using the INTEL 8097 microcontroller, in relation to various sampling frequencies.

REFERENCES

Alkhatib K. Y.

Analytical redundancy scheme for improving reliability of automatic flight control systems for aircraft.

Ph. D Thesis, 1985, Loughborough University, U.K.

Anon

Giants of Georgia

Air International,1984, vol 26, 61-68 & 87-90.

Andry A. N., Shapiro, E. Y., Chung J. C.

Eigenstructure for linear systems

Trans. IEEE, 1983, AES-19(5), 711-729.

Applevich J. D.

Direct computation of canonical forms for linear systems by elementary matrix computation.

Trans. IEEE, 1974, AC-19, 124-126.

Athans M., Falb P. L.

OPTIMAL CONTROL THEORY

McGraw-Hill Book Co., 1966, New York, USA.

Bisplinghoff R. L., Ashley H., Halfman R., L.

PRINCIPLES OF AEROELASTICITY

John Wiley and Sons, 1962, Cambridge, Mass.

Brasch F. M., Pearson J. B.

Pole placement using dynamic compensators.

Trans. IEEE, 1970, AC-15(1), 31-43.

Broussard J. R. Berry P. W.

The relationship between implicit model following and eigenvalue eigenvector placement.

Trans. IEEE, 1980, AC-25, 591-594.

Burris P. M., Bender M. A.

Aircraft load alleviation and mode stabilisation (LAMS).

AFFDL TR-68-161, Nov 1969, WPAFB, Ohio, USA.

Businger P. A., Golub G. H.

Singular value decomposition of a complex matrix.

Comm. ACM, 1969, 12(10), 564-565.

Chalk C. R., Neal T. P., et al

Background information and user guide for Mil-F-8785B(ASG), "Military specifications-flying qualities of piloted airplanes".

AFFDL TR-69-72, 1969, WPAFB, Ohio, USA.

Chang S. S. L.

SYNTHESIS OF OPTIMAL CONTROL

McGraw-Hill Book Co., 1969, New York, USA.

Davison E. J.

On pole assignment in linear systems with incomplete state feedback.

Trans. IEEE, AC-15, June 1970, 348-351.

Dayavansa W. P. M. P., Mukundan R.

Eigenvector structure and dominant eigenvalue/eigenvector placement in linear time-invariant systems using state feedback.

Conf. Procc. 16th Ann. Info. Sciences & Systems,1982, Princeton, 475-479, USA.

Erkelens L. J. J., Schuring J.

Investigation on a passenger ride comfort improvement system with limited control surface actuator performance for a flexible aircraft.

NLR TR-75140 U, Dec 1975, Netherlands.

Fahmy M. M., Tantawy H. S

Eigenstructure assignment via state-feedback control.

Int. Journal of Control, 1984, 40(1), 161-178.

Fahmy M. M., O'Reilly J.

On eigenstructure assignment in linear multivariable systems.

Trans. IEEE, 1982, AC-27(3), 690-693.

Gould J. D.

Effect of active control system control non-linearities on the L-1011-3(ACS) design gust loads.

AIAA paper 85-0755, conf. proc. 26th Structures, Structural dynamics and Materials Conference, 1985, Orlando, USA.

Harvey C. A, Pope R. E.

Study of synthesis techniques for insensitive aircraft control systems.

NASA CR-2803, April 1977, Honeywell Inc. Systems Research Center, Minneapolis, Minnesota, USA.

Holloway R. B.

Introduction of CCV technology into airplane design.

AGARD, Oct 1973.

Jordan D., Sridhar B.

An efficient algorithm for calculation of the Luenberger canonical form.

Trans. IEEE, 1973, AC-18, 292-295.

Kelma V. C., Laub A. J.

The singular value decomposition: Its computation and some applications.

Trans. IEEE, 1980, AC-25(2),164-176.

Klein G., Moore B.C.

Eigenvalue-Generalised eigenvector assignment with state feedback.

Trans. IEEE , 1977, AC-22, 140-141.

Konar A. F., Stone C. R., Mahesh J. K.

Active control synthesis for flexible aircraft

AFFDL-TR-75-146, 1976, Vol-1 & Vol-2, WPAFB, Ohio.

Lehtomaki N. A., Sandell N. S., Athans M.

Robustness results in linear quadratic gaussian based multivariable control designs.

Trans. IEEE, 1981, AC-26, Feb 1981, 75-92.

Luenberger D. G.

Canonical forms for linear multivariable systems.

Trans. IEEE, 1967, AC-12, 290-293.

Luenberger D. G.

Observers for multivariable systems

Trans. IEEE, 1966, AC-11, 90-197.

Luenberger D. G.

Introduction to observers

Trans. IEEE, 1971, AC-16(6), 596-602.

Marshal S. A., Nicholson H.

Optimal control of linear multivariable systems with quadratic performance criteria.

Procc. IEEE, 1970, 117(8), 1705-1713.

Maxwell E. A.

ALGEBRAIC STRUCTURE AND MATRICES

Cambridge University Press, 1965, Cambridge, U.K.

McRuer D., Ashkenas I., Graham D.

AIRCRAFT DYNAMICS AND AUTOMATIC CONTROL

Princeton University Press,1973, Princeton, N. J., USA.

McLean D.

Gust load alleviation systems: A feasibility study.

Report TT7606, 1976, Loughborough University, U.K.

McLean D., Prasad R.A.

A structural load alleviation control system for a large transport aircraft.

Report TT8002, 1980, Loughborough University U.K.

Mendel J. M., Giesking D. L.

Bibliography on the Linear-Quadratic-Gaussian Problem.

Trans. IEEE, 1971, 16(6), 847-869.

Moore B. C.

On the flexibility offered by state feedback in multivariable systems beyond closed-loop eigenvalue assignment.

Trans. IEEE, 1976, AC-21, 689-692.

Mielke R. R., Tung L. J.

Design of multivariable feedback control systems via spectral assignment using reduced order models and reduced order observers.

NASA CR-3889, 1985, Washington D. C., USA.

Milne R. D.

Dynamics of the deformable aircraft.

Aeronautical Research Council, 1964, R&M3345.

Mukhopadhyay V., Newsom J. R.

A multiloop system stability margin study using matrix singular values.

Journal of Guidance Control and Dynamics, 1984, Vol. 7, No. 5, 582-587.

Newberry C. F.

Considerations of stability augmentation systems for large elastic aircraft.

AGARD CP-46, 1969.

Noble B., Daniel J. W.

APPLIED LINEAR ALGEBRA

Prentice Hall, Second Edition, 1977, Englewood Cliffs, N.J., USA.

Oehman I. W.

Analytical Study of the performance of a gust alleviation system for a STOL airplane.

NASA TN D-7201, April 1973, Washington D.C., USA.

Owens T. M., Mielke R. R.

A new gain modification algorithm for spectral assignment.

Proc. IEEE, South Eastern Symposium on Systems Theory, 1982, Vol 14, 51-55.

Porter B., Bradshaw A.

Design of linear multivariable continuous-time output-feedback regulators.

Int. Journal of System Science, 1978, Vol 9, 445-450.

Porter B., Carter J. D.

Design of multi-loop modal control systems for plants having complex eigenvalues.

Trans. Inst. M. C., Vol 1, March 1968, T61-T68.

Porter B., Crossley R.
MODAL CONTROL
Taylor & Francis Limited, 1972

Porter B., D'Azzo J. J [1]
Closed Loop eigenstructure assignment by state feedback in multivariable linear systems.
Int. Journal of Control, 1978, 27(6), 487-492.

Porter B., D'Azzo J.J [2]
Algorithm for closed loop eigenstructure assignment by state feedback in multivariable linear systems.
Int. Journal of Control, 1978, 27(6), 943-947.

Prasad R.A.
Application of optimal control to structural load alleviation control systems.
Ph.D Thesis, 1980, Loughborough University U.K.

Schwanz R. C.
Formulations of the equations of motion of an aeroelastic aircraft.
AFFDL FGC-TM-72-14, Aug 1972, WPAFB, Ohio, USA.

Schwanz R. C., Wells W. R.
Estimation of Elastic aerodynamic parameters.
AGARD CP-172, 1974.

Shapiro E. Y., Chung J. C.
Flight control system synthesis using eigenstructure assignment.
JOTA, 1984, 43(3), 415-429.

Simon J. D., Mitter S. K.
A theory of modal control.
Information and Control, 1968, Vol 13, 316-353.

Sorenson J. A.
Analysis of instrumentation error effects on the identification accuracy of aircraft parameters.
NASA CR-112121, 1972.

Soroka E., Shaked U.

The Eigenstructure of linear high gain systems.

Conf. Procc. American Control Conf., Vol 3, June 1982, 929-933.

Srinathkumar S.

Eigenvalue/Eigenvector assignment using output feedback.

NASA Technical Paper 1118, Feb 1978.

Srinathkumar S.

Eigenvalue/Eigenvector assignment using output feedback.

Trans. IEEE, AC-23, Feb 1978, 79-81.

Stepner D. E., Mehra R. K.

Maximum likelihood identification and optimal input design for identifying aircraft stability and control derivatives.

NASA CR-2200, March 1973.

Stone C.R., Ward M. D., Harvey C. A., et al

Studies of the compatibility of relaxed static stability and manoeuvre load control to C5-A type aircraft.

AFFDL TR-72-38, June 1972, Vol 2, WPAFB, Ohio, USA.

Taylor A. S.

Mathematical approaches to the dynamics of the deformable aircraft.

Aeronautical Research Council,June 1971, R&M3776 (part 1)

Truxal J. G.

AUTOMATIC FEEDBACK CONTROL SYSTEM SYNTHESIS

McGraw-Hill Book Co., 1955, New York, USA.

Wall H. S.

CONTINUED FRACTIONS

D. Van Nostrand Book Co., 1948, New York, USA.

Woodcock D. L

Mathematical approaches to the dynamics of the deformable aircraft.

Aeronautical Research Council, June 1971, R&M3776 (part 2).

Wonham W. M.

On pole assignment in multi-input controllable linear systems.

Trans. IEEE, AC-12(6), Dec 1967, 660-665.

Wonham W. M., Morse A. S.

Feedback invariants of multivariable systems.

Automatica, 1972, Vol 8, 1-18

APPENDIX A

L-1011 TRISTAR MODEL DATA

Coefficient matrices A, B, C, D for the L-1011 Tristar model are presented below, for cruise flight condition, U_0=834.0 ft/sec.

$$A = \begin{bmatrix} -20.0 & 0.0 & 0.0 & 0.0 & 0.0 & 0.0 & 0.0 \\ 0.0 & -25.0 & 0.0 & 0.0 & 0.0 & 0.0 & 0.0 \\ 0.0 & 0.0 & 0.0 & 0.0 & 1.0 & 0.0 & 0.0 \\ -0.744 & -0.032 & 0.0 & -0.154 & -0.0042 & 1.54 & 0.0 \\ 0.337 & -1.12 & 0.0 & 0.249 & -1.0 & -5.2 & 0.0 \\ 0.02 & 0.0 & 0.0386 & -0.996 & -0.0003 & -0.117 & 0.0 \\ 0.0 & 0.0 & 0.0 & 0.5 & 0.0 & 0.0 & -0.5 \end{bmatrix}$$

$$B = \begin{bmatrix} 20.0 & 0.0 \\ 0.0 & 25.0 \\ 0.0 & 0.0 \\ 0.0 & 0.0 \\ 0.0 & 0.0 \\ 0.0 & 0.0 \\ 0.0 & 0.0 \end{bmatrix}$$

$$C = \begin{bmatrix} 0.0 & 0.0 & 0.0 & 1.0 & 0.0 & 0.0 & -1.0 \\ 0.0 & 0.0 & 0.0 & 0.0 & 1.0 & 0.0 & 0.0 \\ 0.0 & 0.0 & 0.0 & 0.0 & 0.0 & 1.0 & 0.0 \\ 0.0 & 0.0 & 1.0 & 0.0 & 0.0 & 0.0 & 0.0 \\ 16.68 & 0.0 & 0.0 & 3.4 & -0.246 & -97.57 & 0.0 \end{bmatrix}$$

$$D = \begin{bmatrix} 0.0 & 0.0 \\ 0.0 & 0.0 \\ 0.0 & 0.0 \\ 0.0 & 0.0 \\ 0.0 & 0.0 \end{bmatrix}$$

APPENDIX B

C-5A GALAXY MODEL DATA

Coefficient Matrix A

	1	2	3	4	5	6	7	8
1	-0.68156D+00	0.32791D+01	-0.35615D-01	-0.71438D-02	-0.24133D-01	0.21332D-01	-0.24404D-01	0.47797D-01
2	-0.55140D+00	-0.11746D+01	0.39579D-01	-0.44709D-01	-0.32990D+00	-0.32436D+00	-0.11995D+00	0.25113D+00
3	-0.14863D+01	0.10534D+00	-0.98741D+00	-0.24874D-01	-0.14662D+00	0.51128D+00	0.17325D-01	-0.25652D+00
4	0.45522D-01	-0.88309D-01	0.14416D-01	-0.46574D+00	-0.67265D-01	-0.58908D-01	-0.76114D-02	-0.30630D-02
5	0.51060D-01	-0.85213D+00	0.51344D-01	-0.72981D-01	-0.12857D+01	-0.40920D+00	-0.34829D-01	-0.61413D-01
6	-0.11068D+01	-0.98721D+00	0.75927D-01	-0.39164D-01	-0.27445D+00	-0.10894D+01	-0.17062D+00	0.43783D+00
7	-0.20164D+00	-0.23495D+00	0.60625D-01	-0.21022D-01	0.48689D-01	-0.10753D+00	-0.86125D+00	0.12357D+00
8	0.46358D+00	0.42046D+00	-0.10741D+00	0.18093D-01	0.35634D-01	0.18446D+00	0.99742D-01	-0.11481D+01
9	0.00000D+00	0.00000D+00	0.10000D+01	0.00000D+00	0.00000D+00	0.00000D+00	0.00000D+00	0.00000D+00
10	0.00000D+00	0.00000D+00	0.00000D+00	0.10000D+01	0.00000D+00	0.00000D+00	0.00000D+00	0.00000D+00
11	0.00000D+00	0.00000D+00	0.00000D+00	0.00000D+00	0.10000D+01	0.00000D+00	0.00000D+00	0.00000D+00
12	0.00000D+00	0.00000D+00	0.00000D+00	0.00000D+00	0.00000D+00	0.10000D+01	0.00000D+00	0.00000D+00
13	0.00000D+00	0.00000D+00	0.00000D+00	0.00000D+00	0.00000D+00	0.00000D+00	0.10000D+01	0.00000D+00
14	0.00000D+00	0.00000D+00	0.00000D+00	0.00000D+00	0.00000D+00	0.00000D+00	0.00000D+00	0.10000D+01
15	0.00000D+00	0.00000D+00	0.00000D+00	0.00000D+00	0.00000D+00	0.00000D+00	0.00000D+00	0.00000D+00
16	0.00000D+00	0.00000D+00	0.00000D+00	0.00000D+00	0.00000D+00	0.00000D+00	0.00000D+00	0.00000D+00
17	0.00000D+00	0.00000D+00	0.00000D+00	0.00000D+00	0.00000D+00	0.00000D+00	0.00000D+00	0.00000D+00
18	0.00000D+00	0.00000D+00	0.00000D+00	0.00000D+00	0.00000D+00	0.00000D+00	0.00000D+00	0.00000D+00
19	0.00000D+00	0.00000D+00	0.00000D+00	0.00000D+00	0.00000D+00	0.00000D+00	0.00000D+00	0.00000D+00
20	0.00000D+00	0.00000D+00	0.00000D+00	0.00000D+00	0.00000D+00	0.00000D+00	0.00000D+00	0.00000D+00
21	0.00000D+00	0.00000D+00	0.00000D+00	0.00000D+00	0.00000D+00	0.00000D+00	0.00000D+00	0.00000D+00
22	0.00000D+00	0.00000D+00	0.00000D+00	0.00000D+00	0.00000D+00	0.00000D+00	0.00000D+00	0.00000D+00
23	0.00000D+00	0.00000D+00	0.00000D+00	0.00000D+00	0.00000D+00	0.00000D+00	0.00000D+00	0.00000D+00
24	0.00000D+00	0.00000D+00	0.00000D+00	0.00000D+00	0.00000D+00	0.00000D+00	0.00000D+00	0.00000D+00

Note : The data presented in this appendix is the computer representation of real numbers.

For example the number -0.35615D-01 (row 1, column 3) represents the number -0.035615.

	9	10	11	12	13	14	15	16
1	-0.63975D+00	-0.65316D+00	-0.17082D+01	0.44958D+01	-0.13601D+01	0.18468D+01	-0.23106D+03	-0.19002D+03
2	-0.10850D+00	-0.16757D+01	-0.10304D+02	-0.57006D+01	-0.49434D+01	0.91053D+01	-0.57617D+03	-0.25322D+04
3	-0.29851D+02	-0.40858D+01	-0.16621D+02	0.40631D+02	-0.58418D+01	-0.66903D+01	-0.33801D+04	0.14194D+04
4	0.26632D+00	-0.12384D+03	-0.86920D+00	-0.15823D+01	-0.15692D+00	0.15112D+01	-0.13323D+03	-0.29227D+03
5	0.13958D+01	-0.64745D+00	-0.19318D+03	-0.15404D+02	-0.97897D+00	-0.31528D+01	-0.14152D+04	-0.25753D+04
6	-0.19816D+00	-0.67868D+00	-0.93687D+01	-0.24252D+03	-0.71834D+01	0.17025D+02	0.80354D+03	-0.25292D+04
7	0.23384D+00	-0.74504D+00	-0.12963D+01	-0.32269D+01	-0.30625D+03	0.60832D+01	-0.13080D+02	-0.65296D+03
8	-0.11571D+00	0.20064D+01	0.14987D+01	0.45063D+01	0.47710D+01	-0.35230D+03	-0.41074D+03	0.11165D+04
9	0.00000D+00	0.00000D+00	0.00000D+00	0.00000D+00	0.00000D+00	0.00000D+00	0.00000D+00	0.00000D+00
10	0.00000D+00	0.00000D+00	0.00000D+00	0.00000D+00	0.00000D+00	0.00000D+00	0.00000D+00	0.00000D+00
11	0.00000D+00	0.00000D+00	0.00000D+00	0.00000D+00	0.00000D+00	0.00000D+00	0.00000D+00	0.00000D+00
12	0.00000D+00	0.00000D+00	0.00000D+00	0.00000D+00	0.00000D+00	0.00000D+00	0.00000D+00	0.00000D+00
13	0.00000D+00	0.00000D+00	0.00000D+00	0.00000D+00	0.00000D+00	0.00000D+00	0.00000D+00	0.00000D+00
14	0.00000D+00	0.00000D+00	0.00000D+00	0.00000D+00	0.00000D+00	0.00000D+00	0.00000D+00	0.00000D+00
15	0.00000D+00	0.00000D+00	0.00000D+00	0.00000D+00	0.00000D+00	0.00000D+00	-0.60000D+01	0.00000D+00
16	0.00000D+00	0.00000D+00	0.00000D+00	0.00000D+00	0.00000D+00	0.00000D+00	0.00000D+00	-0.75000D+01
17	0.00000D+00	0.00000D+00	0.00000D+00	0.00000D+00	0.00000D+00	0.00000D+00	0.00000D+00	0.00000D+00
18	0.00000D+00	0.00000D+00	0.00000D+00	0.00000D+00	0.00000D+00	0.00000D+00	0.00000D+00	0.00000D+00
19	0.00000D+00	0.00000D+00	0.00000D+00	0.00000D+00	0.00000D+00	0.00000D+00	0.00000D+00	0.00000D+00
20	0.00000D+00	0.00000D+00	0.00000D+00	0.00000D+00	0.00000D+00	0.00000D+00	0.00000D+00	0.00000D+00
21	0.00000D+00	0.00000D+00	0.00000D+00	0.00000D+00	0.00000D+00	0.00000D+00	0.00000D+00	0.00000D+00
22	0.00000D+00	0.00000D+00	0.00000D+00	0.00000D+00	0.00000D+00	0.00000D+00	0.00000D+00	0.00000D+00
23	0.00000D+00	0.00000D+00	0.00000D+00	0.00000D+00	0.00000D+00	0.00000D+00	0.00000D+00	0.00000D+00
24	0.00000D+00	0.00000D+00	0.00000D+00	0.00000D+00	0.00000D+00	0.00000D+00	0.00000D+00	0.00000D+00

	17	18	19	20	21	22	23	24
1	-0.30147D+02	-0.48273D+00	-0.70523D+01	-0.91890D+00	0.00000D+00	0.00000D+00	0.00000D+00	0.00000D+00
2	-0.44466D+03	0.27053D+01	-0.10493D+01	-0.11854D+02	0.00000D+00	0.00000D+00	0.00000D+00	0.00000D+00
3	0.25982D+03	0.62979D+00	-0.23132D+02	0.66833D+01	0.00000D+00	0.00000D+00	0.00000D+00	0.00000D+00
4	-0.63867D+02	-0.21372D+00	0.16827D+01	-0.13256D+01	0.00000D+00	0.00000D+00	0.00000D+00	0.00000D+00
5	-0.58207D+03	-0.23009D+01	0.11163D+02	-0.11851D+02	0.00000D+00	0.00000D+00	0.00000D+00	0.00000D+00
6	-0.62504D+03	-0.10079D+01	-0.42601D+01	-0.11528D+02	0.00000D+00	0.00000D+00	0.00000D+00	0.00000D+00
7	-0.17943D+03	-0.32804D+00	-0.42523D-01	-0.29517D+01	0.00000D+00	0.00000D+00	0.00000D+00	0.00000D+00
8	0.32318D+03	0.43848D+00	0.16346D+01	0.50304D+01	0.00000D+00	0.00000D+00	0.00000D+00	0.00000D+00
9	0.00000D+00	0.00000D+00	0.00000D+00	0.00000D+00	0.00000D+00	0.00000D+00	0.00000D+00	0.00000D+00
10	0.00000D+00	0.00000D+00	0.00000D+00	0.00000D+00	0.00000D+00	0.00000D+00	0.00000D+00	0.00000D+00
11	0.00000D+00	0.00000D+00	0.00000D+00	0.00000D+00	0.00000D+00	0.00000D+00	0.00000D+00	0.00000D+00
12	0.00000D+00	0.00000D+00	0.00000D+00	0.00000D+00	0.00000D+00	0.00000D+00	0.00000D+00	0.00000D+00
13	0.00000D+00	0.00000D+00	0.00000D+00	0.00000D+00	0.00000D+00	0.00000D+00	0.00000D+00	0.00000D+00
14	0.00000D+00	0.00000D+00	0.00000D+00	0.00000D+00	0.00000D+00	0.00000D+00	0.00000D+00	0.00000D+00
15	0.00000D+00	0.00000D+00	0.00000D+00	0.00000D+00	0.00000D+00	0.00000D+00	0.00000D+00	0.00000D+00
16	0.00000D+00	0.00000D+00	0.00000D+00	0.00000D+00	0.00000D+00	0.00000D+00	0.00000D+00	0.00000D+00
17	-0.75100D+01	0.00000D+00	0.00000D+00	0.00000D+00	0.00000D+00	0.00000D+00	0.00000D+00	0.00000D+00
18	0.00000D+00	-0.22185D+02	0.00000D+00	0.00000D+00	0.00000D+00	0.00000D+00	0.00000D+00	0.00000D+00
19	0.00000D+00	0.00000D+00	-0.85492D+01	0.00000D+00	0.00000D+00	0.00000D+00	0.00000D+00	0.22185D+02
20	0.00000D+00	-0.50960D+01	0.00000D+00	0.00000D+00	0.10000D+01	0.85492D+01	0.00000D+00	0.00000D+00
21	0.00000D+00	0.90891D+02	0.00000D+00	-0.38953D+02	-0.10192D+02	0.00000D+00	0.00000D+00	0.00000D+00
22	0.00000D+00	0.00000D+00	0.00000D+00	0.00000D+00	0.00000D+00	-0.10983D+02	0.00000D+00	0.10983D+02
23	0.00000D+00	0.00000D+00	0.00000D+00	0.00000D+00	0.00000D+00	0.00000D+00	-0.49524D+00	-0.61315D-01
24	0.00000D+00	0.00000D+00	0.00000D+00	0.00000D+00	0.00000D+00	0.00000D+00	0.10000D+01	0.00000D+00

***** ***** ***** *****

Output Matrix C

	1	2	3	4	5	6	7	8
1	-0.11400D+05	-0.21000D+04	0.11900D+05	-0.11200D+04	-0.10500D+05	0.59600D+04	0.37800D+04	-0.96000D+04
2	-0.16800D+05	-0.17600D+04	-0.13700D+04	-0.10200D+04	-0.17100D+04	0.62100D+04	-0.89423D+03	-0.30200D+04
3	0.21600D+04	0.94467D+03	0.87700D+04	-0.40629D+03	-0.43700D+04	0.40200D+04	0.26300D+04	-0.52800D+04
4	-0.86900D+04	-0.12300D+04	-0.17300D+04	-0.10700D+04	-0.20400D+04	0.54800D+04	-0.10400D+04	0.32600D+04
5	0.32500D+04	0.86850D+03	0.54000D+04	0.57900D+02	0.10600D+04	0.90920D+03	-0.10300D+04	-0.75760D+03
6	-0.45700D+04	-0.45730D+03	-0.19300D+04	-0.10400D+04	-0.17400D+04	0.39800D+04	-0.16400D+04	0.87790D+03
7	-0.20200D+04	-0.36970D+03	0.28400D+04	0.17200D+03	0.30200D+04	-0.10700D+04	-0.14640D+03	-0.19400D+04
8	-0.63700D+04	-0.11000D+04	-0.17900D+04	-0.21580D+03	-0.65703D+03	0.13200D+04	-0.34020D+03	0.21615D+03
9	-0.17600D+04	-0.51300D+03	0.13600D+04	0.99600D+02	0.20200D+04	-0.77770D+03	-0.33910D+03	0.21100D+04
10	-0.36400D+04	-0.70180D+03	-0.13300D+04	-0.15380D+03	-0.82030D+03	0.85790D+03	-0.67800D+02	-0.42360D+03
11	0.18100D+06	0.44700D+06	0.12400D+07	-0.25900D+06	-0.32200D+07	0.20400D+07	0.17300D+07	-0.45100D+07
12	0.35400D+04	-0.80794D+03	-0.52000D+05	-0.24600D+06	-0.52100D+06	0.15200D+07	-0.38700D+06	0.15800D+07
13	0.10600D+06	0.27300D+06	0.98200D+06	-0.99500D+05	-0.13900D+07	0.15000D+07	0.11700D+07	-0.25400D+07
14	0.58500D+03	0.81100D+04	-0.55400D+05	-0.25200D+06	-0.55600D+06	0.15000D+07	-0.37400D+06	0.15100D+07
15	0.50200D+05	0.13000D+06	0.63800D+06	0.18700D+05	0.39900D+06	0.34800D+06	-0.42500D+06	-0.35500D+06
16	-0.44200D+04	-0.48800D+04	-0.52400D+05	-0.24700D+06	-0.40400D+06	0.10700D+07	-0.64000D+06	0.55200D+06
17	0.26800D+05	0.59000D+05	0.38400D+06	0.53100D+05	0.10600D+07	-0.51500D+06	-0.39800D+05	0.86100D+06
18	-0.26000D+03	-0.12400D+04	-0.77000D+04	-0.27000D+05	-0.45400D+05	0.14900D+06	-0.55300D+05	0.57300D+05
19	0.11000D+05	0.25000D+05	0.18200D+06	0.38200D+05	0.79200D+06	-0.39800D+06	-0.14200D+06	0.11000D+07
20	-0.27780D+03	-0.19670D+03	-0.74700D+04	-0.16600D+05	-0.45000D+05	0.79400D+05	-0.15800D+05	-0.24900D+05
21	0.00000D+00	0.00000D+00	0.10000D+01	0.00000D+00	0.00000D+00	0.00000D+00	0.00000D+00	0.00000D+00
22	0.00000D+00	0.00000D+00	0.00000D+00	0.10000D+01	0.00000D+00	0.00000D+00	0.00000D+00	0.00000D+00
23	0.00000D+00	0.00000D+00	0.00000D+00	0.00000D+00	0.10000D+01	0.00000D+00	0.00000D+00	0.00000D+00
24	0.00000D+00	0.00000D+00	0.00000D+00	0.00000D+00	0.00000D+00	0.10000D+01	0.00000D+00	0.00000D+00
25	0.00000D+00	0.00000D+00	0.00000D+00	0.00000D+00	0.00000D+00	0.00000D+00	0.10000D+01	0.00000D+00
26	0.00000D+00	0.00000D+00	0.00000D+00	0.00000D+00	0.00000D+00	0.00000D+00	0.00000D+00	0.10000D+01
27	0.00000D+00	0.00000D+00	0.00000D+00	0.00000D+00	0.00000D+00	0.00000D+00	0.00000D+00	0.00000D+00
28	0.00000D+00	0.00000D+00	0.00000D+00	0.00000D+00	0.00000D+00	0.00000D+00	0.00000D+00	0.00000D+00
29	0.00000D+00	0.00000D+00	0.00000D+00	0.00000D+00	0.00000D+00	0.00000D+00	0.00000D+00	0.00000D+00
30	0.00000D+00	0.00000D+00	0.00000D+00	0.00000D+00	0.00000D+00	0.00000D+00	0.00000D+00	0.00000D+00
31	0.00000D+00	0.00000D+00	0.00000D+00	0.00000D+00	0.00000D+00	0.00000D+00	0.00000D+00	0.00000D+00
32	0.00000D+00	0.00000D+00	0.00000D+00	0.00000D+00	0.00000D+00	0.00000D+00	0.00000D+00	0.00000D+00
33	0.00000D+00	0.00000D+00	0.00000D+00	0.00000D+00	0.00000D+00	0.00000D+00	0.00000D+00	0.00000D+00
34	0.00000D+00	0.00000D+00	0.00000D+00	0.00000D+00	0.00000D+00	0.00000D+00	0.00000D+00	0.00000D+00
35	0.00000D+00	0.00000D+00	0.00000D+00	0.00000D+00	0.00000D+00	0.00000D+00	0.00000D+00	0.00000D+00
36	0.00000D+00	0.00000D+00	0.00000D+00	0.00000D+00	0.00000D+00	0.00000D+00	0.00000D+00	0.00000D+00
37	0.10000D+01	0.00000D+00	0.00000D+00	0.00000D+00	0.00000D+00	0.00000D+00	0.00000D+00	0.00000D+00
38	0.00000D+00	0.10000D+01	0.00000D+00	0.00000D+00	0.00000D+00	0.00000D+00	0.00000D+00	0.00000D+00

	9	10	11	12	13	14	15	16
1	0.12700D+07	-0.27400D+06	-0.33500D+07	0.19600D+07	0.16500D+07	-0.43300D+07	-0.49200D+07	-0.42700D+07
2	-0.79600D+05	-0.27000D+06	-0.57000D+06	0.16300D+07	-0.40200D+06	0.15600D+07	0.35500D+05	0.23200D+06
3	0.10000D+07	-0.10400D+06	-0.14700D+07	0.14400D+07	0.11400D+07	-0.24600D+07	-0.98600D+06	0.15600D+07
4	-0.78100D+05	-0.27600D+06	-0.60700D+06	0.16000D+07	-0.38800D+06	0.15000D+07	0.73200D+05	0.49600D+06
5	0.64700D+06	0.17200D+05	0.35800D+06	0.32100D+06	-0.43600D+06	-0.33200D+06	0.16200D+07	0.16400D+07
6	-0.70600D+05	-0.26400D+06	-0.45100D+06	0.11600D+07	-0.64800D+06	0.52400D+06	0.18500D+07	0.15500D+07
7	0.38400D+06	0.46900D+05	0.10300D+07	-0.50900D+06	-0.49700D+05	0.86200D+06	0.54200D+06	0.14600D+06
8	-0.26400D+05	-0.41200D+05	-0.98000D+05	0.25300D+06	-0.74300D+05	0.49800D+05	0.54100D+07	0.46600D+06
9	0.18100D+06	0.32700D+05	0.78200D+06	-0.39300D+06	-0.15000D+06	0.11100D+07	-0.78100D+06	-0.63200D+06
10	-0.17700D+05	-0.25000D+05	-0.77500D+05	0.14500D+06	-0.28100D+05	-0.30100D+05	0.53100D+07	0.29400D+06
11	-0.31200D+06	0.70600D+06	0.56800D+07	0.13900D+07	0.57200D+06	-0.13000D+06	0.20800D+09	0.97900D+09
12	-0.12400D+05	0.13600D+06	0.26200D+06	-0.10500D+07	0.26800D+06	-0.12400D+07	0.15400D+08	0.21800D+08
13	-0.23700D+06	0.39100D+06	0.30700D+07	0.71000D+06	0.24700D+06	-0.19700D+06	0.11600D+09	0.59000D+09
14	-0.20600D+04	0.13600D+06	0.30200D+06	-0.90600D+06	0.29850D+06	-0.12900D+07	0.12800D+08	0.14100D+08
15	-0.15300D+06	0.15500D+06	0.85700D+06	0.60000D+06	0.81100D+06	-0.70500D+06	0.43500D+08	0.28000D+09
16	0.43500D+04	0.11100D+06	0.13200D+06	-0.68400D+06	0.45900D+06	-0.46000D+06	0.42400D+07	-0.13100D+08
17	-0.87700D+05	0.56200D+05	-0.10800D+06	0.71700D+06	0.31100D+06	-0.12600D+07	0.12800D+08	0.13400D+09
18	0.36800D+04	0.12300D+05	-0.14200D+05	-0.89100D+05	0.60400D+05	-0.14700D+06	0.97700D+06	-0.21900D+07
19	-0.44400D+05	0.13200D+05	-0.25400D+06	0.42600D+06	0.20400D+06	-0.10500D+07	0.14700D+07	0.53100D+08
20	0.77000D+04	0.10100D+05	0.75100D+05	-0.70400D+05	-0.79000D+04	0.11600D+06	-0.28700D+07	-0.12200D+07
21	0.00000D+00	0.00000D+00	0.00000D+00	0.00000D+00	0.00000D+00	0.00000D+00	0.00000D+00	0.00000D+00
22	0.00000D+00	0.00000D+00	0.00000D+00	0.00000D+00	0.00000D+00	0.00000D+00	0.00000D+00	0.00000D+00
23	0.00000D+00	0.00000D+00	0.00000D+00	0.00000D+00	0.00000D+00	0.00000D+00	0.00000D+00	0.00000D+00
24	0.00000D+00	0.00000D+00	0.00000D+00	0.00000D+00	0.00000D+00	0.00000D+00	0.00000D+00	0.00000D+00
25	0.00000D+00	0.00000D+00	0.00000D+00	0.00000D+00	0.00000D+00	0.00000D+00	0.00000D+00	0.00000D+00
26	0.00000D+00	0.00000D+00	0.00000D+00	0.00000D+00	0.00000D+00	0.00000D+00	0.00000D+00	0.00000D+00
27	0.10000D+01	0.00000D+00	0.00000D+00	0.00000D+00	0.00000D+00	0.00000D+00	0.00000D+00	0.00000D+00
28	0.00000D+00	0.10000D+01	0.00000D+00	0.00000D+00	0.00000D+00	0.00000D+00	0.00000D+00	0.00000D+00
29	0.00000D+00	0.00000D+00	0.10000D+01	0.00000D+00	0.00000D+00	0.00000D+00	0.00000D+00	0.00000D+00
30	0.00000D+00	0.00000D+00	0.00000D+00	0.10000D+01	0.00000D+00	0.00000D+00	0.00000D+00	0.00000D+00
31	0.00000D+00	0.00000D+00	0.00000D+00	0.00000D+00	0.10000D+01	0.00000D+00	0.00000D+00	0.00000D+00
32	0.00000D+00	0.00000D+00	0.00000D+00	0.00000D+00	0.00000D+00	0.10000D+01	0.00000D+00	0.00000D+00
33	0.00000D+00	0.00000D+00	0.00000D+00	0.00000D+00	0.00000D+00	0.00000D+00	-0.60000D+01	0.00000D+00
34	0.00000D+00	0.00000D+00	0.00000D+00	0.00000D+00	0.00000D+00	0.00000D+00	0.00000D+00	-0.75000D+01
35	0.00000D+00	0.00000D+00	0.00000D+00	0.00000D+00	0.00000D+00	0.00000D+00	0.10000D+01	0.00000D+00
36	0.00000D+00	0.00000D+00	0.00000D+00	0.00000D+00	0.00000D+00	0.00000D+00	0.00000D+00	0.10000D+01
37	0.00000D+00	0.00000D+00	0.00000D+00	0.00000D+00	0.00000D+00	0.00000D+00	0.00000D+00	0.00000D+00
38	0.00000D+00	0.00000D+00	0.00000D+00	0.00000D+00	0.00000D+00	0.00000D+00	0.00000D+00	0.00000D+00

	17	18	19	20	21	22	23	24
1	-0.37200D+06	0.74600D+04	-0.13200D+06	-0.18300D+05	0.00000D+00	0.00000D+00	0.00000D+00	0.00000D+00
2	0.14200D+06	0.87800D+04	-0.21100D+06	0.11200D+04	0.00000D+00	0.00000D+00	0.00000D+00	0.00000D+00
3	0.10300D+07	-0.27900D+04	0.24000D+05	0.68300D+04	0.00000D+00	0.00000D+00	0.00000D+00	0.00000D+00
4	0.18600D+06	0.62900D+04	-0.11200D+06	0.22900D+04	0.00000D+00	0.00000D+00	0.00000D+00	0.00000D+00
5	0.60200D+06	-0.18100D+04	0.35900D+05	0.71000D+04	0.00000D+00	0.00000D+00	0.00000D+00	0.00000D+00
6	0.46500D+06	0.13900D+04	-0.61000D+05	0.69600D+04	0.00000D+00	0.00000D+00	0.00000D+00	0.00000D+00
7	-0.55700D+05	0.15100D+04	-0.26200D+05	0.63790D+03	0.00000D+00	0.00000D+00	0.00000D+00	0.00000D+00
8	0.15200D+06	0.52330D+03	-0.78300D+05	0.20500D+04	0.00000D+00	0.00000D+00	0.00000D+00	0.00000D+00
9	-0.32600D+06	0.19400D+04	-0.21200D+05	-0.27100D+04	0.00000D+00	0.00000D+00	0.00000D+00	0.00000D+00
10	0.10100D+06	0.17237D+03	-0.44800D+05	0.12900D+04	0.00000D+00	0.00000D+00	0.00000D+00	0.00000D+00
11	0.17300D+09	-0.10100D+07	0.44200D+06	0.45900D+07	-0.44300D+04	-0.46100D+06	0.00000D+00	0.23600D+05
12	0.37200D+07	-0.68800D+05	0.89400D+06	0.10300D+06	-0.47021D+03	-0.89800D+06	0.00000D+00	0.45400D+05
13	0.10300D+09	-0.62600D+06	-0.85000D+05	0.27600D+07	0.18400D+04	0.42500D+05	0.00000D+00	0.68541D+03
14	0.26100D+07	-0.22000D+05	0.82700D+05	0.67900D+05	0.48000D+03	-0.10700D+06	0.00000D+00	0.30800D+04
15	0.48400D+08	-0.30500D+06	-0.12300D+06	0.13100D+07	0.50000D+03	0.10700D+06	0.00000D+00	0.75900D+04
16	-0.24400D+07	0.16300D+05	-0.16300D+05	-0.60700D+05	0.31680D+03	-0.67800D+04	0.00000D+00	-0.55000D+04
17	0.23900D+08	-0.13200D+06	0.14200D+06	0.62700D+06	-0.15300D+04	-0.11500D+06	0.00000D+00	-0.34100D+04
18	-0.47800D+06	0.38600D+04	0.16800D+05	-0.10400D+05	0.39390D+03	-0.14400D+05	0.00000D+00	-0.41500D+04
19	0.96500D+07	-0.53700D+05	-0.41000D+05	0.24900D+06	-0.91780D+02	0.56700D+05	0.00000D+00	-0.28700D+04
20	-0.30300D+06	0.38800D+04	-0.24000D+05	-0.57900D+04	0.15900D+03	0.23400D+05	0.00000D+00	-0.34300D+04
21	0.00000D+00	0.00000D+00	0.00000D+00	0.00000D+00	0.00000D+00	0.00000D+00	0.00000D+00	0.00000D+00
22	0.00000D+00	0.00000D+00	0.00000D+00	0.00000D+00	0.00000D+00	0.00000D+00	0.00000D+00	0.00000D+00
23	0.00000D+00	0.00000D+00	0.00000D+00	0.00000D+00	0.00000D+00	0.00000D+00	0.00000D+00	0.00000D+00
24	0.00000D+00	0.00000D+00	0.00000D+00	0.00000D+00	0.00000D+00	0.00000D+00	0.00000D+00	0.00000D+00
25	0.00000D+00	0.00000D+00	0.00000D+00	0.00000D+00	0.00000D+00	0.00000D+00	0.00000D+00	0.00000D+00
26	0.00000D+00	0.00000D+00	0.00000D+00	0.00000D+00	0.00000D+00	0.00000D+00	0.00000D+00	0.00000D+00
27	0.00000D+00	0.00000D+00	0.00000D+00	0.00000D+00	0.00000D+00	0.00000D+00	0.00000D+00	0.00000D+00
28	0.00000D+00	0.00000D+00	0.00000D+00	0.00000D+00	0.00000D+00	0.00000D+00	0.00000D+00	0.00000D+00
29	0.00000D+00	0.00000D+00	0.00000D+00	0.00000D+00	0.00000D+00	0.00000D+00	0.00000D+00	0.00000D+00
30	0.00000D+00	0.00000D+00	0.00000D+00	0.00000D+00	0.00000D+00	0.00000D+00	0.00000D+00	0.00000D+00
31	0.00000D+00	0.00000D+00	0.00000D+00	0.00000D+00	0.00000D+00	0.00000D+00	0.00000D+00	0.00000D+00
32	0.00000D+00	0.00000D+00	0.00000D+00	0.00000D+00	0.00000D+00	0.00000D+00	0.00000D+00	0.00000D+00
33	0.00000D+00	0.00000D+00	0.00000D+00	0.00000D+00	0.00000D+00	0.00000D+00	0.00000D+00	0.00000D+00
34	0.00000D+00	0.00000D+00	0.00000D+00	0.00000D+00	0.00000D+00	0.00000D+00	0.00000D+00	0.00000D+00
35	0.00000D+00	0.00000D+00	0.00000D+00	0.00000D+00	0.00000D+00	0.00000D+00	0.00000D+00	0.00000D+00
36	0.00000D+00	0.00000D+00	0.00000D+00	0.00000D+00	0.00000D+00	0.00000D+00	0.00000D+00	0.00000D+00
37	0.00000D+00	0.00000D+00	0.00000D+00	0.00000D+00	0.00000D+00	0.00000D+00	0.00000D+00	0.00000D+00
38	0.00000D+00	0.00000D+00	0.00000D+00	0.00000D+00	0.00000D+00	0.00000D+00	0.00000D+00	0.00000D+00

Driving matrix D

	1	2
1	0.00000D+00	0.00000D+00
2	0.00000D+00	0.00000D+00
3	0.00000D+00	0.00000D+00
4	0.00000D+00	0.00000D+00
5	0.00000D+00	0.00000D+00
6	0.00000D+00	0.00000D+00
7	0.00000D+00	0.00000D+00
8	0.00000D+00	0.00000D+00
9	0.00000D+00	0.00000D+00
10	0.00000D+00	0.00000D+00
11	-0.84900D+07	0.31800D+07
12	-0.12700D+08	0.24700D+06
13	-0.61700D+06	0.75600D+06
14	-0.10400D+08	0.82000D+06
15	0.87000D+06	-0.87900D+06
16	-0.55500D+07	0.11200D+06
17	-0.60800D+06	-0.14100D+06
18	-0.17500D+07	-0.51800D+05
19	-0.12300D+07	0.11500D+06
20	0.90200D+07	-0.48900D+05
21	0.00000D+00	0.00000D+00
22	0.00000D+00	0.00000D+00
23	0.00000D+00	0.00000D+00
24	0.00000D+00	0.00000D+00
25	0.00000D+00	0.00000D+00
26	0.00000D+00	0.00000D+00
27	0.00000D+00	0.00000D+00
28	0.00000D+00	0.00000D+00
29	0.00000D+00	0.00000D+00
30	0.00000D+00	0.00000D+00
31	0.00000D+00	0.00000D+00
32	0.00000D+00	0.00000D+00
33	0.60000D+01	0.00000D+00
34	0.00000D+00	0.75000D+01
35	0.00000D+00	0.00000D+00
36	0.00000D+00	0.00000D+00
37	0.00000D+00	0.00000D+00
38	0.00000D+00	0.00000D+00

Control
Driving Matrix B

	1	2
1	0.00000D+00	0.00000D+00
2	0.00000D+00	0.00000D+00
3	0.00000D+00	0.00000D+00
4	0.00000D+00	0.00000D+00
5	0.00000D+00	0.00000D+00
6	0.00000D+00	0.00000D+00
7	0.00000D+00	0.00000D+00
8	0.00000D+00	0.00000D+00
9	0.00000D+00	0.00000D+00
10	0.00000D+00	0.00000D+00
11	0.00000D+00	0.00000D+00
12	0.00000D+00	0.00000D+00
13	0.00000D+00	0.00000D+00
14	0.00000D+00	0.00000D+00
15	0.60000D+01	0.00000D+00
16	0.00000D+00	0.75000D+01
17	0.00000D+00	0.00000D+00
18	0.00000D+00	0.00000D+00
19	0.00000D+00	0.00000D+00
20	0.00000D+00	0.00000D+00
21	0.00000D+00	0.00000D+00
22	0.00000D+00	0.00000D+00
23	0.00000D+00	0.00000D+00
24	0.00000D+00	0.00000D+00